The Effect Of Pipe Roughness On Non-Newtonian Turbulent Flow

by

Fritz Peter van Sittert
B Tech (Civ. Eng.)

A thesis submitted for the degree of
Magister Technologiae
in the Department of Civil Engineering
Cape Technikon

November 1999

Cape Technikon
Cape Town
South Africa

ABSTRACT

The Effect of Pipe Roughness on non-Newtonian Turbulent Flow.

FRITZ PETER VAN SITTERT

Department of Civil Engineering, Cape Technikon, P.O. Box 652, Cape Town 8000, *Republic of South Africa.*

November, 1999

Pipe roughness is known to greatly increase the turbulent flow friction factor for Newtonian fluids. The well-known Moody diagram shows that an order of magnitude increase in the friction is possible due to the effect of pipe roughness. However, since the classical work of Nikuradse (1926 -1933), very little has been done in this area. In particular, the effects that pipe roughness might have on non-Newtonian turbulent flow head loss, has been all but totally ignored.

This thesis is directed at helping to alleviate this problem. An experimental investigation has been implemented in order to quantify the effect that pipe roughness has on non-Newtonian turbulent flow head loss predictions.

The Balanced Beam Tube Viscometer (BBTV), developed at the University of Cape Town, has been rebuilt and refined at the Cape Technikon and is being used for research in this field.

The BBTV has been fitted with pipes of varying roughness. The roughness of smooth PVC pipes was artificially altered using methods similar to those of Nikuradse. This has enabled the accumulation of flow data in laminar and turbulent flow in pipes that are both hydraulically smooth and rough. Newtonian and non-Newtonian fluids have been used for the tests.

The data have been subjected to analysis using various theories and scaling laws. The strengths and problems associated with each approach are discussed and it is concluded that roughness does have a significant effect on Newtonian as well as non-Newtonian flow.

DEDICATION

To my wife Lize.

" In research the horizon recedes as we advance, and is no nearer at sixty than it was at twenty. As the power of endurance weakens with age, the urgency of the pursuit grows more intense.....And research i. always incomplete."

Isaac Casaubon (1875)

ACKNOWLEDGEMENTS

I would like to thank the following persons and organisations;-

Professor P.T. Slatter for his leadership, help, guidance, encouragement and supervision to make this thesis possible.

The directors and staff of Paterson and Cooke Consulting Engineers, especially Dr A Paterson and Dr R Cooke, for their insight, advice, understanding and persistence to make this thesis possible.

My wife and family for their love, support and sacrifices.

The Cape Technikon and Civil Engineering Laboratory for the use of their facilities to make this research possible.

The NRF for their financial support.

Mark Jenkins at the Mechanical Engineering workshop and Alwyn Bester at the Chemical Engineering workshop for their technical assistance.

F P Van Sittert
November 1999

CONTENTS

NOMENCLATURE

Symbol	Description	Unit
A	constant	m^2
	cross sectional area	
A_r	area ratio	
b	constant	
B	constant	
	roughness function	
c	constant	
C	concentration	
d	particle diameter	μm
D	internal pipe diameter	m
E	error function	
	rheological parameter	
E_τ	shear stress prediction error	
f	Fanning friction factor	
g	gravitational acceleration	m/s^2
G	pseudo shear rate	1/s
H	head	m
He	Hedström number	
i	hydraulic gradient	m(water)/m(pipe)
k	constant	
	hydraulic roughness	μm
k_s	sand roughness	μm
K	fluid consistency index	$Pa.s^n$
K'	apparent fluid consistency index	$Pa.s^{n'}$
L	pipe length	m
m	slope	
	rheological parameter	
M	Mass	kg
n	flow behaviour index	
n'	apparent flow behaviour index	
N	number of items	
p	pressure	

Q	volumetric flow rate of slurry	Pa
r	radius at a point in the pipe	m^3/s
	correlation coefficient	m
R	radius of the pipe	m
Re	Reynolds number	
Re_{nn}	non-Newtonian Reynolds number	
Re_r	roughness Reynolds number	
Re_s	non-Newtonian Reynolds number (Slatter & Lazarus)	
S	relative density	
t	time	s
u	point velocity	m/s
u'	dimension less velocity	
V	average slurry velocity	m/s
V_*	shear velocity	m/s
V_s	particle settling velocity	m/s
X	unknown quantity	
	abscissa value	
y	distance from the pipe wall	m
y'	dimension less wall distance	
Y	ordinate value	
Z	stability function	
α	shear stress ratio	
	proportional to	
δ	viscous sub-layer thickness	μm
Δ	increment	
ε	deviation	
κ	stability function	
μ	dynamic viscosity	Pa.s
μ'	apparent dynamic density	Pa.s
ρ	slurry or fluid density	kg/m^3
τ	shear stress	Pa
τ_y	yield stress	Pa
ϕ	function of	
	rheological parameter	

Chapter 1

Introduction

1.1 Introduction

The design of hydrotransport systems has historically been done by scaling the energy gradient and mixture flow rates obtained from a model or prototype pipeline. In the last two decades academic research has advanced substantially, as seen in the proceedings of the numerous hydrotransport conference series, although the use of empirical design equations continues in industry.

Models have been developed for predicting the flow of Newtonian and non-Newtonian fluids. These models contain many variables that include slurry and pipe properties. Slurry properties can be determined very accurately in laboratories. Pipe properties are unique to the type of piping used for the specific application. One of the most important pipe variables is the pipe roughness. Despite the importance of pipe roughness, very little research has been done in this area.

There is a more fundamental need for research on non-Newtonian slurry flow in rough pipes. Slatter (1994) proposed a particle roughness effect which increases the turbulent flow friction factor in a similar manner to pipe roughness in Newtonian turbulent flow. The two mechanisms - the particle roughness and pipe roughness - compete for dominance, and Slatter proposed that if the pipe roughness size exceeded the representative particle size, then pipe roughness would dominate. This was based on very limited experimental evidence, and more experimental investigation is called for.

At present problems still remain in the precise modelling of non-Newtonian fluids. This thesis documents an experimental investigation that has been done in order to determine the effect that pipe roughness has on non-Newtonian turbulent flow behaviour. The balanced beam tube viscometer has been fitted with pipes of varying roughness. The roughness of these pipes has been artificially altered using methods similar to those of Nikuradse (1933). This has enabled the accumulation of flow data in laminar and turbulent flow in pipes that are both hydraulically smooth and rough. Newtonian and non-Newtonian

fluids have been used for the tests.

1.2 Aim and Objectives:

The primary aim of the thesis is to investigate experimentally the effect of pipe roughness on non-Newtonian turbulent flow, especially in the early turbulent flow region and to assess the turbulent flow models in the region.

The secondary objectives of this thesis are:

1. To manufacture a set of test pipes of varying roughness for the Balanced Beam Tube Viscometer (BBTV).

2. To calibrate the test pipes using water.

3. To perform experiments on various Newtonian and non-Newtonian fluids using smooth and rough pipes to establish fundamental behaviour.

4. To analyse the results and compare them with various theoretical model predictions.

1.3 Stating the Problem

Pipe roughness is known to greatly increase the turbulent flow friction factor for the flow of Newtonian fluids in pipes. Most of the pipes used in engineering structures cannot be regarded as being hydraulically smooth, especially at higher Reynolds numbers (Schlichting, 1960). To account for the effects of pipe roughness on head loss, correction factors are generally used for the design of a hydraulic pipeline (Schlichting, 1960). Most of these correction factors are derived empirically and are approximate. In some cases the correction factors work well, but when dealing with non-Newtonian fluids, with many variables, it becomes much more difficult to predict turbulent flow behaviour accurately. In such cases, over-design can prove to be costly and under design could have disastrous effects.

This thesis quantifies the behaviour of fluids tested in rough pipes and how Newtonian and non-Newtonian fluids behave in rough pipes. Different models are applied for predicting the roughness Reynolds number and the friction factors. None of these models produces consistently accurate predictions. Although no solution to this problem is presented, this experimental investigation highlights the problems experienced in dealing with pipe roughness.

1.4 Assumptions and Limitations.

The scope of this research is limited to using smooth PVC pipes and rough pipes similar to those of Nikuradse.

The following research limitations apply:

1. Only non-settling Newtonian and homogeneous non-Newtonian fluids and slurries have been tested.

2. Measurements have been limited to flow rate and pressure drop. No internal flow measurements have been made.

3. The maximum slurry volumetric concentration investigated is approximately 40%.

4. Compressed air is used as the prime mover instead of an in-line pump.

5. It is assumed that no slip occurs between the fluid and suspended particles.

6. No slip occurs at the pipe wall (wall fluid velocity is zero).

7. Constant relative density is assumed for all particles in a mixture.

8. Only rough pipes of 28mm and 46mm diameter and smooth pipes of 5mm, 13mm, 28mm and 46mm diameters are considered.

9. The BBTV is the only instrument used for testing purposes.

1.5 Methodology

1.5.1 Literature Review (Chapter 2)

Pipe roughness has not been fully researched. The most important work done in this field is by Nikuradse (1933). The author has used this work as the basis for experimental work and analysis. Despite an extensive literature search the author could not find any work done on non-Newtonian turbulent flow in rough pipes. However, there has been some work done on Newtonian fluids as well as fracturing gels. The theoretical models and literature are discussed in Chapter 2.

1.5.2 Experimental Work (Chapter 3)

All experimental work has been done using the Balanced Beam Tube Viscometer (BBTV). The instrument was developed at the University of Cape Town and further developed and refined at the Cape Technikon (Slatter, 1995). The BBTV is in fact a miniature pipeline and it has been shown that it is capable of producing valid turbulent flow data and indicating the laminar/turbulent transition region in the eight tubes used. The instrument is the biggest viscometer referenced in the literature and its uses extend beyond viscometry. The BBTV apparatus has been calibrated using water and glycerol. The non-Newtonian investigation was done using CMC, Kaolin and tailings slurries at different concentrations.

1.5.3 Analysis of the Data (Chapter 4)

The data obtained in the test work were analysed using the approach developed by Nikuradse for rough pipes. Newtonian as well as non-Newtonian fluids were tested and the analyses of these results are presented.

1.5.4 Discussion (Chapter 5)

The results in Chapter 4 are discussed using the predictions of Nikuradse as well as the limitations in these predictions when dealing with non-Newtonian fluids.

1.6 Conclusion

This research comprises a detailed investigation into pipe roughness. It identifies and evaluates many of the phenomena present in the flow behaviour of Newtonian and non-Newtonian fluids in rough pipes. The work done is evaluated, conclusions are drawn and further research recommendations are made.

Chapter 2

Theory and Literature Review

2.1 Introduction

The theory and literature relevant to the pipe flow of time independent non-Newtonian slurries is presented.

A large body of literature is available on estimating friction loss or friction pressure gradients for laminar and turbulent flow of Newtonian fluids in smooth pipes. Although not as extensive as for Newtonian fluids, there is a great deal of literature on non-Newtonian fluids for the estimation of friction loss in laminar and turbulent flow in smooth pipes. It has long been known that for laminar flow past solid boundaries, surface roughness has no effect (at least for certain degrees of roughness) on the friction loss of either Newtonian or non-Newtonian fluids (Schlichting, 1960). In turbulent flow however the nature of the flow is intimately associated with the surface roughness. Significant increases in friction loss in turbulent flow over rough surfaces have been reported. Extensive studies have been conducted to quantify the effect of pipe roughness on friction loss in turbulent flow of Newtonian fluids in rough pipes. The phenomenon of turbulent flow of non-Newtonian fluid in rough pipes has received very little attention to date.

2.2 Pipe Roughness

The resistance to flow offered by rough walls is larger than that implied by equations for smooth pipes (Schlichting, 1960). Consequently the laws of friction in rough pipes are of great practical importance and experimental work on them began very early (Reynolds, 1883; Stanton, 1911; Stanton and Pannell, 1914; Nikuradse 1933; Senecal and Rothfus, 1953 and Laufer, 1953). It is difficult to explore the laws of friction in a systematic way because the number of parameters describing roughness is large owing to the great diversity of geometric forms possible. Imagine for instance a pipe wall with identical protrusions, how would you describe the roughness? The drag would depend on the density of distribution of such roughness, i.e. on their number per unit area as well as on their shape, height, type (steel pipe to PVC pipe) and also in the way in which they are distributed over

its surface. It took, therefore, a long time to formulate concise laws to describe the flow of fluids in rough pipes.

L. Hopf (1923) reviewed earlier experimental results and found two types of roughness in relation to the resistance formula for rough pipes and open channels. The first kind of roughness causes a resistance which is proportional to the square of the velocity. This means that the coefficient of resistance is independent of Reynolds number and corresponds to relatively coarse and tightly spaced roughness elements such as coarse sand grains glued on the surface, cement or rough cast iron. In such cases the nature of the roughness can be expressed with the aid of a single roughness parameter k R, known as the relative roughness, where k is the height of a protrusion and R denotes the radius or the hydraulic radius of the conduit in which the fluid is conveyed. From considerations of similitude we may conclude that in this case the resistance coefficient depends on the relative roughness only. The actual relation can be determined experimentally by performing measurements on pipes or channels of differing hydraulic radii but of the same absolute roughness. Such measurements were carried out by K. Fromm (1923) and W. Fritsch (1928).

The second type of resistance formula occurs when the protrusions are more gentle or when a small number of them is distributed over a relatively large area, such as those in wooden or commercial steel pipes. In such cases the resistance coefficient depends both on the Reynolds number and on the relative roughness (Schlichting, 1960).

From the physical point of view it must be concluded that the ratio of the height of protrusions to the boundary layer thickness should be the determining factor (Schlichting, 1960). In particular, the phenomenon is expected to depend on the thickness of the viscous sub-layer δ, so that k/δ must be regarded as an important dimensionless number which is characteristic of the type of roughness. The pipe wall may be considered to be hydraulically smooth in cases were $k < \delta$ or where the boundary layer is so thick that all the roughness particles are contained within the laminar sub-layer. This is similar to the absence of the influence of roughness on resistance in Hagen-Poiseuille flow.

Very systematic, extensive, and careful measurements on rough pipes have been carried out by J. Nikuradse (1933), who used circular pipes covered on the inside as tightly as possible with sand of a definitive grain size glued on to the wall. By choosing pipes of varying

diameters and by changing the size of grain, he was able to vary the relative sand roughness $k_s R$ from approximately 1/500 to 1/15. The regularities of behaviour discovered during the course of these measurements can be correlated with those for smooth pipes in a simple manner.

2.3 Viscometry

Viscometry can be defined as the collection of physical data from tests on a sample of the fluid under investigation for the purpose of establishing the relationship between shear stress and shear rate. The instrument used to measure viscous properties is called a viscometer. There are two main types of viscometers - rotational and tube.

A typical rotational viscometer consists of a concentric bob and cup, one of which is rotated to produce shear in the test fluid contained in the gap between the bob and cup. The shear stress is determined by measuring the torque on one of the elements, and the shear rate is determined from the relative angular velocity between the elements and the measuring gap. A tube viscometer is essentially a small diameter pipeline. The test fluid flows at a controlled, measured rate through the tube and the pressure drop over a known length of the tube is measured.

Although there are many advantages to using the rotational type, for non-Newtonian slurries the tube type is preferred (Wilson *et al.* 1992). The main difficulties associated with the rotational type is that relatively low shear rates are achieved and centrifuge action can occur in the measuring gap (Johnson, 1982; Slatter, 1986 and Shook & Roco, 1991). Centrifuge action causes the readings to decay with time, resulting in the erroneous identification of time dependent (thixotropic) behaviour. Interpretation is further complicated by end effects. On the other hand, the tube viscometer is mechanically simpler, is geometrically similar to a pipe, and is in fact a miniature pipeline (Slatter & Lazarus, 1988).

Ideally, test work for the prediction of turbulent energy gradients from rheology should be performed so that the wall shear stress for the tests is the same as the wall shear stress in the prototype. This is usually not possible as the flow becomes turbulent at these higher shear stresses and flow rates, even in small diameter tube viscometers (Shook & Roco,

1991). Therefore, the rheology obtained is extrapolated, sometimes by several orders of magnitude, to arrive at the required shear stress. The accuracy of the rheological measurements and characterization is therefore of utmost importance. For this reason it is very important that tests are conducted in as many tubes as possible.

2.4 Rheology

In order to do any kind of analysis the rheology of the fluid must be known. Within the context of this thesis, rheology means the viscous characteristics of a fluid. Specifically, rheology is the relationship between shear rate and shear stress, as portrayed on a rheogram.

For Newtonian fluids the relationship between shear stress and shear rate is linear and the viscosity of the fluid is determined only by the slope of the line. The viscosity alone is sufficient to characterise the fluid flow. Where this is not the case, the fluid is non-Newtonian and additional parameters such as the apparent viscosity, the yield stress, dynamic and elastic properties, and the flow behaviour index is required to characterise the fluid.

Non-Newtonian slurries can be modelled using the generalised yield pseudo plastic (Govier & Aziz, 1972 and Hanks, 1979) or Herchel-Bulkley rheological model. The constitutive rheological equation is:

$$\tau = \tau_y - K \left(-\frac{du}{dr} \right)^n \qquad (2.1)$$

where: τ_y = yield stress

K = fluid consistency index

n = flow behaviour index.

The generalised yield pseudoplastic model is sensitive to small variations in the rheological parameters and a reasonable amount of good data in the laminar flow regime is necessary to accurately determine the rheological parameters. The yield pseudoplastic model does not take into account the tendency of certain slurries to have Newtonian viscosities at low and

very high shear rates (Hanks, 1981). This phenomenon is rarely encountered in practice. The model remains the most widely used correlation for non-Newtonian slurries.

Figure 2.1 below shows a rheogram with various non-Newtonian fluids and the shape of the rheogram for each fluid on a linear axis.

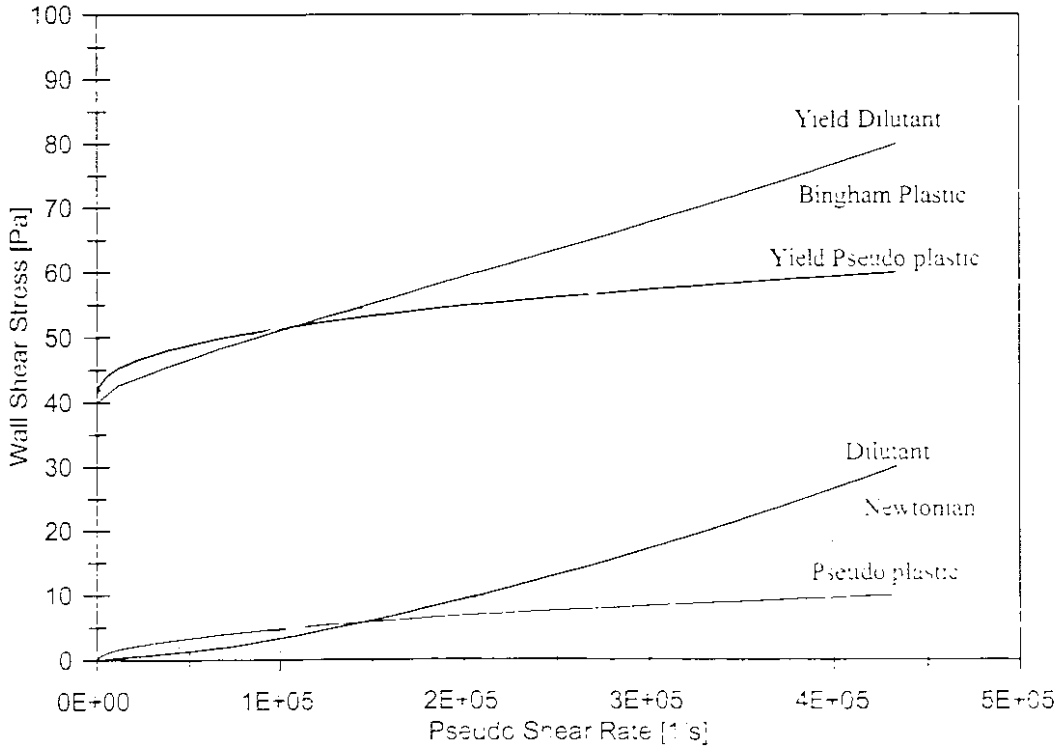

Figure 2.1 Rheological Models

The instrument used for tests in this thesis is a tube viscometer and is called a Balanced Beam Tube Viscometer (BBTV). All the experiments performed and presented in this thesis were done using this instrument. The instrumentation will be described in detail in Chapter 3.

2.5 Rheological Variables

2.5.1 Fluid Consistency Index (K)

The fluid consistency index (K) of a fluid is a measure of its fluidity. The larger the value of K the *less particle mobility* or *thicker* or *more viscous* the fluid (Sive, 1988).

The fluid consistency index is affected by the following (Sive, 1988):

1. Particle Size

   Decreasing particle size increases the degree of non-Newtonian behaviour of a mixture affecting both the fluid consistency index and the flow behaviour index. The resistance to the flow increases as particle size decreases. Only the -74 μm portion plays an important role in the viscous properties of the fluid even though the fluid may consists of a large particle size distribution.

2. Particle Solid Density

   Particle density is significant and smaller particle sizes and higher concentrations are necessary for homogeneous flow as particle density increases. This required increase in mixture concentration results in increased values of the fluid consistency index which means the fluid becomes more viscous or "thick".

3. Shape

   Particle shape combined with the slurry relative density has the single greatest influence on K. The rotation of non spherical particles in a velocity gradient causes an increase in the frequency of inter particle contacts and an apparent increase in the effective concentration and hence fluid consistency. At low concentrations where hydrodynamic effects predominate, this effect is small.

4. Particle Roughness

Rough grains do not slip or roll easily over one another. The effect of adding a lubricant (e.g. soap) to the mixture demonstrates this. The lubricant will cause a substantial change in K for rough particles but will have a limited effect on smooth spheres.

5 Particle Size Distribution

The addition of a relatively small quantity of fine particles to a mixture of coarse particles will result in a significant decrease in K. Addition of a small quantity of coarse particles to a mixture of fines will produce very little change in the value of K.

6 Particle Interactions

Particle interactions cause discrete particles to be sporadically retarded and accelerated. In both stages, inertia affects the amount of energy required by the interaction. This dissipation of energy is manifest as an increase in the fluid consistency index.

2.5.2 The Flow Behaviour Index (n)

The flow behaviour index has some physical meaning where the floc radius in a mixture can be related to the particle radius. The deviation of the flow behaviour index from unity indicates the degree of curvature of the rheogram. K and n thus define the shape of the rheogram.

2.5.3 The Yield Stress (τ_0)

Yield stress is a phenomenon closely associated with electrical attractions (Zeta potential) of particles and hence flocculation. The existence of a yield stress is therefore exclusive to flocculated mixtures (Sive, 1988). The yield stress is a direct consequence of a floc structure in a fine particle mixture. Some additives are available on the market that can, by

2.5 Rheological Variables

2.5.1 Fluid Consistency Index (K)

The fluid consistency index (K) of a fluid is a measure of its fluidity. The larger the value of K the *less particle mobility* or *thicker* or *more viscous* the fluid (Sive, 1988).

The fluid consistency index is affected by the following (Sive, 1988):

1. Particle Size

   Decreasing particle size increases the degree of non-Newtonian behaviour of a mixture affecting both the fluid consistency index and the flow behaviour index. The resistance to the flow increases as particle size decreases. Only the -74 μm portion plays an important role in the viscous properties of the fluid even though the fluid may consists of a large particle size distribution.

2. Particle Solid Density

   Particle density is significant and smaller particle sizes and higher concentrations are necessary for homogeneous flow as particle density increases. This required increase in mixture concentration results in increased values of the fluid consistency index which means the fluid becomes more viscous or "thick".

3. Shape

   Particle shape combined with the slurry relative density has the single greatest influence on K. The rotation of non spherical particles in a velocity gradient causes an increase in the frequency of inter particle contacts and an apparent increase in the effective concentration and hence fluid consistency. At low concentrations where hydrodynamic effects predominate, this effect is small.

4. Particle Roughness

Rough grains do not slip or roll easily over one another. The effect of adding a lubricant (e.g. soap) to the mixture demonstrates this. The lubricant will cause a substantial change in K for rough particles but will have a limited effect on smooth spheres.

5 Particle Size Distribution

The addition of a relatively small quantity of fine particles to a mixture of coarse particles will result in a significant decrease in K. Addition of a small quantity of coarse particles to a mixture of fines will produce very little change in the value of K.

6 Particle Interactions

Particle interactions cause discrete particles to be sporadically retarded and accelerated. In both stages, inertia affects the amount of energy required by the interaction. This dissipation of energy is manifest as an increase in the fluid consistency index.

2.5.2 The Flow Behaviour Index (n)

The flow behaviour index has some physical meaning where the floc radius in a mixture can be related to the particle radius. The deviation of the flow behaviour index from unity indicates the degree of curvature of the rheogram. K and n thus define the shape of the rheogram.

2.5.3 The Yield Stress (τ_y)

Yield stress is a phenomenon closely associated with electrical attractions (Zeta potential) of particles and hence flocculation. The existence of a yield stress is therefore exclusive to flocculated mixtures (Sive, 1988). The yield stress is a direct consequence of a floc structure in a fine particle mixture. Some additives are available on the market that can, by

addition of small quantities, change the yield stress of a fluid without changing the particle size distribution of that mixture.

2.6 Laminar Flow

There are a number of different rheological models that can be used to describe non-Newtonian mixtures. Models that describe the laminar flow of time independent fluids includes the Casson (1959) model and the Herschel-Bulkley (1926) model, which describes a wide variety of different fluids. Non-Newtonian fluids can also be time dependant and viscoelastic (Govier and Aziz, 1972), in which case the models become exceedingly complex. Time dependant and viscoelastic slurries will not be discussed in this thesis.

2.6.1 Time Independent Slurries

Figure 2.2 depicts the various different time independent and time dependant non-Newtonian slurries and the shape of the rheogram for each slurry on linear axes. It is necessary to have a reasonable amount of good data in the laminar flow regime to accurately determine the parameters for the yield pseudo-plastic model. The model is sensitive to small variations in the rheological parameters and requires careful analysis to ensure reproducibility of the model to different data sets.

It is seen in Figure 2.3 that the viscosity of a Newtonian fluid is a constant. In the case of non-Newtonian fluids however, the viscosity changes as the shear rate changes. The fluid consistency index, K, is used to account for the variation in viscosity and mathematically defines the shape of the rheogram. It corresponds only to the steepness of the rheogram and has no physical basis. The flow behaviour index, n, indicates the degree of curvature of the rheogram (Paterson & Cooke, 1997).

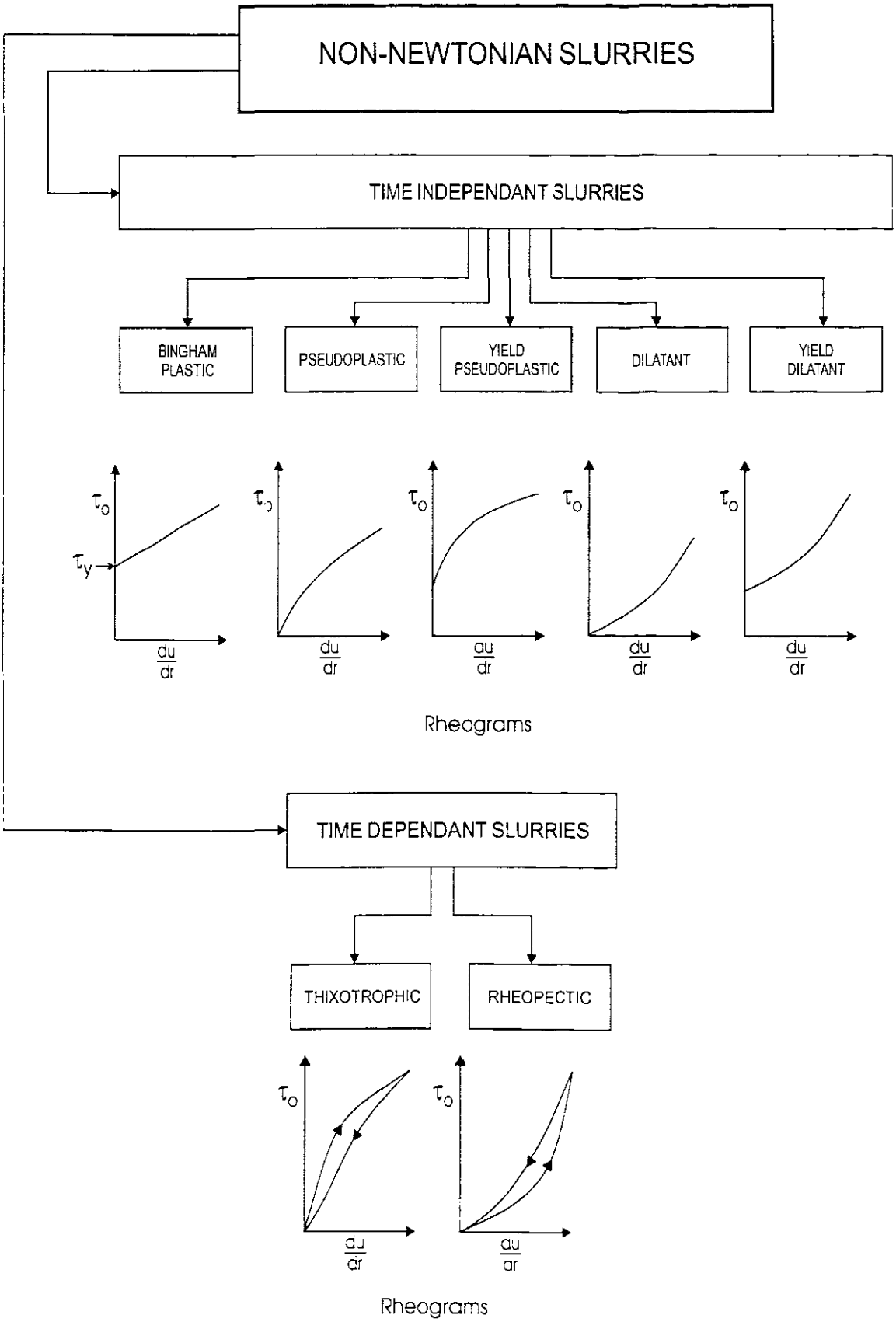

Figure 2.2: Classification of Time Independent and Time Dependant non-Newtonian Slurries. (Paterson and Cooke, 1997)

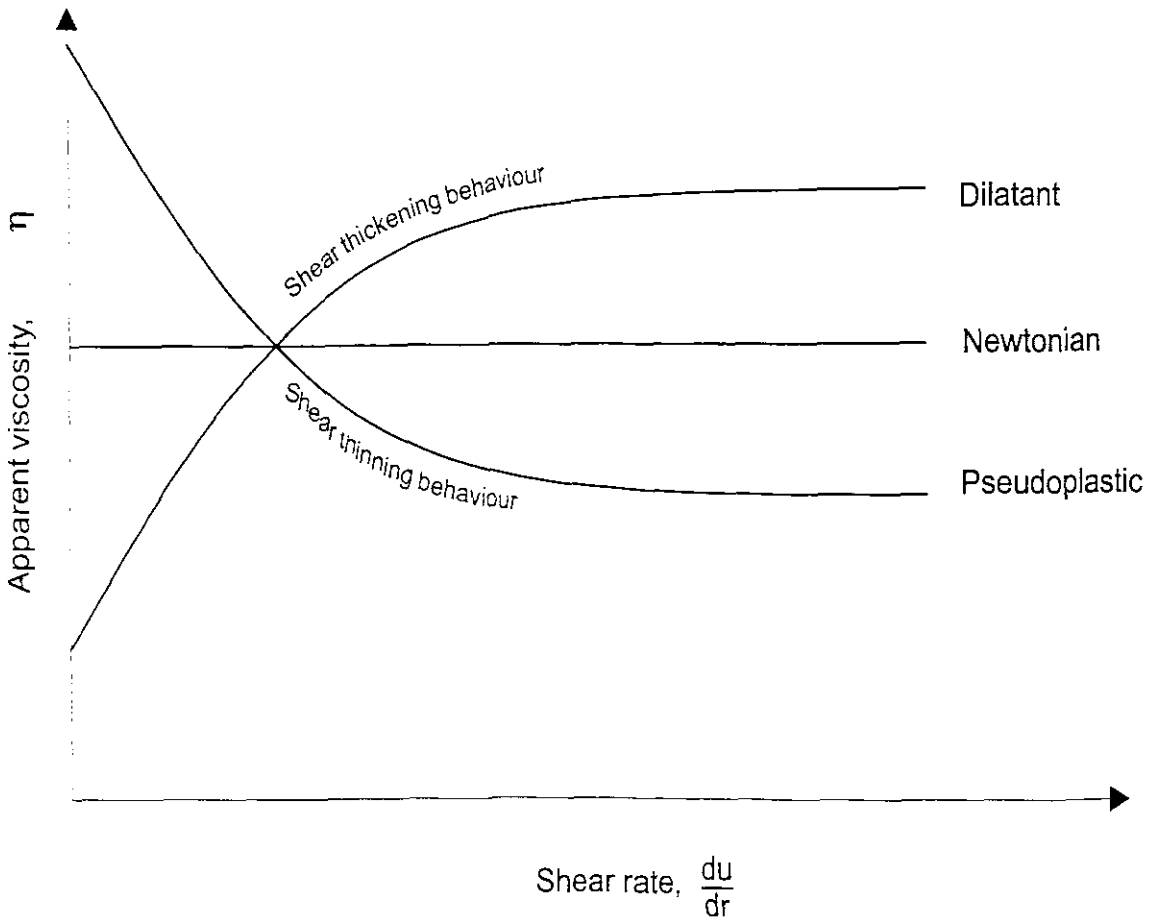

Figure 2.3: Variation of Viscosity in non-Newtonian Slurries (Paterson & Cooke, 1997)

Bingham plastic fluids, yield pseudoplastic fluids and yield dilatant fluids have a yield stress. These fluids have an internal structure that is capable of preventing movement when the applied shear stress is less than the yield stress. The Bingham Plastic model is the most well known and often used (Paterson & Cooke, 1997).

Shear thinning slurries, such as kaolin and coal, have n values less than unity. The progressive shearing of the fluid results in a decreasing interaction between particles and a consequent reduction in apparent viscosity (Paterson & Cooke, 1997).

Dilatant slurries, such as quicksand and some kimberlites, are recognized by an increase in apparent viscosity with increasing shear rates and are known as shear thickening slurries. The flow behaviour index n is greater than unity. They also tend to increase in volume as the shear rate increases and the particles disperse to leave the interstitial spaces only partly filled with liquid.

For laminar pipe flow, volumetric discharge, Q, and average mixture velocity, V, can be determined using the equation (Govier & Aziz, 1972);

$$\frac{32Q}{\pi D^3} = \frac{8V}{D} = \frac{4n}{K\frac{1}{n}\tau_0^3}\left(\tau_0 - \tau_y\right)^{\frac{1+n}{n}}\left[\frac{\left(\tau_0 - \tau_y\right)^2}{1+3n} + \frac{2\tau_y\left(\tau_0 - \tau_y\right)}{1+2n} + \frac{\tau_y^2}{1+n}\right] \quad (2.2)$$

where; $\tau_0 = D\Delta P / 4L$

$V = Q / A.$

It is important to note that this approach can accommodate both the pseudoplastic model (by setting $\tau_y = 0$) and the Newtonian model (by setting $\tau_y = 0$, $K = \mu$ and $n = 1$).

The different slurry types that can be described by the generalized yield pseudoplastic equation are given in Table 2.1.

Table 2.I Time Independent Rheological Models.

Fluid	**Yield Stress** τ_y	**Flow Behaviour Index** **n**	**Constitutive Equation**
Newtonian	0	1	$\tau = \mu\left(-\frac{du}{dy}\right)$
Bingham Plastic	> 0	1	$\tau = \tau_y + K\left(-\frac{du}{dy}\right)$
Pseudoplastic	0	< 1	$\tau = K\left(-\frac{du}{dy}\right)^n$
Yield Pseudoplastic	> 0	< 1	$\tau = \tau_y + K\left(-\frac{du}{dy}\right)^n$
Dilatant	0	> 1	$\tau = K\left(-\frac{du}{dy}\right)^n$

Fluid	Yield Stress τ_y	Flow Behaviour Index n	Constitutive Equation
Yield Dilatant	> 0	> 1	$\tau = \tau_y + K\left(-\frac{du}{dy}\right)^n$

2.6.2 Time Dependant Slurries

Time dependant slurries are those slurries in which the shear stress is dependant upon both the shear rate and the duration of the applied shear. The rheogram relating the shear stress to the shear rate is not unique but depends upon the history of the shear rate. This study does not investigate time dependant slurries.

2.7 Rheological Characterization

The rheology of the slurries used for this investigation was obtained from laminar tube flow data. The rheological constants (τ_y, K and n) are determined from the data in the laminar region and using Equation 2.2 (Lazarus & Slatter, 1986, 1988 and Slatter, 1994). For Newtonian and Pseudoplastic (power law) models, the characterization procedure is much simpler, and the data can be fitted by linear regression.

2.8 Research on Pipe Roughness

The effect that pipe roughness has on turbulent flow behaviour was first investigated by Nikuradse (1933) and Colebrook & White (Colebrook, 1939). Nikuradse performed experiments with pipes that had been purposely roughened by gluing sand particles onto the inner surface. The roughness of these pipes was uniform in size and spatial distribution. Colebrook & White used pipes that were commercially produced and had a more random distribution of roughness.

In the region of laminar flow for Newtonian fluids, Nikuradse found that rough pipes have the same resistance as smooth pipes (Nikuradse, 1933). The critical Reynolds number is equally independent of roughness in both smooth and rough pipes. In the turbulent region there is a range of Reynolds numbers where the rough pipes behave the same as smooth

pipes. In this region the rough pipes are considered to be hydraulically smooth. This range of Reynolds numbers is limited by the relative roughness of the rough pipes. The rougher the pipe the smaller the range in which the rough pipe is considered to be hydraulically smooth. In this region where the pipes are considered to be hydraulically smooth, the friction factor depends on the Reynolds number only. Beginning with a definite Reynolds number whose magnitude increases as k_s/R decreases, the resistance curve for a rough pipe deviates from that for a smooth pipe and reaches the region of the quadratic resistance law at some higher value of Reynolds number, where the friction factor, f, depends on k_s/R only. Figure 2.4 presents the resistance to flow for pipes roughened with sand as presented by Nikuradse (1933).

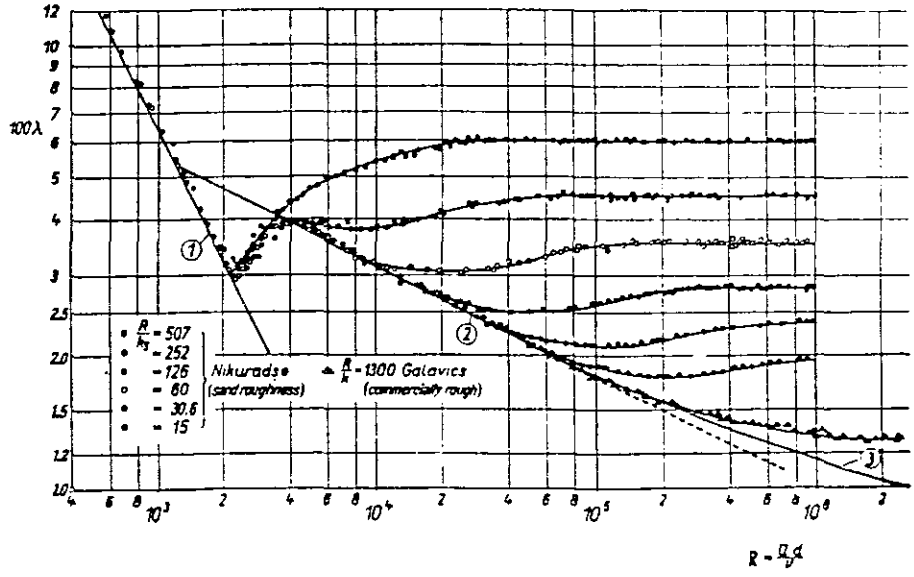

Figure 2.4 Flow Resistance for Rough Pipes (Schlichting, 1960).

2.8.1 Work Done by Nikuradse (1926-1933)

Nikuradse is responsible for the most comprehensive studies of turbulent flow in pipes of well defined roughness, prepared by cementing sand grains to the inside of the pipe walls. Nikuradse obtained both velocity profile and pressure gradient data. The velocity profile data are correlated according to Prandtl's (1927a) modification in which the distance from the pipe wall, y, is made dimensionless by the use of k.

Actual data covering D/k_s values from 30 to 1014 are reasonably well correlated by a value of B = 8.5.

It is therefore necessary to consider the three regimes within turbulent pipe flow, eg. Hydraulically smooth, transitional and completely rough regimes.

1. The hydraulically smooth regime;

$$0 \leq \frac{k_s V_*}{\nu} \leq 5 : f = \varnothing(\mathrm{Re}), \quad (2.3)$$

where;

$$V_* = \sqrt{\frac{\tau_0}{\rho}} \quad (2.4)$$

and;

$$\nu = \frac{\mu}{\rho} \quad (2.5)$$

where; ρ = density

ν = kinematic viscosity

k_s = sand or grain size

R = radius of cross-section.

In this region the viscous sub-layer is thicker than the roughness height or the roughness is so small that all protrusions are contained within the viscous sub-layer thickness.

2. The transition regime;

$$5 \leq \frac{k_s V_*}{\nu} \leq 70 : f = \varnothing\left(\frac{k_s}{D}, Re\right) \tag{2.6}$$

In this region some of the protrusions are higher than the viscous sub-layer and some are smaller. This causes additional resistance to flow and is mainly due to the form drag experienced by the protrusions in the boundary layer.

3. The completely rough regime:

$$\frac{k_s V_*}{\nu} > 70 : f = \varnothing(k_s / D). \tag{2.7}$$

In this region all the protrusions break through the viscous sub-layer and the dominant resistance to flow is due to the form drag which acts on them. The law of resistance *becomes quadratic.*

The velocity distribution for Newtonian turbulent flow in rough pipes is presented by Schlichting, 1960.

$$\frac{u}{V_*} = A \ln\left(\frac{y}{k}\right) + B \tag{2.8}$$

where; $A = 1/\chi$; χ=0.4 (von Kármán's constant)

B = roughness function

k = roughness size

y = distance from pipe wall

u = point velocity.

2.8.1 Work Done by Nikuradse (1926-1933)

Nikuradse is responsible for the most comprehensive studies of turbulent flow in pipes of well defined roughness, prepared by cementing sand grains to the inside of the pipe walls. Nikuradse obtained both velocity profile and pressure gradient data. The velocity profile data are correlated according to Prandtl's (1927a) modification in which the distance from the pipe wall, y, is made dimensionless by the use of k.

Actual data covering D/k_s values from 30 to 1014 are reasonably well correlated by a value of B = 8.5.

It is therefore necessary to consider the three regimes within turbulent pipe flow, eg. Hydraulically smooth, transitional and completely rough regimes.

1. The hydraulically smooth regime;

$$0 \leq \frac{k_s V_*}{\nu} \leq 5 : f = \varnothing(\mathrm{Re}), \quad (2.3)$$

where;

$$V_* = \sqrt{\frac{\tau_0}{\rho}} \quad (2.4)$$

and;

$$\nu = \frac{\mu}{\rho} \quad (2.5)$$

where; ρ = density

ν = kinematic viscosity

k_s = sand or grain size

R = radius of cross-section.

In this region the viscous sub-layer is thicker than the roughness height or the roughness is so small that all protrusions are contained within the viscous sub-layer thickness.

2. The transition regime;

$$5 \leq \frac{k_s V_*}{\nu} \leq 70 : f = \emptyset\left(\frac{k_s}{D}, Re\right) \tag{2.6}$$

In this region some of the protrusions are higher than the viscous sub-layer and some are smaller. This causes additional resistance to flow and is mainly due to the form drag experienced by the protrusions in the boundary layer.

3. The completely rough regime:

$$\frac{k_s V_*}{\nu} > 70 : f = \emptyset(k_s / D). \tag{2.7}$$

In this region all the protrusions break through the viscous sub-layer and the dominant resistance to flow is due to the form drag which acts on them. The law of resistance becomes quadratic.

The velocity distribution for Newtonian turbulent flow in rough pipes is presented by Schlichting, 1960.

$$\frac{u}{V_*} = A \ln\left(\frac{y}{k}\right) + B \tag{2.8}$$

where; $A = 1/\chi$; χ=0.4 (von Kármán's constant)

B = roughness function

k = roughness size

y = distance from pipe wall

u = point velocity.

The velocity gradient near a rough wall is less steep than that near a smooth one (Schlichting, 1960), as can be seen from Figure 2.5.

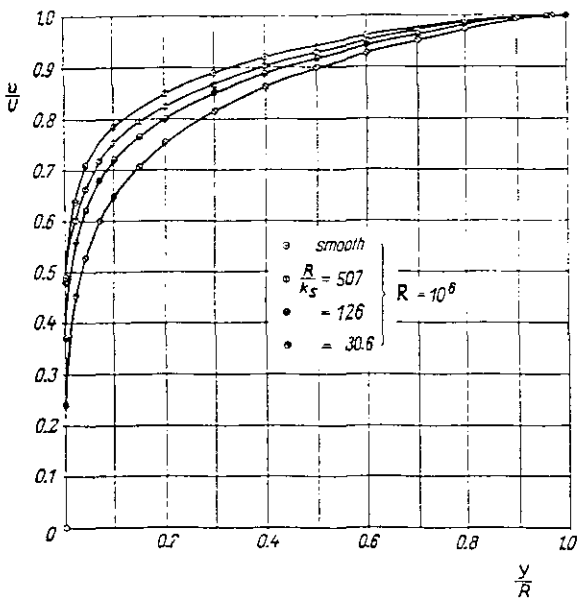

Figure 2.5 Velocity Distribution in Rough Pipes (Nikuradse 1933)

The mean velocity can be obtained by integrating over the cross section of the pipe yielding;

$$\frac{V}{V_*} = 2.5 \ln\left(\frac{R}{k}\right) + B - 3.75. \qquad (2.9)$$

B can be correlated using a roughness Reynolds number;

$$R_{e_r} = \left(\frac{\rho V_* k}{\mu}\right). \qquad (2.10)$$

The roughness function correlation is shown in Figure 2.6. Generally speaking B is a function of the roughness Reynolds number Re_r. The oblique asymptote in Figure 2.6 is the

line which represents smooth wall turbulent flow and can be expressed as (Schlichting, 1960);

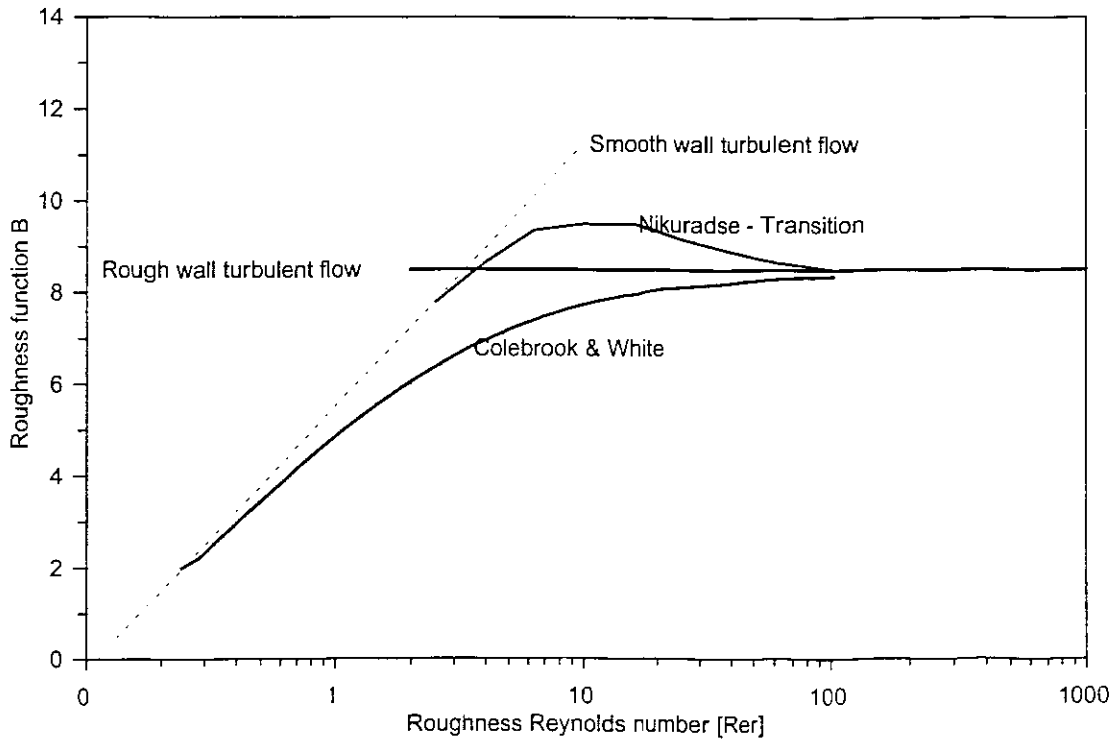

Figure 2.6 Roughness Function Correlation.

The top curve is the locus of data for pipes with uniform roughness from the experiments with sand roughed pipes by Nikuradse. The lower curve represents the locus of data for commercially available (randomly rough) pipes as investigated by Colebrook & White (1937).

The horizontal asymptote in Figure 2.6 is the line B = 8.5 which represents fully developed or rough wall turbulent flow and the velocity distribution can be expressed as;

$$\frac{u}{V_*} = 5.75\log\left(\frac{yV_*}{\frac{\mu}{\rho}}\right) + 8.5. \qquad (2.11)$$

For fully developed rough wall turbulent flow (B = 8.5) the velocity distribution can be integrated over the cross sectional area of the pipe to give the mean velocity and can be expressed as (Schlichting, 1960);

$$\frac{V}{V_*} = 2.5\ln\left(\frac{R}{k}\right) + 4.75. \qquad (2.12)$$

Thus from this equation it can be seen that the behaviour for fully developed rough turbulent flow of Newtonian fluids in pipes is **totally independent of the viscous characteristics of the fluid.**

Nikuradse's friction factor data for rough pipes reflects all three regions of turbulent flow. He correlated the data in the fully developed rough wall turbulent flow regime empirically through the equation;

$$\frac{1}{\sqrt{f}} = 4\log\left(\frac{D}{2k}\right) + 3.48. \qquad (2.13)$$

where; D = internal diameter of pipe

k = relative roughness.

The von Kármán equation is essentially the same;

$$\frac{1}{\sqrt{f}} = 4.06\log\left(\frac{D}{2k}\right) + 3.36. \qquad (2.14)$$

The difference between artificially roughened and naturally randomly rough pipes can be seen as the difference between the two data loci in Figure 2.6. The locus of the naturally random pipes (Colebrook & White, 1938) shows a gradual and smooth transition between the two asymptotes, while the artificially roughened (Nikuradse, 1933) locus shows a distinct maximum value in the roughness, B. However, the asymptotes apply equally to

both cases.

2.8.2 Newtonian Fluids in Rough Pipes (Colebrook 1938).

The velocity distribution for Newtonian turbulent flow in rough pipes is;

$$\frac{u}{V_*} = A \ln\left(\frac{y}{k}\right) + B, \tag{2.15}$$

where; A = constant

B = roughness function.

The logarithmic law for velocity distribution is valid in rough pipes except that the constant of integration must reflect the roughness size (Schlichting, 1960).

B can be correlated using a roughness Reynolds number

$$Re_r = \frac{\rho V_* k}{\mu}, \tag{2.16}$$

The oblique asymptote in Figure 2.6 is the line;

$$B = 2.5 \ln Re_r + 5.5, \tag{2.17}$$

which represents the equation for smooth wall turbulent flow.

The horizontal asymptote is the line B = 8.5 which represents fully developed rough wall turbulent flow.

The top curve is the locus of data for pipes with uniform roughness from the experiments with sand roughened pipes by Nikuradse (Schlichting,1960).

The lower curve is the equation of Colebrook and White (1939) and represents the locus of data for commercially available (randomly rough) pipes. This equation is widely used for the design of Newtonian pipelines.

For fully developed rough turbulent flow (B = 8.5) the velocity distribution can be integrated over the cross sectional area of the pipe to give the mean velocity;

$$\frac{V}{V_*} = 2.5\ln\left(\frac{R}{k}\right) + 4.75. \qquad (2.18)$$

It can be concluded that the behaviour for the fully developed rough wall turbulent flow of Newtonian fluids in pipes is totally independent of the viscous characteristics of the fluid.

Equation 2.18 may be expressed in Reynolds number - friction factor format as;

$$\frac{1}{\sqrt{f}} = -4\log\left(\frac{k}{3.7D}\right). \qquad (2.19)$$

2.8.3 Work Done by Moody (1944)

The turbulent flow friction factor relations for smooth pipe or smooth wall turbulence, partially rough wall turbulence and fully rough wall turbulence are presented graphically in Figure 2.8 as presented by Moody (1944).

These relations and their graphical counterpart represent our best current knowledge of the effect of Re and k/D on the turbulent friction factor (Govier and Aziz, 1972). We must remember, however, that k_s is the equivalent sand grained roughness and that natural roughness must be expressed in terms of the sand grain roughness, which would result in the same friction factor. This is not easily achieved, in fact the only way it can be done is by comparison of the behaviour of a naturally rough pipe with a sand roughened pipe (Govier and Aziz, 1972).

Moody (1944) has made such comparisons, and his widely used chart giving the absolute and relative sand grained roughness of a variety of pipe wall materials is reproduced in Figure 2.9. Moody's roughness is typical of the materials indicated, but we cannot expect them to be precise for any given material (Govier and Aziz,1972). When it is possible to obtain the results of a flow test through a pipe of identical or closely similar material to that to be used, one may calculate the friction factor, and hence the effective k/D directly.

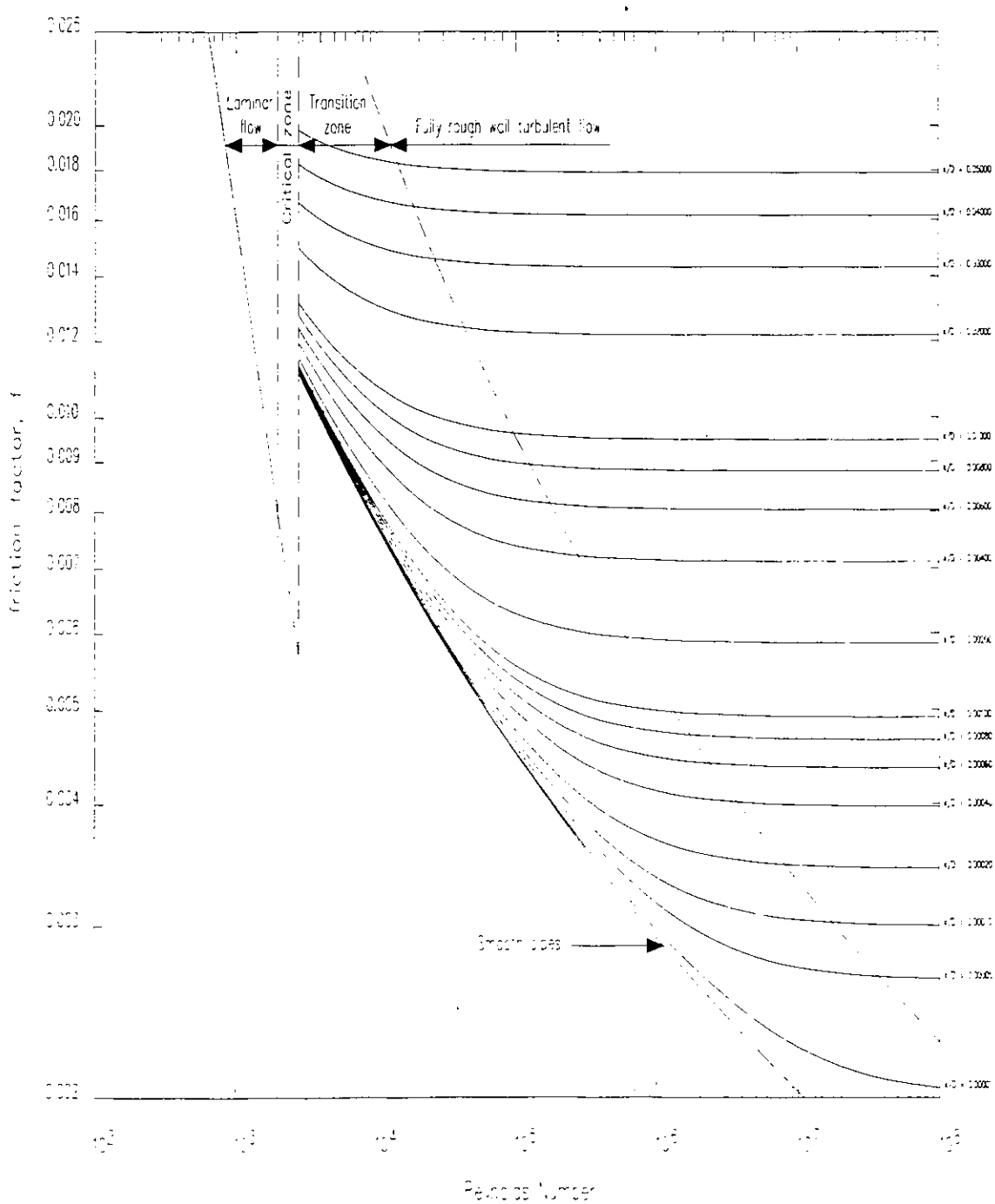

Figure 2.8 Pipe Friction Factors for Turbulent Flow. (Moody, 1944)

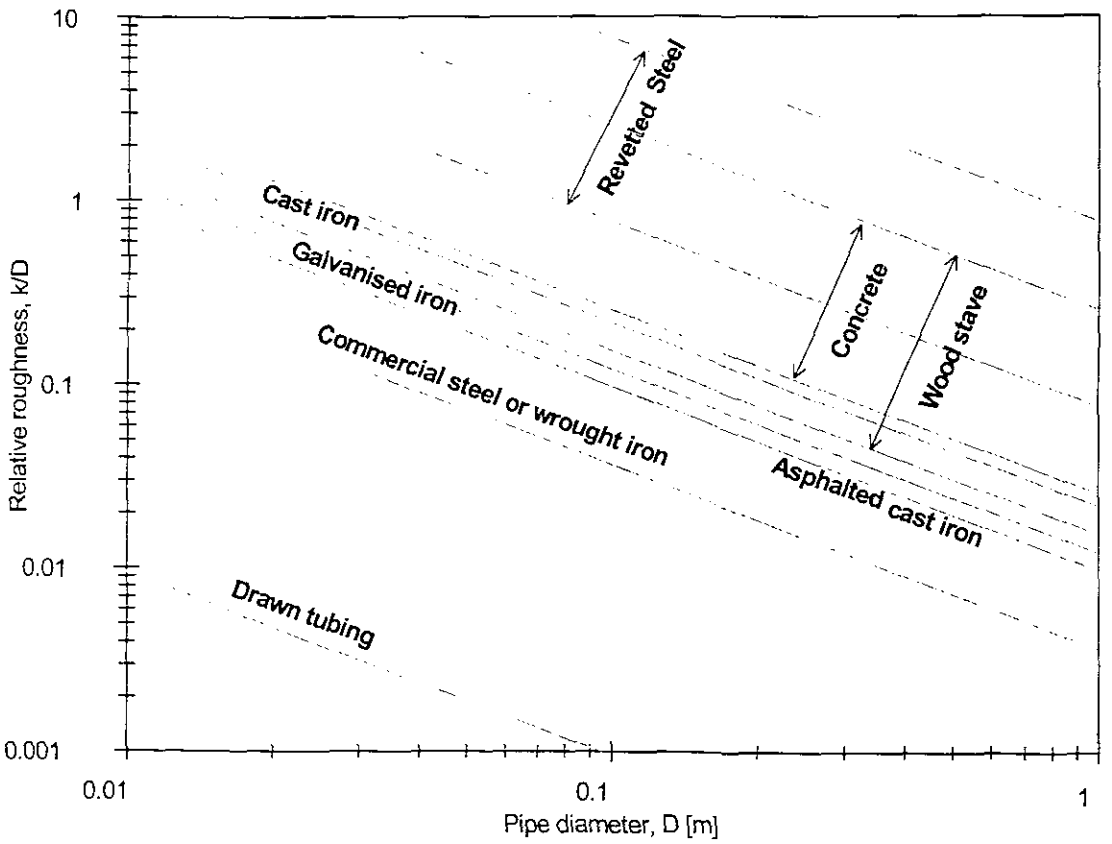

Figure 2.9 Relative Roughness of Pipes. (Moody, 1944)

2.8.4 Work Done by Torrance (1963)

Torrance derived a model for fully developed rough wall turbulent flow for non-Newtonian fluids in pipes using the yield pseudoplastic rheological model as the starting point. The mean velocity is given by;

$$\frac{V}{V_*} = \frac{2.5}{n}\ln\left(\frac{R}{k}\right) + 8.5 - \frac{3.75}{n}. \qquad (2.20)$$

The von Kármán constant is now assigned the value of 0.4n. The Torrance model for the fully developed rough wall turbulent flow of non-Newtonian fluids in pipes indicates that the behaviour is dependant on the viscous characteristics of the fluid. Torrance makes no comment on partially rough wall turbulent flow.

2.8.5 Work Done by Govier and Aziz (1972)

Govier and Aziz define the roughness Reynolds number as:

$$Re_k = \frac{k}{D} Re \sqrt{\frac{f}{2}}. \qquad (2.21)$$

They predicted that as long as the roughness was "buried" in the laminar sub-layer (Re_k = <5) it would be ineffective. In fact it is found (Schlichting, 1960) that roughness makes itself felt at $Re_k > 3$, and to a value of Re_k of about 70 the friction factor depends upon both the relative roughness, k/D, and the Reynolds number. Above $Re_k = 70$ the Nikuradse data, and other recent data, show that the friction factor is dependent upon the relative roughness alone. Thus, they present three regions of turbulent flow in a pipe;

a. Smooth wall turbulence
b. Partially rough wall turbulence
c. Fully rough wall turbulence

Figure 2.10 shows the boundaries between smooth wall and partially rough wall given by $Re_k = 3$, and the boundary between partially rough wall and fully rough wall turbulence given by $Re_k = 70$. The region of laminar flow and the transition from laminar to turbulent flow, the transition region, is also presented in the figure. This graph can be used for all pipe diameters and all smooth and rough pipes.

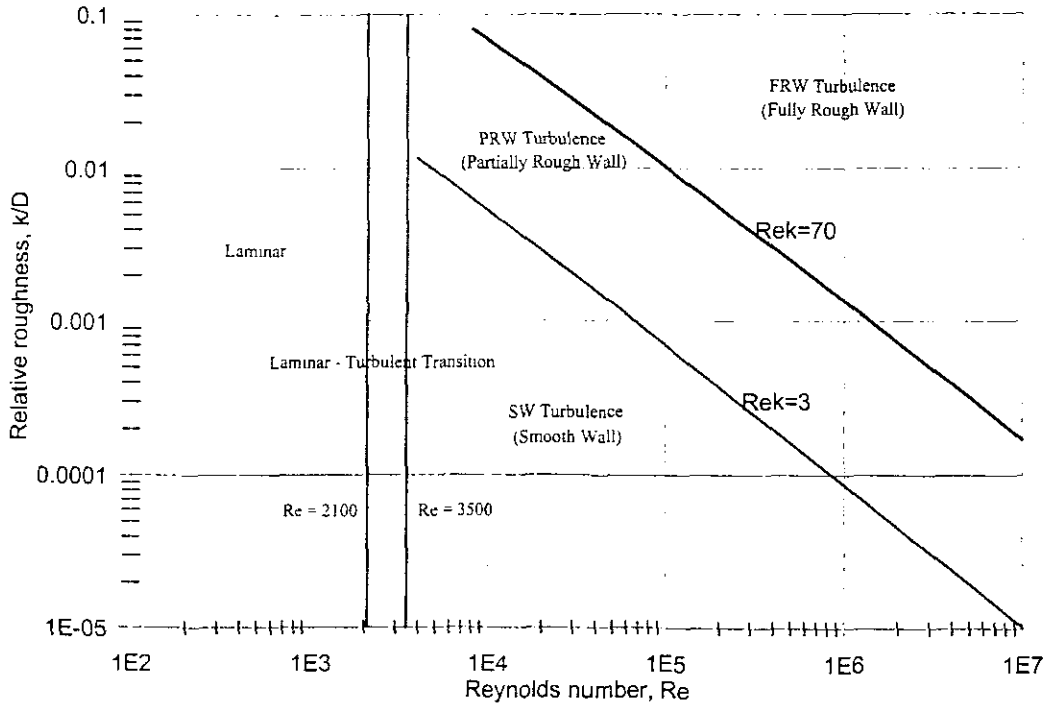

Figure 2.10 Regions of Laminar and Turbulent Flow (Govier and Aziz, 1972)

2.8.6 Work Done by Wilson & Thomas (1985)

Wilson & Thomas based their work on the enhanced microscale viscosity effects of non-Newtonian fluids. The model uses an area ratio A_r, based on postulated thickening of the viscous sub-layer. The area ratio is given by;

$$A_r = 2\left[\frac{1+\frac{\tau_y}{\tau_0}n}{1+n}\right]. \qquad (2.22)$$

The viscous sub-layer thickness is;

$$\delta_{nn} = A_r \delta_n . \tag{2.23}$$

Where: δ_n = Newtonian viscous sub-layer thickness

δ = Non-Newtonian viscous sub-layer thickness

The velocity distribution is given by;

$$u^+ = \frac{u}{V_*} = 2.5 \ln\left(\frac{\rho V_* y}{\mu}\right) + 5.5 + 11.6\left(A_{r-1}\right) - 2.5 \ln\left(A_r\right). \tag{2.24}$$

The mean velocity is calculated as;

$$\frac{V}{V_*} = \frac{V_N}{V_*} + 11.6\left(A_r - 1\right) - 2.5 \ln A_r - \Omega \tag{2.25}$$

V_N is the mean velocity for the equivalent Newtonian fluid based on a secant viscosity from the yield pseudoplastic rheogram.

Ω accounts for the blunting of the velocity profile caused by the yield stress and is given by;

$$\Omega = -2.5 \ln\left(1 - \frac{\tau_y}{\tau_0}\right) - 2.5 \frac{\tau_y}{\tau_0}\left(1 + 0.5 \frac{\tau_y}{\tau_0}\right). \tag{2.26}$$

Pipe roughness can be accommodated in the model by using the appropriate roughness when determining V_N. This is only approximate since the interaction between the pipe roughness and the laminar sub-layer will clearly be different when the thickened laminar sub-layer is present.

2.8.7 Work Done by Berman (1986)

Berman studied the effect of pipe roughness on drag reduction for commercially available rough pipes on polymer solutions and his findings is as follow;

The transition from smooth to rough wall turbulent flow occurs at $k^+ \sim 3$ and results in a minimum value of the friction factor. He defines a dimensionless roughness as;

$$k^+ = kV_* / \nu. \qquad (2.27)$$

Where: k = roughness height

ν = kinematic viscosity

V_* = friction velocity

As the Reynolds number is increased, the roughness height becomes much larger than the height of the viscous sub-layer and the Fanning friction factor becomes a constant in the completely rough regime. Berman predicts that the Fanning friction factor becomes a constant where $k^+ > 50$.

In non-uniform roughness such as commercial pipes and tubes, the friction factor vs Reynolds number behaviour can be matched with the uniform roughness data to give an apparent k. The Colebrook-White equation as already discussed represents all friction factor vs Reynolds number data for both smooth and rough pipes for Newtonian fluids.

Berman examined evidence that the maximum drag reduction corresponds to the transition from smooth to rough wall turbulent flow behaviour where k^+ is a constant for all the fluids tested.

2.8.8 Work Done by Slatter (1994)

To correlate the roughness function B, Slatter formulated a roughness Reynolds number in terms of the yield pseudoplastic model. By analogy with the Newtonian approach, the roughness Reynolds number for a yield pseudoplastic slurry can be formulated as follows:

$$Re_r = \frac{8\rho V_*^2}{\tau_y + K\left[\frac{8V_*}{D}\right]^n}. \qquad (2.28)$$

The mean velocity can be obtained by integrating over the cross section of the pipe yielding:

$$\frac{V}{V_*} = \frac{1}{\chi}\ln\left(\frac{R}{d_{85}}\right) + B - 3.75. \qquad (2.29)$$

where; χ = von Kármán's constant

d_{85} = 85% particle roughness

The roughness function B was correlated against the roughness Reynolds number in the same way as for Newtonian turbulent flow.

2.8.9.1 Smooth wall turbulent flow is summarised as follow:

If $Re_r \leq 3.32$ then $B = 2.5 \ln Re_r + 5.5$. This is analogous with smooth wall turbulent flow and;

$$\frac{V}{V_*} = 2.5\ln\left(\frac{R}{d_{85}}\right) + 2.5\ln Re_r + 1.75. \qquad (2.30)$$

2.8.9.2 Fully developed rough turbulent flow:

If $Re_r > 3.32$ then B = 8.5. This is analogous with fully developed or rough wall turbulent flow and will yield a constant value for the Fanning friction factor f;

$$\frac{V}{V_*} = 2.5\ln\left(\frac{R}{d_{85}}\right) + 4.75, \tag{2.31}$$

which reduces to;

$$\frac{1}{\sqrt{f}} = 4.07\log\frac{3.34D}{d_{85}}. \tag{2.32}$$

The average percentage error when calculating the roughness function, B, using this correlation is 9.2% with a standard deviation of 7.8%, and a log standard error of 0.0024% when compared to kaolin data (Slatter,1994).

This correlation produces an abrupt transition from the smooth to the rough flow condition.

2.9 Some Conflicting Arguments by Researchers in the Past

For Newtonian fluids in turbulent flow, a rough pipe contributes to a larger friction factor for a given Reynolds number than a smooth pipe does. The friction factor is a function of both Reynolds number and the relative roughness, k/D. Nikuradse's (1933) roughness criterion k_s seem to be problematic and some authors (Kamphuis, 1974) have a problem using this roughness criteria to correlate to relative roughness and to describe the flow in rough pipes. According to these authors (Kamphuis, 1974) this roughness must be a factor of not only the sand grain size but the particle angularity, shape, density etc.

Since Nikuradse's (1932) experiments on flow in sand roughened pipes, several investigators (Colebrook, 1938; Churchill, 1973; Chen, 1979; Zigrang, 1982; Serghides, 1984) have suggested correlations for fully turbulent flow of Newtonian fluids in rough pipes. Serghdes (1984) recently compared the accuracy of several equations. Some of these correlations are not explicit and thus are relatively difficult to use. Chen's (1979) equation

is explicit and correlates friction factor, pipe-roughness parameters, pipe diameter, and Reynolds number for transition and turbulent flow regions. The phenomenon of turbulent flow of non-Newtonian fluids in rough pipes has not been explored fully and flow data in rough pipes are extremely rare.

A relationship analogous given to that by Dodge and Metzner has been provided by Dodge (1957) for the case of turbulent flow of non-Newtonian fluids. Virk (1971) summarized the work on the drag-reduction phenomenon in rough pipes since Dodge's findings. In his experimental investigation, Virk examined the physics of drag reduction in rough pipes, emphasizing the flow regimes associated with incipient and asymptotic maximum drag reduction. Virk used polymer solutions such as polyetholeneoxide (PEO) and polyacrylamide (PAM). Durst and Rastogi (1977) developed a model that accounts for low Reynolds number effects in the immediate vicinity of the wall and the influence of the polymer additives in smooth and rough pipes in accordance with experimental results available in the literature. Bewersdorff & Berman (1987) recently reported the effects of pipe roughness on drag reduction in commercial pipes.

Few studies have dealt with the effect of pipe roughness on friction loss of non-Newtonian fluids, particularly with more "concentrated" solutions. Using hydraulic fracturing fluids, Shah (1984) showed that the friction factor of non-Newtonian fracturing fluids in turbulent flow in rough pipes is a function of both Re (generalized Reynolds number) and k/d, while Dodge's proposed equation gives friction factors as a function of k/d only. Because rough pipe data was limited, no satisfactory correlation was developed.

2.10 Conclusion

The literature relevant to the flow of Newtonian and non-Newtonian slurries in rough pipes was reviewed, and the relevant theoretical models presented.

2.10.1 Laminar Flow

The yield pseudoplastic model has mainly been reviewed for the flow of non-Newtonian slurries. This model is not restrictive and allows for both a yield stress and rheogram curvature. Although the model is sensitive to small changes in the rheological parameters,

laminar flow in different diameters can be used to verify the results. The viscometry of non-Newtonian slurries is best performed using a tube viscometer (Balanced Beam Tube Viscometer). Rheological characterization can be accurately performed using the Lazarus & Slatter (1988) method. The accuracy of the rheology of a slurry is more important for turbulent flow predictions than in laminar flow.

2.10.2 Turbulent Flow

Smooth wall Newtonian turbulent flow can be modelled using the classical universal logarithmic velocity distribution. Rough wall Newtonian turbulent flow can be modelled using a logarithmic velocity distribution with a roughness function and a roughness Reynolds number to correlate the roughness function. Partially rough wall Newtonian turbulent flow can be modelled using the Colebrook-White relation which is a combination of the smooth and rough turbulent flow laws.

To model non-Newtonian turbulent flow parameters such as apparent viscosity, the yield stress, dynamic and elastic properties, and the flow behaviour index are needed to characterise the fluid.

There are a number of models that can be used to describe non-Newtonian mixtures. Models that describe the laminar flow of time independent fluids include the Casson (1959) model and the Herschel-Bulkley (1926) model which describes a wide variety of different fluids. The best known model to characterise the laminar flow are the generalised yield pseudoplastic model and is the most widely used by industry.

There are a lot of models available that predicts the turbulent flow of non-Newtonian fluids in pipes. Some of the best known models are the Dodge and Metzner (1959), Torrance (1963), Wilson (1985), and the Slatter model (1994). All these models are dependant on the rheological characterisation of the fluid which can be obtained using the Casson (1959) or Herschel-Bulkley (1926) model in the laminar flow region.

Non-Newtonian fluids can also be time dependant and viscoelastic (Govier and Aziz, 1972), in which case the models become more complex. Time dependant slurries are those slurries in which the shear stress is dependant upon the both the shear rate and the duration

of the applied shear. These types of slurries were not tested in the thesis and will not be discussed further.

2.10.3 Roughness Effect

The surface roughness of the pipe wall affects the relationship between wall shear stress and velocity, or friction factor and Reynolds number. As portrayed in the Moody diagram, the effect of pipe roughness is to increase the friction factor over that for a smooth pipe.

Roughness may be attributable to the nature of the wall substance and the method of its manufacture as in the case of new steel, cast iron, and cement-asbestos pipe. Further, it may be influenced by erosion and corrosion. Such roughness is referred to as natural roughness and has a random size distribution. In addition, roughness may be artificially created, usually for experimental purposes, as by the attachment of sand grains or other objects to the pipe wall surface.

A full description of roughness would require a complete definition of its geometry, including the height, length, width, and shape of any protrusions or indentations and their distribution. This is seldom possible, and it has become customary to think of roughness either as natural or artificial and to measure artificial roughness in terms of the mean height of the sand grain, or other protuberance, and finally to relate natural roughness empirically to the artificial roughness.

Additionally it is recognized from dimensional analysis considerations that the effect of roughness is not due to its absolute dimensions but rather to its dimensions relative to that of the pipe. Thus a relative roughness is defined as k/D, where k is the mean protruding height of relatively uniformly sized, uniformly distributed, tightly packed sand grains. In the case of naturally rough walls, k is the height of the uniform sand grains which would give the roughness effect observed.

The effect of wall roughness in turbulent flow has been found to depend not only on the relative roughness, k/D, but also on the Reynolds number. This is attributed to the viscous sub-layer which exists in contact with the wall. If the sub-layer is sufficiently thick to cover the wall roughness (as at low Reynolds numbers), the roughness will not be effective,

however, if the sub-layer is thin compared with the roughness of the wall (as at high Reynolds numbers) the roughness will be effective.

2.11 Research Aspects Identified

It is clear from the conclusions that there is a definite need for further research in this field. Aspects requiring further research are identified below.

2.11.1 Experimental Work

Very little experimental work on pipe roughness has been performed since the work of Nikuradse (1926-1933) Only a few sources could be found which deal with non-Newtonian fluids. Clearly there is a need to quantify experimentally the effect of pipe roughness. The first main objective of this thesis is to design and execute experiments to accumulate data on the behaviour of non-Newtonian fluids in rough pipes.

2.11.2 Analytical Work

Apart from the work of Slatter (1994) there has been no theoretical analysis which has focussed on roughness effects in non-Newtonian turbulent flow. The model of Torrance and Wilson and Thomas will however allow for roughness effects to be analysed.

There has been no work published which focusses on the evaluation of these analytical models for rough wall non-Newtonian turbulent flow.

The second main objective of this thesis is to evaluate these analytical models against the experimental data which has been accumulated.

Chapter 3

Apparatus and Experimental Work

3.1 Introduction

The apparatus and methods used to gather data for determining the effect of pipe roughness on non-Newtonian turbulent flow are presented in this chapter.

The BBTV was fitted with pipes of varying roughness. The roughness of the pipes was artificially altered using a method similar to that of Nikuradse (1933). This enabled the accumulation of flow data in laminar and turbulent flow in pipes that are both hydraulically smooth and rough. Both Newtonian and non-Newtonian fluids were tested.

The apparatus used for the tests was developed specifically with the following objectives in mind:

- to measure the rheology accurately
- to test over as wide a range of flow rates and diameters as possible
- to test over as wide a range of slurries and slurry relative densities as possible
- to do test work using artificially roughened pipes
- to compare the test results to the classical work of Nikuradse in order to gain confidence in the instrument and procedures
- to accumulate a data base to evaluate the effect of pipe roughness on non-Newtonian turbulent flow
- to prove to industry an instrument that is a useful tool for test work when designing a slurry pipeline system.

Fluids tested for this thesis range from Newtonian (water, glycerol) to non-Newtonian slurries (CMC, Kaolin and tailings). Full details of all the fluids tested are presented in Table 4.4 and Appendix A. Pipe diameters range from 5 mm to 46 mm nominal bore with mean velocities ranging from 0.01 m/s to 24 m/s. An important aspect of the experiments is that exactly the same slurry was used for each test set. A test set is a serious of tests using different pipe diameters and surface roughness for the same slurry at the same relative

density.

3.2 Apparatus/Description of the BBTV

The lack of a database for non-Newtonian fluids has initiated an enormous amount of research (Slatter, 1994) and there is consensus that the viscous characteristics of a fluid must play an important role in the flow behaviour.

The BBTV was originally developed by Hydrotransport Research at the University of Cape Town, South Africa in the 1980's (Lazarus & Sive, 1984, Lazarus & Slatter, 1986 and Neill, 1988). Figure 3.1 shows a schematic diagram and Figure 3.2 shows a photograph of the new BBTV, which has been built and refined at the Cape Technikon.

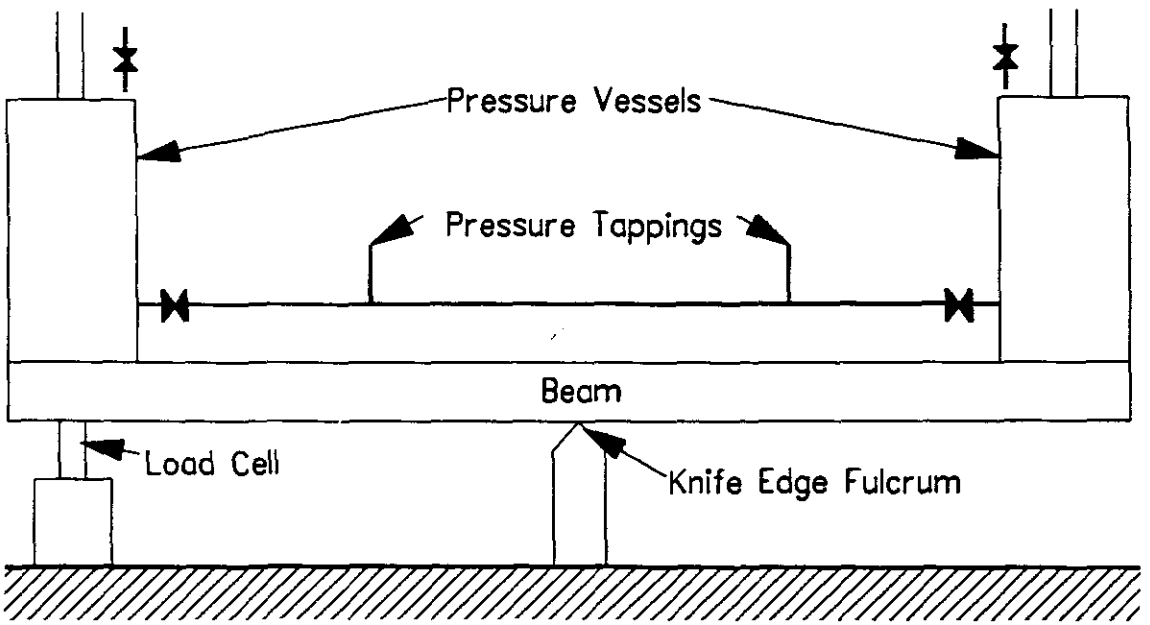

Figure 3.1: Schematic Diagram of the BBTV.

The viscometer consisted of two 224 litre pressure vessels rated at 24 bar and mounted on a steel I-beam 10 m long. The pressure vessels are manufactured from 500 mm diameter, 24 bar glass reinforced (GRP) pipes, with specially manufactured flanges at both ends. The total height of each vessel is 1.14 m which includes a volume safety factor of 25 percent. The wall thickness of the tank is 5 mm.

On the top cover plate provision is made for a fill port, a vent with a silencer, a pressure gauge and a 50 mm diameter galvanised steel pipe for compressed air supply. The bottom cover plate is provided with a drain valve for sampling and cleaning. Two outlets, 25mm and 50 mm nominal bore galvanised steel pipes are provided to the test tubes. The cover plates are bolted to the flanges using thirty-six bolts of 12 mm diameter. The bolts run the length of the vessel and narrow face rubber gaskets are used for the seal and are 2 mm thick.

The BBTV is balanced on a knife edge as can be seen on Figure 3.1. The left-hand side of the BBTV is fixed to a load cell and the right-hand side is cantilevered. The load cell prevents the BBTV from moving and measures the mass transfer of the test fluid between the two pressure vessels. The load cell output is logged at regular time intervals and the average slurry velocity is obtained from the mass transfer rate. The pressure drop across a known length of the tube is measured using a differential pressure transducer. A test comprises a series of "runs" where a run is defined as the collection of a set of mass, time and pressure readings. This data is processed and a run will yield a single co-ordinate of $\{V;\Delta p\}$. Test section entry lengths can be changed to detect undeveloped flow or time dependency. The BBTV is supported at each side with side bracing to prevent the instrument from falling over. The side bracing is fixed to the BBTV with hinges in such a way that it does not interfere with the load cell reading.

The two pressure vessels are connected with four clear reinforced PVC pipes of nominal diameters 5 mm, 13 mm, 28 mm, 46 mm respectively. Baker *et al* (1979) recommends that at least two diameter test pipes should be used to ensure that time dependancy and wall shear stress anomalies can be detected. The tubes are transparent to allow the operator to observe the change in flow patterns from laminar to turbulent flow or settling in the pipe.

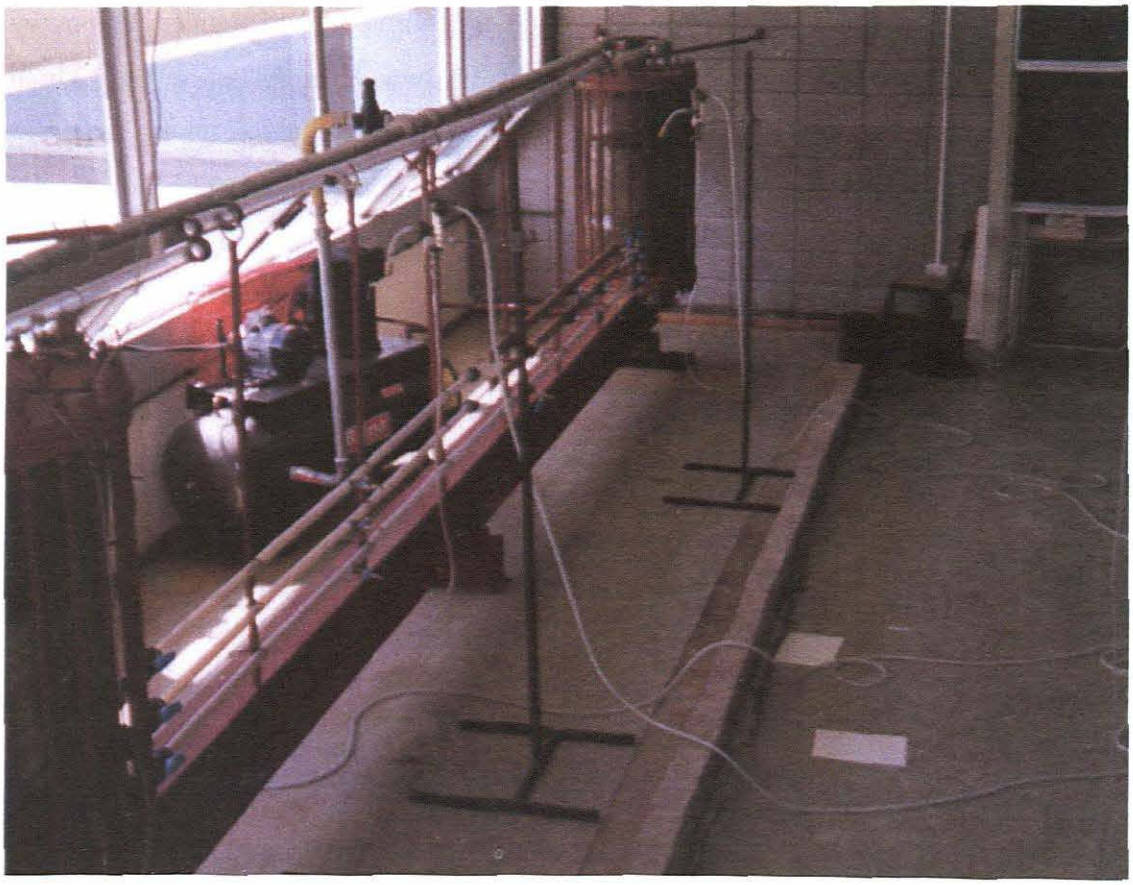

Figure 3.2: Photograph of the BBTV.

Rough pipes were made to fit between the unions at either side of the BBTV. Only rough pipes of nominal diameters of 28 mm and 46 mm were made. The 5 mm and 13 mm pipes were too small to be able to make rough pipes. A table of all the pipe details is presented in Chapter 4 and Appendix A. The precise diameters of the various pipes were determined by filling the pipes up with water and weighing them. This precision is required since a rheogram point inherently contains the fourth power of the diameter. All the pipes on the BBTV are isolated by valves on either end of the pipe. To select a pipe for test work requires only the opening of the right "set" of valves. Air pressure is provided by the air compressor seen in Figure 3.2. The air compressor is connected to the pressure vessels by a 50mm galvanised steel pipe. The valves on the 50mm steel pipe are connected in such a way that the one half of the 50mm steel pipe could be used to pressurise the one vessel and the other end could be used to act as a vent to atmosphere for the receiving vessel.

The flow rate of the fluid in the selected tube is measured directly from first principles by weighing the fluid transported through the tube over a given time interval. This has two advantages. Firstly, the problems and errors inherent in the calibration and use of a secondary transducer such as a magnetic flux flow meter is eliminated (Heywood *et al,* 1993) and secondly, theoretically there is no quantitative limitation on the flow that can be measured.

The BBTV has a set of pressure tappings on each pipe for determining the head loss or wall friction loss during a test run. The pressure tapping is situated at least 50 diameters away from any up stream disturbances and 20 diameters from any down stream disturbances (Govier & Aziz, 1972 and Hanks, 1981). This avoids the effects of entrance losses, exit losses and hydraulic grade line curvature due to developing flow. The hydraulic effective length is thus equal to the physical distance between the tappings (L). The pressure tappings are connected to solids collection pods filled with water. These pods collect any air or solids that end up in the pressure tappings during a test run. The solids collecting pods are connected on the one side to a pressure tapping and on the other side to a differential pressure transducer cell (DPT cell). An in line flushing/bleeding facility is connected to the pods and DPT cells to flush the line from any air or solids collected by the solids collecting pods. The DPT cell is also connected to a water over mercury manometer board for calibration purposes.

The primary output from the viscometer consists of successive voltage readings representing load cell input (power supply voltage), load cell output and DPT output. These are converted into volumetric flow rate and differential pressure for analysis. The operator has the facility to manually reject the non-steady state flow readings taken during acceleration. These are distinguishable as nonlinear differential pressures.

The viscometer is capable of rheological characterising fluids such as water and slurries (Slatter 1986, Lazarus and Sive 1985). The viscometer is also a miniature pipeline and is capable of collecting turbulent flow data and indicating the laminar-turbulent flow transition (Slatter 1986).

3.3 Instrumentation

3.3.1 Flow Measurement

A load cell is used to determine the slurry mass distribution between the two vessels. A typical flow measurement consists of 20 (minimum) to 60 (maximum) readings of mass versus time.

A least square linear regression on this data yields the mass flow rate (dm/dt). Q_m and V_m can be calculated from (dm/dt) as follows;

$$Q_m = \frac{\frac{dm}{dt}}{\rho_m} \tag{3.1}$$

and

$$V_m = \frac{Q_m}{A} = \frac{\frac{dm}{dt}}{\rho_m A}. \tag{3.2}$$

The load cell can operate in both tension and compression and has a resolution of 1N and a range of ± 5500N (combined error of 0.03%).

Four strain gauges are bonded in the positions of maximum strain. The strain gauges are connected in a Wheatstone Bridge.

A Voltage regulator power supply is used for the input voltages and is set at a nominal 12V. The output voltage of the bridge varies linearly with applied force and is proportional to the input voltage. The output voltage is divided by the input voltage, giving a non-dimensional load cell reading (V/V) which is independent of input voltage and temperature fluctuations.

3.3.2 Differential Pressure Measurement

A Gould PDH 3000 series differential pressure transducer (DPT) is used. The DPT has an accuracy of 0.25% and a maximum range of 30 Psi (210 kPa) and is connected to a 24V power supply. The output is 4-20 mA and is linear with the pressure differential across the two halves of the cell. The current output is converted to a 40 - 200 mV output over a 10 Ω series resistor.

The range and the span on the DPT are manually adjustable.

3.3.3 Computer Hardware

The computer hardware used for high speed data acquisitioning and processing consists of;

1. An HP-87C computer with;
   (i) an HP82901M double flexible disc drive
   (ii) a HP3421A data acquisition unit (analogue to a digital converter).

The HP-87C is a 128k RAM basic computer with I/O and Advanced Programming ROM's and an interface loop (IL) peripheral.

The data acquisition unit (DAU) is equipped with a 10-channel multiplexer and is used as a software controlled digital voltmeter to read various analogue input channels.

The computer is connected to the data acquisition unit by an interface loop and to the other three peripheral devices by an interface bus.

3.3.4 Pressure Tappings

The BBTV measures mass transfer rates from a load cell and differential pressure from a DPT. The accuracy of the DPT depends mainly on two factors;

1. The DPT calibration
2. The geometry of the pressure tappings

The calibration of the DPT is straight forward because the operator has direct control of the calibration and is able to accept or reject the calibration even before testing has started. The calibration procedure is discussed in Section 3.11.

Figure 3.3 shows a typical pressure tapping. The only way to find out that the pressure tappings were made properly is to do a clear water test. Provided that the DPT cell and load cell calibrations are good, any gross errors in the clear water test analysis will be due to poor pressure tappings.

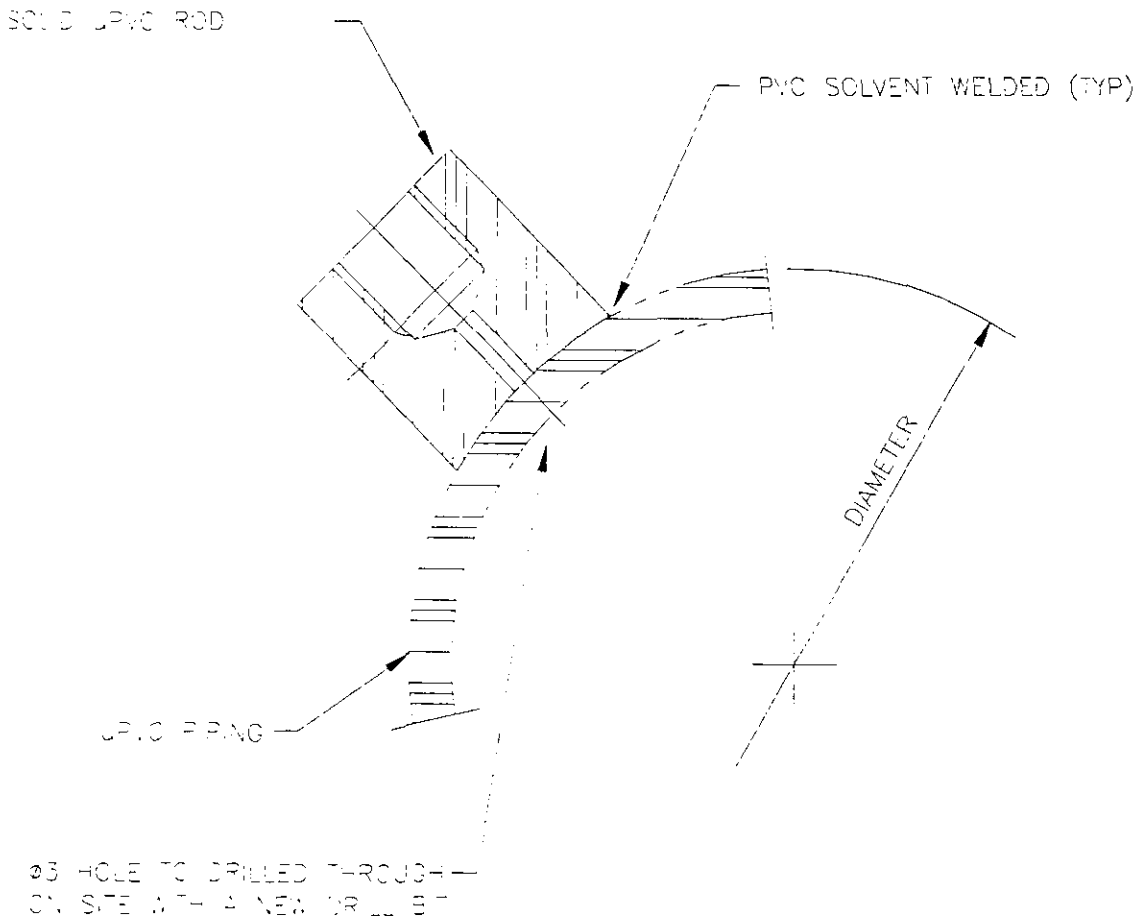

Figure 3.3: Typical Pressure Tapping.

The author found that a 40mm diameter solid PVC rod is of adequate size for making most pressure tappings. A pressure tapping in the pipe wall is normally made at 45^0 from the horizontal. The length to diameter ratios of the hole drilled in the pressure tapping is very important. The tappings must have length to diameter ratios greater than four to ensure accurate readings (Hanks, 1981). The diameter of the tappings should not be too large, and

generally 3 mm to 5 mm diameter holes are used. Great care must be taken to remove any burrs from the inside edge of each tapping. The hole must be drilled at low speed with a new steel drill bit to ensure that the hole is evenly cut on the inside. Drilling at high speed causes burrs on the inside of the pressure tapping. It is important to glue the tapping onto the pipe and only when the glue is dry to drill the hole in the pressure tapping. Tappings cut *in-situ* using grinders or cutting torches are not acceptable and can lead to large pressure measurement errors.

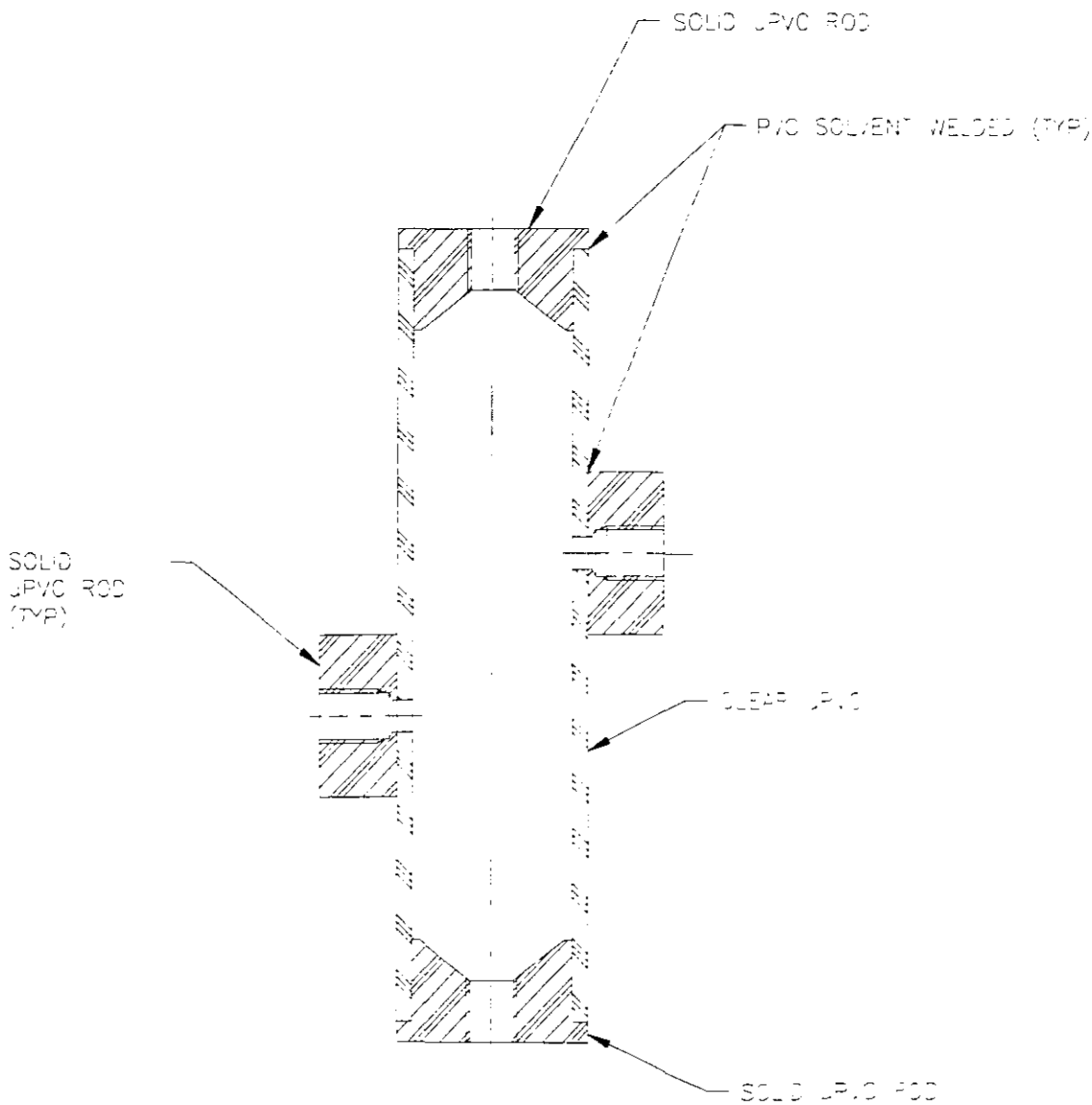

Figure 3.4: Typical Solid Collection Pod.

Each tapping is fed through a valve to an isolating pod which collects any solids that may enter the pressure tapping. Each pod has a valve at the top and the bottom. The top valve

is for flushing away the air and the bottom valve is for flushing away the solids collected in the pods. Clear water lines connect the pods to the manometer and differential pressure transducer. Figure 3.4 shows a typical design of a solid collection pod.

3.3.4.1 End effects

One of the greatest advantages of the BBTV is that end effects are quickly detected because of the method used for testing. The BBTV is constructed in such a way that every second data point is taken from the fluid flowing in the opposite direction in the pipe. For instance the first data point would be taken pumping from the left-hand vessel to the right-hand vessel. The second data point would then be taken the other way around. Because of this way of testing an end effect would be picked up within the first few test runs. Figure 3.5 shows how a typical end effect would look taken from real data from the BBTV. This test data is taken from clear water tests done on the BBTV in the 5mm pipeline. It is important to note that an end effect in a pipeline is not always given by scattered data but could be found from actual test data as shown in Figure 3.5 which shows two definite patterns.

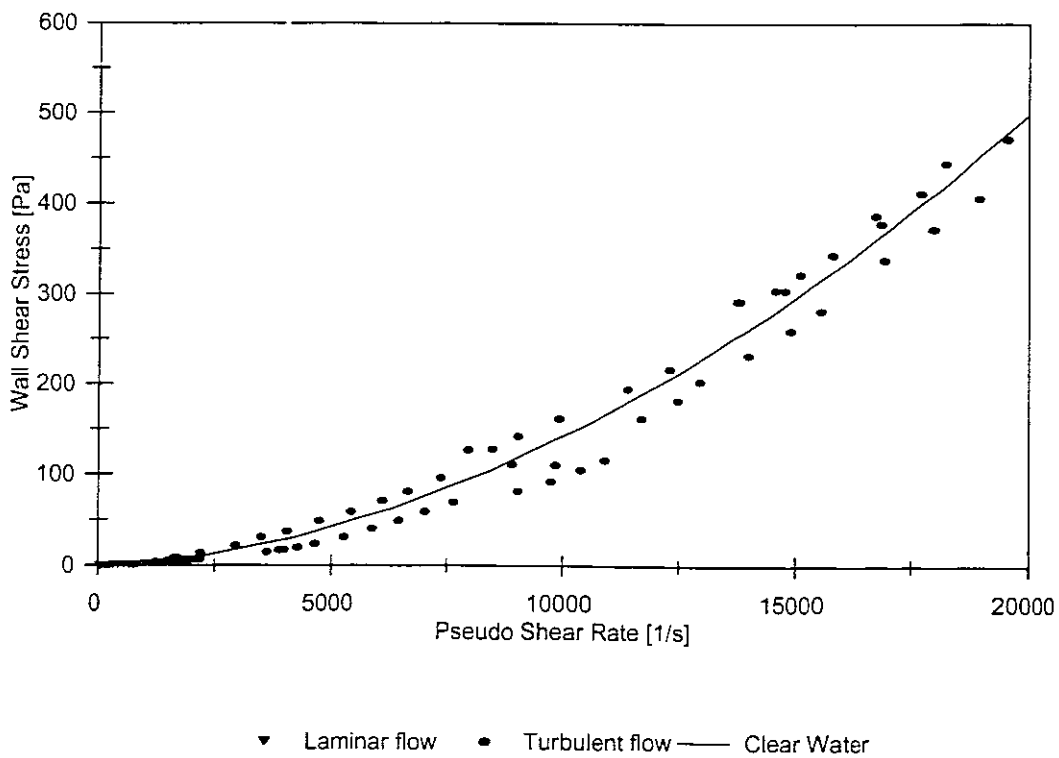

Figure 3.5: Typical End Effects Caused by Bad Tappings.

3.4 Analysis Techniques

Govier & Aziz, (1972) recommends that tube viscometer data be transformed using the Rabinowitch-Mooney relationship. This method has been found to have practical problems (Lazarus & Slatter, 1988). The technique used to fit the laminar pipe flow equation directly to the tube data (Lazarus & Slatter, 1986 and Neill, 1988) using least squares regression analysis will be used in this study.

3.5 Rough Pipes

One of the most difficult problems of constructing the test apparatus was to produce the rough pipes. The criteria were well defined, and the length of the pipes (5m) as well as the internal diameters of the pipes (46 mm and 28 mm) made it difficult. Various samples were made and compared with each other in order to find the best artificially made rough pipes able to maintain a uniform roughness throughout the pipe wall. The author found that a mixture of PVC glue and acetone was the best solution to glue the sand to the inside of the pipes.

Sand was sieved out in two different grades. Two sieves of 300μm and 600μm were used to sieve out the sand grains of the roughest pipes. The sand grains captured between these two sieves were used to make the rough pipes. The same procedure was used for the 250μm and 150μm sieves. In both cases two rough pipes were made of nominal diameters of 50 and 28mm.

A slurry of PVC glue, acetone and sand were made up and poured through the pipe. The pipe was then systematically rolled to ensure that the slurry evenly covered the whole surface of the pipe. The pipe was then stood vertically and all excess slurry was poured off. Air from the compressor was then used to blow through the pipe to ensure that the pipe dried quickly. During the drying process the pipe was rolled horizontally every 10 minutes for the first hour to ensure that the slurry mixture would not accumulate at the bottom of the pipe. These procedures were repeated for all the rough pipes with the different grading of sand.

After the pipes had sufficiently dried, the tappings were put on 50 diameters from any

disturbance in the pipeline. The diameter of the pipes was determined by using water and weighing the pipes.

Clear water tests were done on the various pipes to determine the hydraulic roughness of the test pipes. All the rough pipe details are listed in Table 4.2 of Chapter 4 and the clear water tests presented in Appendix A.

3.6 The BBTV Manometer and DPT Circuit

The fluid circuit diagram of the BBTV DPT and manometer board is shown in Appendix D. For a test run the pods are connected to the pressure tappings. The circuit is used to flush air and solids from all lines and to set up a differential mercury/water head for calibration of the DPT. The high pressure water supply is passed through an air trap to clear the water from any air while bleeding the lines.

The following operations are performed from the manometer board;

- Air and solids are flushed from all tubes and pods and through the DPT.
- A variable differential of water over mercury head is set up in, and read off, the manometer tubes for calibration purposes.
- The DPT is connected to the pressure tapping for data logging.
- The water over mercury manometer tube head is visible during testing to provide a visual confirmation of head loss measurements in the 5 mm and 13 mm diameter tubes. Time constraints for a run in the 28 mm and 46 mm pipes make it very difficult to apply this method for these pipes.

3.7 Operating Procedure

Instrumentation used and the operational procedure for performing a test run are discussed in this section.

3.7.1 Data Acquisition and Processing Techniques

Data from the BBTV are collected electronically via a Data Acquisition System. The data are then processed to give the final measured variables of average velocity and differential pressure over a known length of pipe.

3.7.2 Data Acquisition System

The data acquisition system consists of a computer, data acquisition unit (DAU) and transducers as shown in Appendix D. The DAU measures the flow rate via the load cell and the differential pressure via the differential pressure transducer. Thus, the primary output from the viscometer consists of successive voltage readings representing load cell output and DPT output. These outputs are logged at regular time intervals. These time intervals could be changed to suit the needs of the operator.

3.7.3 Processing Techniques

The load cell is used to determine the slurry mass distribution between the two vessels. A typical flow measurement consists of a number of readings of mass versus time. The slope of a least square linear regression on these data yields the mass flow rate. The volumetric flow rate and velocity can be calculated from the mass flow rate.

The differential pressure transducer output is logged each time the load cell output is logged. The average of the pressure differences computed from these readings is taken as the pressure difference across a known pipe length.

3.8 Measured Variables and Calibration

The measurement of force (mass) and differential pressure is done using transducers. The load cell and DPT give a 4 to 20 mA output. The DAU converts this signal to a voltage reading. The load cell are calibrated using different known weights. For each weight applied the DAU will display a different voltage reading. The response from the transducer is a linear relationship. The load cell a DPT is each calibrated using the voltage reading output. A calibration procedure is required to establish the functional relationship between

transducer signal and measured quantity.

3.9 Linear Regression

The response from the transducers used for the experimental work was linear. The linear relationship arises from the difference in voltage output from the DAU and the difference in pressure or force (load) applied to the transducers.

Calibration equations derived from least square's linear regression are used to process transducer readings (Spiegel, 1972). The correlation coefficient, r, provides an objective measure of how well the line represents the data (*op cit*). A value of $r = 1$ implies a perfect fit. Calibrations done on the BBTV were accepted for r values in the range $0.9999 \leq r \leq 1$.

In general the fit is not perfect and at each point there remains a small but finite difference or residual error. The highest residual error from a calibration provides a measure of the maximum absolute error involved in the use of the transducer under test conditions.

The least square's regression line of a set of N physically observed measurements, Y on the corresponding set of N transducer readings X is (Spiegel, 1972);

$$Y = mX + c \tag{3.3}$$

where

$$m = \frac{N\Sigma XY - (\Sigma X)(\Sigma Y)}{N\Sigma(X^2) - (\Sigma X)^2} \tag{3.4}$$

and

$$c = \frac{\Sigma Y\Sigma(X^2) - \Sigma X\Sigma(XY)}{N\Sigma(X^2) - (\Sigma Y)^2} \tag{3.5}$$

The regression coefficient, r, is calculated from;

$$r = \frac{N\Sigma XY - (\Sigma X)(\Sigma Y)}{\sqrt{[N\Sigma(X^2) - (\Sigma X)^2][N\Sigma(Y^2) - (\Sigma Y)^2]}} \tag{3.6}$$

The residual error E_{res} is defined by;

$$E_{res} = \left|Y_{obs} - (mX + c)\right| \tag{3.7}$$

3.10 Load Cell

The load cell on the BBTV is calibrated by applying an external force on the instrument using standard weights (Slatter, 1986). The load cell is used to calculate the mean mixture flow rate (Q_m). Calculations are derived from first principals. During a test run a graph is plotted of the difference in mass versus time.

The equations to determine the mean velocity V_m is as follows;

$$Q_m = \frac{dM / dt}{\rho_m} \tag{3.8}$$

where;

$$V_m = \frac{Q_m}{A} \tag{3.9}$$

This is the most accurate way of determining the mean mixture flow rate (Q_m) and are derived from first principles. Figures 3.7 displays typical calibration results for the load cell.

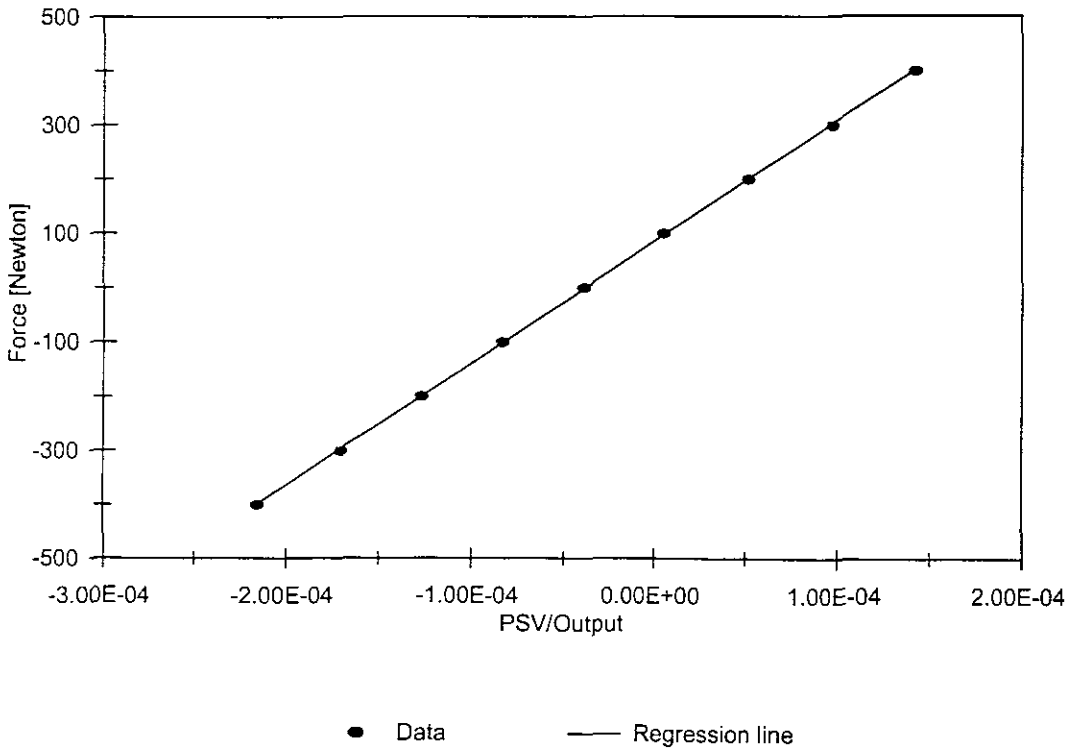

		Regression Output:
Constant		84.0785
Std Err of Y Est		2.7434
R Squared		***0.9999***
No. of Observations		9.0000
Degrees of Freedom		7.0000
X Coefficient(s)	2241317.9796	
Std Err of Coef.	7938.5899	

Figure 3.6: Load Cell Calibration Data and Linear Regression Analysis.

The following steps are followed to calibrate the load cell;

1. Check the load cell output from the DAU. The voltage reading should be constant and should only change when an external load is applied on either side of the BBTV. If the voltage reading is zero, a weight on the left-hand side of the BBTV should display a positive reading and a load on the right-hand side a negative reading.

2. Start the programme for load cell calibrations. It is important to thoroughly inspect the instrument to check that there is no other equipment that could interfere with the calibration. It is also preferred that the instrument is empty when a calibration on the load cell is done.

3. Always start with no load placed on the BBTV and take a reading. This would be the first data point.

4. Take the first standard weight and place it on the left-hand vessel where the centroid is marked out. Put the value of the weight into the programme and take a reading. This would be the second data point. The voltage reading should display a positive reading.

5. Repeat step four on the right-hand vessel after removing the first weight from the left-hand vessel and vice versa for each data point.

6. A standard number of nine readings are required to do a proper calibration. After the calibration procedure is finished, remove all the weights from the instrument.

The programme will take ten readings for each applied force, and do a least square linear regression which yields the calibration equation:

$$(\text{Applied load}) = \text{mX(Transducer output)} + \text{c}\,, \qquad (3.10)$$

where;
m = gradient of the calibration line
c = ordinate intercept of the calibration line.

The load cell calibration procedure can be performed again at any time during a test series.

Tips on the load cell calibration;

1. At least one day before the calibration takes place the load cell must be taken off the BBTV to release it from internal strain.

2. When the load cell is put back on the BBTV check the voltage reading from the DAU. Turn the screw that attach the load cell to the BBTV up or down until the Voltage reading from the DAU displays ± zero. In this way the BBTV is balanced against the load cell to display a 0-Voltage reading at 0 mass differential between the two pressure vessels.

3. When calibration procedures are in progress, close all windows in the laboratory as any draught may influence the output readings of the load cell.

4. After a load has been placed on the BBTV allow sufficient time for the load cell to absorb the weight before a data point is taken.

5. Putting the weight precisely on the centroid of the vessel is of critical importance for obvious reasons.

6. After the load cell has been calibrated, no tampering of the load cell is allowed as it may influence the readings and the calibration of the load cell. (Eg. adjusting the screws on the load cell after the calibration).

7. After the load cell has been calibrated, the power supply to the load cell must stay on at all times. Once the power supply has been switched off the load cell needs to be calibrated again.

8. The range of weights used to calibrate the load cell must cover the hole range of the minimum to the maximum weight initiated on the load cell at any time. Eg. The maximum density of the slurry tested will probably be 2000 kg/m^3. The volume of the vessel = 224 litres. The maximum weight placed on the load cell = 448kg. The range of weights used for the calibration must range from zero to 450kg (also make sure that the maximum weight is within the range of the load cell).

3.11 Differential Pressure Transducers (DPT)

The differential pressure transducer is used to measure the head loss in a given length of

pipe using the pressure tappings. It is important to calibrate over the full range of the DPT. The span of the DPT must also accommodate the highest pressures achieved in the 5 mm pipe and the lowest pressures achieved in the 46 mm pipe for the hole range of velocities. This is not always possible depending on the density of the slurry tested. Sometimes the range needs to be adjusted during a test series which results in recalibration of the DPT.

It would be preferable to have two DPT's, one for operating at high range and one for operating at low range. When operated at high range the low range DPT could be isolated on the manometer board and when operating at low range the high range DPT could be isolated on the manometer board. Figure 3.8 shows typical calibrations results and linear regression analysis from the DPT.

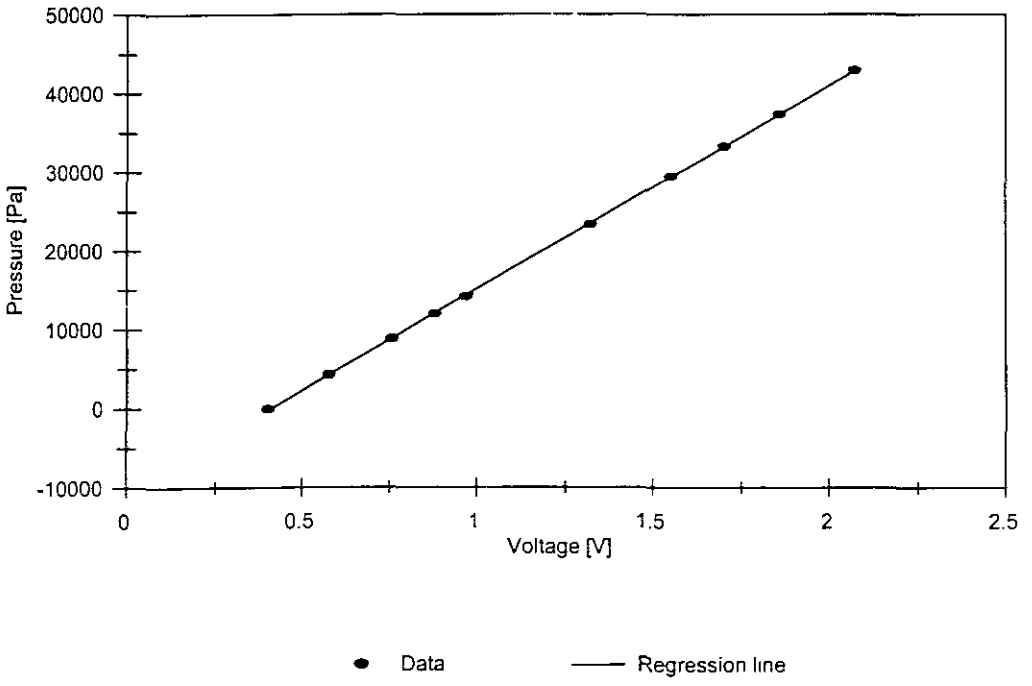

Regression Output:

Constant	-10550.9577
Std Err of Y Est	120.6705
R Squared	***0.99994***
No. of Observations	10
Degrees of Freedom	8
X Coefficient(s)	25761.3562
Std Err of Coef.	70.0623

Figure 3.8: DPT Calibration Data and Regression Analysis.

The following procedure is used to calibrate the differential pressure transducer (DPT) on the BBTV;

1. Air and solids are flushed from all the lines.

2. Isolate the DPT and close the valves on the tappings. Put the manometer board under pressure by opening the high pressure water supply. Check all the pipes for any leakages and repair if necessary before any calibration takes place.

3. Release the pressure in the line and open both sides of the DPT to vent to atmosphere. Check if the DP cell output is 4 mA (zero pressure). If the DP cell output is not 4 mA the zero span must be changed until the output of the DPT is reading 4 mA.

4. Close the high pressure discharge side of the DPT. Set up a differential head in the glass water/mercury manometer board equal to the maximum pressure differential needed for the tests. Check the DPT output. If the reading is not 20 mA the range of the span must be changed until the output of the DPT is 20 mA. Make sure that the low pressure side of the DPT is open the atmospheric pressure and only the high pressure side of the DPT is open to the manometer board.

5. Calibrations can start by entering the appropriate programme for calibrating the DPT. Start calibrating by applying the maximum pressure differential first and working to zero differential pressure for the last reading. A minimum of 10 readings is needed for a proper calibration.

6. At each pressure differential sufficient time must be allowed for the DPT to give a constant output.

7. The head differential is physically measured with a tape measure and the DPT output is logged at the same time.

8. The differential head is changed and the process repeated. Always try to end the last reading with zero differential pressure.

The pressure difference on the water/mercury manometer board is given by;

$$\Delta p = (S_{Hg} - S_w)\rho_w gH. \quad (3.11)$$

The calibration equation is obtained by performing a linear regression on the pressure difference and transducer Voltage output.

3.12 Measured Variables

Physical properties of the slurry were measured and will be discussed in this section.

3.12.1 Slurry Relative Density

The relative density of the slurry (mixture) is the ratio of the mass of the mixture to the mass of an equivalent volume of fluid (water). The relative density of the slurry is related to the volumetric concentration as follows;

$$S_m = S_w + C_v(S_s - S_w). \quad (3.12)$$

Determining the slurry relative density is a very important variable. It is used to determine the mixture velocity V_m from the mass transfer rate and needles to say it must be done very accurately.

In homogeneous non-Newtonian slurries the density and concentration are assumed to be uniform. Density (ρ) and relative density of the mixture (S_m) are determined by performing the following steps;

1. A clean, dry one litre volumetric flask is weighed to the nearest 0.01g (M_1).

2. A slurry sample was taken in the volumetric flask at the sampling point in the pipe line while pumping from the one vessel to the other. The volume of the slurry taken is approximately 950 ml.

3. The flask plus slurry is weighed (M_2).

4. The flask is filled with water up to the graduated mark and weighed (M_3).

5. The flask is emptied, filled with clear water and weighed again (M_4).

The mixture relative density S_m is defined as;

$$S_m = \frac{\rho_m}{\rho_w} \tag{3.13}$$

which can be restated as;

$$S_m = \frac{\text{mass of slurry sample}}{\text{mass of equal volume of water}} = \frac{M_2 - M_1}{(M_4 - M_1) - (M_3 - M_1)} \tag{3.14}$$

ρ_m is calculated from;

$$\rho_m = S_m \rho_w . \tag{3.15}$$

3.12.2 Solids Relative Density

The relative density of the solids (S_s) is determined using test method 6B for fine-grained soils from BS 1377 (1975).

3.12.3 Volumetric Concentration

The volumetric concentration is the ratio of the volume of solids to the total volume of the mixture;

$$C_v = \frac{(S_m - S_w)}{(S_s - S_w)} . \tag{3.16}$$

3.12.4 Internal Pipe Diameter

The internal pipe diameter (D) is determined by measuring the mass of water (M_w) required to fill a known length of pipe (L). The diameter is calculated from;

$$D = \sqrt{\frac{4M_w}{\pi \rho_w L}}. \tag{3.17}$$

3.12.5 Slurry Temperature

The temperature of the slurry is measured by dipping a mercury thermometer into the slurry through the filling valve on top of the left-hand vessel of the BBTV. The BBTV is unique in the sense that even after extensive tests the temperature of the slurry does not change significantly. The reason for this is that there is no in line devices (pump etc.) that can cause the temperature to rise during testing. Only pipe friction causes a slight increase in temperature during testing.

In the case of a pipe loop with an in-line pump, the energy input by the pump causes the slurry temperature to rise significantly. The prime mover on the BBTV is compressed air from a compressor. The pressure vessels are pressurised and the slurry is forced through the pipe from one vessel to the other. The BBTV is also built inside an air-conditioned laboratory. The temperature of the slurry is mainly affected by the external room temperature which is usually 25 ^{0}C. The temperature during a whole test series on the BBTV would thus be limited to a temperature variation of $\pm$ 2 ^{0}C. In all the tests presented in this thesis no significant flow behaviour variance was found due to temperature effects.

3.12.6 Particle Size Distributions

For fluids like water, CMC and Glycerol no particle size distributions were done as these fluids are single phase liquids and the material dissolves completely in water. In the case of kaolin and the tailings slurry, the particle size distributions were done and are presented in Figure 3.8 and 3.9.

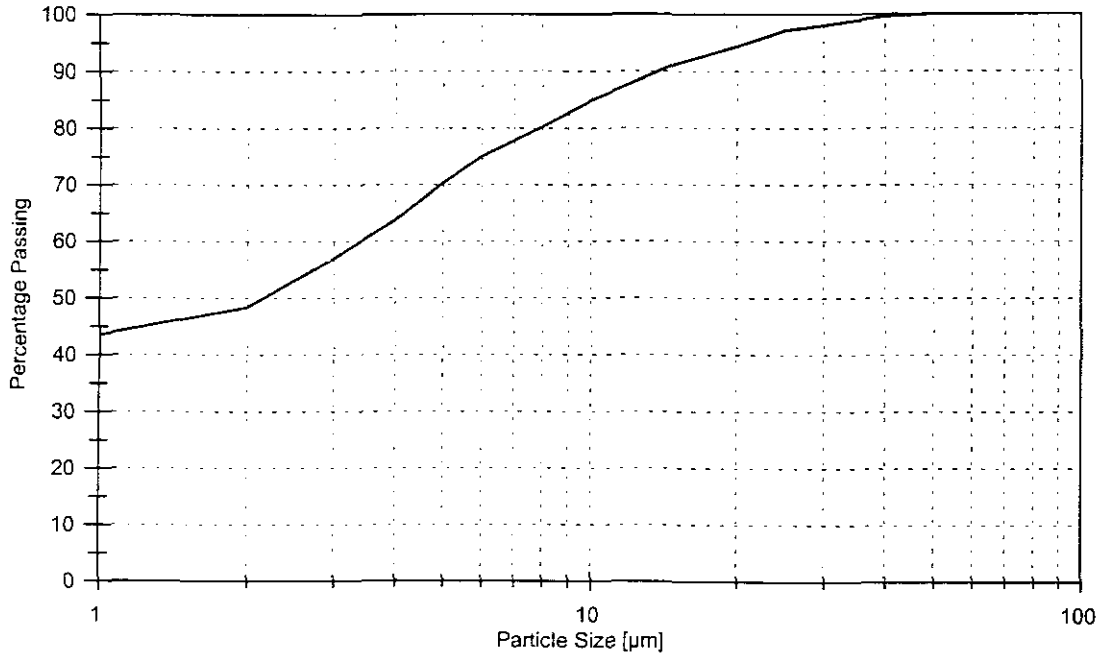

Figure 3.8: Particle Size Distribution for Kaolin.

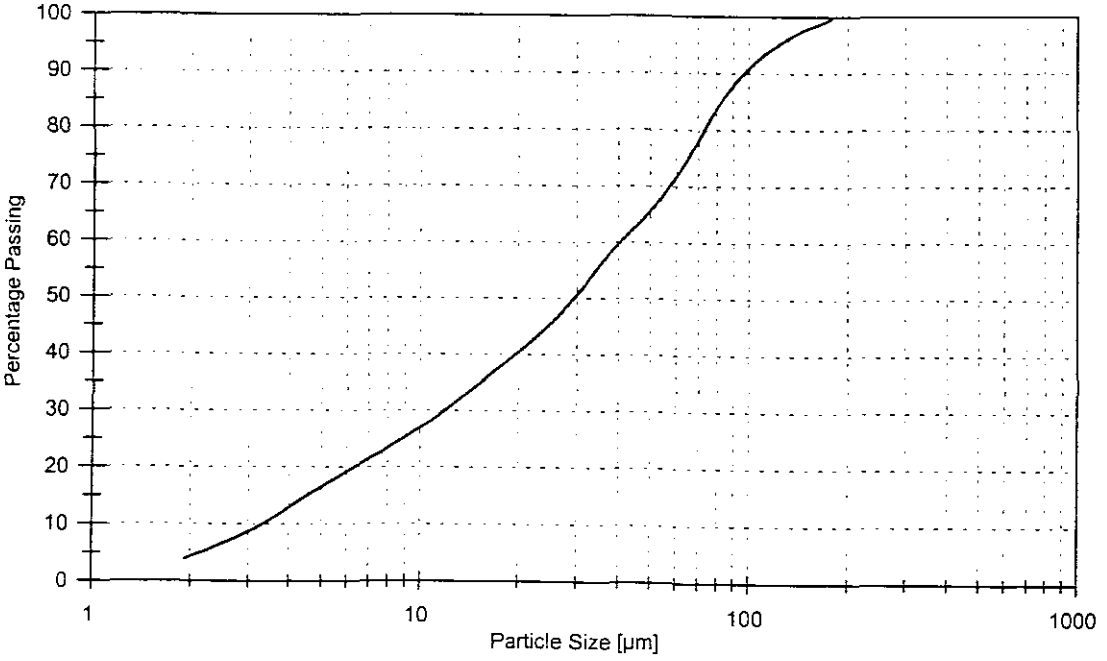

Figure 3.9: Particle Size Distribution for Tailings.

The particle size distributions were determined using a Malvern 2600/3600 Particle Sizer

VF.6. The calibration of the instrument was confirmed using standard calibration particles.

It should be noted that the particle size distributions produced by the Malvern instrument do not necessarily agree with those obtained by other methods. Any comparison of particle size distributions using different measuring techniques should therefore be undertaken with caution.

3.13 Derived Variables

The following variables are derived from the measured variables and will be discussed in this section.

3.13.1 Average Slurry Velocity

As stated before the average slurry velocity is derived from the mass distribution vs time graphs produced by the load cell. The formula is derived from first principals and is the most accurate way of determining the average slurry velocity.

The average or mean slurry velocity (V_m) is defined as the volumetric flow rate (Q_m) divided by the cross sectional area (A) of the pipe and is calculated from;

$$V_m = \frac{Q}{A} = \frac{4Q}{\pi D^2} = \frac{4M}{\pi \rho_m t D^2} \tag{3.18}$$

where;
M = mass of slurry derived from the load cell
ρ_m = mixture density
t = time in seconds

3.13.2 Wall Shear Stress

The wall shear stress (τ_0) is determined from the water/mercury manometer head difference (ΔH) over a known length of pipe (L), ie, the test section, as follows;

$$\tau_0 = \frac{D\Delta p}{4L}. \tag{3.19}$$

where;

$$\Delta p = \rho_w g \Delta H \left(S_{Hg} - S_w\right) \tag{3.20}$$

The head loss in meter of water per meter of pipe length can be derived from;

$$\Delta p = \frac{\rho_w g \Delta H}{L}. \tag{3.21}$$

3.13.3 Pipe Wall Roughness

The hydraulic pipe roughness (k) of the smooth pipes is determined from tests using clear water in each pipe size. Mean velocity and wall shear stress are measured for velocities over the full test range and roughness is determined using the Colebrook White equation (Colebrook and White, 1939). For partially rough wall turbulent flow the friction factor can be calculated from;

$$\frac{1}{\sqrt{f}} = -4\log\left[\frac{k}{3.7D} + \frac{1.26}{Re\sqrt{f}}\right] \tag{3.22}$$

and k is calculated from;

$$k = 3.7D\left(10^{\left(1/4\sqrt{f}\right)} - \frac{1.26}{Re\sqrt{f}}\right) \tag{3.23}$$

This procedure establishes the Colebrook White equation as the standard for calculating

smooth pipe roughness.

For the rough pipes the equation of Nikuradse (1933) was used to determine the pipe roughness for fully developed rough wall turbulent flow and the friction factor calculation changes to;

$$\frac{1}{\sqrt{f}} = 4\log\left(\frac{3.7D}{k}\right) \tag{3.24}$$

The pipe roughness is calculated using equation 3.23.

3.14 Instrument Measurement Errors

Whenever scientific experimental work is done, it is important to quantify the magnitude of the errors associated with the measured data and computed results. The expected error for a particular measurement can be determined if the functional relationship which defines the measurements is known. These errors are presented below.

3.14.1 Differential Pressure Transducer (DPT)

The error in the measurement of head using the DPT was taken as the largest residual error from the calibrations, which was 1 mm of mercury/water head.

3.14.2 Density and Relative Density Measurements

A standard of three relative density measurements was taken on each slurry tested. If the difference on the three measurements varied by more than 1%, the procedure was repeated. In general the density difference did not vary by more than 0.5%.

The errors in the individual measurements of relative density using a mass balance that read to the closest 0.001g were extremely small and were not taken as representative of the true errors involved in this measurement.

3.14.3 Slurry Temperature

The error in the measurement of slurry temperature using the mercury thermometer was less than 0.5 ^{0}C.

3.14.4 Force Measurements

The maximum combined error to be expected from the load cell output was given in the specifications as 0.03%.

3.15 Linear Regression Analysis

The calibration equation for the various transducers is derived from a linear regression analysis.

The linear regression method (Lipson and Shetch, 1973) of least squares is employed. The sum of the squares of the deviations (ε) is minimised in the y-direction. This is done since the random variation exists in the y values while the x values are held constant.

The resulting equation is;

$$y = mX + c + \varepsilon \tag{3.25}$$

where ε is the measure of deviation of the data points in the y-direction.

3.16 Correlation Analysis

The correlation coefficient (r) is defined as the quantitative measure of association between two variables x and y, where;

r = 1, perfect correlation

r = 0, no correlation

and;

$$r = \pm\sqrt{\frac{\text{explained variation}}{\text{total variation}}}. \tag{3.26}$$

In terms of variables;

$$r = \pm\sqrt{\frac{\sum\left(y_{est}\bar{y}\right)^2}{\sum\left(y-\bar{y}\right)^2}} \tag{3.27}$$

where;

y - actual measurement

$\bar{y}$ - mean value of y

y_{est} - correlation estimates of y

Expanding;

$$r = \frac{n\sum xy - \sum x\sum y}{\left\{\left[n\sum x^2\left(\sum x\right)^2\right]\left[n\sum y^2 - \left(\sum y\right)^2\right]\right\}^{1/2}} \tag{3.28}$$

The value of r is significant in r^2 of the total variation in y and can be accounted for by the least square line, and $(1 - r^2)$ is unaccountable. Therefore, physical (explained) variation is r^2 while random (unexplained) variation is $(1 - r^2)$.

This error analysis has been used to quantify the following errors.

3.17 Combined Errors

When a quantity involves more than one independent measurement, then the errors will combine in the following way. Errors are assumed to be randomly distributed following the Gaussian distribution and can be quantified using the procedure recommended by

Brinkworth (1968). The highest expected error can be determined using a root mean square approach.

In general for a given quantity X which is a function of several variables (measurements) the quantity X is a function of n other quantities ie;

$$X = \Phi(a, b, c, \ldots\ldots\ldots\ldots n) \tag{3.29}$$

The error in X due to measurement n (i.e. $(\triangle X)_n$) can be found by;

$$\frac{\Delta X_n}{X} = \left(\frac{\delta X}{\delta n}\right)\frac{\Delta n}{X} \tag{3.30}$$

or expanding;

$$\frac{\Delta X}{X} = \left(\frac{\delta X}{\delta n}\right)\frac{n}{X}\frac{\Delta n}{n} \tag{3.31}$$

The maximum possible error in X is given by the sum of the errors of the n contributory measured quantities;

$$\left(\frac{\Delta X}{X}\right)_{max} = \sum\left(\frac{\delta X}{\delta n}\frac{n}{X}\frac{\Delta n}{n}\right) \tag{3.32}$$

The expected highest error is given by the square root of the sum of the squared values of each term ensures that all contributions will be positive and can be expressed as;

$$\left(\frac{\Delta X}{X}\right)^2_{exp} = \sum\left(\frac{\delta X}{\delta n}\right)^2\left(\frac{n}{X}\right)^2\left(\frac{\Delta n}{n}\right)^2 \qquad (3.33)$$

where;

X - overall result

ΔX - error in the overall result

n - quantity measured (e.g. flow, weight, etc.)

Δn - error in the quantity measured in units of measurement.

3.17.1 Errors in Measured Parameters

Fluctuations of the analogue outputs of the transducers occur in any measurement system. The discrete readings of the data acquisition unit may be taken at an extreme analogue fluctuation value. This could be accounted for by using statistical techniques. Systematic errors will appear in the mean value of any measurement and statistical methods will not disclose them. These errors are in the following form;

- Scale errors
- Static response
- Dynamic response errors
- Interference
- Personnel error.

Clear water tests, in which experimental results and theoretical predictions can be compared, were performed in each tube diameter to ensure that systematic errors were minimised.

3.17.2 Pipe Diameter

The internal pipe diameter is determined by measuring the mass of water that fills a section

of pipe of length L using the equation given by;

$$D = \sqrt{\frac{4M_w}{\rho_w \pi L}}. \tag{3.34}$$

The maximum error is given by;

$$\left(\frac{\Delta D}{D}\right)^2 = \left(\frac{1}{2}\sqrt{\frac{4}{\pi \rho_w M_w L}}\right)^2 \left(\frac{M_w}{D}\right)^2 \left(\frac{\Delta M_w}{M_w}\right)^2 + \left(-\frac{1}{2}\sqrt{\frac{4M_w}{\pi \rho_w L^3}}\right)^2 \left(\frac{L}{D}\right)^2 \left(\frac{\Delta L}{L}\right)^2 \tag{3.35}$$

Possible errors which exist in the measurement of L and M_w where;

L - length of pipe

M_w - mass of water contained in the pipe.

The highest expected errors in the pipe diameter for the BBTV are give in Table 3.1

Table 3.1: Highest expected error for pipe diameters on the BBTV.

Description	Pipe Diameter D [mm]	Highest Expected Error in Diameter [mm]	Highest Expected Measurement Error ΔD/D [%]
Smooth pipes	5.78	±0.1945	± 6.3646
Smooth pipes	13.12	±0.1620	± 1.2345
Smooth pipes	28.34	±0.1018	± 0.3593
Smooth pipes	46.04	±0.0455	± 0.0989
28-2515 Rough pipes	27.03	±0.3678	± 0.7197
28-6030 Rough pipes	27.18	±0.1950	± 0.7174

Description	Pipe Diameter D [mm]	Highest Expected Error in Diameter [mm]	Highest Expected Measurement Error $\Delta D/D$ [%]
45-2515 Rough pipes	44.73	±0.1174	± 0.2626
45-6030 Rough pipes	45.44	±0.1583	± 0.3385

Notes;

1. Water temperature : 23 ^{0}C
2. Water density : 998 kg/m^3

17.3 Error in Mean Velocity Measurements

Velocities between 0.01m/s and 22m/s are measured using the equation;

$$V_m = \frac{4Q_m}{\pi D^2} = \frac{4M_m}{t\rho_m \pi D^2} = \frac{2F}{t\rho_m \pi D^2 g}. \quad (3.36)$$

The mass distribution between the two vessels is measured using the load cell. The load cell is calibrated using the equation given by;

$$F = m(v / v) + c. \quad (3.37)$$

The slope of the calibration curve is determined by a least square linear regression shown in Figure 3.7. The slope is given by;

$$m = \frac{F}{(v/v)}. \tag{3.38}$$

and the maximum error may be approximated as;

$$\left(\frac{\Delta m}{m}\right) = \sqrt{\left(-\frac{F}{(v/v)^2}\frac{(v/v)}{m}\frac{(\Delta v/v)}{(v/v)}\right)^2} + \sqrt{\left(\frac{1}{(v/v)}\frac{F}{m}\frac{\Delta F}{F}\right)^2}. \tag{3.39}$$

The largest error in the measurement of the dimension less load cell output is 0.03%. The largest error in the measurement of applied force $\Delta F/F$ is 0.0274%. Therefore the maximum error in slope $\Delta m/m$ is 0.057%.

The maximum error in F is given by;

$$\left(\frac{\Delta F}{F}\right) = \sqrt{\left(\frac{v}{v}\frac{m}{F}\frac{\Delta m}{m}\right)^2} + \sqrt{\left(m\frac{v/v}{F}\frac{\Delta v/v}{v/v}\right)^2}. \tag{3.40}$$

The maximum error in V_m calculated using the slope of the graph of mass versus time is approximated by;

$$\begin{aligned}\left(\frac{\Delta V_m}{V_m}\right) &= \sqrt{\left(\frac{2}{t\rho_m\pi D^2 g}\frac{F}{V_m}\frac{\Delta F}{F}\right)^2} \\ &= \sqrt{\left(\frac{-2F}{t^2\rho_m\pi D^2 g}\frac{t}{V_m}\frac{\Delta t}{t}\right)^2} \\ &= \sqrt{\left(\frac{-4F}{t\rho_m\pi D^3 g}\frac{D}{V_m}\frac{\Delta D}{D}\right)^2} \\ &= \sqrt{\left(\frac{-2F}{t\rho_m^2\pi D^2 g}\frac{\rho_m}{V_m}\frac{\Delta\rho}{\rho_m}\right)^2}\end{aligned} \tag{3.41}$$

The largest error in the measurement of time $\Delta t/t$ is 0.10 %. The largest error in the measurement of mixture density $\Delta p_m/p_m$ is 0.50 %. The maximum errors in velocity are presented in Table 3.3.

Table 3.2: Maximum Expected Errors in Velocity.

Nominal Diameter [mm]	Maximum Percentage Error in Velocity [%]
46	0.053
28	0.14
13	0.655
5	3.376

3.17.4 Differential Pressure Transducers

Shear stresses between 1 and 600 Pa is measured. This involves the measurement of differential pressure between 1 and 250 kPa. The error in differential head is given by the accuracy of the pressure transducers and the accuracy with which the calibration manometers can be read.

The calibration curve for the DPT is given by;

$$p = mV + c \tag{3.42}$$

where;

p - differential head output

V - transducer output voltage.

The errors in the measurement of the differential pressure are calculated in the same way as for the load cell. The accuracy of the DP cell is 0.250 %. The largest error in the measurement of applied pressure is 0.070 %. The maximum error in the calibration slope $\Delta m/m$ is calculated to be 0.320 %.

The equation used to calculate the shear stress at the wall is given by;

$$\tau_0 = \frac{D\Delta p}{4L}. \tag{3.43}$$

The maximum error in τ_0 is given by;

$$\frac{\Delta\tau_0}{\tau_0} = \sqrt{\left(\frac{\Delta p}{4L}\frac{D}{\tau_0}\frac{\Delta D}{D}\right)^2} + \sqrt{\left(\frac{D}{4L}\frac{\Delta p}{\tau_0}\frac{\Delta\Delta p}{\Delta p}\right)^2} + \sqrt{\left(\frac{-D\Delta p}{4L^2}\frac{L}{\tau_0}\frac{\Delta L}{L}\right)^2}. \tag{3.44}$$

The largest error in the measurement of the length between pressure tappings $\Delta L/L$ is 0.200 %. The maximum errors in shear stress are presented in Table 3.3. and the highest expected error at different shear stresses are presented in Figure 3.10.

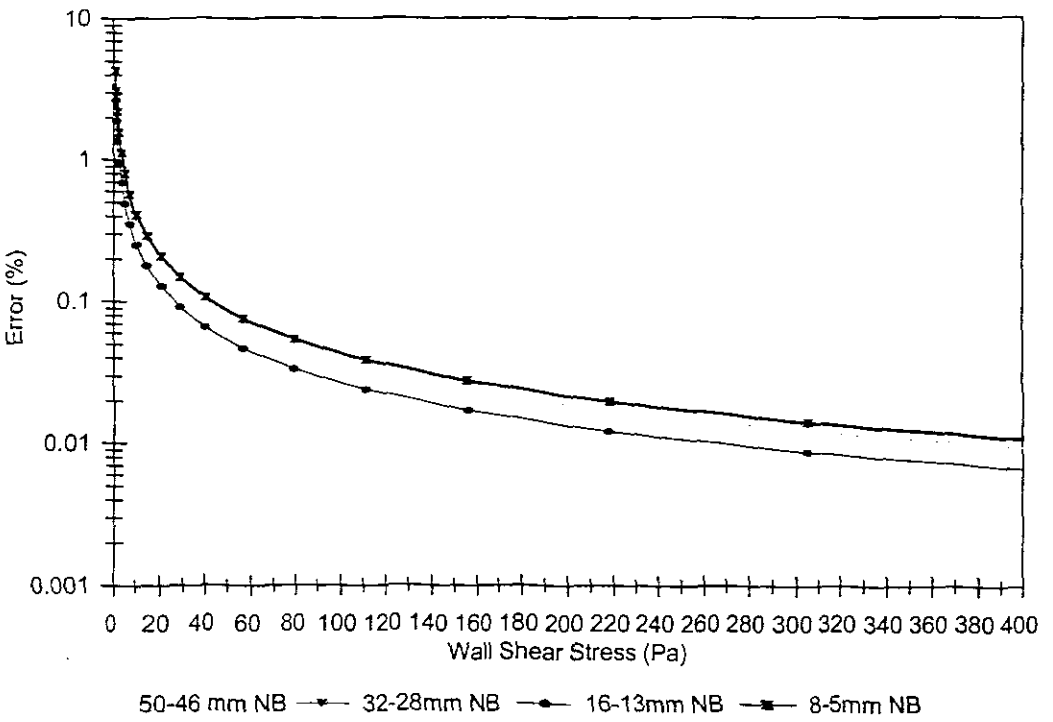

Figure 3.10: The Highest Expected Error Calculated Using the DPT at Different Shear Stresses.

Table 3.3: Maximum Expected Error in Shear Stress.

Nominal Diameter [mm]	Maximum Percentage Error in Shear Stress [Pa]
46	3.728
28	4.184
13	2.641
5	4.305

The maximum error in the above experimental measurements is within acceptable limits.

3.17.5 Pipe Roughness

The pipe roughness was determined using clear water tests over the full velocity range. The errors are summarised in Table 3.4.

Table 3.4: Errors in Pipe Roughness Using Clear Water Tests.

Pipe description	Diameter [mm]	Roughness [μm]	Standard deviation [%]	Average error [%]	Maximum error [%]
Smooth	5.78	1.4	2.198	2.588	7.674
Smooth	13.12	0.81	3.87	5.962	10.126
Smooth	28.34	5.59	1.169	1.851	3.863
Smooth	46.04	1.04	2.558	3.741	9.218
28_2515 Rough pipe	27.03	136	1.277	4.294	6.608
28_6030 Rough pipe	27.18	266.4	2.607	4.904	8.14
46_2515 Rough pipe	44.73	48.3	1.545	3.314	5.777
46_6030 Rough pipe	45.44	656	2.237	2.892	7.918

3.18 Experimental Procedure

The experimental procedures pertaining to tests on the BBTV are presented in this section.

3.18.1 The BBTV

The following procedure is followed to run a test on the BBTV.

1. One day before testing is started, all the instrumentation is switched on to warm up.

2. All the piping connected to the BBTV is pressurised by the main water supply. The system is left for half an hour and then all the pipes are systematically checked for leaks. The valves on the manometer board are also isolated individually and pressurised to check for any leakages through the valves.

3. Flush all the lines connecting the manometer board to the pressure tappings and DPT to make sure no air is present in these lines. Close the lines at the isolating valves after flushing to make sure no air is introduced during the preparation period.

4. Make sure that both vessels are completely empty before attaching the load cell to the BBTV. Calibrate both the load cell and DPT as described in sections 3.10 and 3.11.

5. Fill only the left-hand vessel completely full of slurry and make sure the right-hand vessel is completely empty. Pump the slurry from one vessel to the other for at least 20 minutes to ensure good mixing. The 28mm pipe is used for the mixing process at velocities greater than 6 m/s. This procedure was found to be the optimum for mixing and is a combination of time used to pump from one vessel to the other and the velocity of the slurry introduced in the receiving tank that helps with the mixing proses within the vessel.

6. After the mixing process the slurry is pumped from the one vessel to the other in the 28 mm pipe at a velocity of approximately 2m/s. While the fluid flows from the one vessel to the other, a sample is taken from the sampling point in the line. This

procedure is repeated three times to have a total of three samples for relative density measurements.

7. Determine the relative density and slurry temperature before tests are started and enter the variables into the computer programme set up for testing. The relative density and temperature should be checked frequently during the test period.

8. Make sure all the test tube valves on the BBTV are closed. Set the appropriate pressure to be tested and pressurise the vessel containing the slurry.

9. Select the pipe to be tested and open the valve on the receiving side. Make sure the air vent on the receiving vessel is also open. All the other valves must be closed.

10. Open the isolating valves on the pressure tappings and make sure the cross over section on the manometer board is set correctly depending on the direction of flow.

11. Open the valve on the high pressure side of the pipe slowly to make sure that the pipe is filled with slurry. Open the valve fully to reach stable flow. Wait for a few moments to reach stable flow before data logging is started on the computer. The data logger will collect readings from the load cell and DPT at specified time intervals.

12. At the end of the run, the valve is slowly closed, avoiding water hammer. This is very important because water hammer can be severe on the BBTV.

13. Choose the correct data logging points on the computer and plot the data point.

14. All these previous steps are taken to get one data point. Repeat the procedure from point 8 to get the next data point.

Tips;

- When testing always try to start from the middle velocity range ± 5 m/s. Test to the top velocity range and then test the low velocity ranges.

- When starting a run always fill the pipe with slurry first (by opening the valve slowly and letting the pipe fill with slurry) before completely opening the valve to reach stable flow. This will minimise the amount of air introduced into the solids collecting pod and minimise the times the pods need to be flushed during a test series.

- To test laminar flow select an adequate pressure to pressurise the vessel, usually 1bar. The flow rate is then controlled by opening and closing the pinch valves and keeping the pressure constant at 1bar.

- One run produces a data point (V; Δp). The run is repeated until sufficient data points have been acquired (normally 40 data points).

3.19 Material/Fluids Tested

The following fluids were tested in the BBTV. Appendix A contains a table of all the fluid properties.

3.19.1 Water

Ordinary tap water was used for all the clear water tests. The temperature of the water was measured carefully because it affects the viscosity and the density of the fluid.

3.19.2 CMC (Carbonyl Methyl Cellulose)

CMC (used in wall paper glue) originally is in a powder form. The BBTV was filled three quarters with tap water and then the CMC was added. CMC was added to water to the desired concentration and then air was bubbled through the mixture to speed up the mixing process. This mixing process would continue for at least a day before any testing would commence. CMC dissolves naturally in water and even after the mixture was left for days no settling occurred. Before testing started the mixture is pumped around for at least 15 minutes. Relative density measurements were taken before testing commenced. Temperature measurements were taken regularly throughout testing.

3.19.3 Glycerol

Glycerol naturally comes in liquid form. 100 % Glycerol was mixed up with tap water to achieve different relative densities. The same mixing process was used for Glycerol as for CMC.

3.19.4 Kaolin

Kaolin slurry was prepared from dry kaolin pellets. The mixture was prepared by mixing kaolin pellets and tap water in a concrete mixer to the desired concentration before the mixture were poured into the BBTV. Kaolin settles out over time and very good mixing must occur before a test is conducted.

3.19.5 Tailings

The mine tailings were received in slurry form. The slurry was poured into the BBTV and diluted to the desired concentration. The tailings also settle out with time and the same mixing procedure occurs as for kaolin slurry.

3.20 Results and Discussion

The results are presented in Chapter 4 and Appendix A. Each pipe test is presented by plotting the data on various graphs.

3.20.1 Pressure Gradient Tests

Test data from the BBTV can be grouped into test sets. A test set can be defined as a group of tests (different diameter pipes) that were performed on the same slurry (same relative density). A pseudo shear diagram of each test set is plotted which displays the wall shear stress ($D\Delta P/4L$) on the y - axis and the pseudo-shear rate ($8V/D$) on the x - axis. A typical pseudo-shear diagram is shown in Figure 3.11.

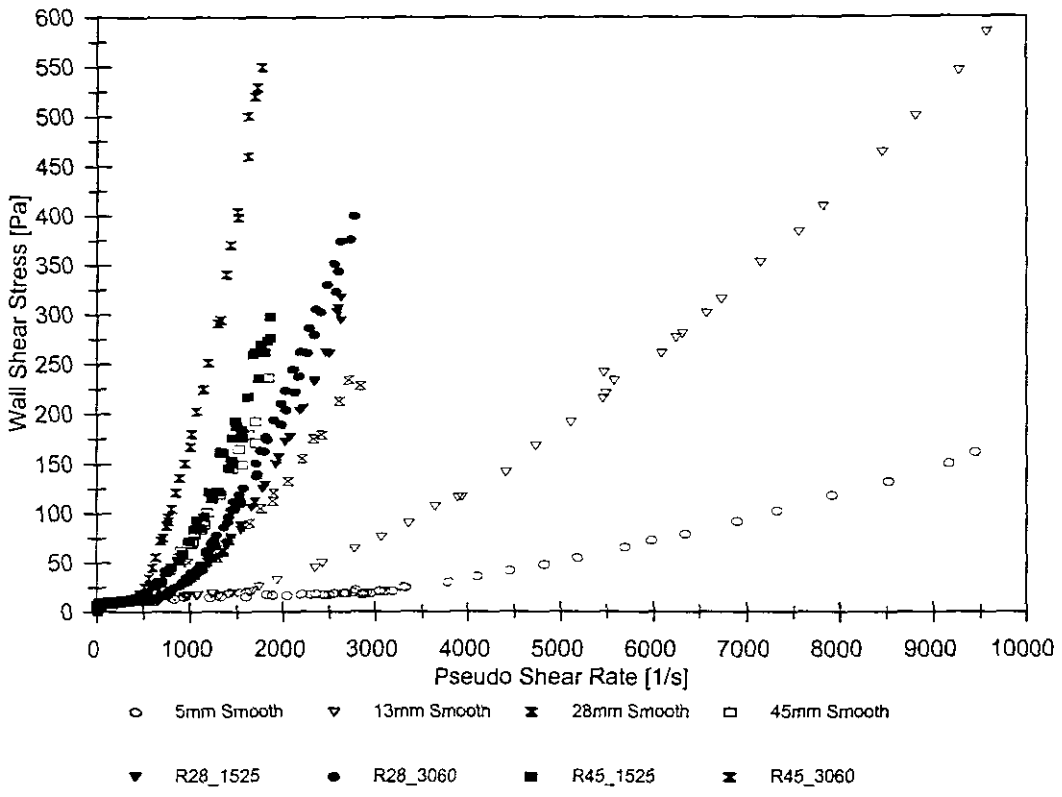

Figure 3.11: Typical Pseudo Shear Diagram of Kaolin Slurry, 5% by Volume.

The diagram shows graphically the change in behaviour between the laminar and turbulent regimes. The locus of the viscous data in the laminar region is coincident for the different tube diameters and the rheological constants (τ_y, K and n) can be determined from the data in the laminar region (rheological characterisation).

The change from laminar to turbulent flow is visible by observation of the slurry particles in the transparent tubes during testing. In laminar flow the slurry particles move gradually along the pipeline in the direction of flow. In turbulent flow the slurry particles move in all directions although the net flow of the particle would still be in the direction of flow.

The change from laminar to turbulent flow can also be seen by connecting the manometer board to the pressure tappings. In laminar flow the differential head displayed by the manometer would be stable with very little variation. In turbulent flow the head produced by the flow would vary much more and would not be as stable as produced by laminar flow. The differential pressure transducer cutput also shows significantly more variation

in the transition region during a test. This evidence supports the notion that true turbulence is indeed occurring. The critical point at which turbulence begins for each pipe size can be clearly seen on the pseudo-shear diagram. The bigger the pipe the earlier the transition from laminar to turbulent flow occurs. The critical velocity occurs at the intersection where the flow changes from laminar to turbulent.

3.20.2 The Influence of Diameter

Figure 3.11 shows that pipe diameter has no influence on the wall shear stress at a given pseudo-shear rate in the laminar regime for the same concentration. This is an indication that the slurry is time independent and that the slurry properties have not changed during a test series. With very high concentration slurries only laminar flow was achieved in the smaller pipes.

As mentioned before the laminar/turbulent critical point occurs at lower pseudo-shear rates for larger pipes than for smaller diameter pipes (Bowen, 1961). Roughness has no effect on the transition or critical point and is only governed by the pipe diameter.

3.20.3 The Influence of Concentration

The influence of concentration on pipe flow behaviour can be seen in Figure 3.12. Only the data sets of the two roughest pipes the R45_6030 and the R28_6030 are presented. This figure shows that for a given pipe diameter the increase in relative density would cause the wall shear stress to increase for the same pseudo shear rates. The kaolin data presented in Figure 3.12 shows that for a pseudo shear rate of 500 1/s the wall shear stress increases from 10 Pa at a relative density of 1.080 to 50 Pa at a relative density of 1.177.

The transition point from laminar to turbulent flow for the same diameter pipe increases as the concentration increases. At the lowest relative density the transition of the R45_6030 data set occurs at a pseudo shear rate of approximately 480 1/s. At the highest relative density of 1.177 the transition occurs at a pseudo shear rate of approximately 800 1/s.

In the fully developed rough wall turbulent flow region the pressure gradient is practically the same for the same diameter pipe irrespective of the solids concentration of the fluid. At

a pseudo shear rate of 1650 1/s the wall shear stress is approximately 450 Pa's for all the concentrations presented.

The initial turbulent flow region however, gave quite different results. Pipe roughness seems to have the greatest influence in this region. This is also the core of the thesis as this region is the region in which designers are the most interested. The reason for this is that most pipelines are designed to operate in this region. This region has proved to be the most economical for pipeline design. The data however shows that the most variances occur in this region which makes it difficult to gave accurate predictions in this area. For a pseudo shear rate of 800 1/s in the R46_6030 data set the wall shear stress varied from 150 Pa's at the lowest relative density to 50 Pa's for the highest relative density. The reason for this change in behaviour is because the viscous forces increase with an increase in relative density. The data presented in Figure 3.12 confirms the findings of Bowen (1961) and Harris & Quader (1971).

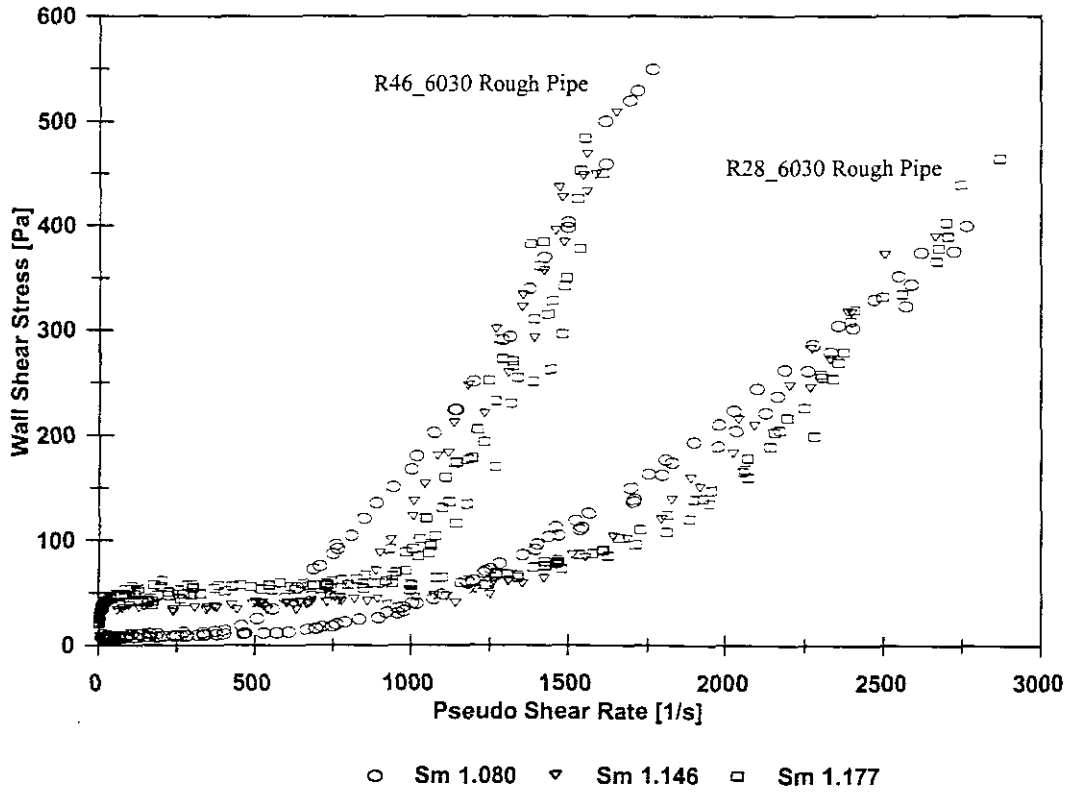

Figure 3.12: The Effect of the Increase in Concentration for Kaolin.

3.20.4 Settling and Homogeneity

Fluids such as water, CMC, and Glycerol homogeneity were not a problem. Fluids such as kaolin and the tailings slurry were slow settling slurries and settling did occur if the slurry was left to stand for several hours. Great caution was taken when these slurries were tested to ensure they were very well mixed before any testing was started. It was therefore assumed that all the slurries tested could be analysed as homogeneous suspensions.

3.20.5 Particle Size Distributions

Particle size distributions were only done on Kaolin slurry and the Tailings. The results are presented in section 3.12.6. The particle size distributions were done according to the Malvern 2600/3600 Particle Sizer VF.6.

The particle size distribution is a very important physical property of a slurry. For the same slurry a difference in particle size distribution would cause a difference in the slurry flow behaviour. The -74μm part of the slurry plays an important role in the viscous characteristics of the slurry (Gillies, 1984). Degradation of the slurry in the pipe loop is a problem and measurement of the particle size distribution during a test is very important as the slurry degrades during the test series. In a pipe loop slurry degradation is a serious problem as the pump would break down the slurry and change the flow behaviour. One of the biggest advantages of the BBTV is that physical degradation caused by pumps is not a problem. In all the tests done on the BBTV no significant degradation of the slurry was detected.

3.21 Discussion

The accuracies of the velocity and pressure measurements are dependant on the accuracy of the response of the processing technique used, and are not only dependent on the accuracy of the transducers and their calibrations. This means that the accuracy of the final velocity value is influenced by the accuracy of the mass/time linear regression. The final pressure differential value is influenced by the standard deviation of the individual values used for the average. These two factors must be taken into account when developing operational procedure for standard pressure gradient tests. The maximum number of

individual data points should be taken during a run to eliminate this problem. If this is done, it will minimise the above two sources of error.

The following precautions have been accumulated from operational experience;

1. The right-hand vessel is on a cantilever and may be set into oscillatory motion when disturbed during a run. This will show up as an inclined sine wave on the mass versus time graphs and the data should be discarded.

2. Make sure no slurry leaks through the tubes that are not in use.

3. Make sure that no valves on the manometer board leak as this will influence the pressure readings.

4. Allow a short time (± 5 seconds) for the flow to stabilize before taking measurements.

5. If the slurry insolation pods fill up with slurry above the outlet or get air in them, they must be flushed.

6. At high concentration the pressure tappings may become blocked by solids causing an error in the pressure reading.

7. At the end of a run air may be drawn into the pipe. This should be avoided because it aerates the slurry and sets the viscometer into oscillatory motion.

8. Test the rough and smooth pipes randomly so that the laminar pipe data overlaps and any error in one of the pipes could be picked up immediately.

The BBTV has several advantages in comparison with pumped pipe loop test rigs;

- Often relatively large pilot plants have to be built in order to provide a representative scale of the original plant.

- Normally the pipe test rig is limited to two pipe diameters. This is due to the fact that a good range of velocities must be obtained for testing purposes.

- Before tests can commence, the pipeline conditions must first reach steady state. The time to reach steady state can be anything from 4 to 8 minutes.

- The velocity of the slurry is measured by means of flow meters. Several flow meters are normally required on a pilot plant for the different test sections. Some flow meters perform better on different kinds of slurry than others. Ideally two different kinds of flow meters should be placed into one line to verify their correct operation. This is usually very costly.

- During the test run the slurries is recycled numerous times and both the pump action and pipeline length adversely affect the slurry temperature. The temperature rise necessitates the installation of heat exchanges.

- Pumps are used to drive the slurry through the pipe system. The pump action results in degradation of the particles and it is only fair to doubt the correctness of the final data.

- A relatively large sample of slurry is needed for a pump loop test which is costly to transport to the test facility.

- Operational cost of such a installation is high, for example pump and motor maintenance.

- The cost of installing a pump test facility compared to that of the BBTV is high.

The disadvantages of the BBTV are;

- The instrument is limited to a large pipe size of 50 mm diameter.

- The instrument requires a slurry sample of at least 250 litres. Care must be taken that a representative sample of the slurry is tested.

- It is unlikely that the BBTV would be able to detect time dependent behaviour which has a relatively long time constant.

- Only homogeneous slurries can be tested in the BBTV.

Despite these disadvantages, it is a versatile instrument and accurate head loss and visual flow data can be collected over wide ranges of diameter and velocity for laminar, laminar/turbulent transition and turbulent tube flow. It is rare, if not unique to be able to combine all of these features on a single instrument. The BBTV is therefore useful not only for routine rheological analyses and characterisations - as its name implies - but it is also a valuable and versatile research tool.

3.22 Conclusions

- Apparatus for the reliable collection of pipeline test data for non-Newtonian slurries over wide range of pipe diameters and velocity in both the laminar and turbulent regimes was constructed and commissioned using clear water tests. The BBTV was used to test all the fluids presented in this thesis and has been shown to be a useful instrument to test over the full range of laminar and turbulent flow.

- The calibration and test procedures for the BBTV are well established and provide for valid and accurate pipeline data measurement.

- The experimental errors have been shown to be within acceptable limits to give accurate and reliable data.

- The solid materials used for slurry preparation were kaolin slurry and the tailings. These slurries were tested over as wide a range of concentrations as possible.

- Homogeneous fluids tested were water, CMC and glycerol.

- These slow settling and homogeneous mixtures were tested to cover as wide a range of different fluids as possible to establish their different kind of behaviour in a

pipeline. All the results are presented in Appendix A.

- This data base is used against Nikuradse's findings (1933) to compare the behaviour of the different fluids tested in smooth and rough pipes.

- Smooth and sand roughened pipes has been shown to behave significantly differently in a given diameter pipe for the same concentration of slurry.

- Good clear water tests presented in Appendix A verified the correct operation of the instrument to ensure accurate data.

- It can be concluded that the BBTV is a reliable instrument and can be used to generate accurate data for homogeneous and slow settling mixtures over wide ranges of laminar and turbulent flow.

3.23 Recommendations

- A differential pressure transducer that can read both positive and negative pressures should be implemented on the BBTV. This will eliminate the cross over section on the manometer board and make the operation of the BBTV easier.

- The computer and data acquisition unit need to be updated to make it easier for the operator to analyse the results immediately and reduce the time needed to complete a test.

- The compressor needs to be placed outside the laboratory to eliminate noise pollution during testing.

- Adequate drainage must be provided around the BBTV as the floor becomes slippery when wet.

- The pressure vessels must be modified to make more space to put the weights on the instrument when the load cell is calibrated.

- A permanent thermometer should be installed in one of the pressure vessels.

3.24 Future Work

- Test work on rough pipes should continue to further the understanding of the behaviour of different fluids in turbulent flow.

- The test programme should continue to support the validation of the instrument and refinement of the operation procedure and processing techniques using Newtonian and non-Newtonian fluids.

- Different kinds of roughness needs to be investigated such as mixing kaolin with sand or differed particle size distributions of the same slurry.

- A proper data base needs to be set up so that the data base would be readily available for research purposes.

- Larger rough pipes (>50mm diameter) need to be investigated on a pipe loop driven by a pump and the data compared with the BBTV test results.

Chapter 4

Analysis of Results

4.1 Introduction

This Chapter presents the analysis of the test data. The measured test data is presented in detail in Appendix A. The author will start by discussing the clear water test results and then the data obtained for the various fluids tested.

4.2 Clear Water Tests, Nikuradse and Colebrook & White

It is very important to do clear water tests to confirm the operation of any instrument. If the clear water tests are acceptable, the instrument can be used to determine the behaviour of any other fluid. The BBTV was used to test all the different fluids presented in this thesis. The BBTV was first fitted with smooth pipes with nominal internal diameters from 6 mm up to 46 mm. After the clear water tests were completed using smooth pipes, the BBTV was fitted with rough pipes of the same diameter.

Clear water tests are very important for the following reasons:

- Clear water tests are used to calibrate the instrument.
- If something is wrong with the differential pressure transducer (DPT) or the load cell calibrations, it will be evident from the clear water tests.
- The Colebrook & White equation is used to determine the roughness of the smooth pipes and the equation of Nikuradse is used to determine the roughness of the rough pipes.
- Clear water is a Newtonian fluid which is well documented (Nikuradse, 1933 and Colebrook & White, 1938-1939) and we know how it behaves in a pipe. It is good practice to start testing a known fluid before testing a non-Newtonian fluid of unknown properties.

4.3 Clear Water Test Analysis

All the clear water tests for the smooth and rough pipes are presented in Appendix A. The smooth pipe properties are presented in Table 4.1.

Table 4.1: Smooth Pipe Properties

Pipe	Internal Diameter [mm]	Hydraulic Roughness [μm]
8x6 mm Clear PVC	5.78	1.07
16x13 mm Clear PVC	13.12	0.87
32x28 mm Clear PVC	28.34	5.9
50x46 mm Clear PVC	46.04	1.33

The smooth pipes show typical roughness values expected for a clear PVC pipe. The roughness ranges from 0.8 μm to almost 6 μm which is well within the ranges (0 to 20 microns) documented for clear PVC pipes (Govier & Aziz, 1972). The smooth pipes were tested at velocities from 0 to 12 m/s for the 5.78 mm, 28.34 mm and 46.04 mm smooth pipe and up to 18 m/s for the 13.12 mm smooth pipe. The data corelates very well with Colebrook & White.

After the smooth pipes were tested and the author was satisfied that the BBTV and instrumentation gives accurate results, the BBTV was fitted with a series of rough pipes. A summary of the rough pipe properties is given in Table 4.2.

Table 4.2: Rough Pipe Properties

Pipe	Internal Diameter [mm]	Sand Roughness [μm]	Hydraulic Roughness [μm]	k/D
R28_1525	27.03	150 to 250	136	0.0050
R28_3060	27.18	300 to 600	291	0.0098
R46_1525	44.73	150 to 250	42	0.0011
R46_3060	45.44	300 to 600	672	0.0144

The procedure of how the rough pipes were made is described in detail in Chapter 3. Essentially the author tried to simulate the process Nikuradse (1933) used to make sand roughened pipes. Appendix A shows the roughness of the different pipes using the clear water test data and Colebrook & White. The roughness of the sand roughened pipes varies from about 42 μm to 672 μm.

The author expected the rough pipes which were made from the same sand grain sizes, to be more or less of the same hydraulic roughness. After the clear water tests were completed, it became evident that this was not the case. Still, the data from the clear water tests were in good agreement with Nikuradse's predictions for hydraulic roughness.

4.3.1 Friction Factor Reynolds Number Analysis for Water

The Colebrook & White friction factor was plotted against the Newtonian Reynolds number in Figure 4.1. The formulae are presented in Chapter 2.The solid line which runs along the smooth pipe data represents the Prandtl equation for smooth wall turbulent flow. This also verifies that the data presented from the smooth pipes are correct. The solid line on the left of the figure represents laminar flow where the friction factor equals 16/Re. Laminar flow for water was only achieved in the 5.78mm pipe. The region between the laminar flow line and the smooth wall turbulent flow is called the transition region, where the flow is neither fully laminar nor fully turbulent. The different flow regions have been discussed in more detail in Chapter 2 using the Moody diagram.

The smooth pipe data shows very good agreement with the smooth wall correlation as shown in Figure 4.1. The results presented in Figure 4.1 represent all smooth and rough pipe data obtained from the clear water tests. All the smooth pipe data seem to group themselves on one curve, showing typical smooth pipe behaviour. These data are only slightly separated depending on the difference in hydraulic roughness between the smooth pipes. As the diameter increases the data also shifts from the left to the right of the graph as the Newtonian Reynolds number increases with increase in diameter. Even at high Reynolds numbers, greater than 500 000, the friction factors of the smooth pipes are still decreasing which indicates that the flow has not yet developed to fully rough wall turbulent flow. At fully developed rough wall turbulent flow the friction factor become a constant irrespective of the viscosity of the fluid.

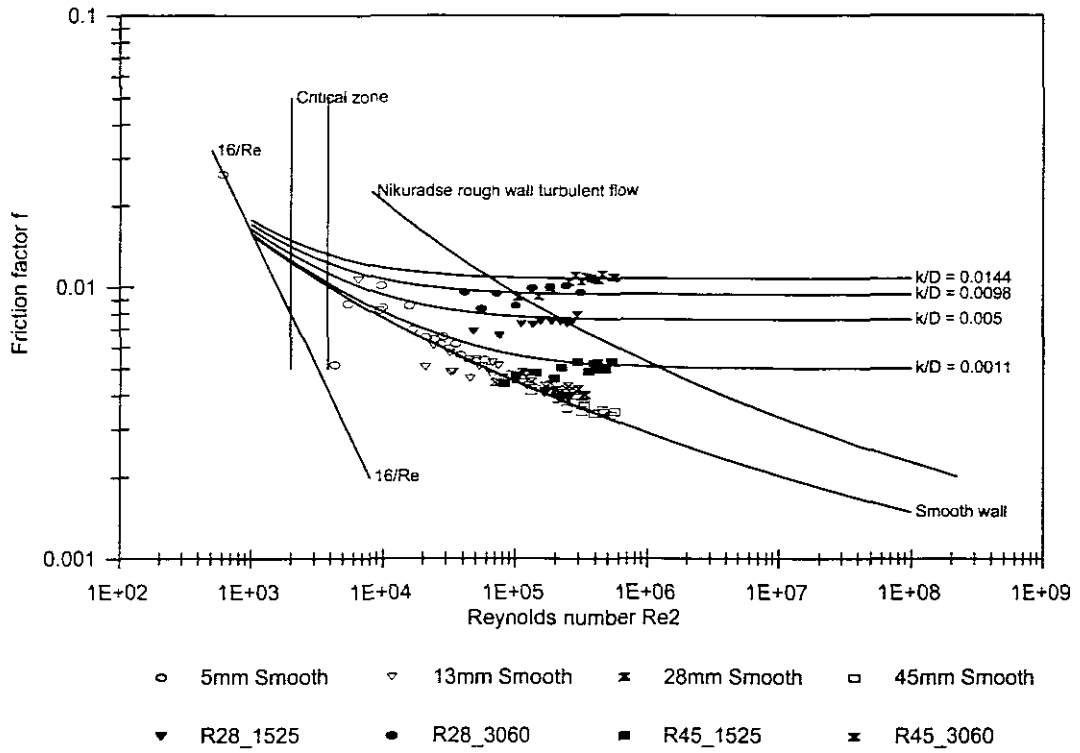

Figure 4.1: Colebrook & White Friction Factor vs Newtonian Reynolds Number for Water.

In Figure 4.1 the effect of roughness is clearly shown by the sudden increase in the friction factor for the rough pipes. All the smooth pipe data lie on one curve where the rough pipe data already start to separates in the early turbulent flow region. The R45_1525 pipe which has the lowest roughness of 42 μm, settles on the lowest k/D value for the rough pipes and the R45_3060, which is the roughest pipe of 672 μm, settles on the highest k/D value. The two 28 mm pipes which have intermediate roughness also settle between these two pipes with their friction factors separated by their differences in roughness.

Table 4.3: Constant Friction Factor Values for Fully Developed Rough Wall Turbulent Flow for Rough Pipes.

Pipe	k/D ratio	Re [Newtonian]	Rer	f [Colebrook & White]
R28_1525	0.0050	295 850	94	0.00769
R28_3060	0.0098	309 061	229	0.00975
R45_1525	0.0011	530 287	26	0.00496
R45_3060	0.0144	562 458	612	0.01089

Table 4.3 shows the friction factor for the rough pipes at the highest Reynolds number tested. It is clear from Figure 4.1 that the greater the roughness of the pipe, the sooner the fully developed rough wall turbulent flow is reached. In the case of the data set R45_1525, fully developed rough wall turbulent flow has not been fully reached and the friction factor keeps changing as the Reynolds number increases. At low Reynolds numbers the rough pipe data deviates from the smooth wall turbulent flow curves and starts at values lower than predicted for their respective k/D values. As the Newtonian Reynolds number increases the friction factor value of the rough pipes increases until it eventually settles on the respective k/D curves predicted for those rough pipes.

4.3.2 Roughness Function Correlation

In Figure 4.2 the roughness function B versus the roughness Reynolds number is plotted. The different lines on the curve have been explained in detail in Chapter 2 and will only be discussed briefly again.

The top curve is the locus of data presented by Nikuradse for pipes roughened with sand. The lower curve represents the locus of data by Colebrook & White for commercially available rough pipes. For fully developed rough wall turbulent flow the roughness function B approaches the value of 8.5 which represents the horizontal line on the curve. The oblique asymptote is the line which represents smooth wall turbulent flow.

The rough pipe data is in good agreement with the transition curve of Nikuradse. There is good agreement between the data where the roughness function B = 8.5 and where the friction factor becomes a constant at fully developed rough wall turbulent flow. Comparing Figure 4.1 and Figure 4.2 it is clear that the data in the transition zone on Figure 4.2 are the same data points in Figure 4.1, where the friction factor is still changing as the Reynolds number changes.

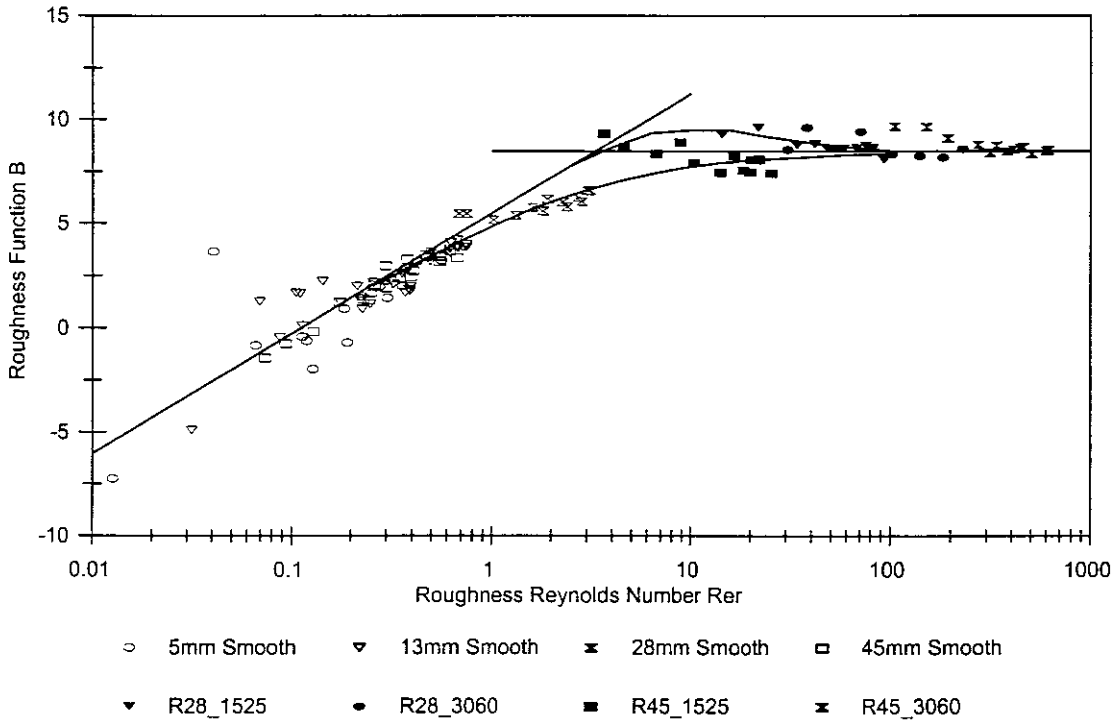

Figure 4.2: Roughness Function B vs Roughness Reynolds Number for Water.

4.4 Non-Newtonian Test Analysis

4.4.1 Introduction

After the clear water test analysis was finished, the author tested a variety of non-Newtonian fluids. Detailed figures are presented of all the non-Newtonian tests in Appendix A. Table 4.4 is a summary of the slurry properties.

4.4.2 Rheological Characterisation

All the slurries tested by the author are characterised as homogeneous slurries. In other words, a two phase solid mixture in which the solids do not settle out. This is strictly not true because with the most homogeneous slurries the solids will settle out with time. This may take a couple of days or even months. Some authors use the term "slow settling slurries".

Only the fluids that contain solids like the kaolin slurry and the tailings' slurry are not pure homogeneous mixtures. Glycerol and CMC are considered to be pure homogeneous

mixtures as the different mixtures do not contain any solid particles and the mixture is homogeneous.

The rheological characterisation procedure consists of using the data points in laminar flow to extract the rheological constants τ_y, K and n. These parameters are important because they are used in all the formulas to analyse roughness behaviour, as discussed in Chapter 2.

Table 4.4: Non-Newtonian Slurries Properties.

Slurry Type	Slurry Relative Density	Solids Density	Viscous Properties		
	S_m	S_s	τ_y	K	n
Glycerol	1.0906	N/A	0	0.00274	1.000
	1.1433		0	0.00802	1.000
CMC	1.0129	N/A	0	0.84959	0.026
	1.0269		0	0.12106	0.827
	1.0372		0	0.37011	0.787
Kaolin	1.0803	2.65	5.505	0.28786	0.463
	1.1460		14.286	0.87945	0.443
	1.1779		35.789	0.27887	0.617
Tailings	1.7309	3.7	2.584	0.00287	1.202
	1.8012		4.960	0.01689	1.001

4.4.3 Turbulent Flow in Rough Pipes

In this section the turbulent flow of the non - Newtonian fluids in the rough pipes will be discussed. The different models are applied and the effect of the roughness will be shown. The transition region will also be looked at, as well as the influence of pipe roughness in the transition region. In this section only the modelling of the rough pipes will be shown. The smooth pipe data is shown in Appendix C.

4.4.3.1 Turbulent Flow Data and Modelling of Glycerol.

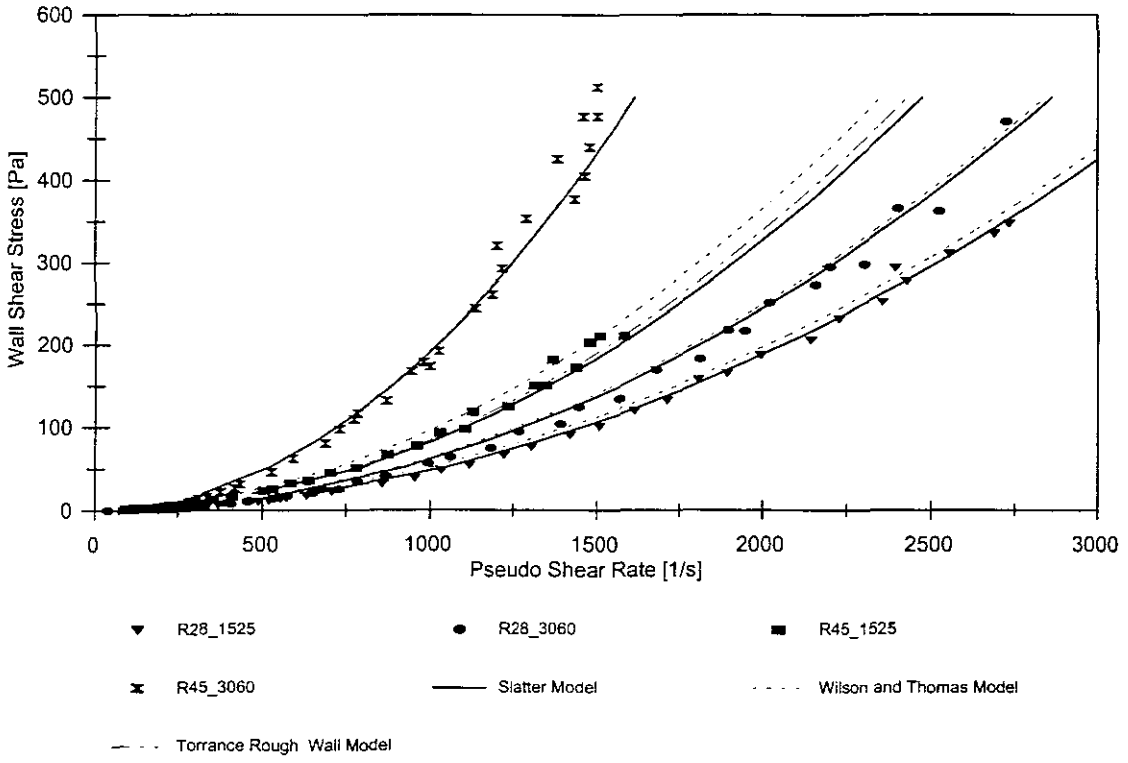

Figure 4.3: Glycerol at a Slurry Relative Density of 1.0906

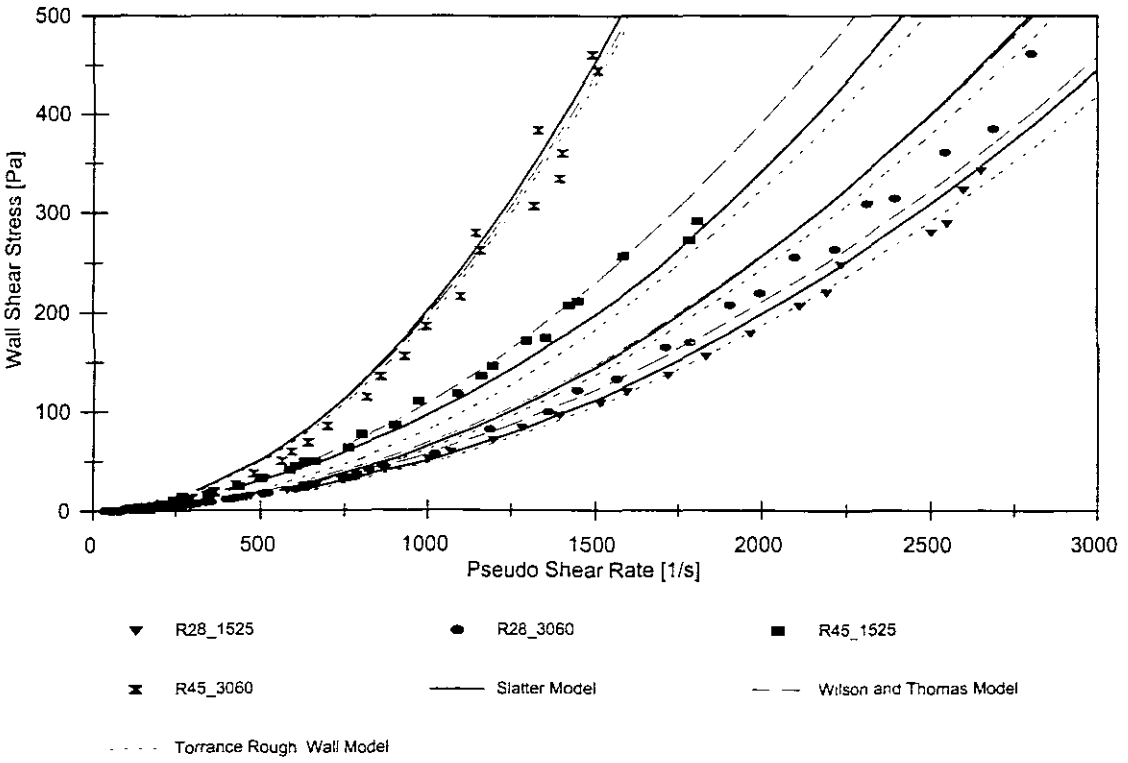

Figure 4.4: Glycerol at a Slurry Relative Density of 1.1433

In both cases the models seem to fit the turbulent flow rough pipe data for Glycerol very

well. All three models that have been used predict the turbulent flow data very accurately and there are very little differences between these models at the various densities.

4.4.3.2 Turbulent Flow Data and Modelling for CMC.

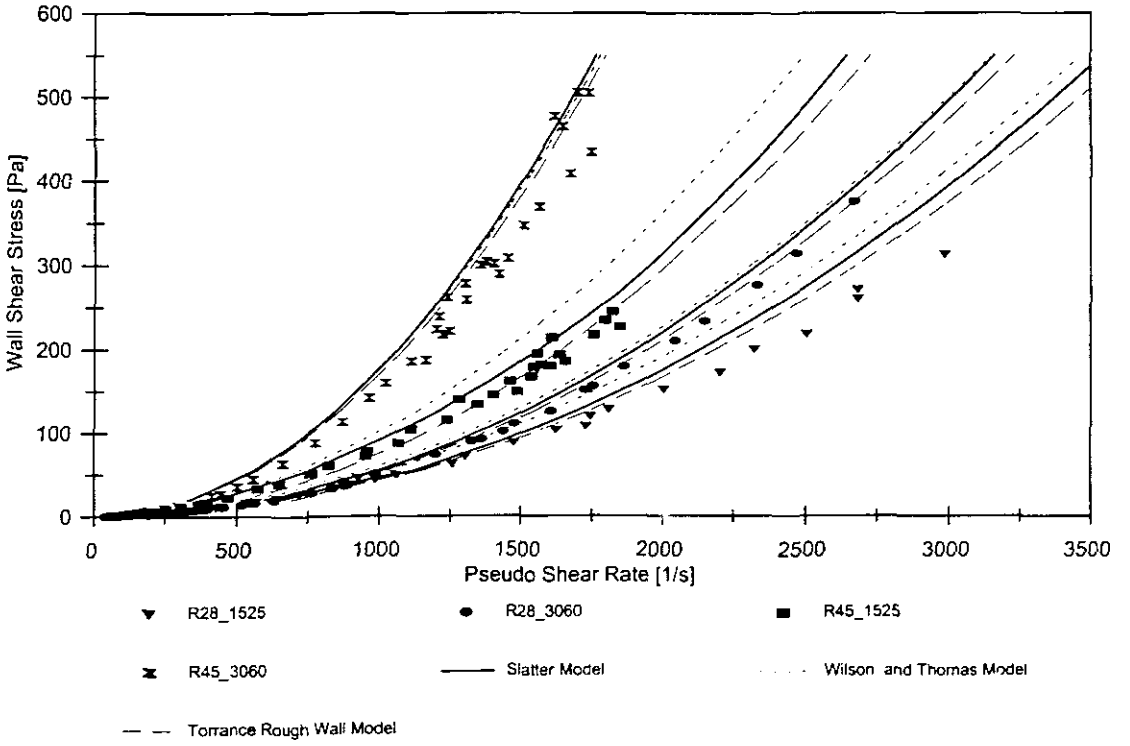

Figure 4.5: CMC at a Slurry Relative Density of 1.0129

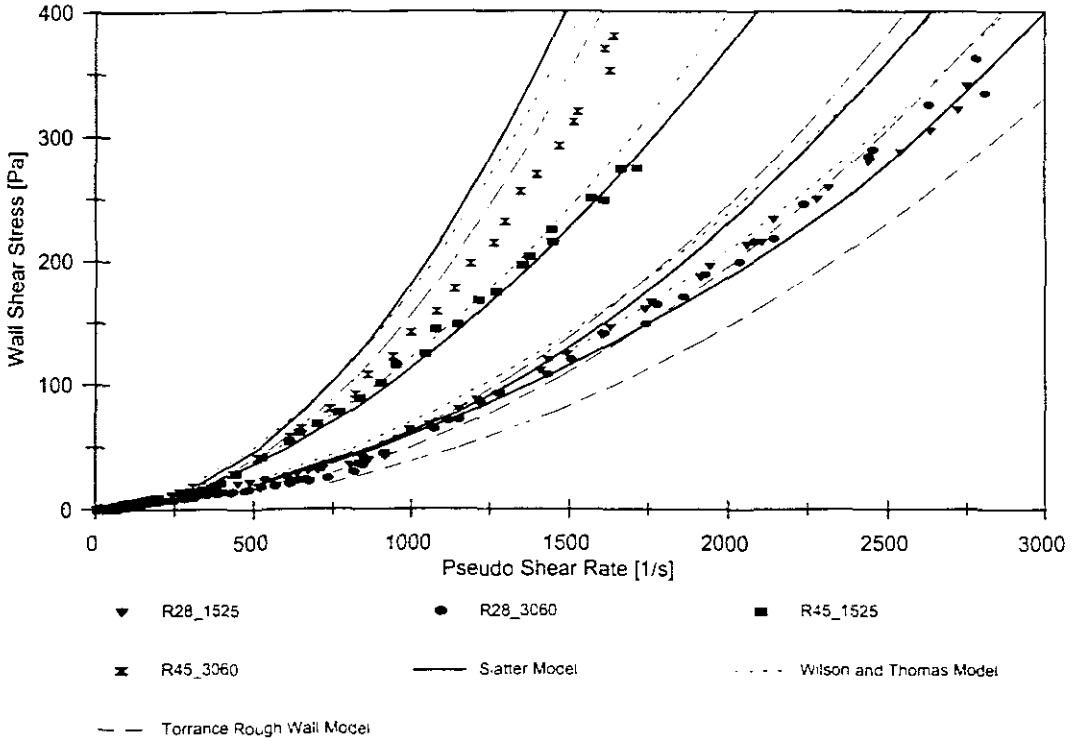

Figure 4.6: CMC at a Slurry Relative Density of 1.0269

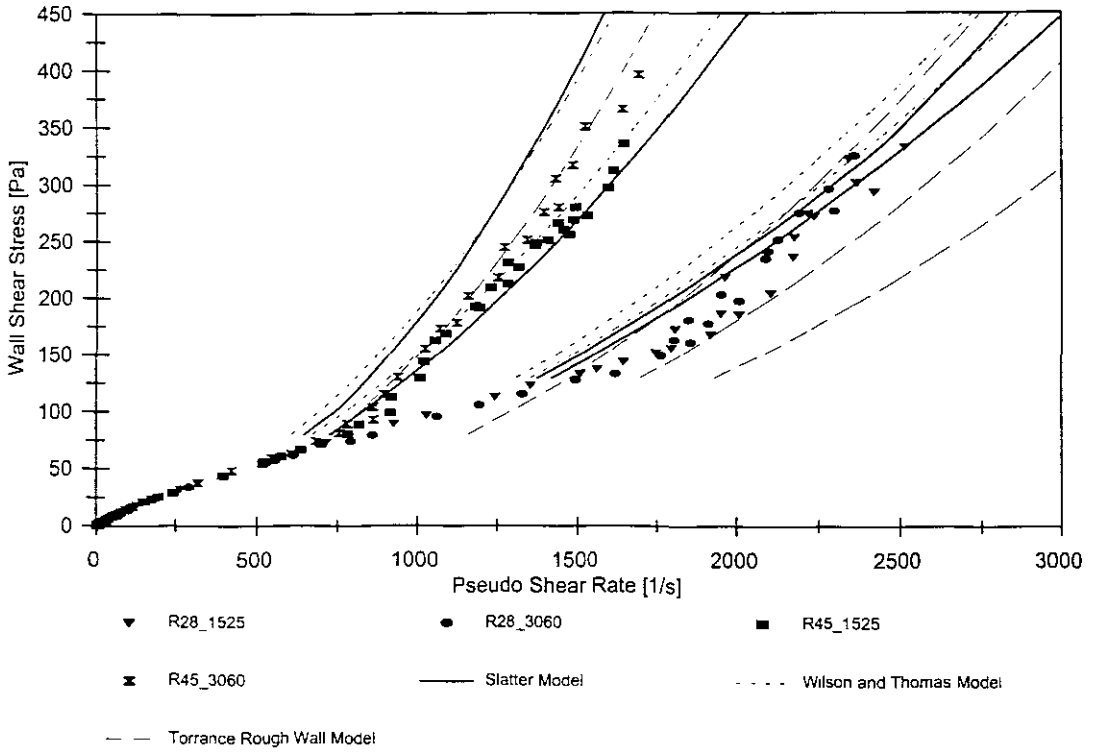

Figure 4.7: CMC at a Slurry Relative Density of 1.0372

As the relative density of CMC increases from 1.0129 to 1.0372, the models become increasingly inaccurate. At a relative density of 1.0129 all the models tend to over predict slightly. As the relative density increases the Torrance rough wall turbulent flow model start to under predict the turbulent flow where the Slatter and the Wilson model consistently over predict the turbulent flow.

As the relative density increases from 1.0129 to 1.0372 more smooth wall turbulent flow data is achieved and less fully developed rough wall turbulent flow over the same velocity range. The increase in relative density causes the smooth wall turbulent flow to dominate at higher pseudo shear rates. Only when fully developed rough wall turbulent flow is reached, does the roughness start to dominate and the smooth and rough pipe data separate from each other.

In all cases the models predict the smooth pipe turbulent flow data very well (Appendix C). The transition from laminar to turbulent for the same diameter smooth and rough pipe seem to be occurring at the same pseudo shear rate.

4.4.3.3 Turbulent Flow Data and Modelling for Kaolin

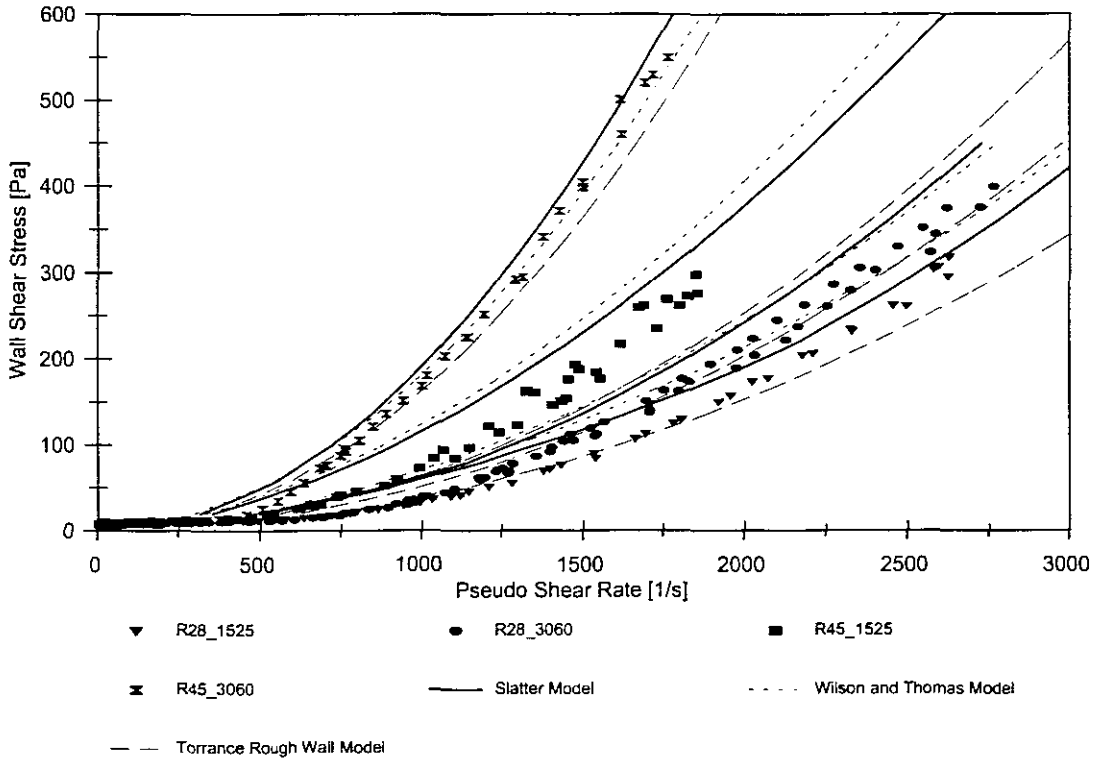

Figure 4.8: Kaolin at a Slurry Relative Density of 1.0803

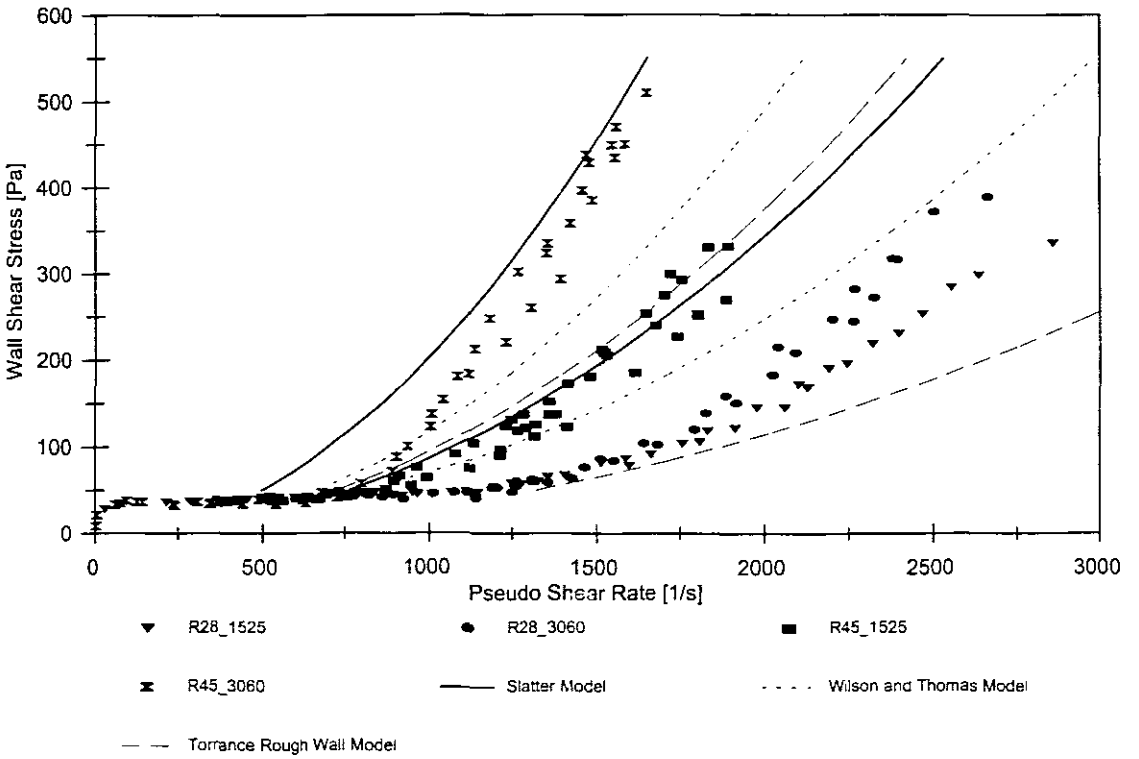

Figure 4.9: Kaolin at a Slurry Relative Density of 1.146

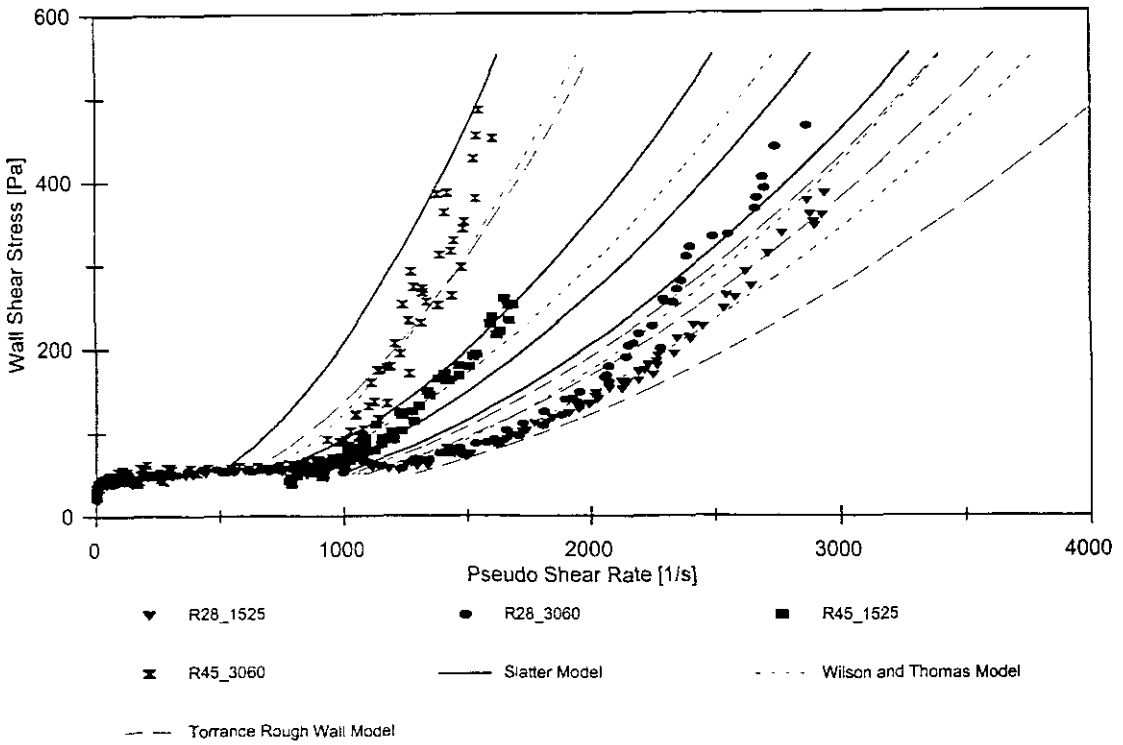

Figure 4.10: Kaolin at a Slurry Relative Density of 1.1779

The models did not perform that well predicting the turbulent flow for kaolin in the rough pipes at different relative densities. The Slatter and Wilson model tend to over predict the turbulent flow in the rough pipes. The Torrance rough wall turbulent flow model seems to under predict the turbulent flow of kaolin in the rough pipes. In general all the models perform badly in the early turbulent flow region. As the data reaches fully developed turbulent flow the models generally perform better.

The transition from laminar to turbulent flow for rough pips occurs at the same pseudo shear rates as for the smooth pipes. The models accounts for the roughness effects by shifting to the left of the smooth pipe turbulent flow prediction. This causes the models to be inaccurate in the early turbulent flow region as the transition from laminar to turbulent flow for the smooth and the rough pipes are the same.

All the models fit the smooth pipe data very well and the results are presented in Appendix C.

4.4.3.4 Turbulent Flow Data and Modelling for Tailings

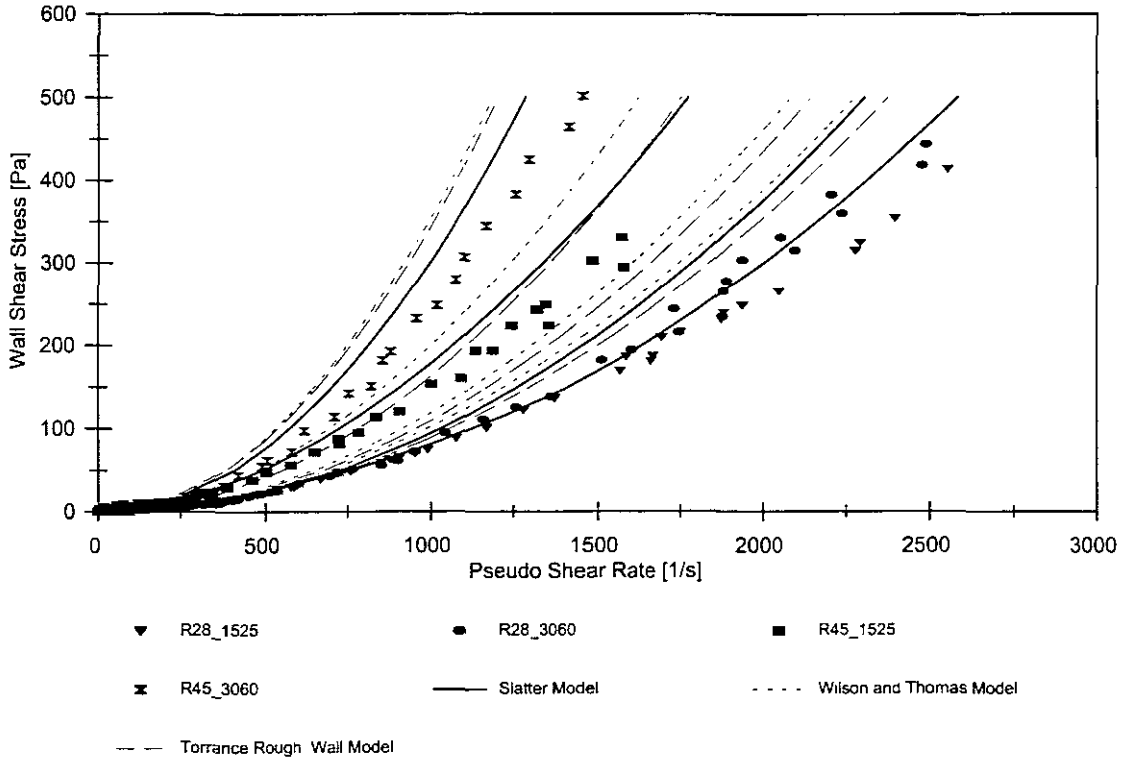

Figure 4.11: Tailings at a Slurry Relative Density of 1.7309

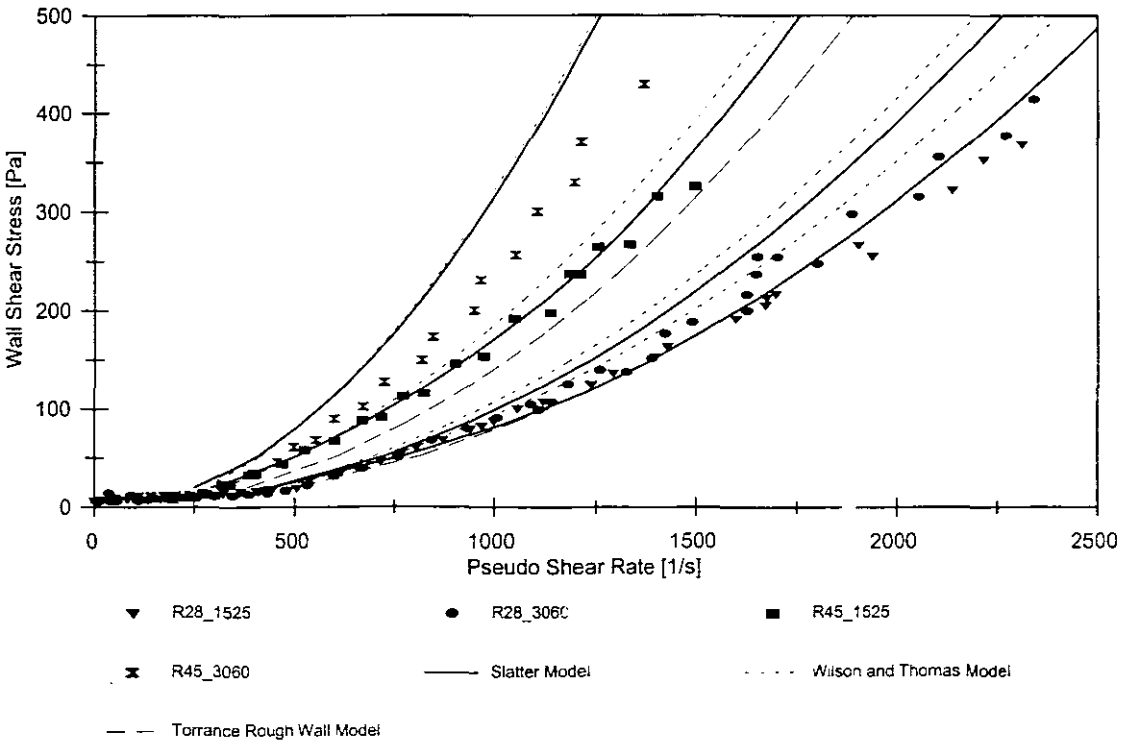

Figure 4.12: Tailings at relative density of 1.8012

Tailings were tested at relative densities of 1.7309 and 1.8012. In both cases the models

tend to over predict the 45mm rough pipe. The models performed slightly better when predicting the turbulent flow of the 28mm rough pipes. In general the models performed better at the higher relative density.

In the smooth pipe range the models performed fairly well with accurate predictions in the 28mm and 45mm nominal diameter pipe range. The models did not perform well in the 5mm to 13mm diameter pipe range and tend to over predict the turbulent flow. The models seem to perform the worst at the low concentration and a better fit was achieved at the higher concentration.

The transition from laminar to turbulent flow for the smooth and the rough pipes of the same diameter occurs at the same pseudo shear rates, and the models predict this very well.

4.4.4 Roughness Function Correlation

In this section the roughness Reynolds number formulated by Slatter (1994,1995a) will be used and correlated against the roughness function B (Nikuradse, 1933). The different test fluids will be presented and discussed in this section.

4.4.4.1 Glycerol Test Results

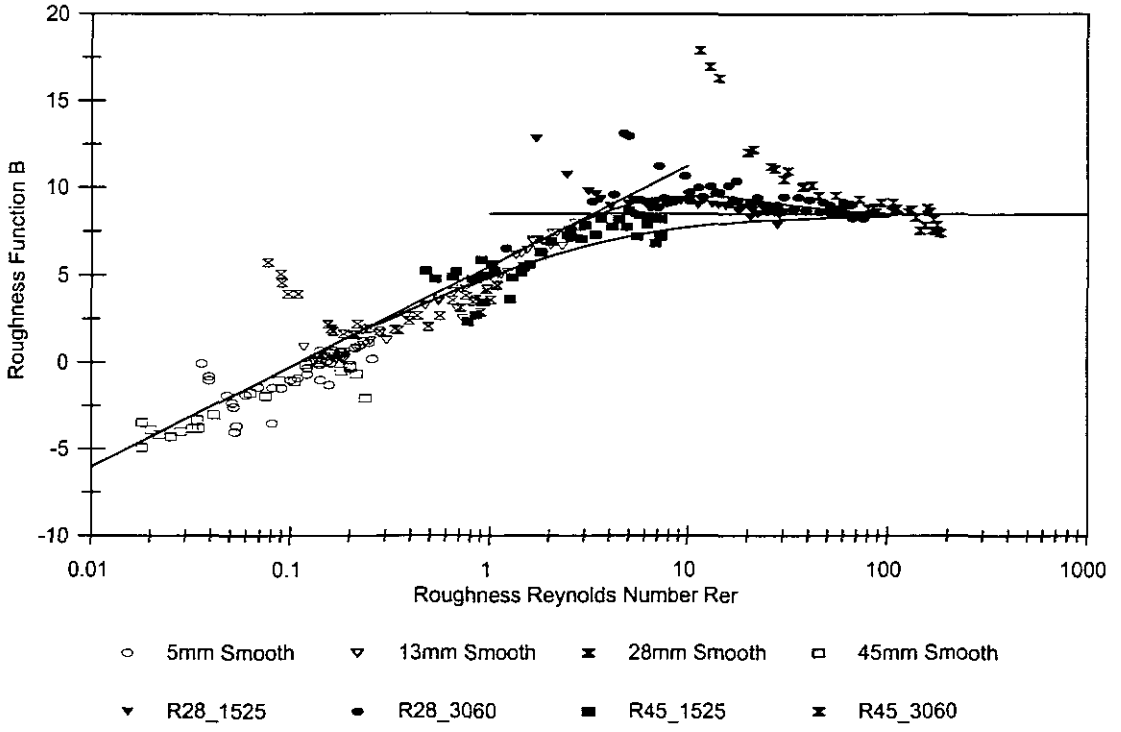

Figure 4.13: Roughness Function B vs Roughness Reynolds Number for Glycerol at a Slurry Relative Density of 1.0906

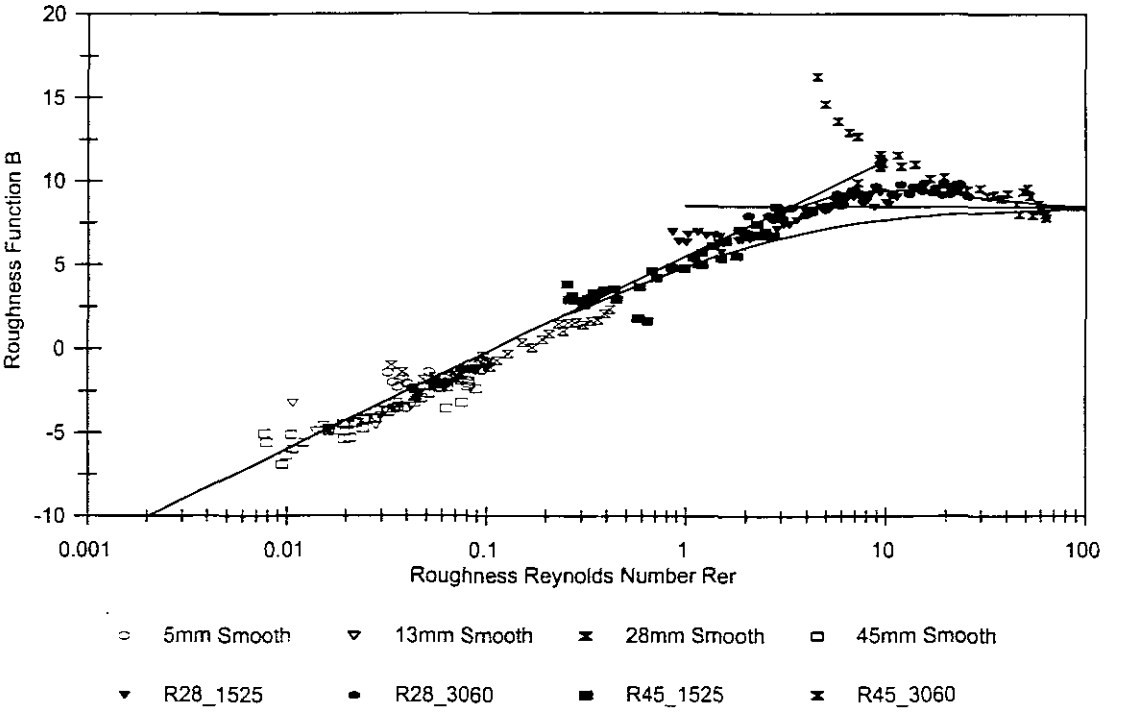

Figure 4.14: Roughness function B vs Roughness Reynolds number for Glycerol at a slurry relative density of 1.1433

In both cases there is a very good correlation in the prediction of the roughness function B and the smooth and rough pipe data.

It is clear that at both densities the B-value of the data is separated by pipe roughness. All the smooth pipe data follow the oblique asymptote which represents smooth wall turbulent flow. The rough pipe data start at the top curve which represents Nikuradse's transition curve for sand roughened pipes. In both cases the rough pipe with the lowest roughness start at the lowest B-value on the transition curve and as the Reynolds number increases the data follows the shape of the curve. The roughest pipe in both cases settles on the horizontal asymptote which represents fully developed rough wall turbulent flow with a B-value of 8.5. The rough pipe data is also separated from the left to the right of the curve as the roughness increases. There is no diameter effect as it is incorporated in the roughness Reynolds number.

Most of the rough pipes have a short "tail" which starts off with B-values higher than the transition curve and migrates downwards until it lies on the transition curve. This data is in the critical flow zone area where the flow is neither laminar nor turbulent.

4.4.4.2 CMC Test Results

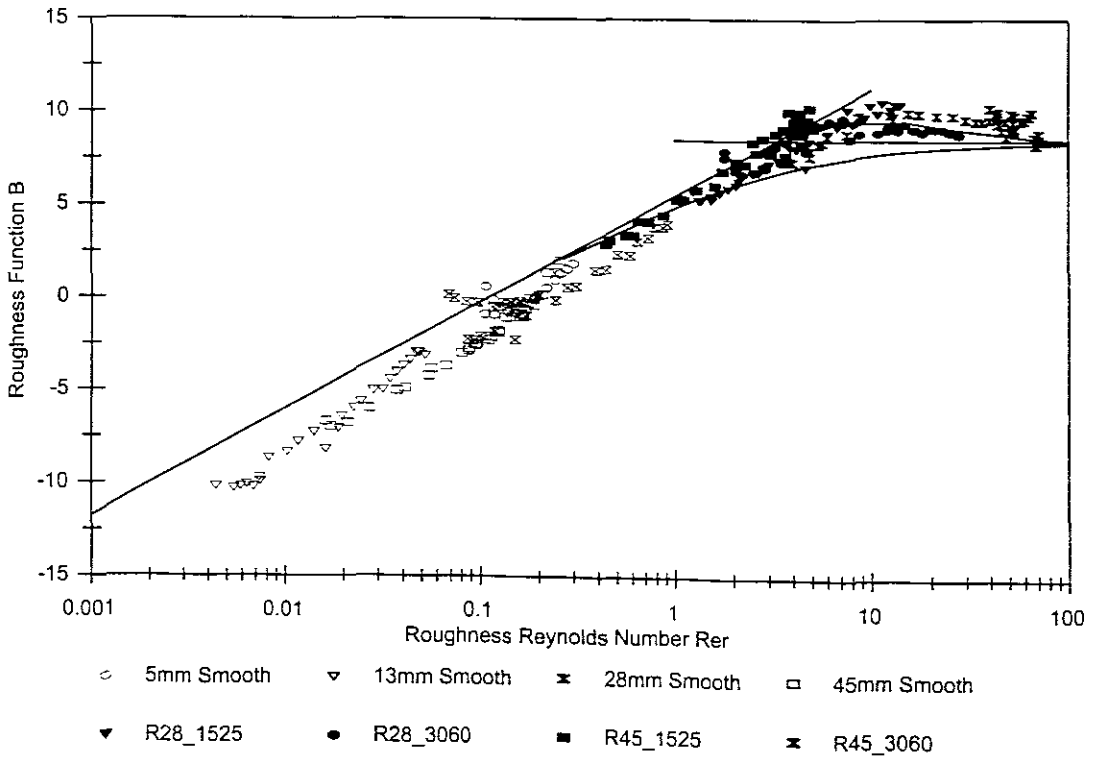

Figure 4.15: Roughness Function B vs Roughness Reynolds Number for CMC at a Slurry Relative Density of 1.0129

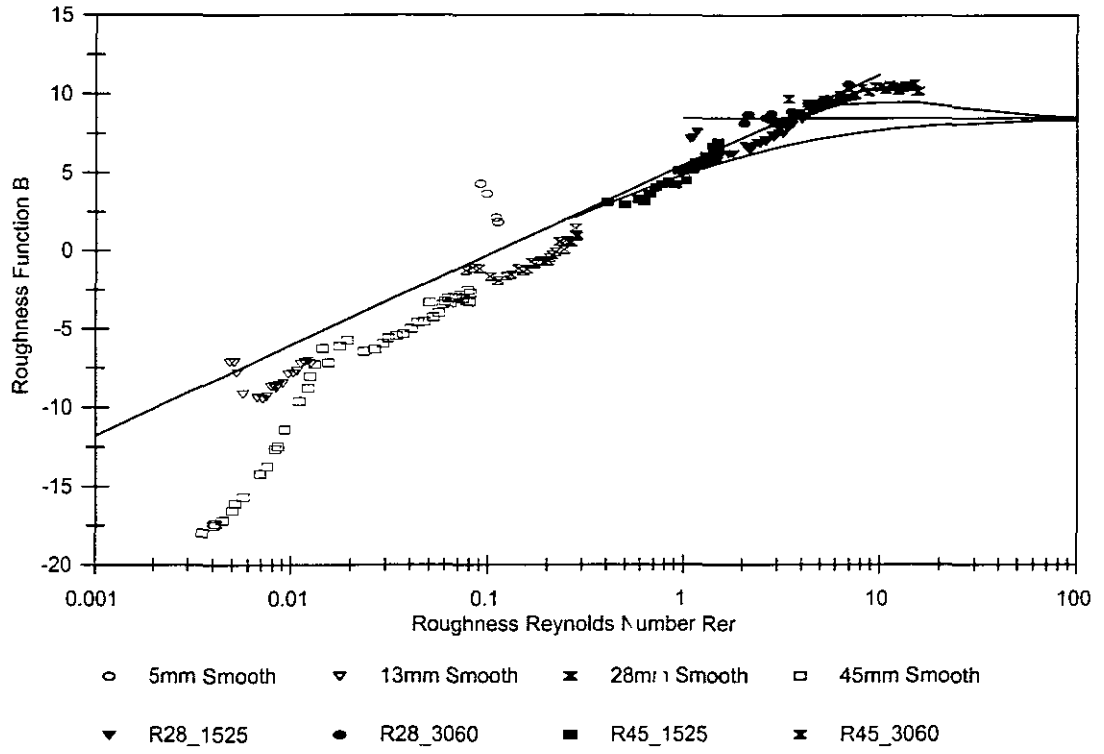

Figure 4.16: Roughness Function B vs Roughness Reynolds Number for CMC at a Slurry Relative Density of 1.0269

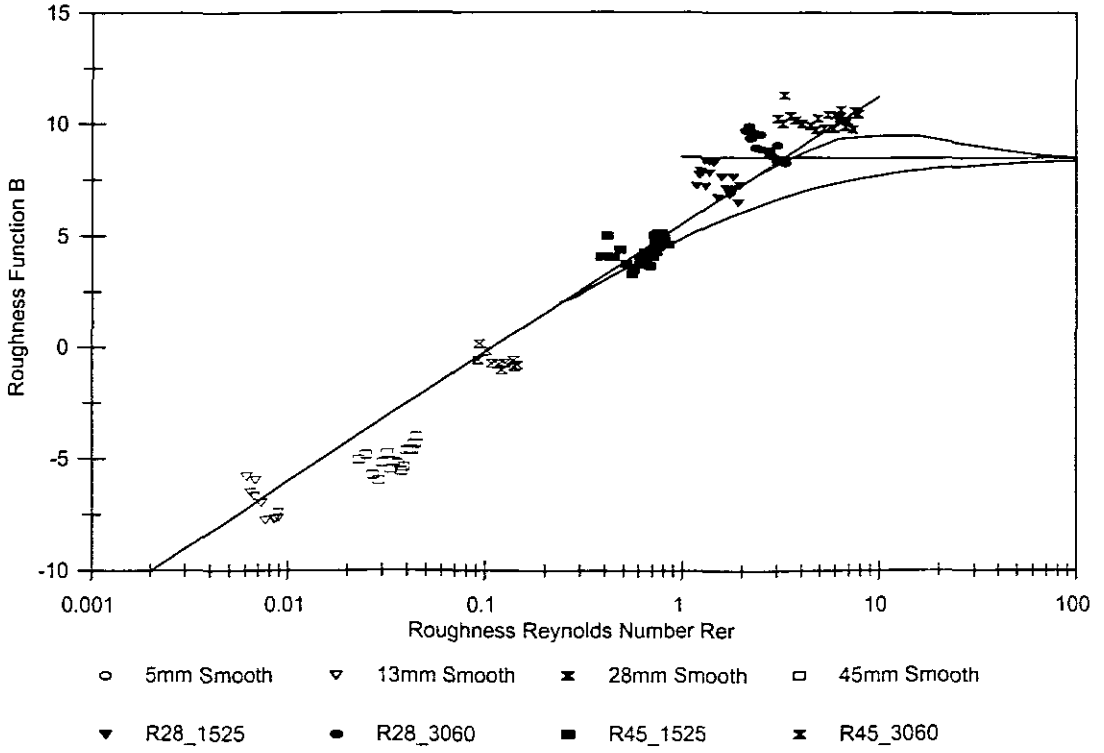

Figure 4.17: Roughness Function B vs Roughness Reynolds Number for CMC at a Slurry Relative Density of 1.0372

CMC was tested at three relative densities ranging from 1.0129 to 1.0372. As the relative density increases the amount of measured turbulent data decreased. The smooth pipe data in all cases follows the oblique asymptote for smooth wall turbulent flow.

The B-values of the smooth pipe data consistently falls below the smooth wall turbulent flow line. This could be due to the rheological characterisation as the roughness Reynolds number is sensitive to change in the rheological parameters. However, good correlation is achieved in the rough pipe data.

The rough pipe data represents a very good fit for all relative densities tested. The B-values of the different rough pipes are separated again by the difference in hydraulic roughness between the pipes. In this case fully developed rough wall turbulent flow was not achieved and all the rough pipe data accumulates on the top transition curve which represent the transition between smooth wall turbulent flow and fully developed rough wall turbulent flow for sand roughened pipes.

4.4.4.3 Kaolin Test Results

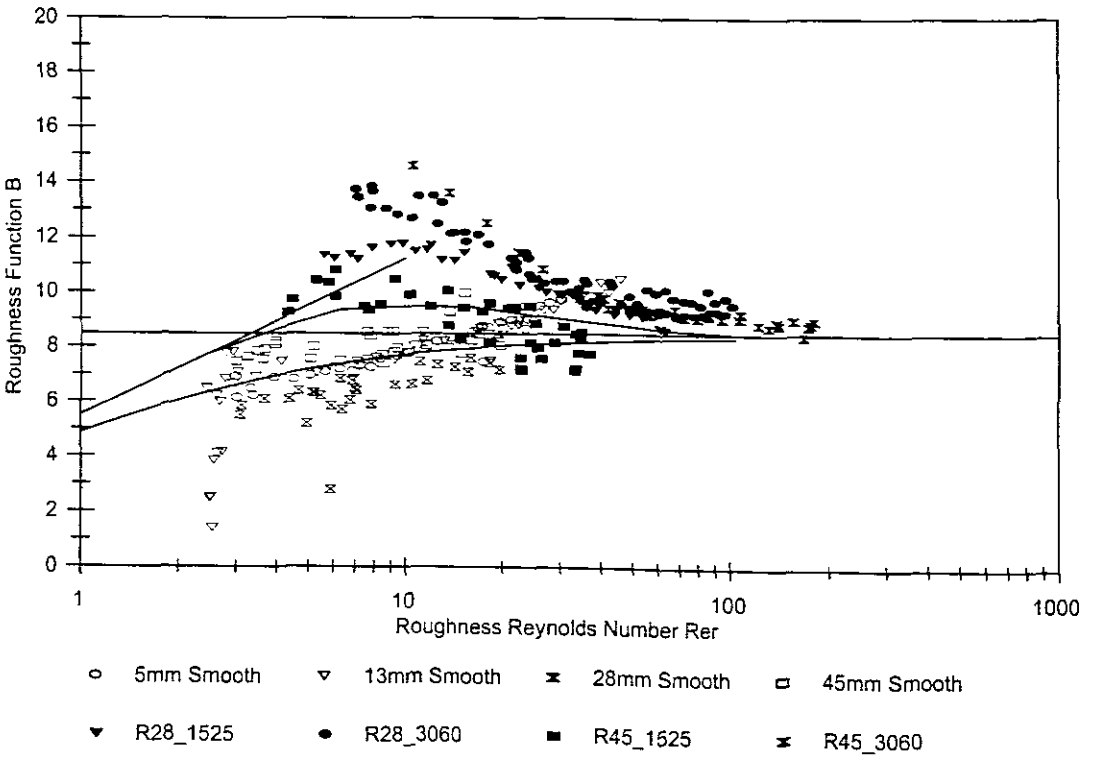

Figure 4.18: Roughness Function B vs Roughness Reynolds Number for Kaolin at a Slurry Relative Density of 1.0803

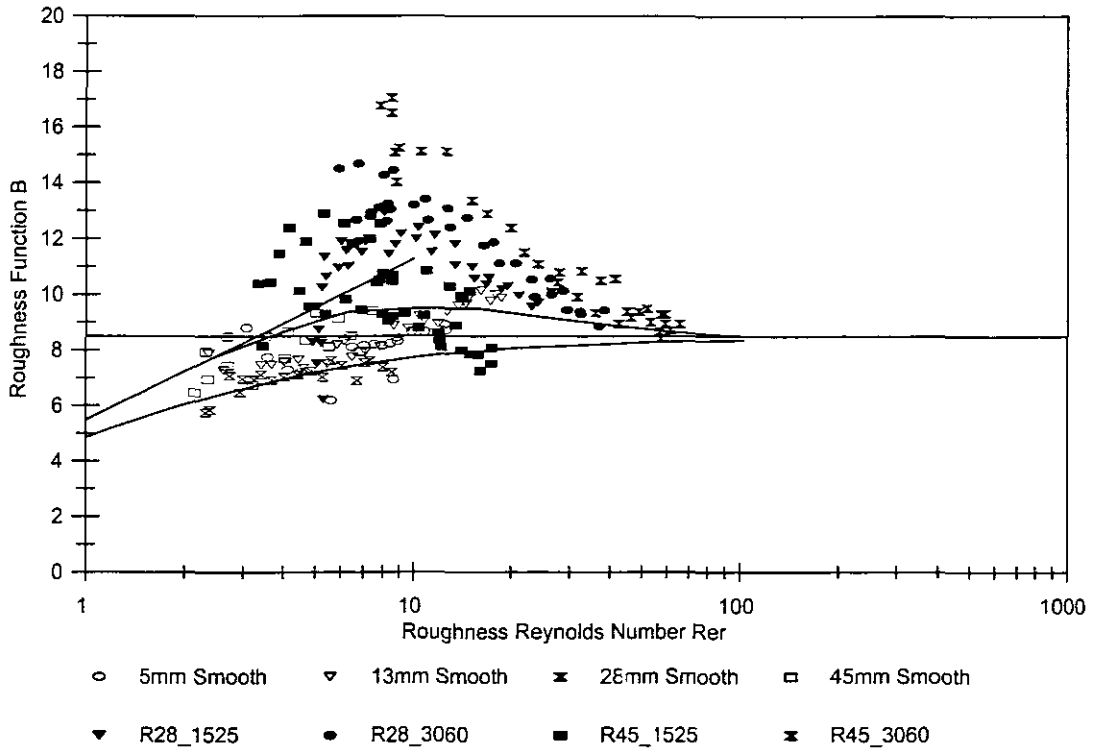

Figure 4.19: Roughness Function B vs Roughness Reynolds Number for Kaolin at a Slurry Relative Density of 1.146

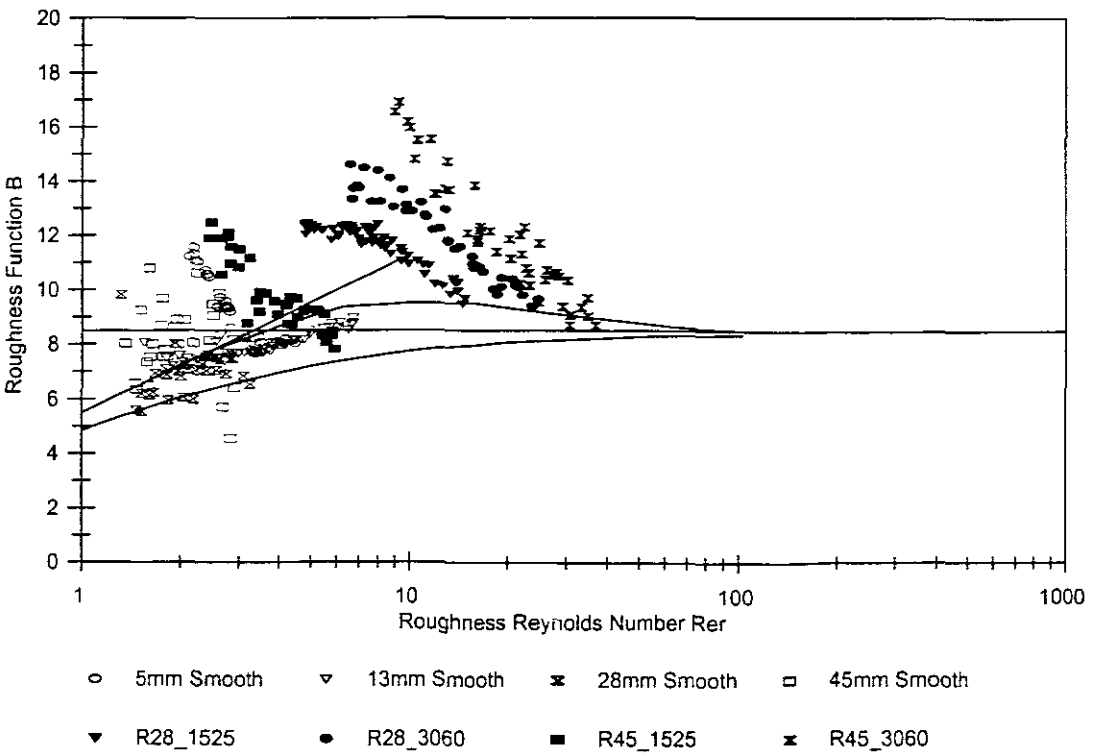

Figure 4.20: Roughness Function B vs Roughness Reynolds Number for Kaolin at a Slurry Relative Density of 1.1779

Kaolin was tested at three relative densities. The smooth pipe data accumulates on the

bottom curve which represents Colebrook & White's curve for commercially available rough pipes. In this case the roughness of the smooth pipes were taken as 15μm which is the d_{85} percentile particle of the kaolin slurry. All the smooth pipe data lie on top of each other and there is very little difference in the B-values. The increase in relative density causes the smooth pipe data to shift from the right of the curve to the left.

The rough pipe data behaves distinctly different. At the different relative densities the rough pipe data are mainly separated by the B-values where the roughness Reynolds number range for all sets of data is approximately within the same range. As the relative density increases the data shifts to the left of the curve as the roughness Reynolds number decreases for the same velocity range. The increase in relative density also seems to alter slightly higher B-values. The rough pipe with the lowest hydraulic roughness is shifted to the left of the curve and as the hydraulic roughness of the rough pipes increases the data are shifted to the right of the curve.

In all the tests for kaolin, the B-values are higher than predicted for rough pipes in the transition zone where the pipe with the greatest hydraulic roughness has the highest B-values. As the hydraulic roughness of the rough pipes decrease so do the B-values. The shape of the rough pipe data curves is the same as Nikuradse's transition curve, but the B-values are higher.

The B-values seem to be insensitive to change as the relative density increases. The roughness Reynolds number range changes for each data set as the relative density increases.

4.4.4.4 Tailings Test Results

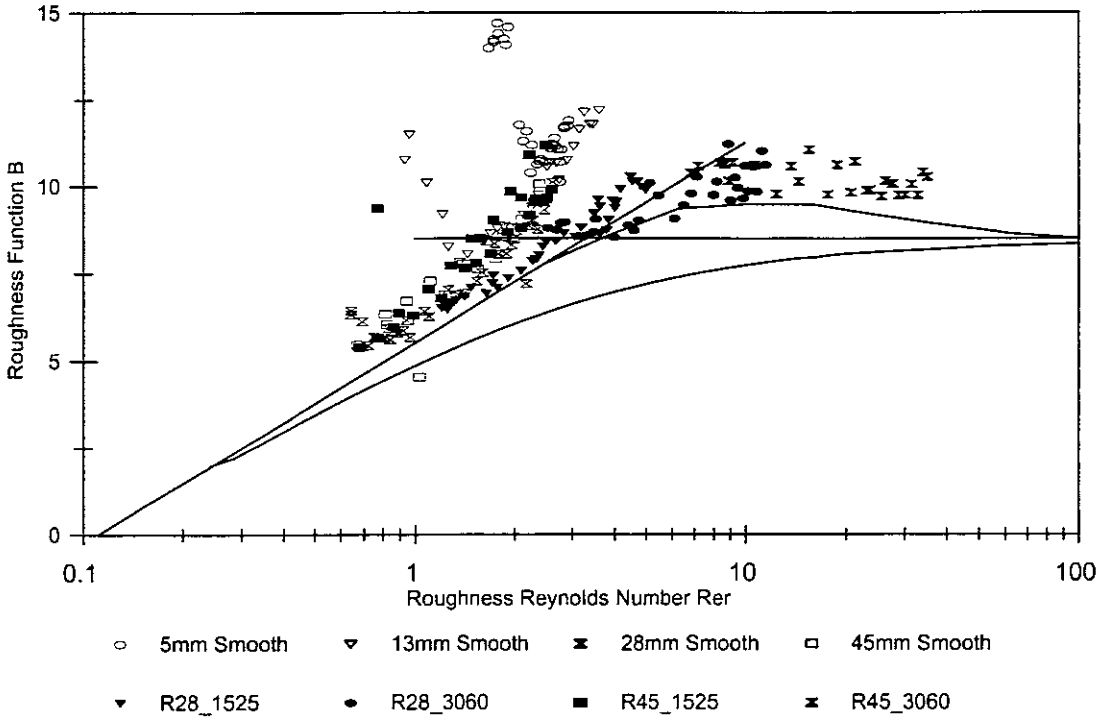

Figure 4.21: Roughness Function B vs Roughness Reynolds Number for Tailings at a Slurry Relative Density of 1.7309

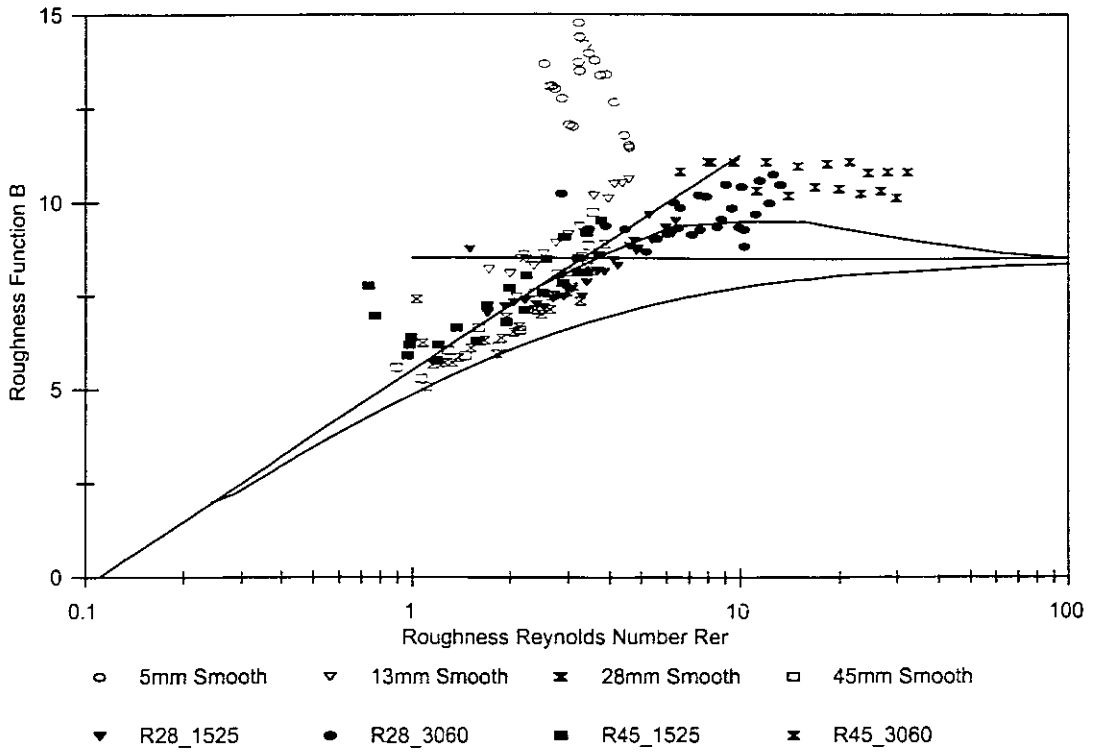

Figure 4.22: Roughness function B vs Roughness Reynolds number for Tailings at a slurry relative density of 1.8012

Tailings were tested at two relative densities of 1.7309 and 1.8012. At a relative density of 1.7309 the smooth pipe data lies very high on the oblique asymptote which represents smooth wall turbulent flow. The slope of the data points seems to be the same as this oblique asymptote but the B-values of the data are slightly higher than this line. The results indicate that there are a lot of smooth pipe data that falls within the critical flow zone and the data lie well above the smooth wall turbulent flow line. At a relative density of 1.8012 the smooth pipe data fitted the smooth wall turbulent flow line better but there are still some data that falls in the critical flow zone. The representative pipe roughness of the smooth pipe data was taken as 85 μm that was the d_{85} percentile particle size of the tailings.

At both relative densities the rough pipe data agrees very well with top transition curve although the B-values are slightly higher. The data again seems to be separated by the pipe roughness from the left of the curve to the right where the roughest pipe data would be shifted to the right. In both cases fully developed rough wall turbulent flow was not achieved and all the rough pipe data lies on top of the top transition curve for sand roughened pipes. The data indicates that an increase in slurry relative density also slightly increases the B-values.

Both smooth and rough pipe data are grouped quite closely together where most of the smooth pipes data would lie to the left of the curve and the sand roughened pipes to the right of the curve. Very little of the rough pipe data falls within the critical flow zone where this is not the case for the smooth pipes.

4.4.5 Friction Factor vs Non - Newtonian Reynolds Number

In this section the Fanning friction factor will be correlated against the non-Newtonian Reynolds number of Slatter & Lazarus (1993). All the test fluids will be presented and discussed in this section.

4.4.5.1 Glycerol Test Results

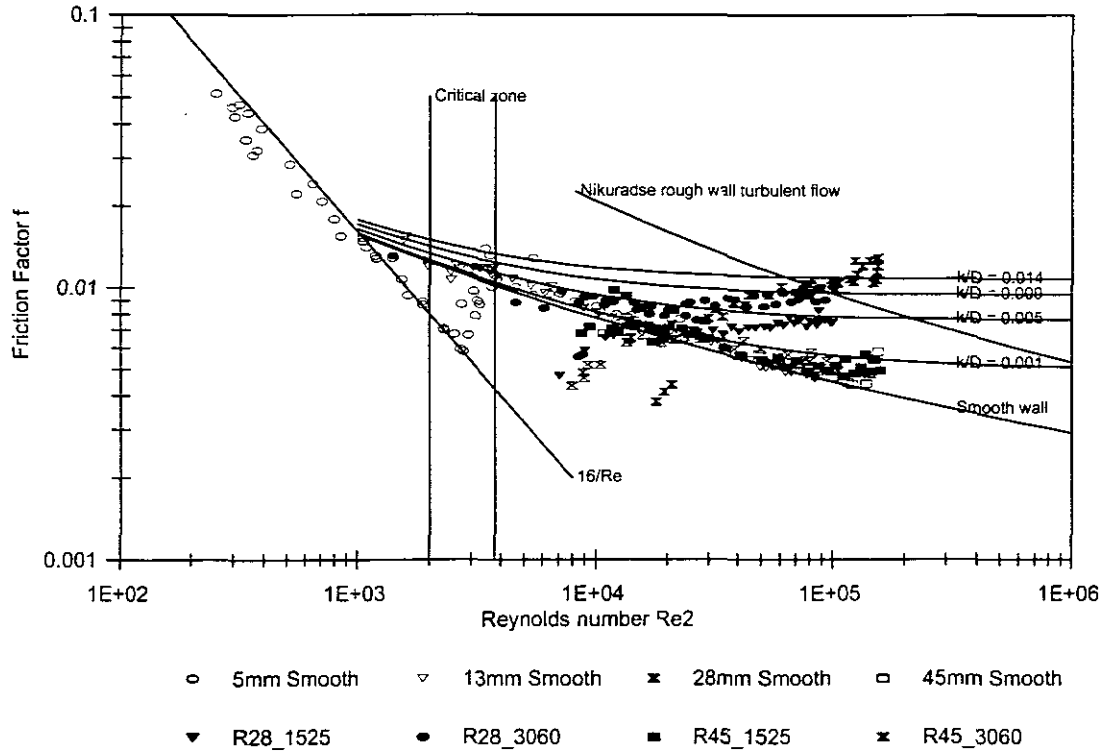

Figure 4.23: Fanning Friction Factor vs non-Newtonian Reynolds Number for Glycerol at a Solution Relative Density of 1.0906

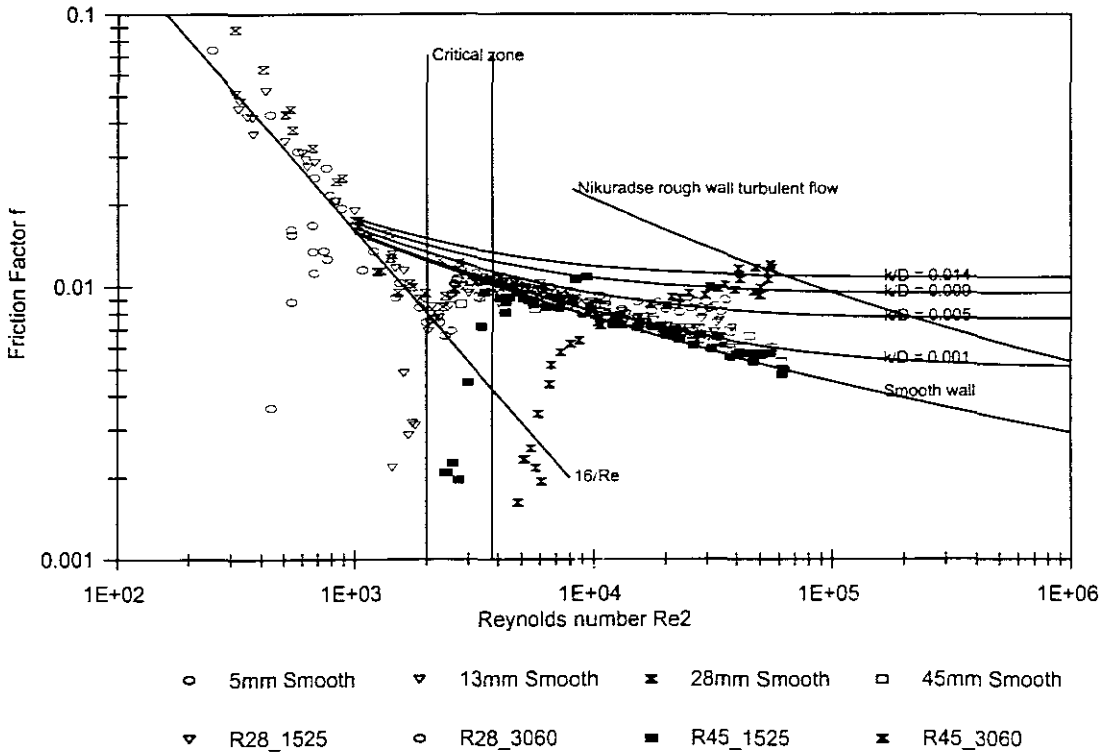

Figure 4.24: Fanning Friction Factor vs non-Newtonian Reynolds Number for Glycerol at a Solution Relative Density of 1.1433

The smooth pipe data of glycerol behaves as expected. As pipe diameter decreases, more laminar flow is achieved and is clearly seen from the 5mm smooth pipe data. The smooth pipe data are grouped closely together and follow the same pattern at both relative densities. The rough pipe data behaves quite differently than the smooth pipe data.

All the laminar smooth pipe data falls on the 16/Re line. The rough pipe data behaved quite differently and no data followed the 16/Re line. At low Reynolds numbers the data would start at low friction factor values and would steadily increase as the Reynolds number increases. At the higher Reynolds numbers the friction factors settle on the different k/D values predicted for those rough pipes. The transition from laminar to turbulent flow occurs in the critical zone for the smooth pipes. There seems to be no definite pattern for the rough pipes.

In both cases of different relative densities the friction factors of the rough pipes are still increasing until fully developed rough wall turbulent flow is reached. Once fully developed rough wall turbulent flow is reached the friction factor stops changing and follows a straight line.

4.5.5.2 CMC Test Results

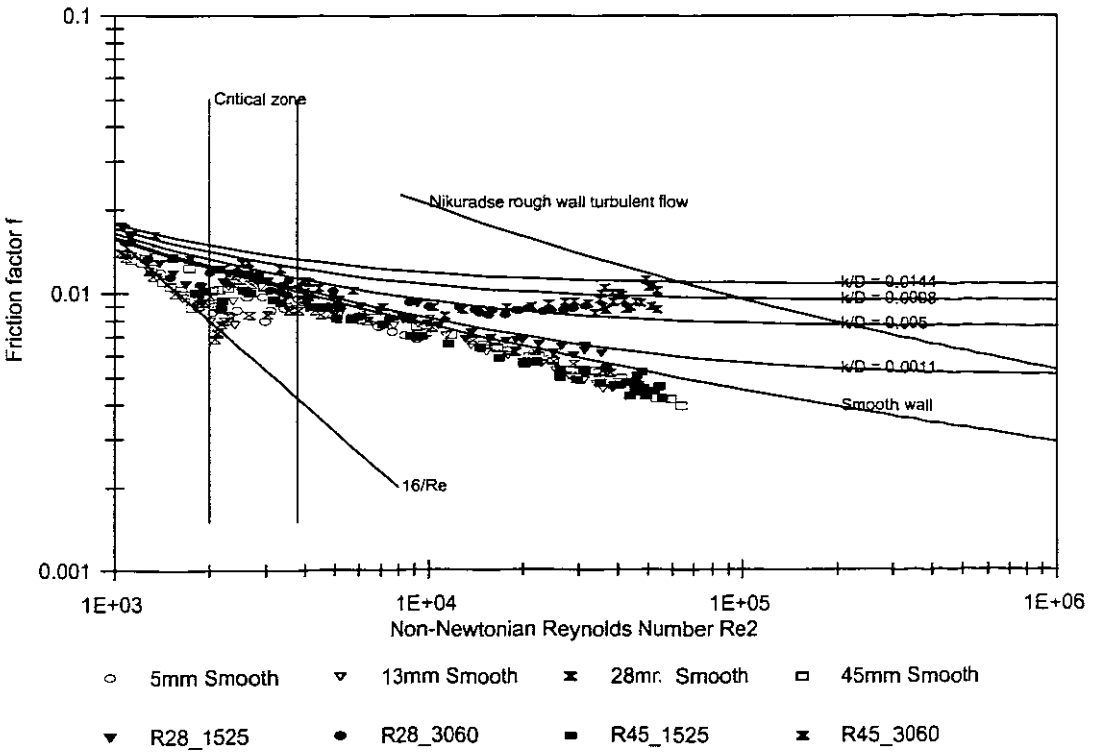

Figure 4.25: Fanning Friction Factor vs non-Newtonian Reynolds Number for CMC at a Solution Relative Density of 1.0129

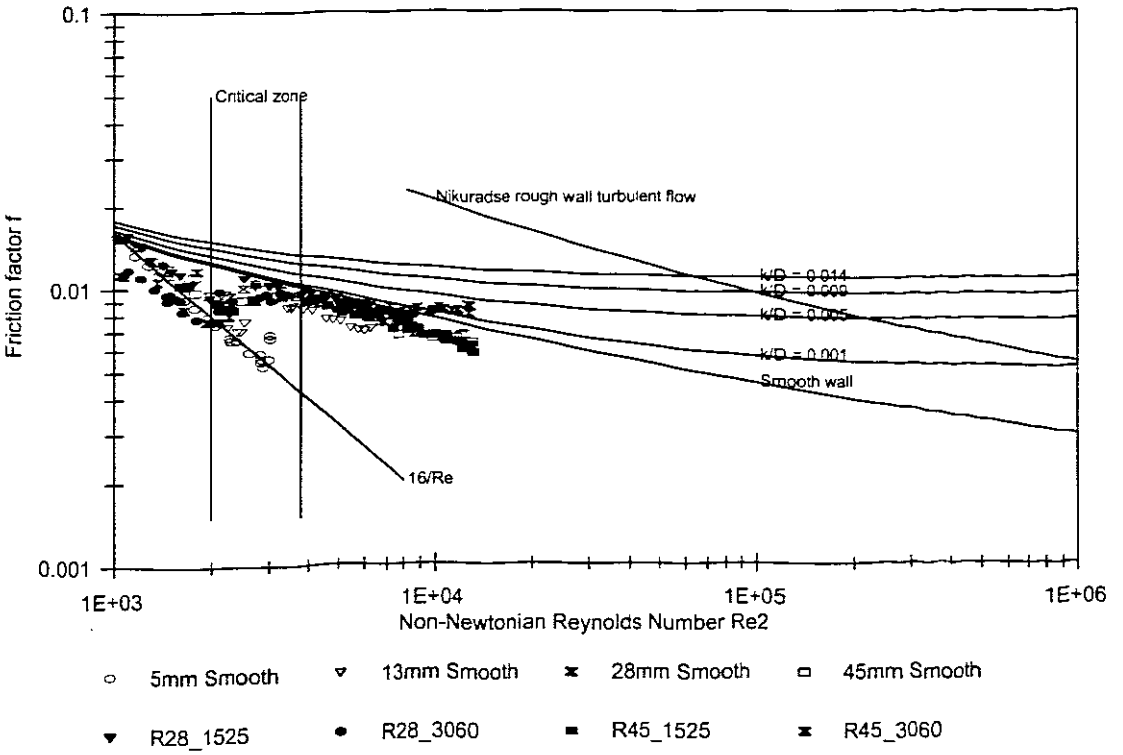

Figure 4.26: Fanning Friction Factor vs non-Newtonian Reynolds Number for CMC at a Solution Relative Density of 1.0269

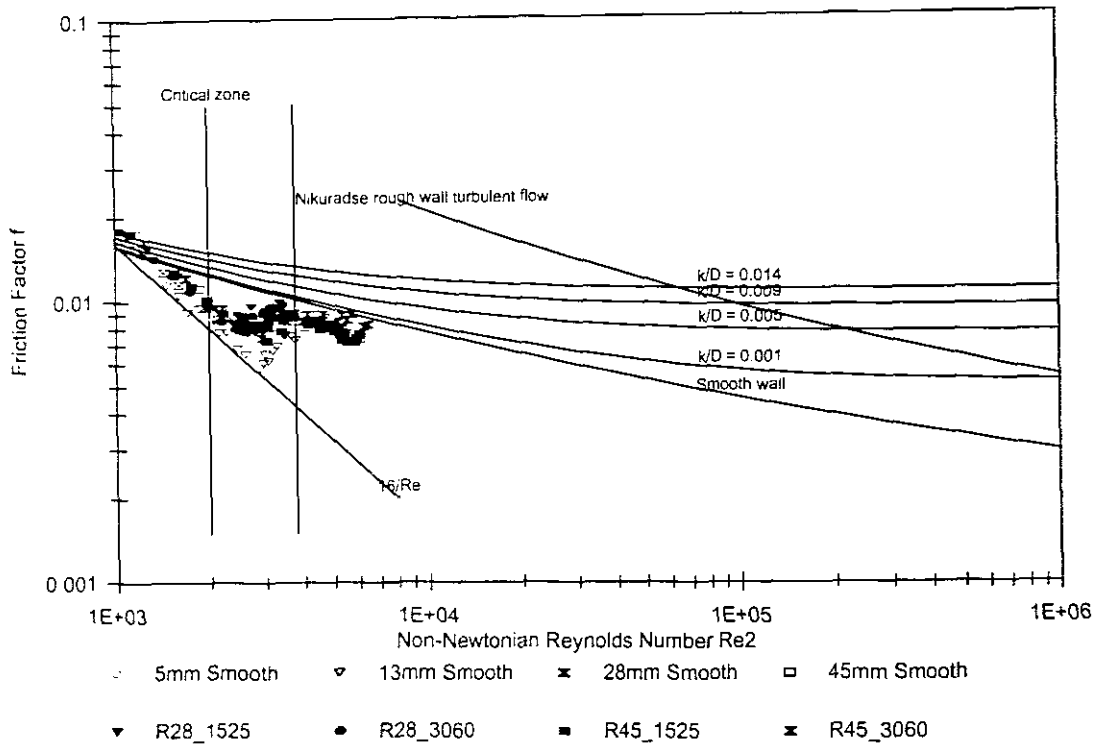

Figure 4.27: Fanning Friction Factor vs non-Newtonian Reynolds Number for CMC at a Solution Relative Density of 1.0372

CMC was tested at three slurry relative densities. In all cases the smooth and rough pipe data behave similar except at high Reynolds numbers. At all three slurry relative densities the laminar flow data of the smooth and rough pipes falls on the 16/Re line.

The transition from laminar to turbulent flow in the critical zone occurs at the same Reynolds numbers for the smooth and the rough pipes.

The smooth and rough pipe data start to separate in the smooth wall turbulent flow region. The smooth and rough pipe data separate at the same Reynolds numbers irrespective of the relative density. As the relative density increases the data shifts to the left of the curve as the Reynolds number decreases for the same velocity range. No fully developed rough wall turbulent flow was achieved and it is difficult to predict if the data would settle on their respective k/D curves in this region.

All the friction factor data lie slightly below the smooth wall turbulent flow line. This may be due to drag reduction in the smooth and the rough pipes where the friction factors is less than predicted for smooth wall turbulent flow.

4.5.5.3 Kaolin Test Results

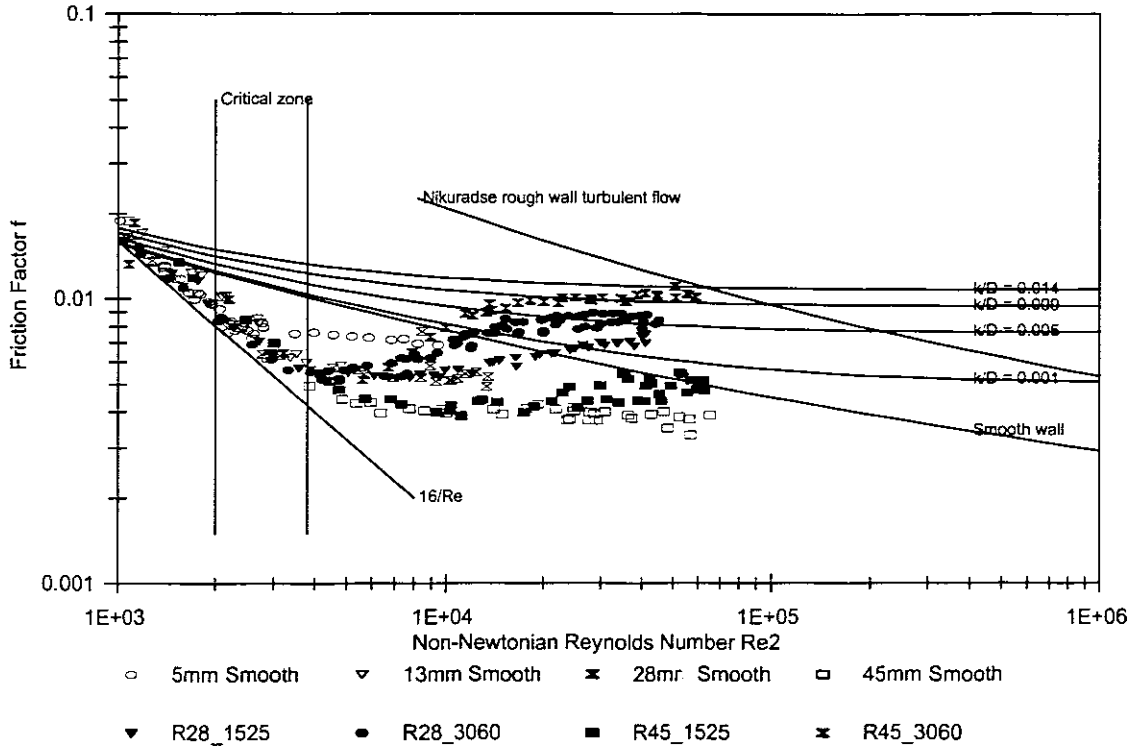

Figure 4.28: Fanning Friction Factor vs non-Newtonian Reynolds Number for Kaolin at a Slurry Relative Density of 1.0803

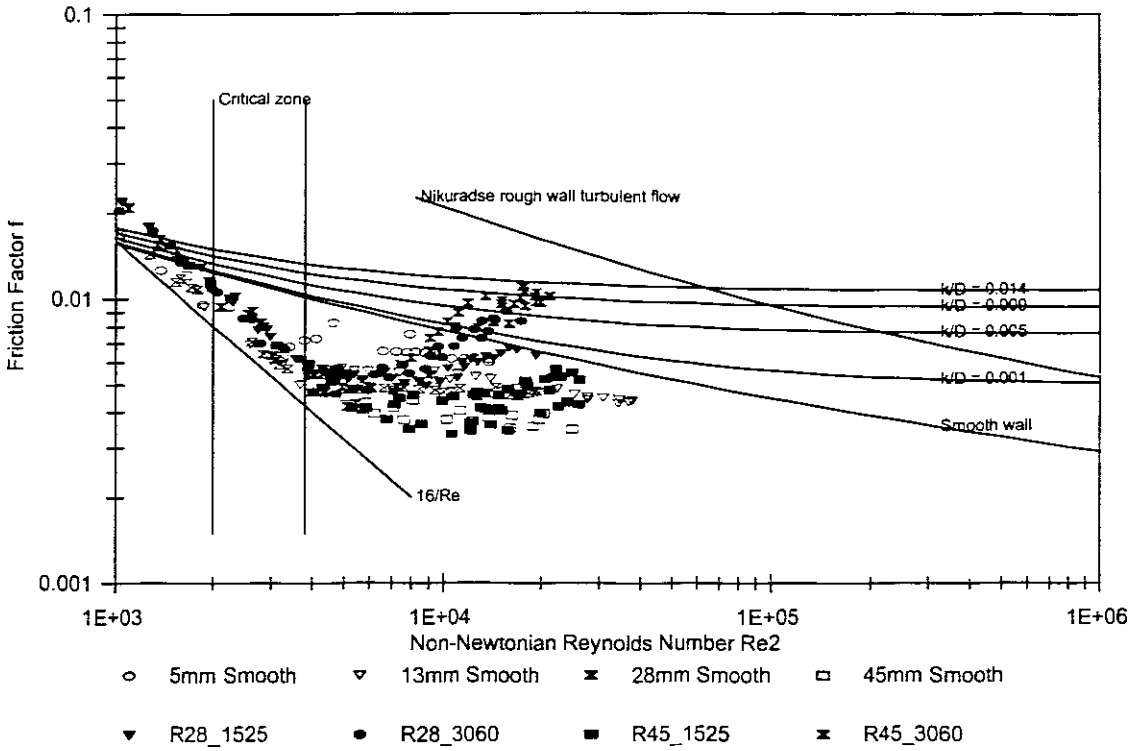

Figure 4.29: Fanning Friction Factor vs non-Newtonian Reynolds Number for Kaolin at a Slurry Relative Density of 1.1146

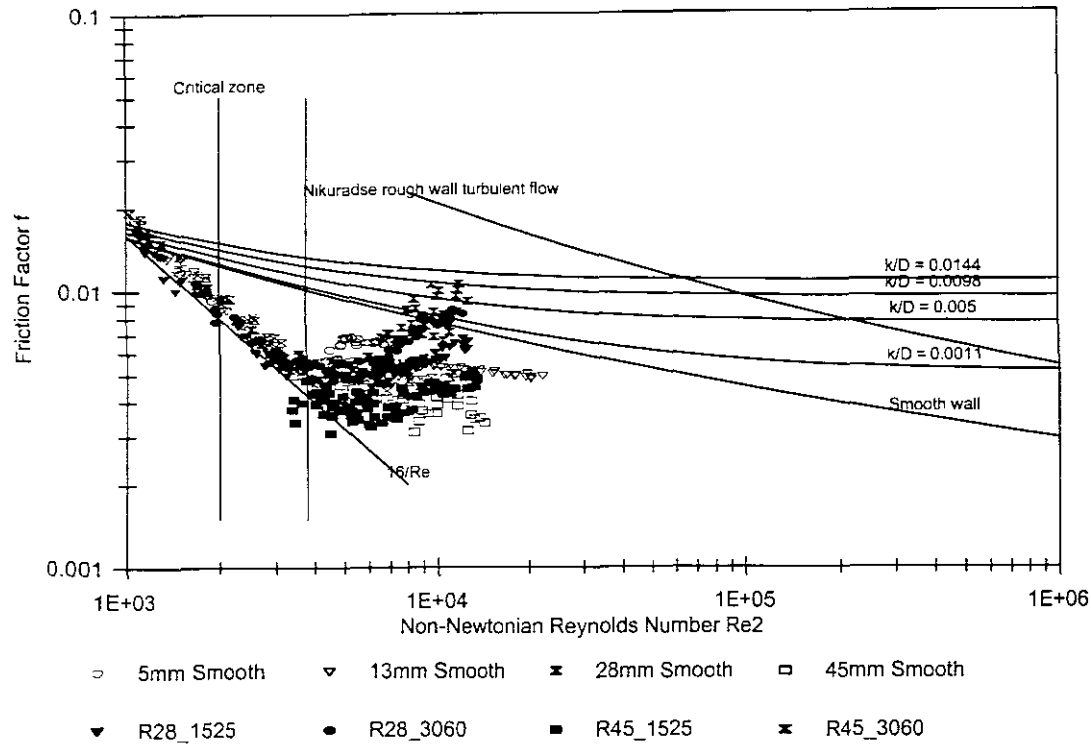

Figure 4.30: Fanning Friction Factor vs non-Newtonian Reynolds Number for Kaolin at a Slurry Relative Density of 1.1779

Kaolin was tested at three relative densities that ranged from 1.0803 to 1.1779. In all of the cases laminar flow for the smooth and rough pipes behaved the same and fall slightly above the 16/Re line.

In all the cases of different slurry relative densities, the transition from laminar to turbulent flow occurs outside the critical zone. This could be due to the Reynolds number used for this analysis. The separation of the smooth and rough pipe friction factors occurs at approximately within the same Reynolds number rang.

All the data in the early turbulent flow region lies well below the smooth wall turbulent flow curve. This is again a case of drag reduction in the smooth and the rough pipes. As the Reynolds number increases the friction factors of the different pipes increases as well. As the slurry relative density increases the range of Reynold numbers, which the data covers, decreases. The slope at which the friction factors increases in the smooth wall turbulent flow region also decreases as the slurry relative density increases. At the highest slurry relative density it is difficult to tell the difference between the smooth and the rough pipe friction factors. No fully developed rough wall turbulent flow was achieved in all the test cases.

4.5.5.4 Tailings Test Results

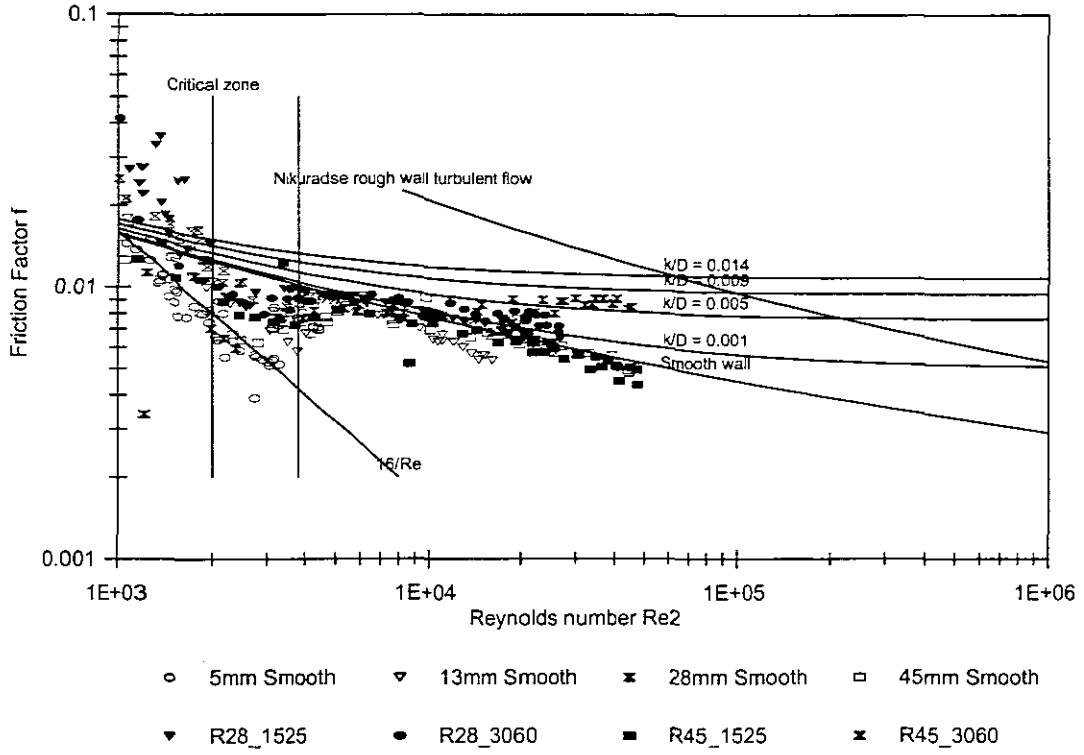

Figure 4.31: Fanning Friction Factor vs non-Newtonian Reynolds Number for Tailings at a Slurry Relative Density of 1.7309

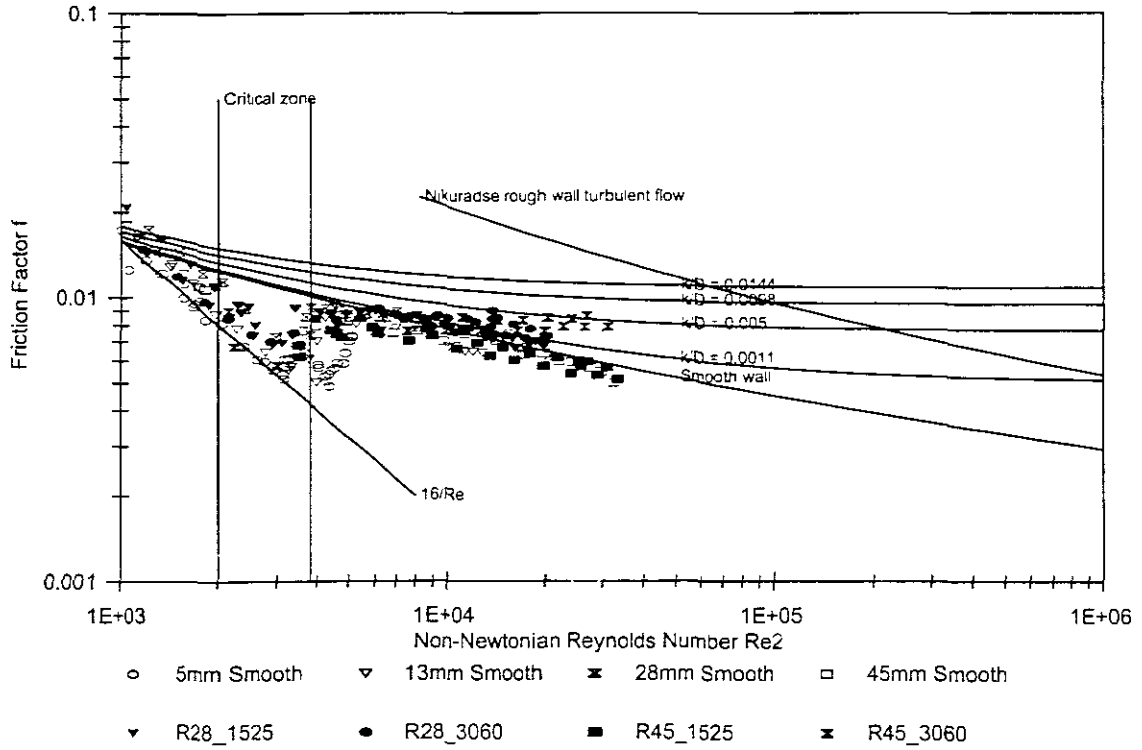

Figure 4.32: Fanning Friction Factor vs non-Newtonian Reynolds Number for Tailings at a Slurry Relative Density of 1.8012

Tailings were tested at two different slurry relative densities of 1.7309 and 1.8012. The smooth and rough pipe data behaved similarly at both relative densities.

At both slurry relative densities the laminar data of the smooth and rough pipes settled slightly above the 16/Re curve.

The transition from laminar to turbulent flow for both the smooth and the rough pipes occur in the critical zone and over the same Reynolds number range.

Both the smooth and the rough pipe data fall on the smooth wall turbulent flow line. Only at higher Reynolds numbers do the friction factors of the rough pipes start to increase and deviate from the smooth wall turbulent flow line. As the slurry relative density increases the split of the smooth and rough pipe friction factors occur at lower Reynolds numbers. The slope at which the friction factor increases become less as the slurry relative density increases.

No fully developed rough wall turbulent flow was achieved at both slurry relative densities.

4.6 Conclusions

- The clear water test results correlate well with the established correlations documented in the literature for Newtonian analysis.

- In most cases the transition from laminar to turbulent flow occurs at the same Reynolds number for the same diameter pipes for all the test fluids.

- The transition from laminar to turbulent flow for the smooth and the rough pipes did not always occur inside the critical zone. This could be due to the Reynolds number used for analysis.

- Roughness does have a significant effect on the turbulent flow hydraulic gradient, and consequently on the friction factor.

- All the models performed badly predicting the early turbulent flow region of the

slurries tested.

- The roughness function B-values for slurries, with solid particles present, behaves differently than predicted by Nikuradse for Newtonian fluids.

Chapter 5

Discussion

5.1 Introduction

In this chapter all the result's presented in Chapter 4 are discussed. The emphasis in this Chapter would specifically be on the turbulent flow and how it is being influenced by pipe roughness.

5.2 Rheological Characterisation

Only smooth pipe data were used for rheological characterisation purposes. For each test fluid at least two different models were used to predict the laminar flow. In each case the best fit to the laminar data was used for the modelling purposes. In Appendix B the rheological characterisation results will be presented and discussed in more detail.

The generalised pseudo plastic model (Govier & Aziz, 1972) has been used for all rheological analysis. In some cases, like kaolin the laminar data at low pseudo shear rates deviated from this model. In these cases the low pseudo shear rate data were rejected for the rheological characterisation. This approach works as there was good agreement between the data and the models used for analysis purposes. This analysis technique was adopted in all the cases where the laminar flow deviated from the general pseudo plastic type of behaviour.

5.2.1 Laminar Flow in Rough Pipes

In all the tests conducted only the laminar flow obtained by the smooth pipes were used for rheological characterisation. The reason for this is that some of the rough pipe data did not behave the same as the smooth pipe data. Specific references are section B3 in Appendix B. These differences in behaviour were picked up for Glycerol, CMC and Kaolin. No sufficient data for the tailings could not be picked up because at these low flow rates the tailings started to settle out in the test pipes and consequently the laminar data achieved were not reliable enough.

It was not the objective of this thesis to test at such low flow rates and the amount of data accumulated at these low pseudo shear rates are to little to quantify precisely what happens at these low pseudo shear rates. The data are sufficient to predict accurately that roughness in some specific applications does effect the laminar flow of fluids in rough pipes. Research in this specific field of interest must continue.

5.3 Transition From Laminar to Turbulent Flow

The transition from laminar to turbulent flow is an important parameter as the flow behaviour of the test fluid changes drastically after this region. It is important to compare the rough pipe results to the smooth pipe results to see if there is any significant change in behaviour between the smooth and the rough pipes.

The transition from laminar to turbulent flow for the smooth pipe data and the rough pipe data are consistent in all the fluids tested. The rough pipe transition agreed well with the smooth pipes and in all the tests the transition from laminar to turbulent flow for the smooth and the rough pipes occurred within the same Reynolds number range. It was not the objective of this thesis to investigate this further but further research in this field must go on.

5.4 Particle Roughness and Pipe Hydraulic Roughness

In all the tests done either the d_{85} percentile particle roughness of the slurry or the pipe roughness was used. In the tests done for Water, Glycerol and CMC the pipe roughness has been used for analysis purposes as the fluid did not have any solid particles present.

For tests done with kaolin and tailings, the d_{85} percentile particles size was used when this number was **greater than the pipe roughness** (Slatter, 1994).

The author could not find any comparison between the hydraulic roughness, k, determined in the clear water tests and the representative sand roughness k_s. Table 5.1 presents the comparison between the hydraulic roughness determined by the clear water tests and the representative sand roughness, k_s.

Table 5.1: Hydraulic Roughness vs Representative Sand Roughness.

Pipe	Internal Diameter [mm]	Sand Roughness [μm]	Hydraulic Roughness [μm]	k/D
R28_1525	27.03	150 to 250	136	0.0050
R28_3060	27.18	300 to 600	291	0.0098
R46_1525	44.73	150 to 250	42	0.0011
R46_3060	45.44	300 to 600	672	0.0144

The author tried to simulate the method Nikuradse used to make sand roughened pipes as already discussed in section 3.5 of this thesis. There are however a lot of problems associated with the analysis method used to analyse the rough pipes.

Nikuradse used the representative sand particle size k_s for analysis purposes. There are a lot of problems associated with the use of this method and are already discussed in section 2.2 of this thesis. Some of the important facts will be highlighted in this discussion again.

Nikuradse assumed that the representative roughness of the sand roughened pipes were a function of the average height of the representative sand particle alone. Table 5.1 indicates that there is no comparison between the average representative sand particle size and the hydraulic roughness. A lot of research has gone into finding a proper comparison method between the representative sand particle size and the hydraulic roughness as already discussed in section 2.9.

Some of the important reasons why the author could not find any relationship between the hydraulic roughness and the representative sand particle size is summarised below (Schlichting, 1960):

- The hydraulic roughness is not a function of the representative height, h, of the sand particle alone.

- The hydraulic roughness is a function of the concentration of the sand particles per unit area.

- The shape and angularity of the particle plays an important role in determining the hydraulic roughness of the pipe.

- The average representative sand particle size cannot be used as representative for determining the hydraulic roughness. Colebrook & White (1937) concluded that only a few big particles that are not representative of the pipe physical roughness can have a significant change in the hydraulic roughness.

- The method used to attach the sand to the inside of the pipe influences the surface roughness of the pipes greatly.

Taking all of the above parameters into account it is understandable that the author could not find any comparison between the representative average sand particle height and the hydraulic roughness. The rough pipes with similar sand grading also did not compare well with each other for the same reasons as discussed in the above summary. For this reason the author decided to use the hydraulic roughness for analysis purposes.

5.5 Roughness Does Have a Significant Effect

Pipe roughness definitely has a significant effect on the pressure gradient in a pipeline. Figure 5.1 presents kaolin data at a relative density of 1.080 for the 46 NB clear PVC pipes of different roughness.

This figure is very important as it shows the effect of pipe roughness in all three classic regions viz.; laminar flow, smooth wall turbulent flow and fully developed rough wall turbulent flow.

5.5.1 The Laminar Flow Region

The results indicate that pipe roughness has no influence on the laminar flow region. This is however not true for all cases as roughness does influence the laminar flow for certain fluids tested. This is discussed in detail in Appendix B section B3 and will not be repeated in this section.

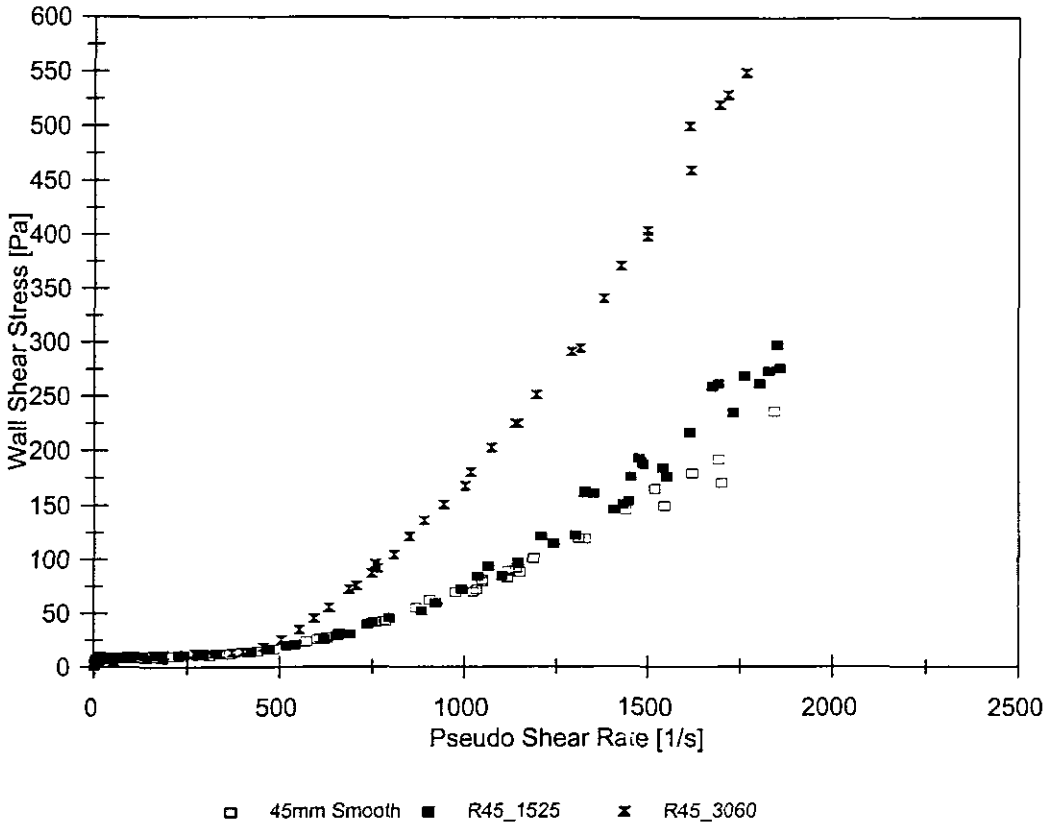

Figure 5.1: The effect of pipe roughness on the same diameter pipe for kaolin at a relative density of 1.080.

5.5.2 Smooth Wall Turbulent Flow Region

This is one of the most important regions as this is the area in which most designers are interested in. The reason for this is that it is the most economical region to design a pipeline in. In laminar flow there is the danger that solids can settle out in the pipeline and in the fully developed turbulent flow the energy loss in the pipeline is to high which leaves the smooth wall turbulent flow region as the optimal for design purposes.

It is important to notice that for the smooth wall turbulent flow region all the pipe follows the same pressure gradient. The smooth wall turbulent flow region starts approximately at a pseudo shear rate of 250 1/s. At a pseudo shear rate of 500 1/s the roughest pipe reach fully developed rough wall turbulent flow and the pressure gradient of this pipe increases rapidly. The smooth wall turbulent flow region continues until a pseudo shear rate of approximately 1300 1/s where the last rough pipe reaches fully develop rough wall

turbulent flow and the pressure gradient increases more than that of the smooth pipe. The results indicate that for the smooth wall turbulent flow the pressure gradient is the same for all the pipes irrespective of the pipe roughness.

5.5.3 Fully Developed Rough Wall Turbulent Flow.

For the fully developed rough wall turbulent flow there is a significant change in the pressure gradient and the pressure in the pipe increases drastically in this area. The reason for this is that the friction factor is a function of the pipe roughness alone irrespective of viscous properties of the fluid. As the pipe roughness of the pipe increases so does the effect on the pressure gradient as can be seen from Figure 5.1.

5.6 Viscous Sub - Layer Thickness vs Rough Wall Turbulent Flow

In this section the viscous sub-layer thickness is compared to the pipe roughness size at the transition from smooth wall turbulent flow to rough wall turbulent flow. In classical pipe flow theory it is assumed that the viscous sub-layer thickness is the same thickness as the height of the pipe roughness at the transition between the smooth wall turbulent flow and fully developed rough wall turbulent flow (Massey,1960). Figure 5.2 shows the relationship between the pipe roughness of the roughest pipe of 672μm and the viscous sub-layer thickness when the flow changes from smooth wall turbulent flow to fully developed rough wall turbulent flow for all the fluids tested.

It is clear that there is a very good comparison between the data and the pipe roughness. It is important to note that the data is interpolated by visual inspection of the pseudo shear diagrams. The viscous sub-layer prediction is also highly dependant on the rheological characterisation and needless to say, this must be done as accurately as possible. The results show some scatter but could be due to the error in the visual inspection and interpolating data from the pseudo shear diagrams.

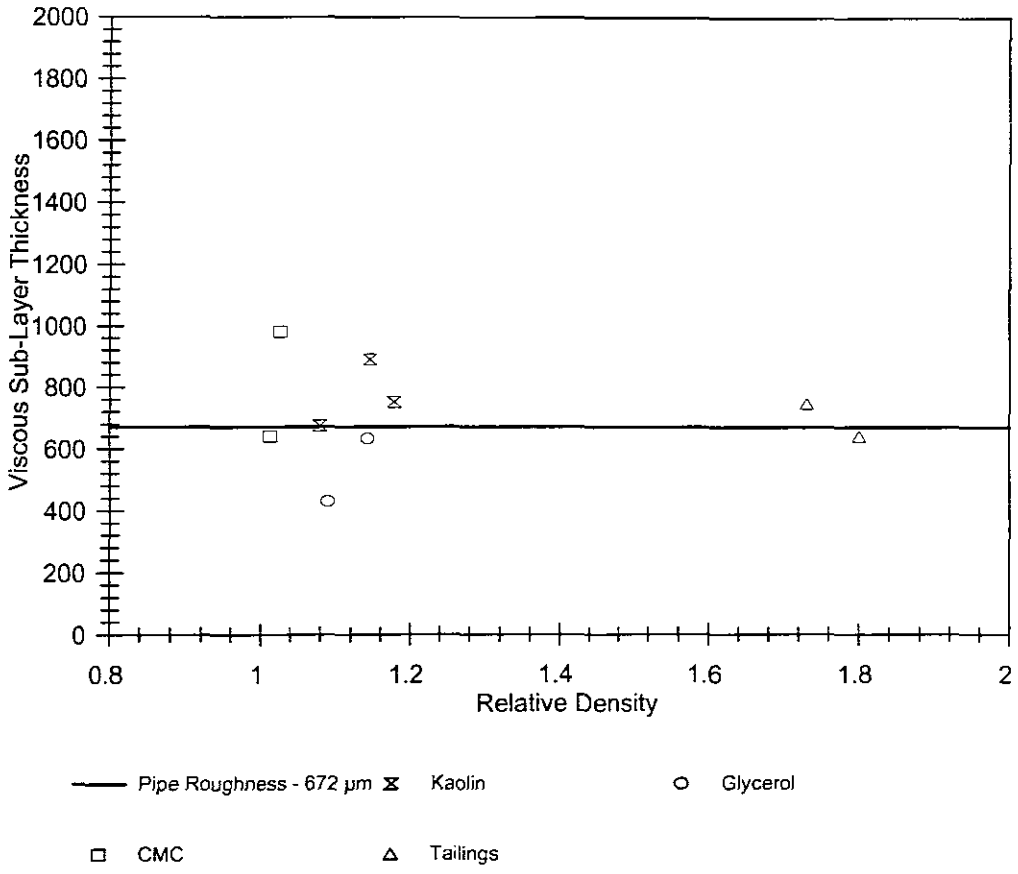

Figure 5.2: Viscous sub-layer thickness vs pipe roughness

5.7 Turbulent Flow Modelling of the Smooth and Rough Pipes

Turbulent flow and turbulent flow modelling have been discussed in Chapter 4. In general the models performed badly for predicting the rough pipe turbulent data. The models performed the worst in the early turbulent flow region. The models accurately predicted the turbulent flow of the smooth pipes, as shown in Annexure C. This highlights the need for a turbulent flow model which accommodates pipe roughness accurately for pipes of higher roughness.

This is also the core of this thesis as the early turbulent flow region is very important for reasons discussed earlier in this chapter. None of the models produced accurate and consistent results which highlights the need for a model that can predict the early turbulent flow region accurately for rough pipes as most of the pipes used in industry cannot be considered as being hydraulically smooth.

5.8 Roughness Function B vs Roughness Reynolds Number

The roughness function B seems to be sensitive to change in the rheological characterisation. A small change in the rheological parameters seems to significantly change the position of the data sets on the roughness function B graph (Chapter 4).

The increase in relative density does not seem to have a significant effect on the test fluids. For Glycerol and CMC the increase in relative density grouped the rough pipe data closer together. In the case of kaolin and tailings, where solid particles were present in the mixture the roughness effect separated the data sets more as the viscosity of the fluid increased.

The pipe roughness separates the data and as the relative roughness of the pipe increases the data shifts from the left of the curve to the right. In the case of kaolin and tailings the roughness also affects the height of the data above the transition curve. As the pipe roughness increases the data would have higher B-values in the transition region for the same Reynolds number as for the equivalent pipe of lower roughness.

In the fully developed rough wall turbulent flow region the data of all the fluids tested tends to settle at values close to 8.5 which confirms the predictions of Nikuradse (1939). This also supports the fact that in general the turbulent flow models performed better in the fully rough wall turbulent flow region where the data correlates well with the value of 8.5.

In the transition region however there were great differences between the transition curve of Nikuradse and the data. This only happened with fluids with solid particles present such as kaolin and tailings. The turbulent flow models also performed the worst in this area which is to be expected as all the models are a function of the roughness function B-value. If the data correlated well with the roughness function B graph, the turbulent flow modelling were accurate but if the correlation was bad the turbulent flow modelling also did not correlate very well with the data.

5.9 Fanning Friction Factor vs Non-Newtonian Reynolds Number

In Chapter 4 the Fanning friction factor was plotted against a non-Newtonian Reynolds number Re_2 (Slatter & Lazarus, 1993).

There seems to be no difference in the friction factor for the smooth and the rough pipes in the laminar flow region except for a few isolated cases which are discussed in detail in Appendix B.

The change in the friction factor for the smooth and the rough pipes in the critical zone seems to be random and no definite pattern is established. The change in friction factors for the smooth and the rough pipes seems to be similar for the same diameters in this region.

In the turbulent flow region the rough pipes behaved significantly differently from the smooth pipes and have larger friction factor values than for smooth pipes. All the smooth pipe data followed the smooth wall turbulent flow curve accurately where the rough pipes would separate from the smooth pipe data and follow their respective k/D curves. Fully developed rough wall turbulent flow was rarely achieved in the tests done and the friction factor for the rough pipes continued to increase at the high Reynolds numbers.

5.10 The Effect of The Increase in Relative Density

The increase in relative density has the biggest influence on the turbulent flow modelling of the rough pipes although it does not significantly effect the roughness function B-values. Figure 5.3 clearly illustrates this problem. The models discussed in Chapter 2 are a function of a lot of variables which the Reynolds number and the Roughness function B are of the important ones.

Figure 5.3 present different data sets of kaolin and tailings in the R45_6030 rough pipe. The data is presented at different relative densities for the same diameter pipe with the same hydraulic roughness. It is clear that the B-values for the kaolin and tailings slurry does not follow the relationship as displayed by the solid lines predicted by the different models. Only at high Reynolds numbers do the data and the models correlate well.

The turbulent flow models are inaccurate at predicting the turbulent flow of the rough pipes in the early turbulent region. It is also the area on the roughness function B graph where the data and the prediction line are separated the most. The turbulent flow models are also sensitive to the increase in relative density where the data shows that the increase in relative density does not significantly affect the B-values.

All the data for the same fluid at the different relative densities are grouped close together and indicate that the Reynolds number used for analysis is correct.

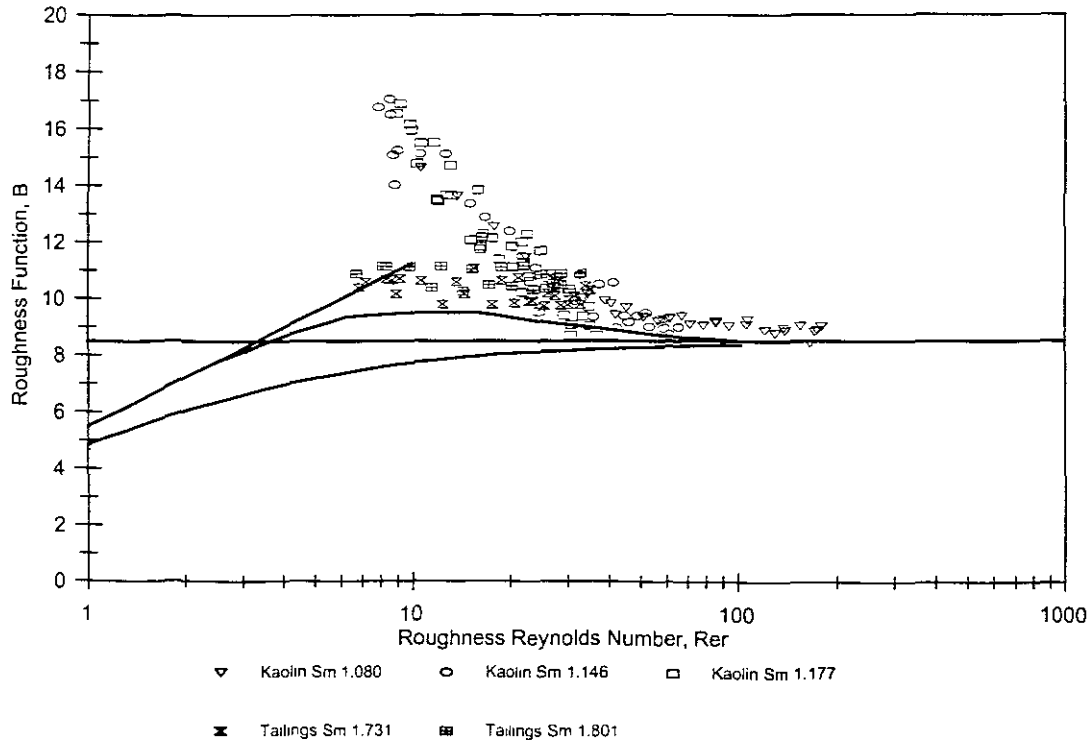

Figure 5.3: The Effect of the Increase in Relative Density on Kaolin and Tailings Slurry for the R45-6030 Pipe.

5.11 Conclusions

Laminar Flow

- Only the smooth pipe data were used for rheological characterisation, as the rough pipe laminar flow was unpredictable.

- Roughness does have some effect on laminar pipe flow but the data obtained from the different tests is not enough to establish a definitive pattern.

Transition Region

- The transition from laminar to turbulent flow for the same diameter smooth

and rough pipes occurs within the same velocity range.

Turbulent Flow

- Pipe roughness does have a significant effect on the pressure gradient.

- The data indicates that the effect of pipe roughness is the same for a Newtonian as well as a non-Newtonian fluid.

Viscous Sub-Layer Thickness

- The viscous sub-layer thickness correlates well with the height of the hydraulic pipe roughness of the R46_3060 pipe at the point where the smooth and rough pipe data separates in the fully developed rough wall turbulent flow region.

Friction Factor

- In laminar flow the smooth and the rough pipe friction factors were the same except for the isolated cases discussed in Annexure B.

- The friction factors for the smooth and the rough pipes were similar for the smooth and the rough pipes in the critical zone for the same diameter pipes.

- The smooth and the rough pipes gave significantly different friction factors in the turbulent flow region.

Roughness Function B-Values

- Slurries with solid particles (kaolin and tailings) seem to have a significant effect on the B-values in the transition region.

- The B-values are sensitive to rheological characterisation and viscosity.

- In the cases where the data and the roughness function B values correlate well the turbulent flow modelling also agreed well with the data.

The Effect of The Increase In Relative Density

- The increase in relative density does have a significant effect on the turbulent flow models but does not significantly affect the roughness function B-values.

Rheological Characterisation

- The roughness function B and the turbulent flow models are sensitive to changes in the rheological parameters τ_y, K and n.

Chapter 6

SUMMARY AND CONCLUSION

6.1 Summary

The effect of pipe roughness on non-Newtonian turbulent flow has been investigated and presented. Roughness is a real problem and none of the pipes used in engineering structures can be considered as being hydraulically smooth.

This thesis investigates the effect that pipe roughness has specifically on turbulent flow for Newtonian and non-Newtonian fluids. Newtonian fluids were used to confirm Nikuradse's findings and to verify the correct operation of the rough pipes. The author simulated the method used by Nikuradse to manufacture the rough pipes. The data obtained from the rough pipes were correlated against Nikuradse's findings and presented.

Very little work could be found that dealt specifically with this area of interest and only Nikuradse's findings could be used for the Newtonian fluids tested. The non-Newtonian test results are also presented and discussed in this thesis. It is hard to believe that research in this field has been neglected for so long as the results show significant errors in the turbulent flow models for predicting the turbulent flow head loss in rough pipes.

The main area of interest and also the core of this thesis is the prediction of the turbulent flow for non-Newtonian fluids in the early turbulent flow region. It is important to predict the early turbulent flow accurately as most pipelines are designed to operate in this area. The test results show that the biggest error between the turbulent flow models and the data occurs in this region. This necessitates the development of a model that can predict the turbulent flow of non-Newtonian fluids in rough pipes accurately.

Research in this field must continue as there are still many "unknowns" to explore and will be discussed at the end of this chapter.

6.2 Conclusions

The conclusion of all the chapters will be discussed in this section.

6.2.1 Chapter 1: Introduction

In Chapter 1 the problem was stated and the aims and objectives set out. The main conclusions of Chapter 1 are;

- Pipes used in engineering structures cannot be considered as being hydraulically smooth and we have got to allow for a roughness effect in the design of a pipeline.
- Pipe roughness is a problem and predictions of the roughness effect is inaccurate.
- There is a need for experimental work in this area.

6.2.2 Chapter 2: Theory and Literature Review

In Chapter 2 the theory of pipe roughness has been evaluated and the available literature reviewed. The main conclusions of Chapter 2 are;

- There is not sufficient literature available on pipe roughness.
- The greatest research on roughness (Nikuradse, 1933) was on Newtonian fluids. Very little have been done on non-Newtonian fluids.
- There are models that allow for a roughness effect in predicting the turbulent flow of non-Newtonian fluids.

6.2.3 Chapter 3: Experimental Investigation

In Chapter 3 the experimental investigation is documented. The main conclusions of Chapter 3 are;

- The BBTV can be used for determining accurate rheology.
- The BBTV is a versatile instrument in which turbulent flow in smooth and rough pipes can be tested for the same fluid under the same conditions.
- Both laminar and turbulent flow were achieved in the same instrument (BBTV).
- The error analysis is within acceptable limits for accurate analysis of the data.

6.2.4 Chapter 4: Analysis

In Chapter 4 the analysis of the test results was done. The main conclusions of this Chapter were;

- The clear water test results correlate well with the literature documented for Newtonian analysis.
- Nikuradse's formula for calculating the friction factor for fully developed rough wall turbulent flow was used to calculate the pipe roughness of the rough pipes.
- The Colebrook & White friction factor was used to calculate the pipe roughness of the smooth pipes.
- In most cases the transition from laminar to turbulent flow occurs at the same velocity for the same diameter pipes irrespective of the roughness of the pipes.
- The transition from laminar to turbulent flow for the smooth and the rough pipes did not always occur inside the critical zone. This could be due to the Reynolds number used for analysis.

- Roughness does have a significant effect on the turbulent flow friction factor.

- All the models performed badly in predicting the early turbulent flow region of the fluids tested.

- The classical roughness function B-values for slurries behaves differently than predicted by Nikuradse for Newtonian fluids.

6.2.5 Chapter 5: Discussion

In Chapter 5 the analysis of Chapter 4 was discussed. The conclusions of this Chapter are as follow;

Laminar Flow

- Only the smooth pipe data were used for rheological characterisation as the rough pipe laminar flow was unpredictable.

- Roughness does have some effect on laminar pipe flow but the data obtained from the different tests are not enough to establish a specific pattern.

Transition Region

- The transition from laminar to turbulent flow for the smooth and the rough pipes occurs within the same Reynolds number range.

- The non-Newtonian Reynolds number Re_2 is appropriate for all the analysis used in this thesis as it incorporates the yield stress.

The Early Turbulent Flow Region

- The smooth and rough pipe data are co-linear on a pseudo shear diagram for

the same diameter.

Turbulent Flow

- Pipe roughness does have a significant effect on the pressure gradient.
- The data indicates that the effect of pipe roughness is similar for a Newtonian as well as a non-Newtonian fluid.
- For fully developed rough wall turbulent flow the smooth and the rough pipes gave similar wall shear stresses for the same pseudo shear rate irrespective of the concentration and rheology of the fluid.

Viscous Sub-Layer Thickness

- There seems to be good correlation between the viscous sub-layer thickness and the height of the pipe roughness at the point where the flow changes from smooth wall turbulent flow to fully developed rough wall turbulent flow.

Friction Factor

- In laminar flow the smooth and the rough pipe friction factors were the same.
- The friction factors for the smooth and the rough pipes were similar in the smooth wall turbulent flow region for the same diameter pipes.
- The smooth and the rough pipes gave significantly different friction factors in the rough wall turbulent flow region.

Roughness Function B-Values

- Slurries with solid particles (kaolin and tailings) seem to have significant

different B-values in the transition region from true homogeneous Newtonian to non-Newtonian fluids.

- The B-values are sensitive to rheological characterisation and viscosity.

- For fully developed rough wall turbulent flow the data of **ALL** the test fluids gave results close to 8.5.

- Smooth wall turbulent data from both the smooth and rough pipes correlated well with the smooth wall turbulent flow predictions.

The Effect of the Increase in Relative Density

- The increases in the relative density do not have a significant effect on the roughness function B-values but significantly affect the turbulent flow models.

Turbulent flow modeling

- The turbulent flow models performed consistently accurately in predicting the smooth pipe turbulent flow for all the fluids tested.

- The turbulent flow models gave reasonable results predicting the fully developed rough wall turbulent flow for the rough pipes.

- The turbulent flow models performed badly in predicting the turbulent flow of the rough pipes in the early turbulent flow region.

- When the rheological characterization was close to a Bingham plastic the turbulent flow models performed better.

6.3 Future Work

1. Research in this specific field of interest must go on.

2. Rough pipes of bigger diameters need to be made and tested in a pump test rig.

3. The effect of pipe roughness on laminar flow needs to be further investigated.

4. Differed kinds of roughness need to be explored.

5. A new model needs to be developed to accommodate pipe roughness accurately.

6. More slurries with solid particles need to be tested with rough pipes to establish the flow behavior accurately.

7. A more reliable method needs to be established to correlate sand roughness to hydraulic roughness accurately.

The Effect Of Pipe Roughness On Non-Newtonian Turbulent Flow

by

Fritz Peter van Sittert
B Tech (Civ. Eng.)

A thesis submitted for the degree of
Magister Technologiae
in the Department of Civil Engineering
Cape Technikon

November 1999

APPENDICES

Cape Technikon
Cape Town
South Africa

APPENDIX A

CLEAR WATER TEST RESULTS

TEST RESULTS

Test Fluid	Solids density (S_s)	Slurry Relative Density (S_m)	Solids Concentration by Volume (C_v)	Pipe Name	Page
				R45_1525	A27
				R45_3060	A28
CMC	N/A	1.013	N/A	5 Smooth	A29
				13 Smooth	A30
				28 Smooth	A31
				45 Smooth	A32
				R28_1525	A33
				R28_3060	A34
				R45_1525	A35
				R45_3060	A36
CMC	N/A	1.027	N/A	5 Smooth	A37
				13 Smooth	A38
				28 Smooth	A39
				45 Smooth	A40
				R28_1525	A41
				R28_3060	A42
				R45_1525	A43
				R45_3060	A44
CMC	N/A	1.037	N/A	5 Smooth	A45
				13 Smooth	A46
				28 Smooth	A47
				45 Smooth	A48
				R28_1525	A49
				R28_3060	A50
				R45_1525	A51
				R45_3060	A52
Kaolin	2.65	1.080	4.85 %	5 Smooth	A53
				13 Smooth	A54

Test Fluid	Solids density (S_s)	Slurry Relative Density (S_m)	Solids Concentration by Volume (C_v)	Pipe Name	Page
				28 Smooth	A55
				45 Smooth	A56
				R28_1525	A57
				R28_3060	A58
				R45_1525	A59
				R45_3060	A60
Kaolin	2.65	1.146	8.85 %	5 Smooth	A61
				13 Smooth	A62
				28 Smooth	A63
				45 Smooth	A64
				R28_1525	A65
				R28_3060	A66
				R45_1525	A67
				R45_3060	A68
Kaolin	2.65	1.177	10.73 %	5 Smooth	A69
				13 Smooth	A70
				28 Smooth	A71
				45 Smooth	A72
				R28_1525	A73
				R28_3060	A74
				R45_1525	A75
				R45_3060	A76
Tailings	3.70	1.731	27.07 %	5 Smooth	A77
				13 Smooth	A78
				28 Smooth	A79
				45 Smooth	A80
				R28_1525	A81
				R28_3060	A82

Test Fluid	Solids density (S_s)	Slurry Relative Density (S_m)	Solids Concentration by Volume (C_v)	Pipe Name	Page
				R45_1525	A83
				R45_3060	A84
Tailings	3.70	1.801	29.67 %	5 Smooth	A85
				13 Smooth	A86
				28 Smooth	A87
				45 Smooth	A88
				R28_1525	A89
				R28_3060	A90
				R45_1525	A91
				R45_3060	A92

CLEAR WATER TEST ANALYSIS

APPARATUS

Facility	BBTV
Pipe name	5 Smooth
Diameter (mm)	5.78
Pipe roughness (μm)	1.1
Material	Clear Water
Operator	FvS
Supervisor	PTS

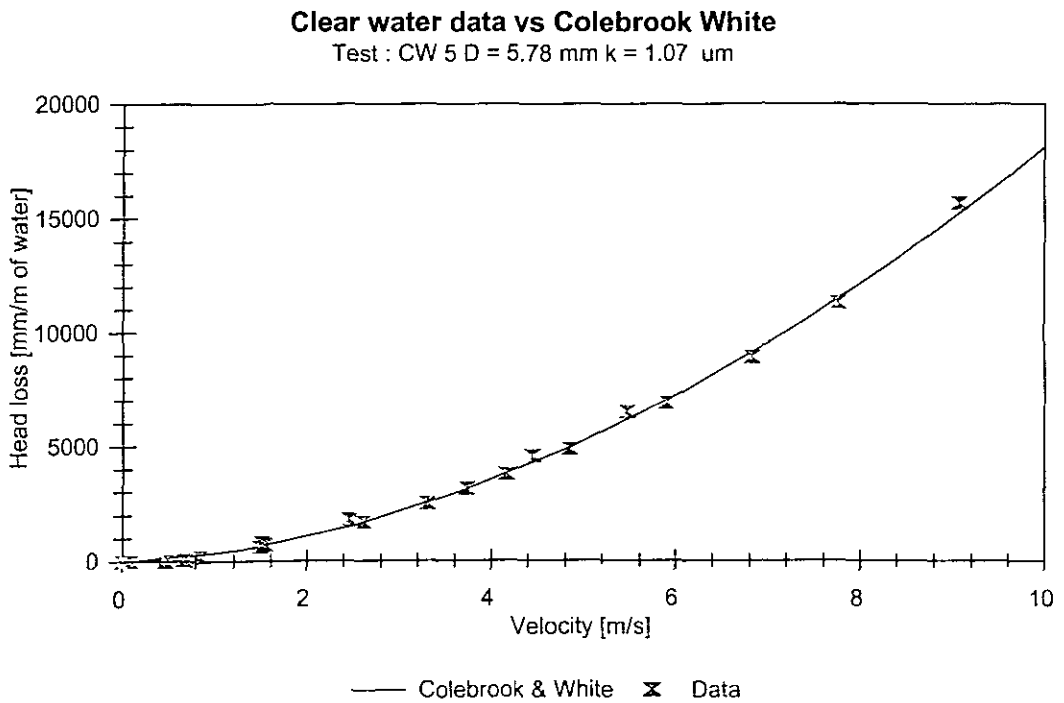

APPARATUS

Facility	BBTV
Pipe name	13 Smooth
Diameter (mm)	13.12
Pipe roughness (μm)	0.87
Material	Clear Water
Operator	FvS
Supervisor	PTS

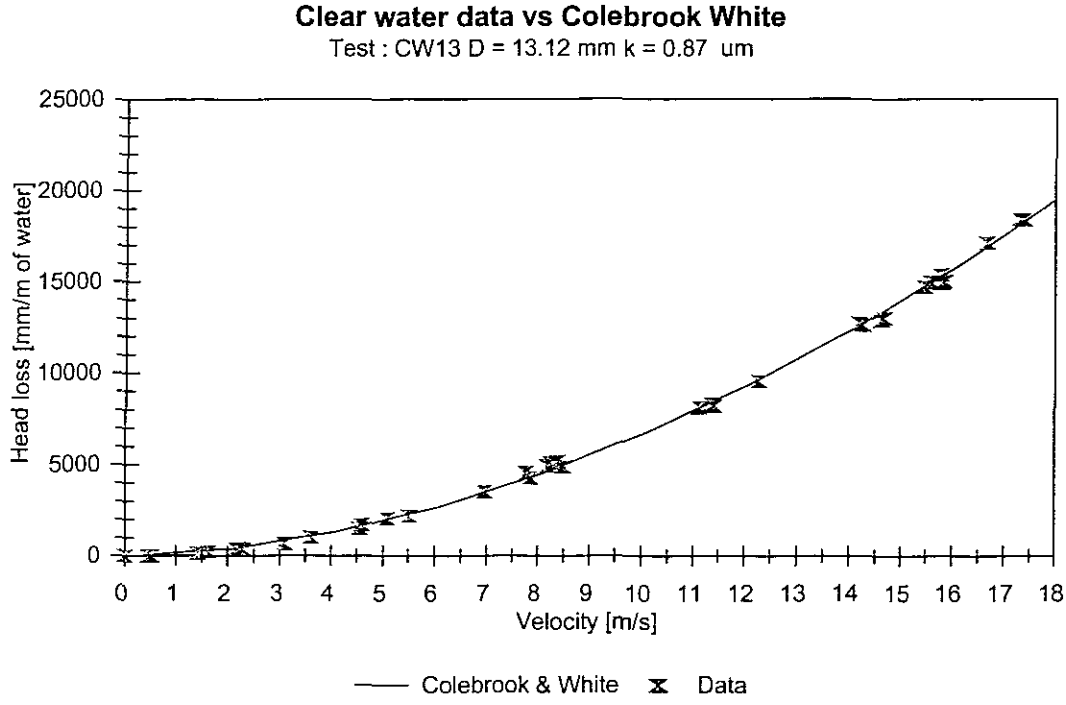

APPARATUS

Facility	BBTV
Pipe name	28 Smooth
Diameter (mm)	28.34
Pipe roughness (μm)	5.9
Material	Clear Water
Operator	FvS
Supervisor	PTS

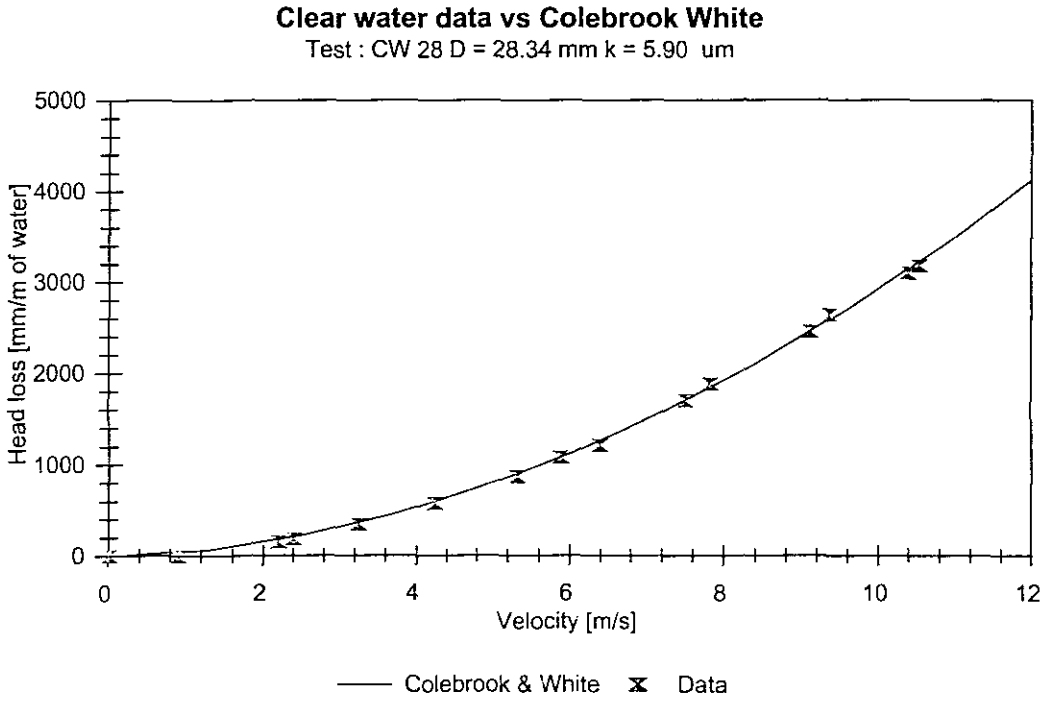

APPARATUS

Facility	BBTV
Pipe name	45 Smooth
Diameter (mm)	46.04
Pipe roughness (μm)	1.33
Material	Clear Water
Operator	FvS
Supervisor	PTS

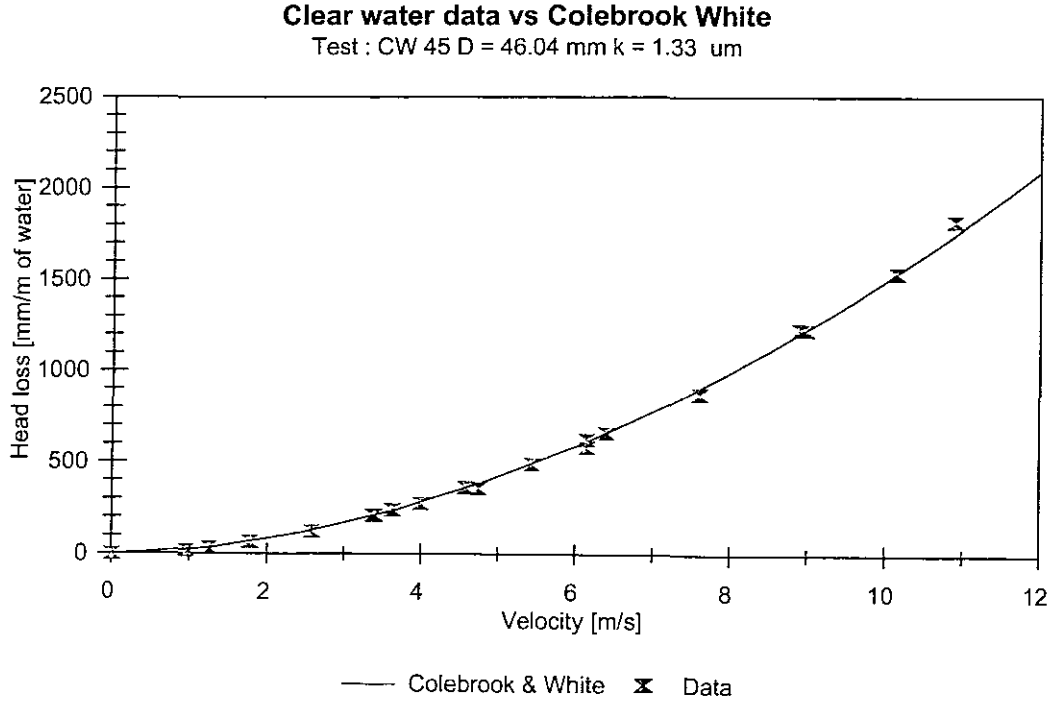

APPARATUS

Facility	BBTV
Pipe name	R28_1525
Diameter (mm)	27.03
Pipe roughness (μm)	136
Material	Clear Water
Operator	FvS
Supervisor	PTS

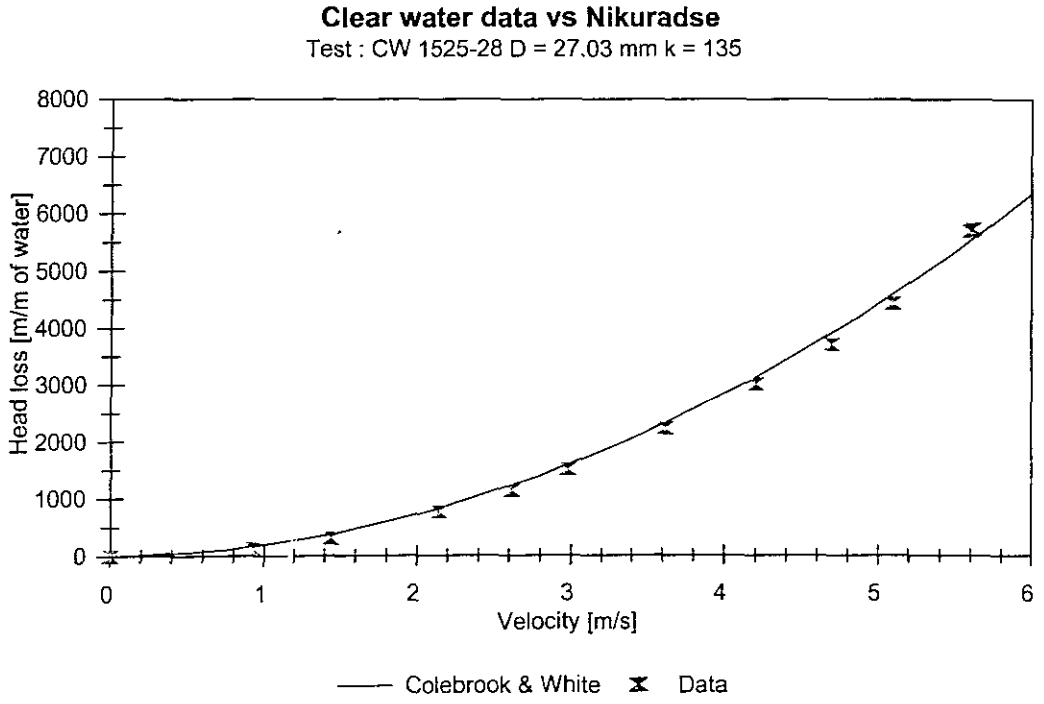

APPARATUS

Facility	BBTV
Pipe name	R28_3060
Diameter (mm)	27.18
Pipe roughness (μm)	291
Material	Clear Water
Operator	FvS
Supervisor	PTS

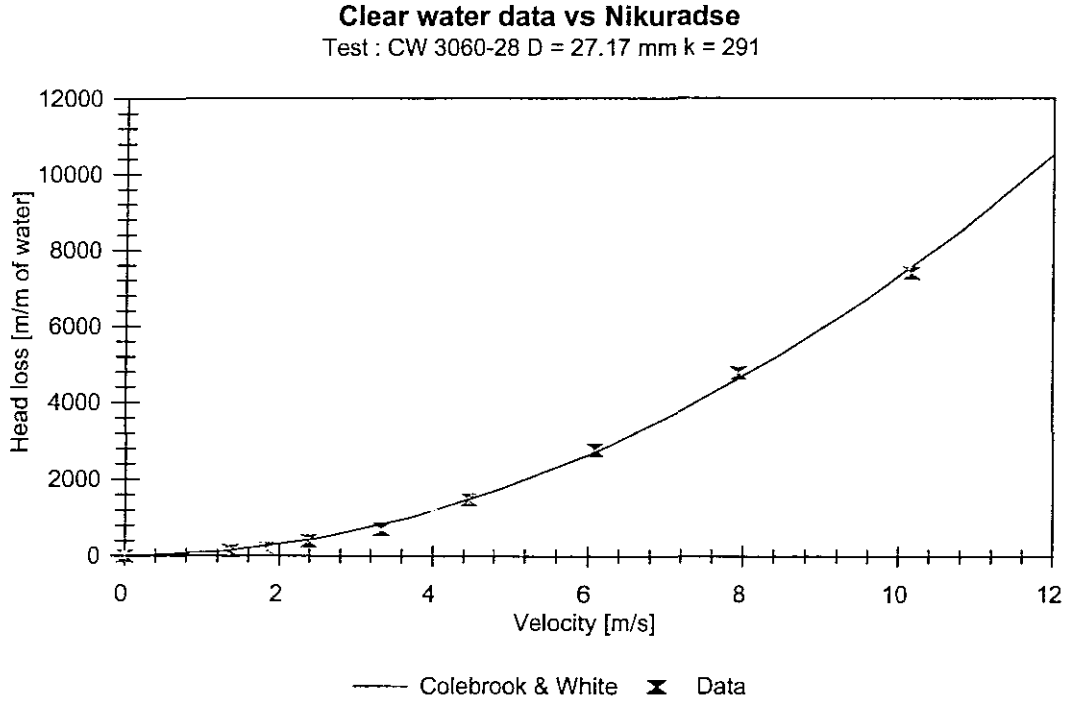

APPARATUS

Facility	BBTV
Pipe name	R45_1525
Diameter (mm)	44.73
Pipe roughness (μm)	42
Material	Clear Water
Operator	FvS
Supervisor	PTS

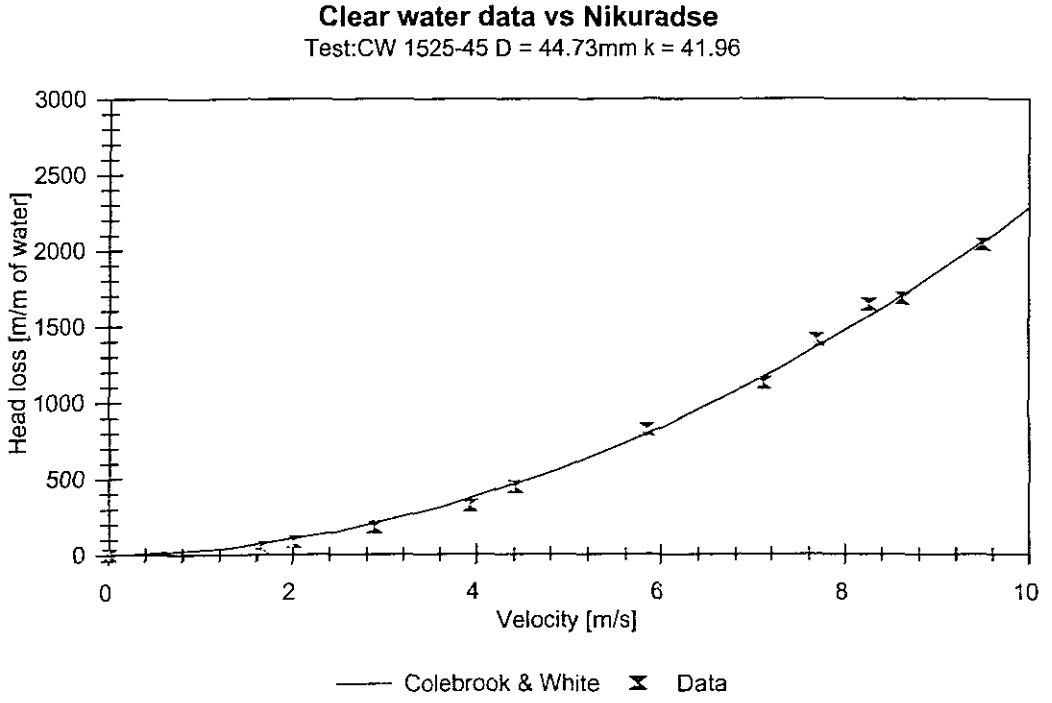

APPARATUS

Facility	BBTV
Pipe name	R45_3060
Diameter (mm)	45.44
Pipe roughness (μm)	672
Material	Clear Water
Operator	FvS
Supervisor	PTS

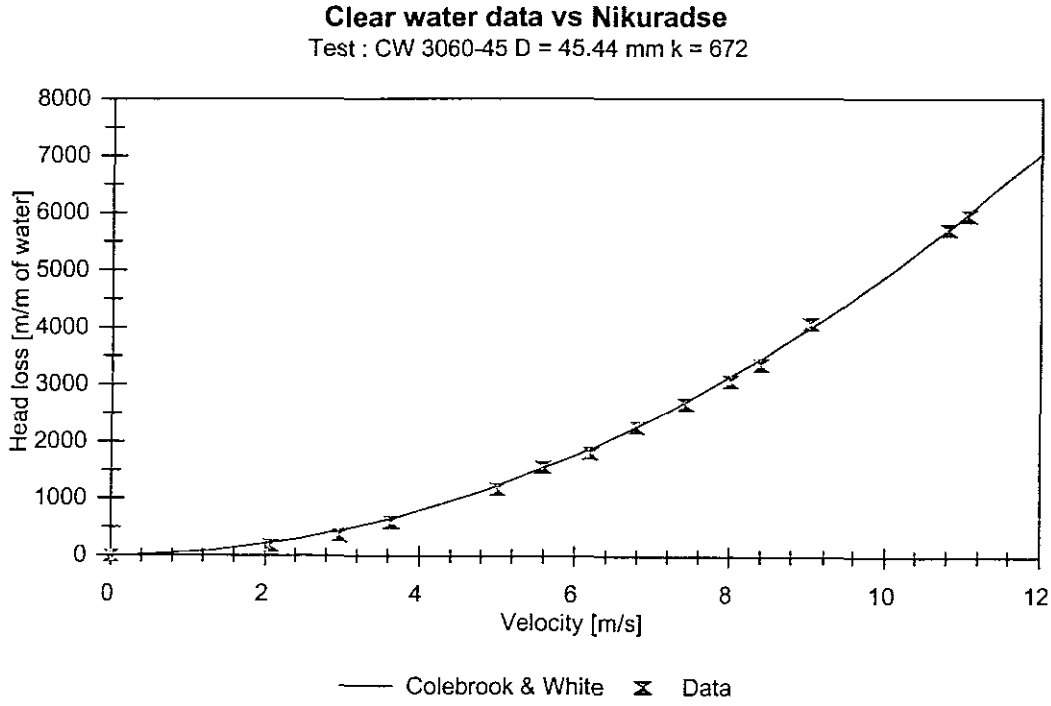

GLYCEROL TEST RESULTS $S_m = 1.090$

APPARATUS

Facility	BBTV
Pipe name	5 Smooth
Diameter (mm)	5.78
Pipe roughness (μm)	1.1
Material	Glycerol
Operator	FvS
Supervisor	PTS

SLURRY PROPERTIES

Solids Relative Density	N/A
Fluid Relative Density (S_m)	1.0906
Volumetric Concentration	N/A
Viscosity (Pa.s)	.00274
Representative Particle Size	N/A

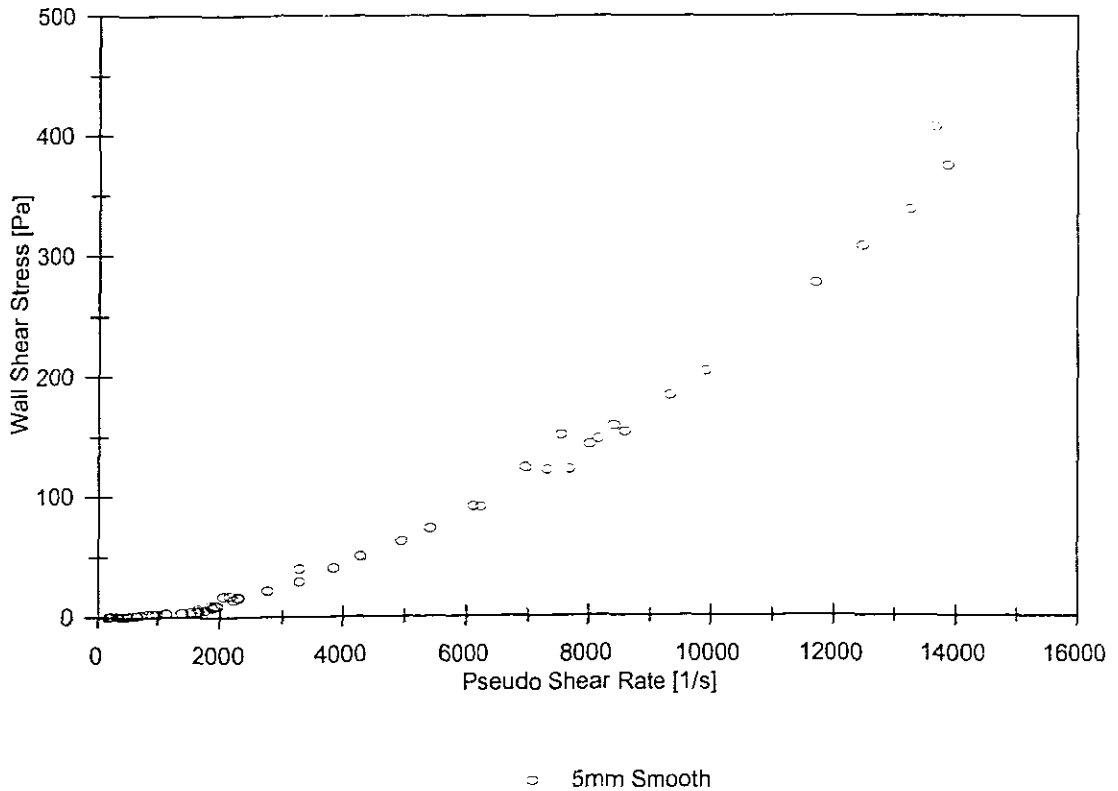

APPARATUS

Facility	BBTV
Pipe name	13 Smooth
Diameter (mm)	13.12
Pipe roughness (μm)	0.9
Material	Glycerol
Operator	FvS
Supervisor	PTS

SLURRY PROPERTIES

Solids Relative Density	N/A
Fluid Relative Density (S_m)	1.0906
Volumetric Concentration	N/A
Viscosity (Pa.s)	.00274
Representative Particle Size	N/A

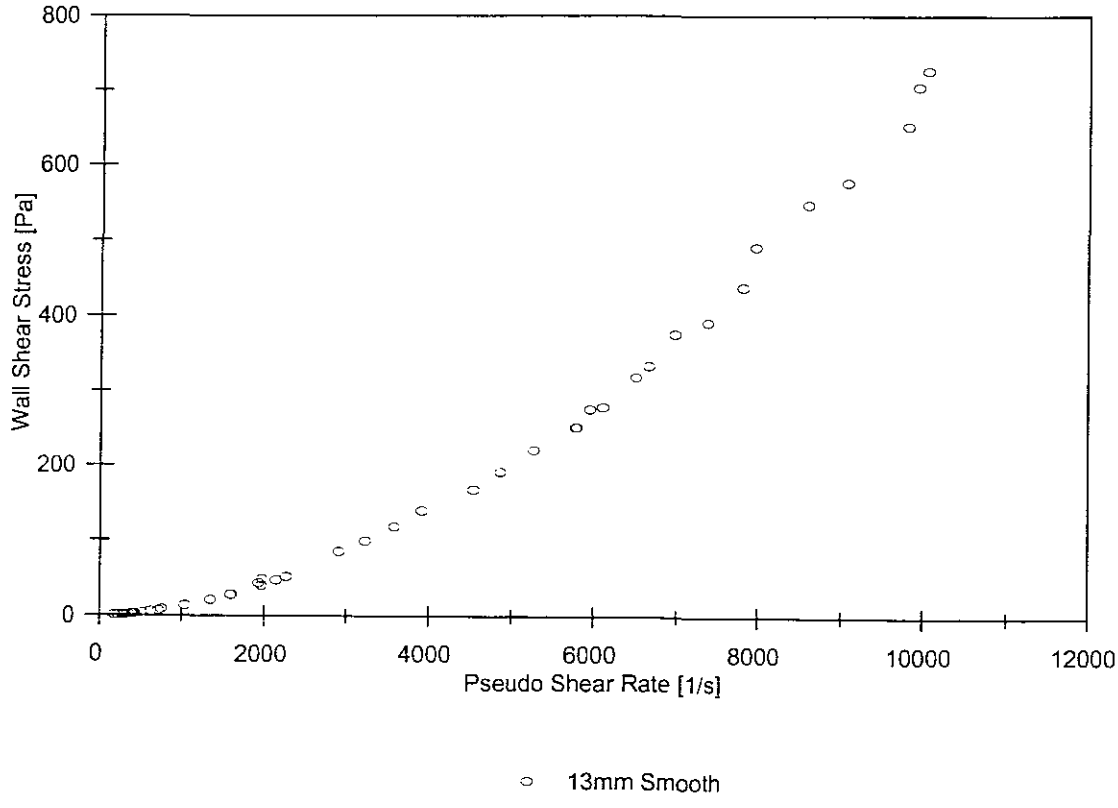

APPARATUS

Facility	BBTV
Pipe name	28 Smooth
Diameter (mm)	28.34
Pipe roughness (μm)	5.9
Material	Glycerol
Operator	FvS
Supervisor	PTS

SLURRY PROPERTIES

Solids Relative Density	N/A
Fluid Relative Density (S_m)	1.0906
Volumetric Concentration	N/A
Viscosity (Pa.s)	.00274
Representative Particle Size	N/A

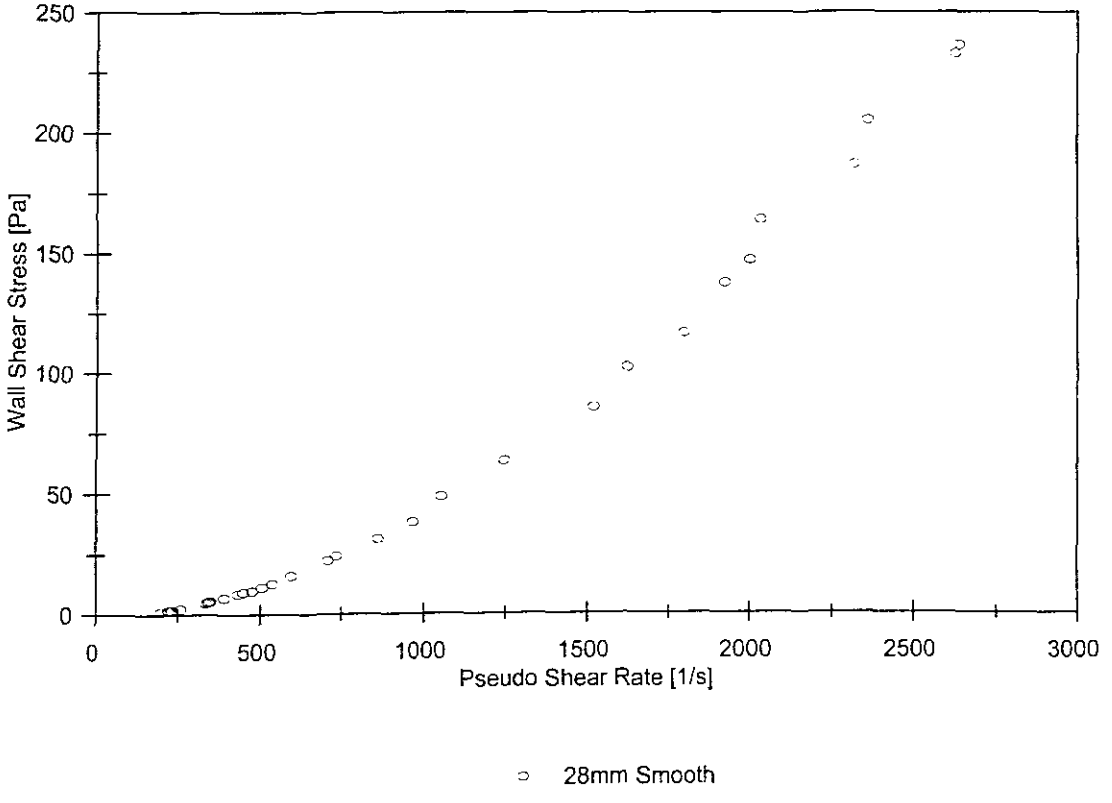

APPARATUS

Facility	BBTV
Pipe name	45 Smooth
Diameter (mm)	45.04
Pipe roughness (μm)	1.3
Material	Glycerol
Operator	FvS
Supervisor	PTS

SLURRY PROPERTIES

Solids Relative Density	N/A
Fluid Relative Density (S_m)	1.0906
Volumetric Concentration	N/A
Viscosity (Pa.s)	.00274
Representative Particle Size	N/A

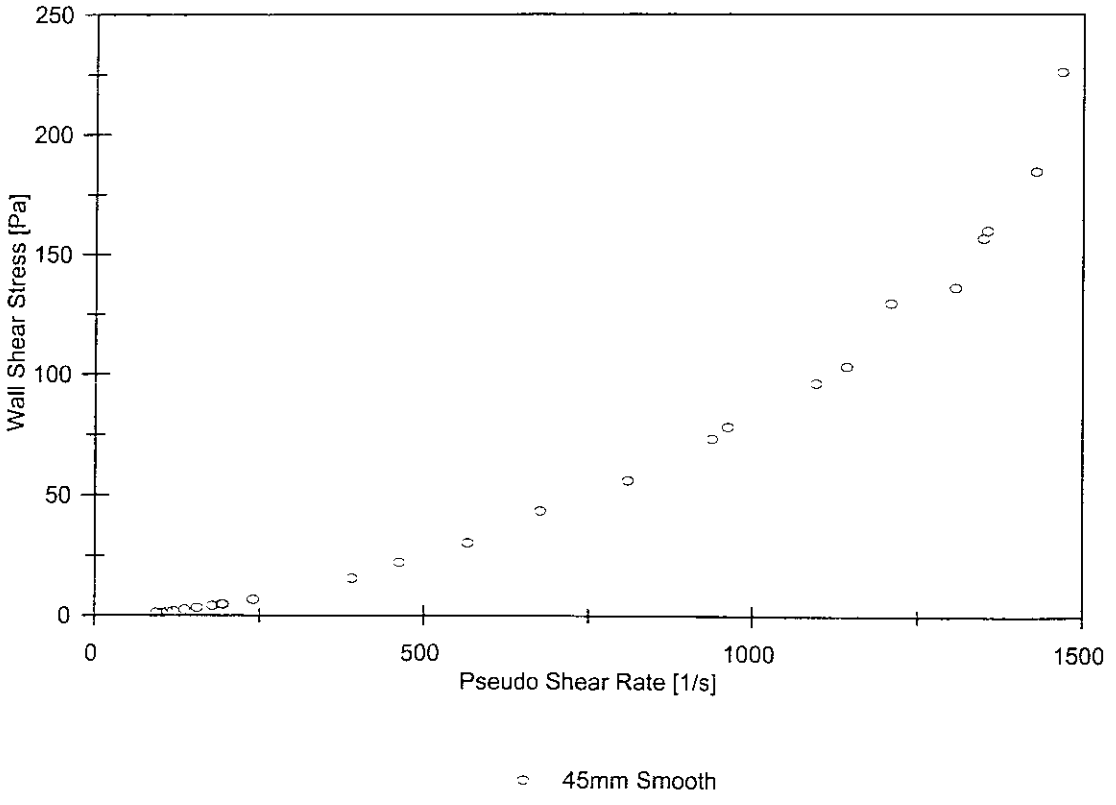

APPARATUS

Facility	BBTV
Pipe name	R28-1525
Diameter (mm)	27.03
Pipe roughness (μm)	136
Material	Glycerol
Operator	FvS
Supervisor	PTS

SLURRY PROPERTIES

Solids Relative Density	N/A
Fluid Relative Density (S_m)	1.0906
Volumetric Concentration	N/A
Viscosity (Pa.s)	.00274
Representative Particle Size	N/A

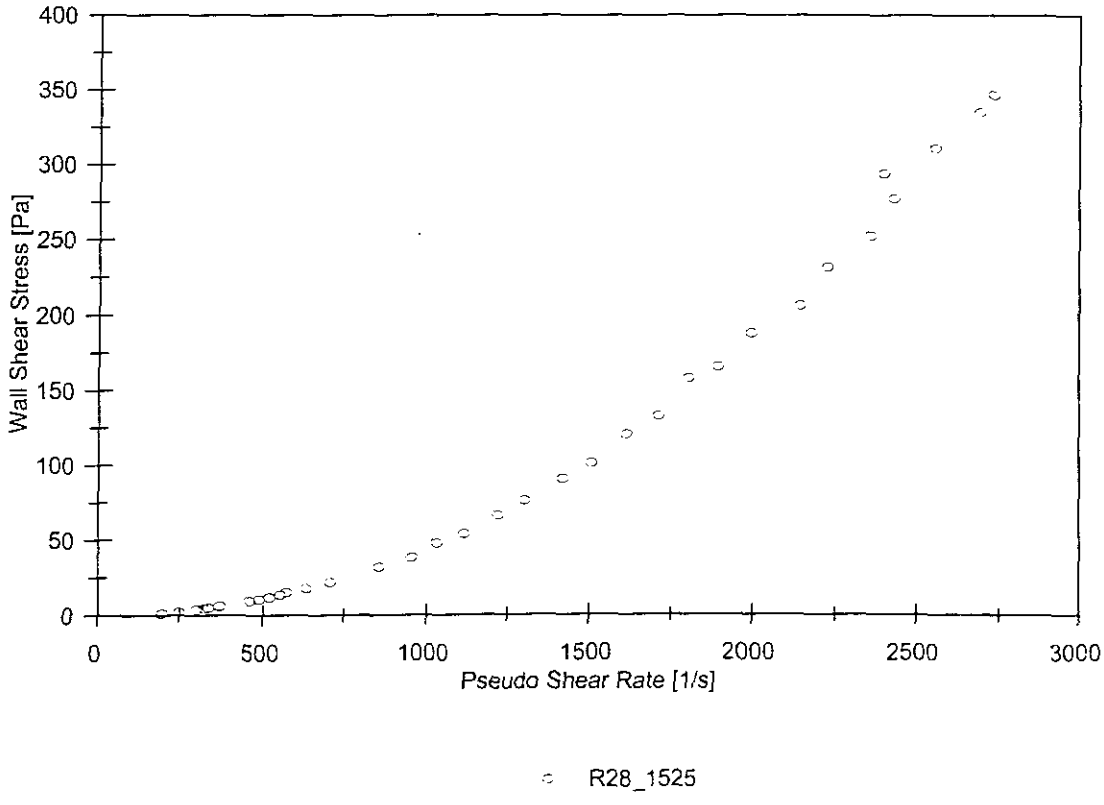

APPARATUS

Facility	BBTV
Pipe name	R28-3060
Diameter (mm)	27.17
Pipe roughness (μm)	291
Material	Glycerol
Operator	FvS
Supervisor	PTS

SLURRY PROPERTIES

Solids Relative Density	N/A
Fluid Relative Density (S_m)	1.0906
Volumetric Concentration	N/A
Viscosity (Pa.s)	.00274
Representative Particle Size	N/A

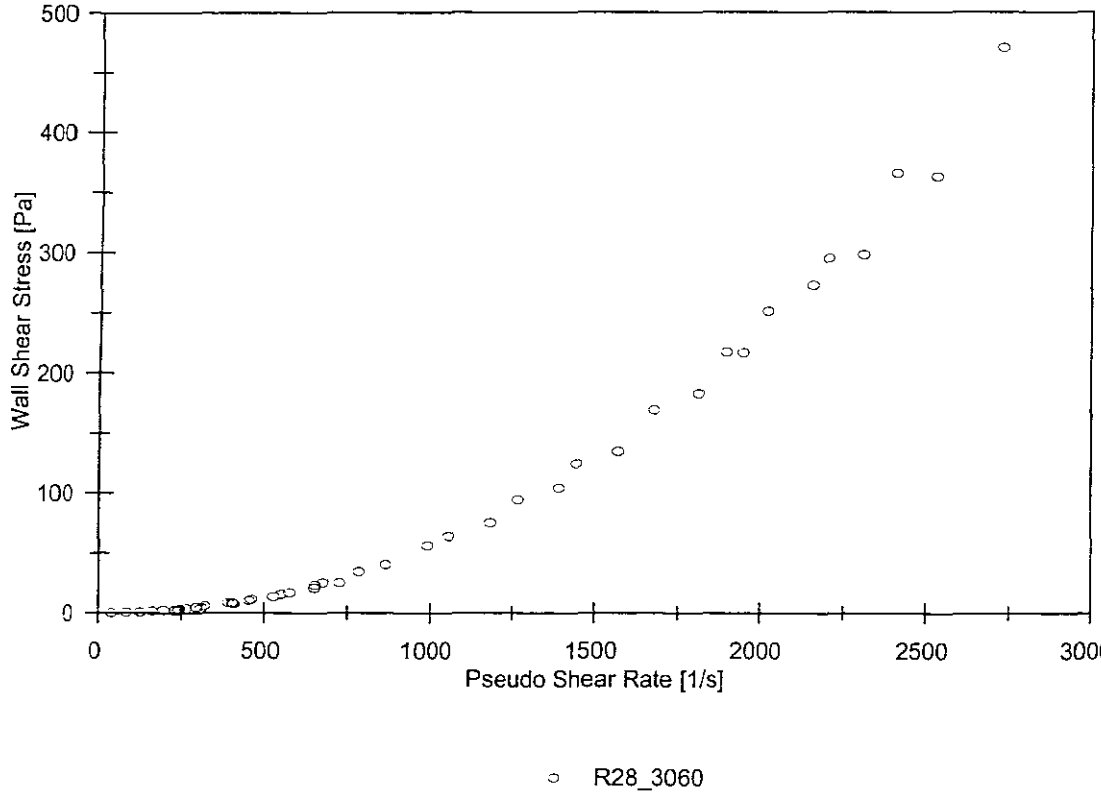

APPARATUS

Facility	BBTV
Pipe name	R45-1525
Diameter (mm)	44.73
Pipe roughness (μm)	42
Material	Glycerol
Operator	FvS
Supervisor	PTS

SLURRY PROPERTIES

Solids Relative Density	N/A
Fluid Relative Density (S_m)	1.0906
Volumetric Concentration	N/A
Viscosity (Pa.s)	.00274
Representative Particle Size	N/A

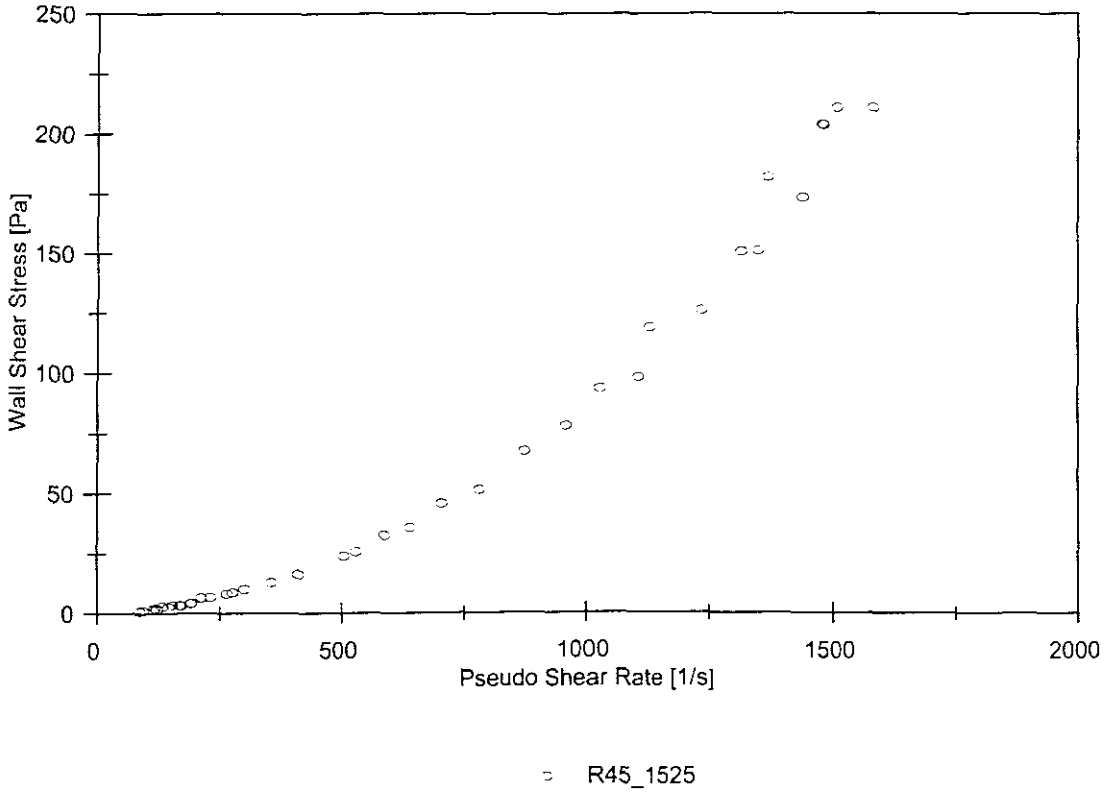

APPARATUS

Facility	BBTV
Pipe name	R45-3060
Diameter (mm)	45.44
Pipe roughness (μm)	672
Material	Glycerol
Operator	FvS
Supervisor	PTS

SLURRY PROPERTIES

Solids Relative Density	N/A
Fluid Relative Density (S_m)	1.0906
Volumetric Concentration	N/A
Viscosity (Pa.s)	.00274
Representative Particle Size	N/A

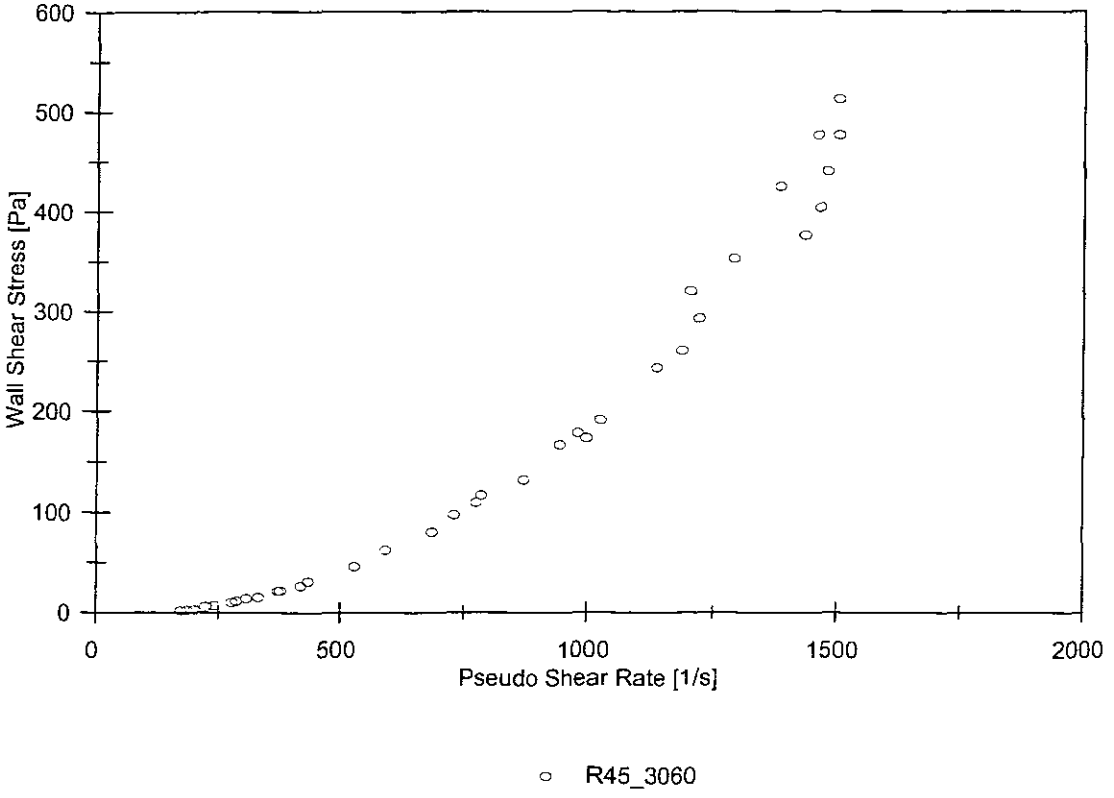

GLYCEROL TEST RESULTS $S_m = 1.1433$

APPARATUS

Facility	BBTV
Pipe name	5 Smooth
Diameter (mm)	5.78
Pipe roughness (μm)	1.1
Material	Glycerol
Operator	FvS
Supervisor	PTS

SLURRY PROPERTIES

Solids Relative Density	N/A
Fluid Relative Density (S_m)	1.1433
Volumetric Concentration	N/A
Viscosity (Pa.s)	.00824
Representative Particle Size	N/A

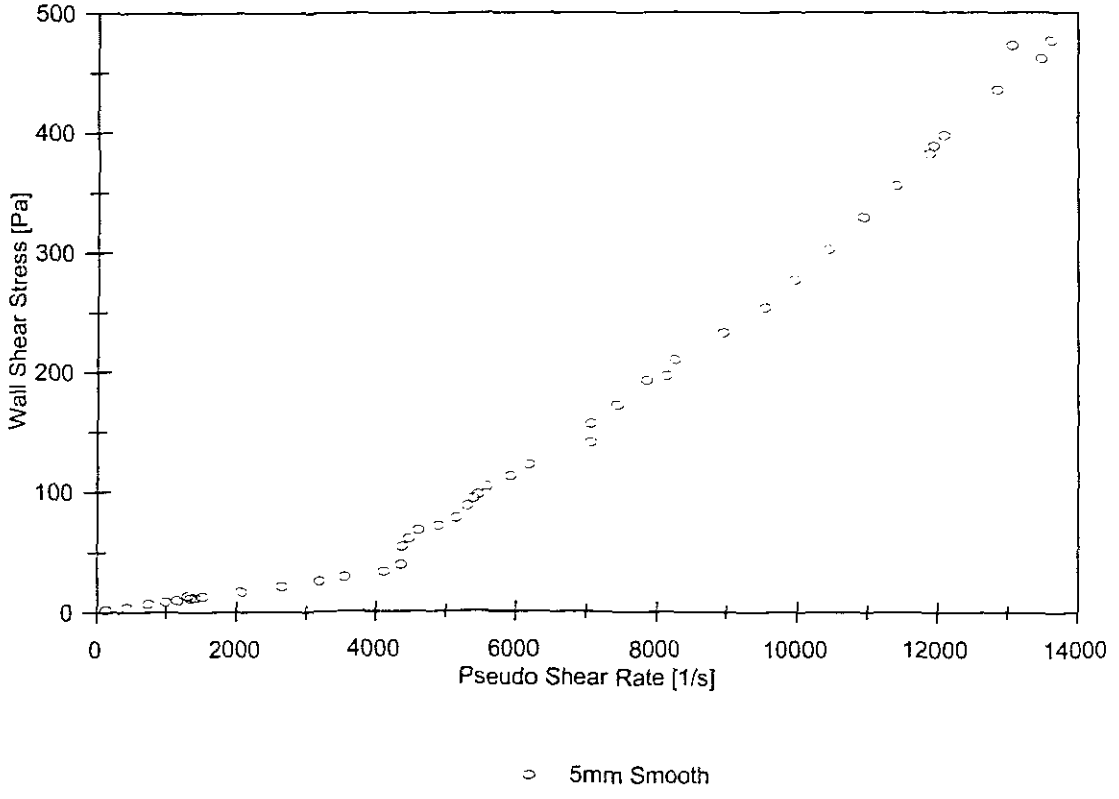

APPARATUS

Facility	BBTV
Pipe name	13 Smooth
Diameter (mm)	13.12
Pipe roughness (μm)	0.9
Material	Glycerol
Operator	FvS
Supervisor	PTS

SLURRY PROPERTIES

Solids Relative Density	N/A
Fluid Relative Density (S_m)	1.1433
Volumetric Concentration	N/A
Viscosity (Pa.s)	.00824
Representative Particle Size	N/A

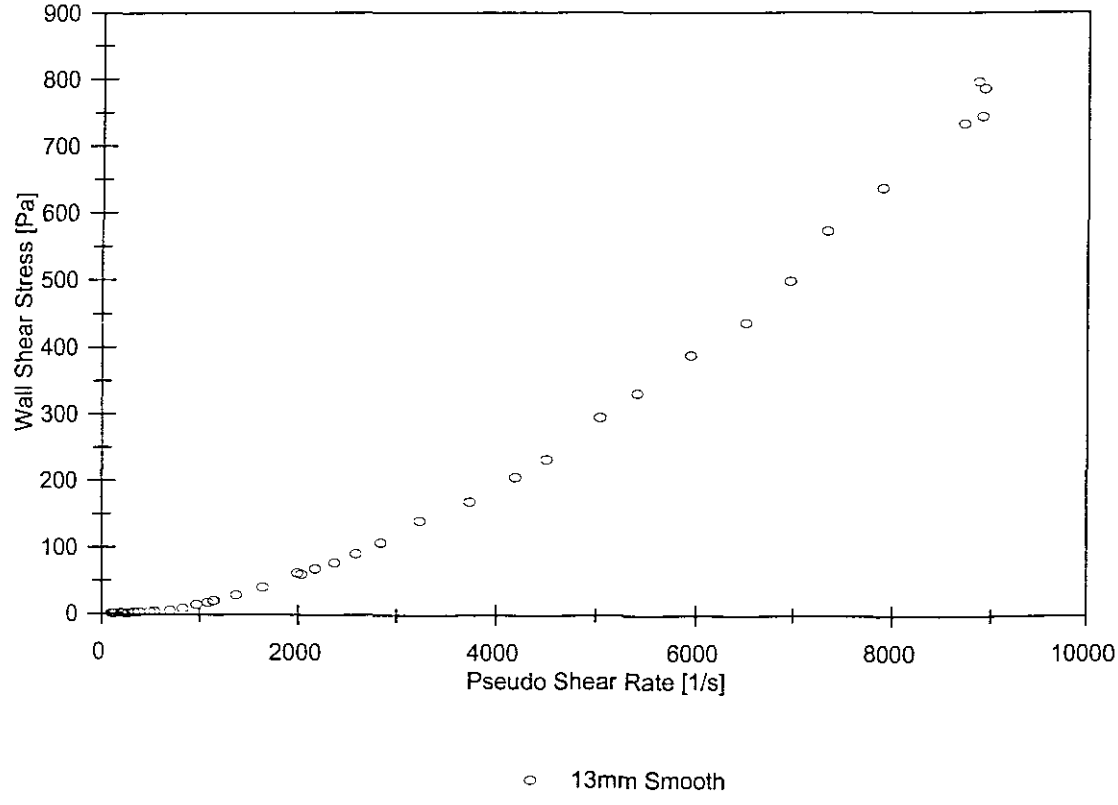

APPARATUS

Facility	BBTV
Pipe name	28 Smooth
Diameter (mm)	28.34
Pipe roughness (μm)	5.9
Material	Glycerol
Operator	FvS
Supervisor	PTS

SLURRY PROPERTIES

Solids Relative Density	N/A
Fluid Relative Density (S_m)	1.1433
Volumetric Concentration	N/A
Viscosity (Pa.s)	.00824
Representative Particle Size	N/A

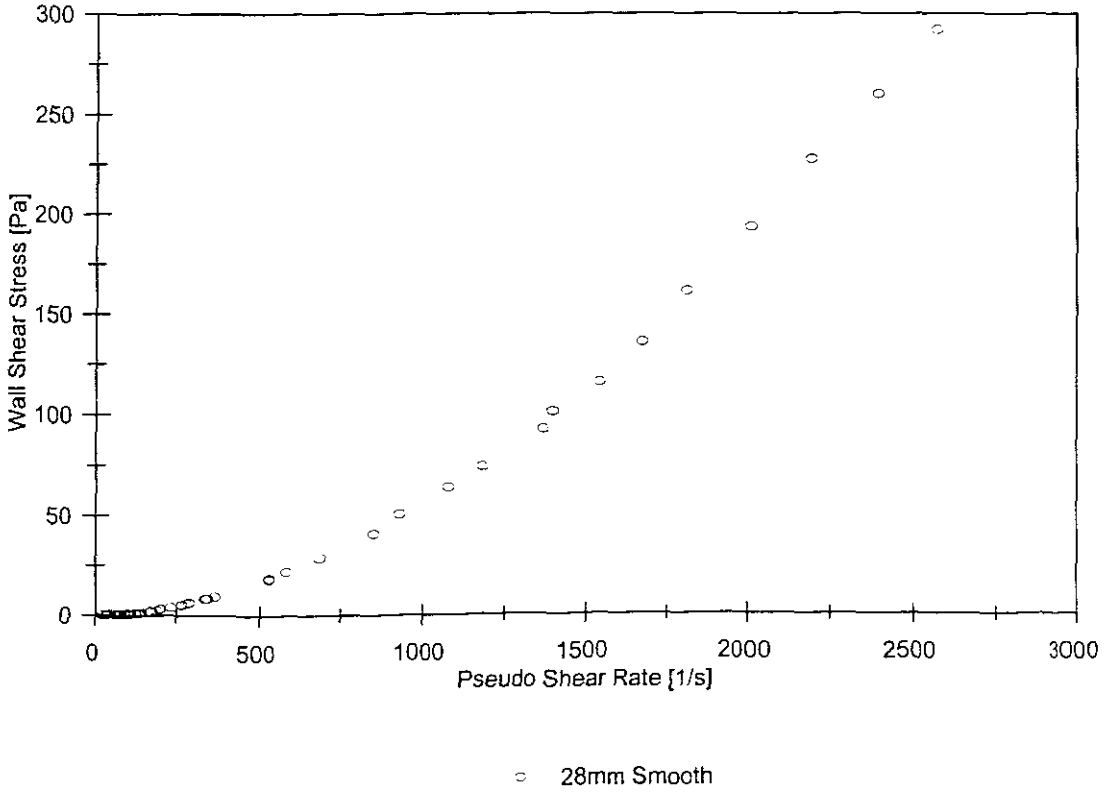

APPARATUS

Facility	BBTV
Pipe name	45 Smooth
Diameter (mm)	45.04
Pipe roughness (μm)	1.3
Material	Glycerol
Operator	FvS
Supervisor	PTS

SLURRY PROPERTIES

Solids Relative Density	N/A
Fluid Relative Density (S_m)	1.1433
Volumetric Concentration	N/A
Viscosity (Pa.s)	.00824
Representative Particle Size	N/A

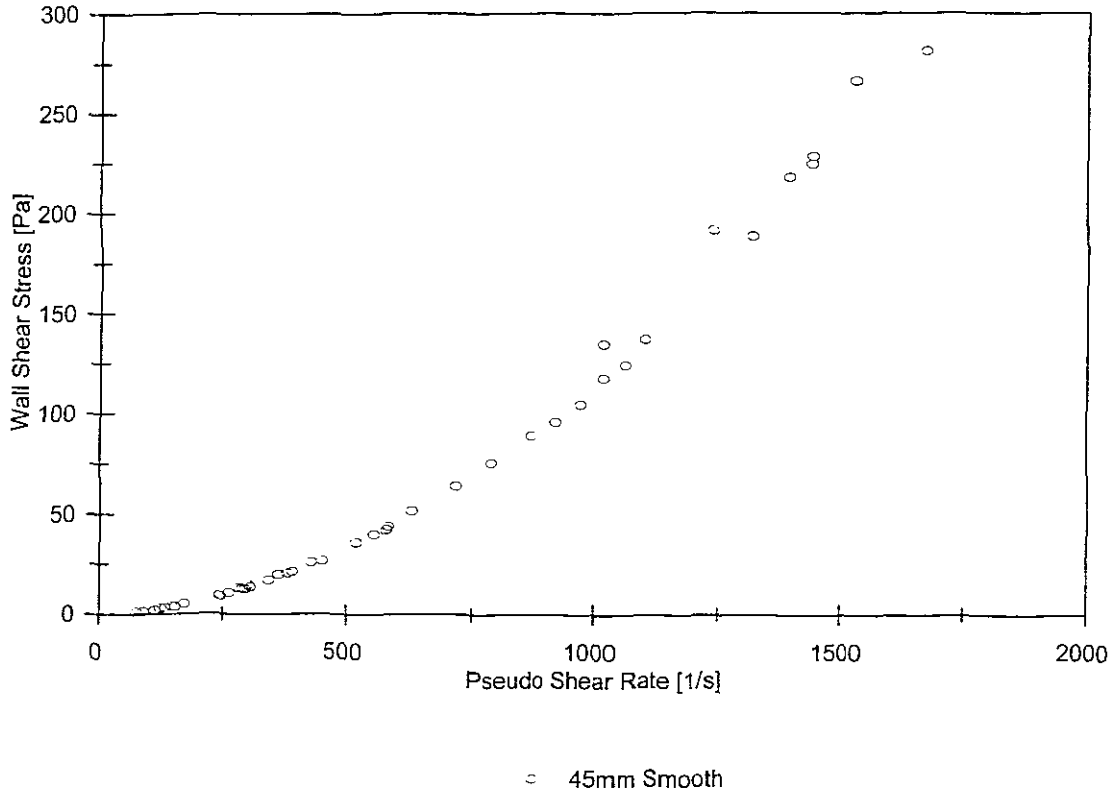

APPARATUS

Facility	BBTV
Pipe name	R28-1525
Diameter (mm)	27.03
Pipe roughness (μm)	136
Material	Glycerol
Operator	FvS
Supervisor	*PTS*

SLURRY PROPERTIES

Solids Relative Density	N/A
Fluid Relative Density (S_m)	1.1433
Volumetric Concentration	N/A
Viscosity (Pa.s)	.00824
Representative Particle Size	N/A

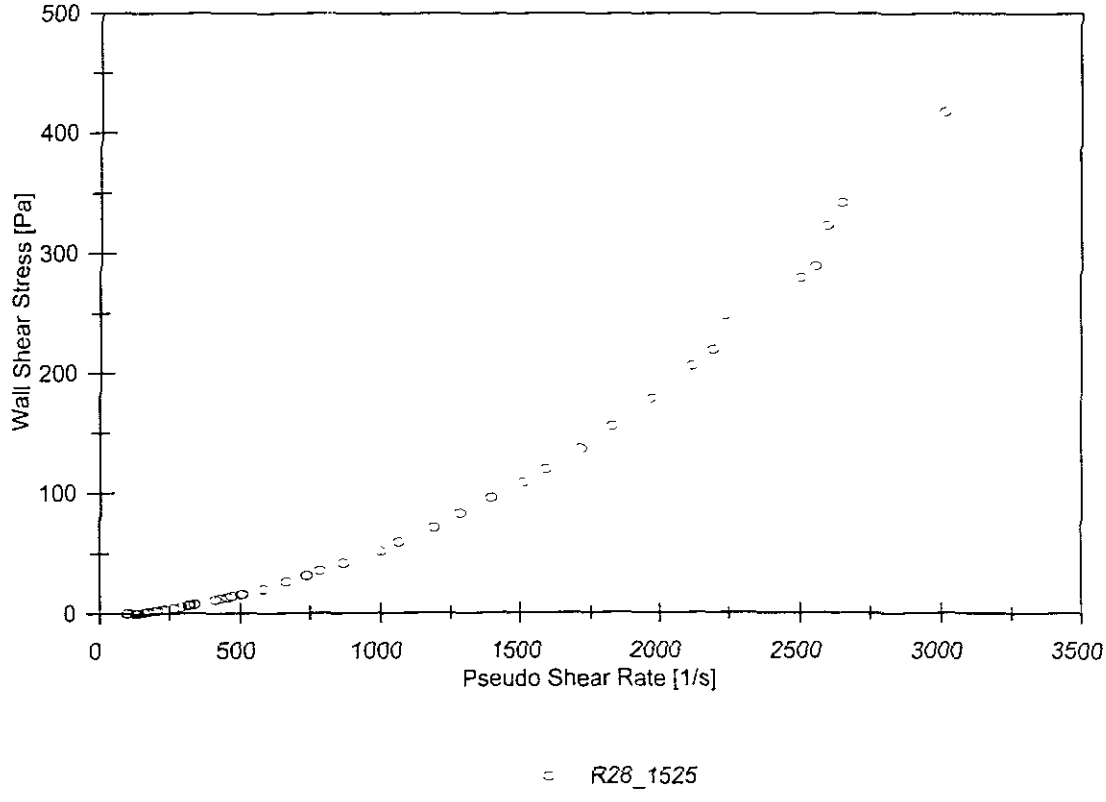

APPARATUS

Facility	BBTV
Pipe name	R28-3060
Diameter (mm)	27.17
Pipe roughness (μm)	291
Material	Glycerol
Operator	FvS
Supervisor	PTS

SLURRY PROPERTIES

Solids Relative Density	N/A
Fluid Relative Density (S_m)	1.1433
Volumetric Concentration	N/A
Viscosity (Pa.s)	.00824
Representative Particle Size	N/A

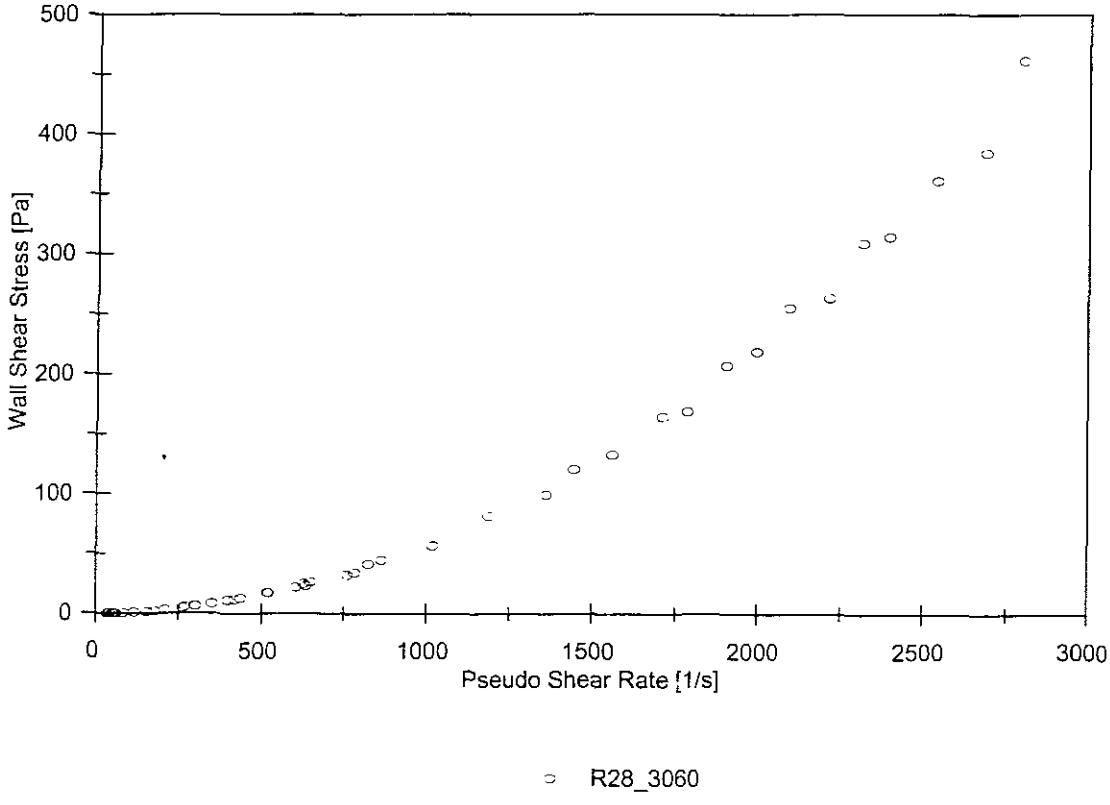

APPARATUS

Facility	BBTV
Pipe name	*R45-1525*
Diameter (mm)	44.73
Pipe roughness (μm)	42
Material	Glycerol
Operator	FvS
Supervisor	PTS

SLURRY PROPERTIES

Solids Relative Density	N/A
Fluid Relative Density (S_m)	1.1433
Volumetric Concentration	N/A
Viscosity (Pa.s)	.00824
Representative Particle Size	N/A

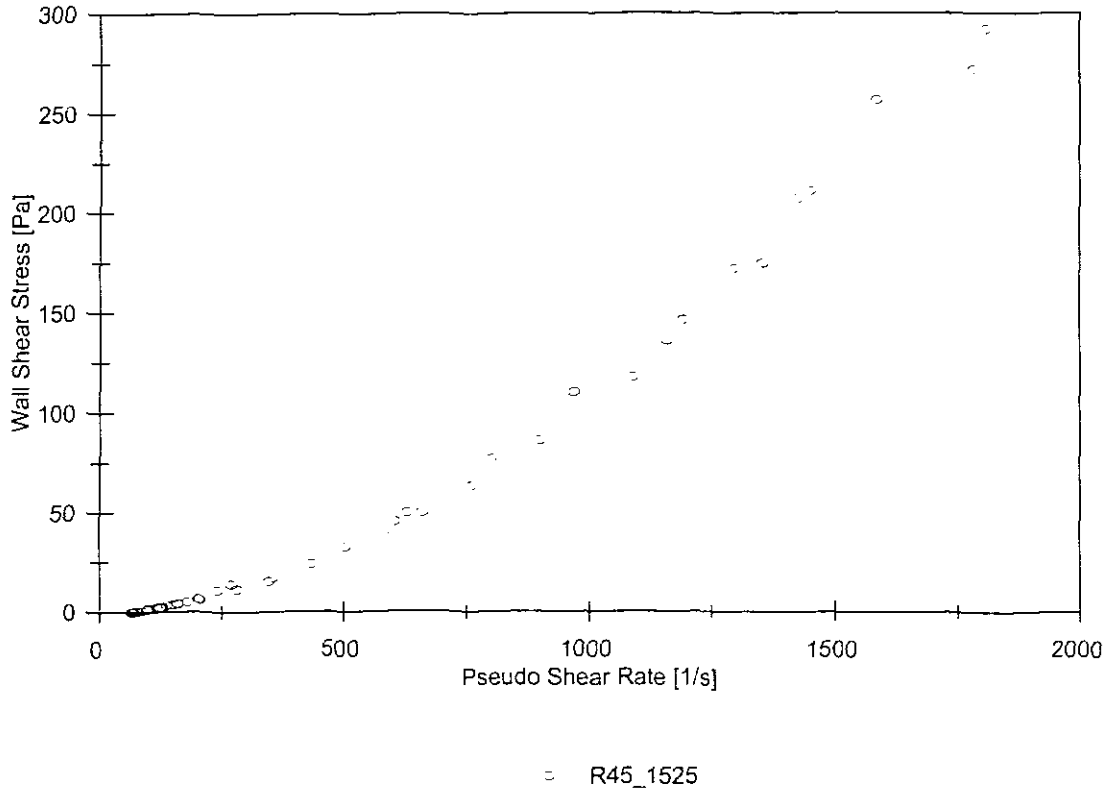

APPARATUS

Facility	BBTV
Pipe name	R45-3060
Diameter (mm)	45.44
Pipe roughness (μm)	672
Material	Glycerol
Operator	FvS
Supervisor	PTS

SLURRY PROPERTIES

Solids Relative Density	N/A
Fluid Relative Density (S_m)	1.1433
Volumetric Concentration	N/A
Viscosity (Pa.s)	.00824
Representative Particle Size	N/A

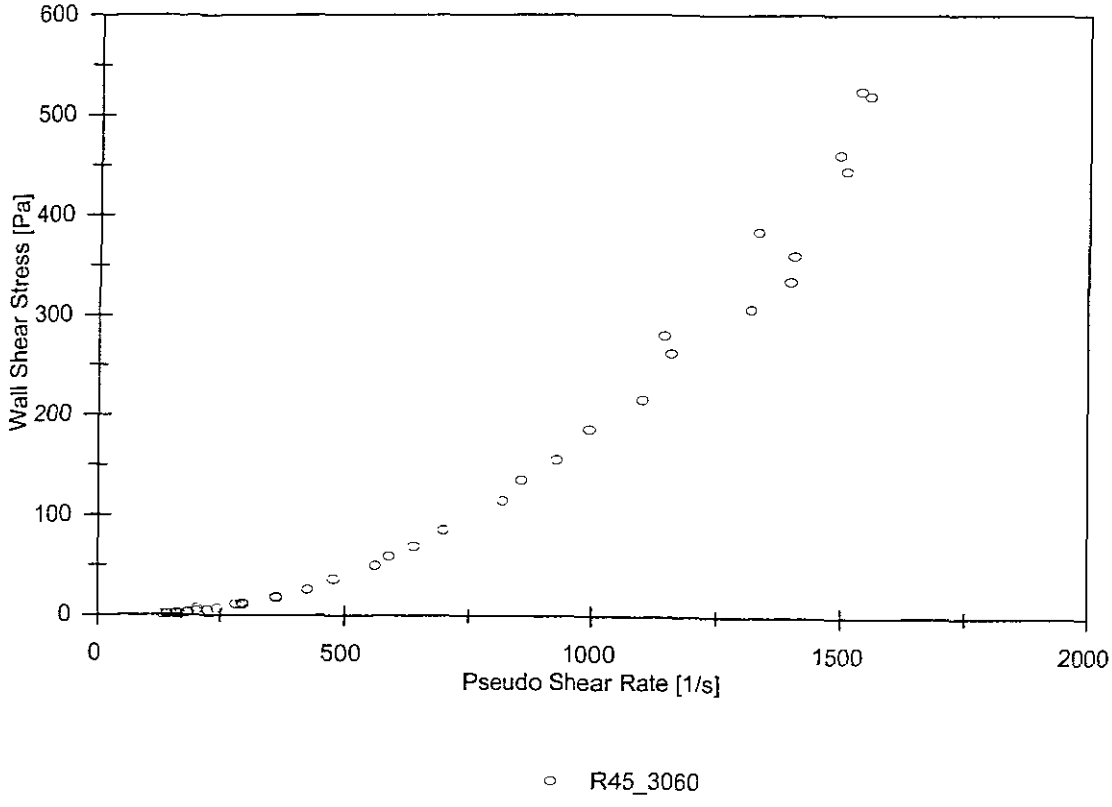

CMC TEST RESULTS $S_m = 1.0129$

APPARATUS

Facility	BBTV
Pipe name	5 Smooth
Diameter (mm)	5.78
Pipe roughness (μm)	1.1
Material	CMC
Operator	FvS
Supervisor	PTS

SLURRY PROPERTIES

Solids Relative Density	N/A
Fluid Relative Density (S_m)	1.0129
Volumetric Concentration	N/A
Yield Stress, τ_y (Pa)	0
Fluid Consistency Index, K ($Pa.s^n$)	0.02592
Flow Behaviour Index, *n*	0.84959
Representative Particle Size	N/A

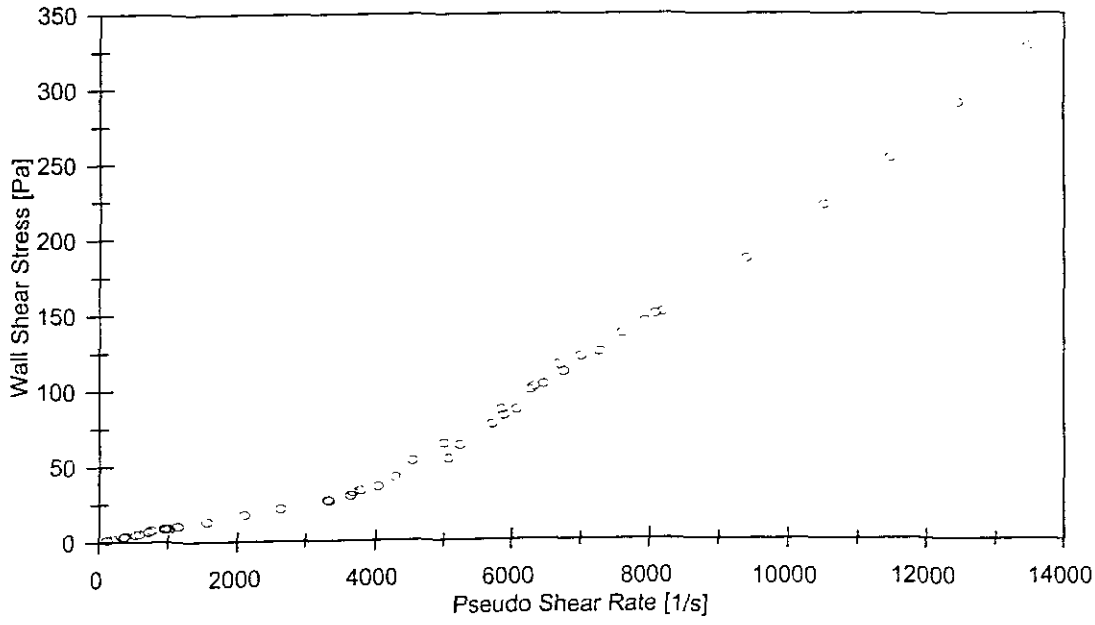

APPARATUS

Facility	BBTV
Pipe name	13 Smooth
Diameter (mm)	13.12
Pipe roughness (μm)	0.9
Material	CMC
Operator	FvS
Supervisor	PTS

SLURRY PROPERTIES

Solids Relative Density	N/A
Fluid Relative Density (S_m)	1.0129
Volumetric Concentration	N/A
Yield Stress, τ_y (Pa)	0
Fluid Consistency Index, K (Pa.s^n)	0.02592
Flow Behaviour Index, n	0.84959
Representative Particle Size	N/A

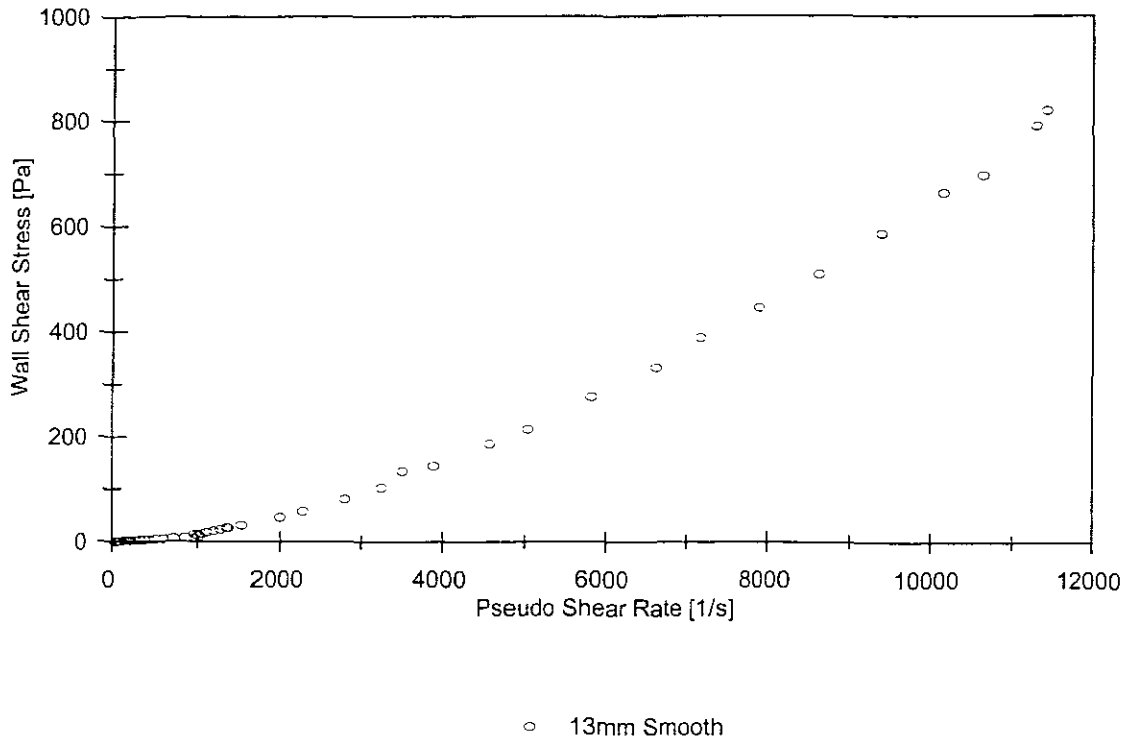

APPARATUS

Facility	BBTV
Pipe name	28 Smooth
Diameter (mm)	28.34
Pipe roughness (μm)	5.9
Material	CMC
Operator	FvS
Supervisor	PTS

SLURRY PROPERTIES

Solids Relative Density	N/A
Fluid Relative Density (S_m)	1.0129
Volumetric Concentration	N/A
Yield Stress, τ_y (Pa)	0
Fluid Consistency Index, K ($Pa.s^n$)	0.02592
Flow Behaviour Index, n	0.84959
Representative Particle Size	N/A

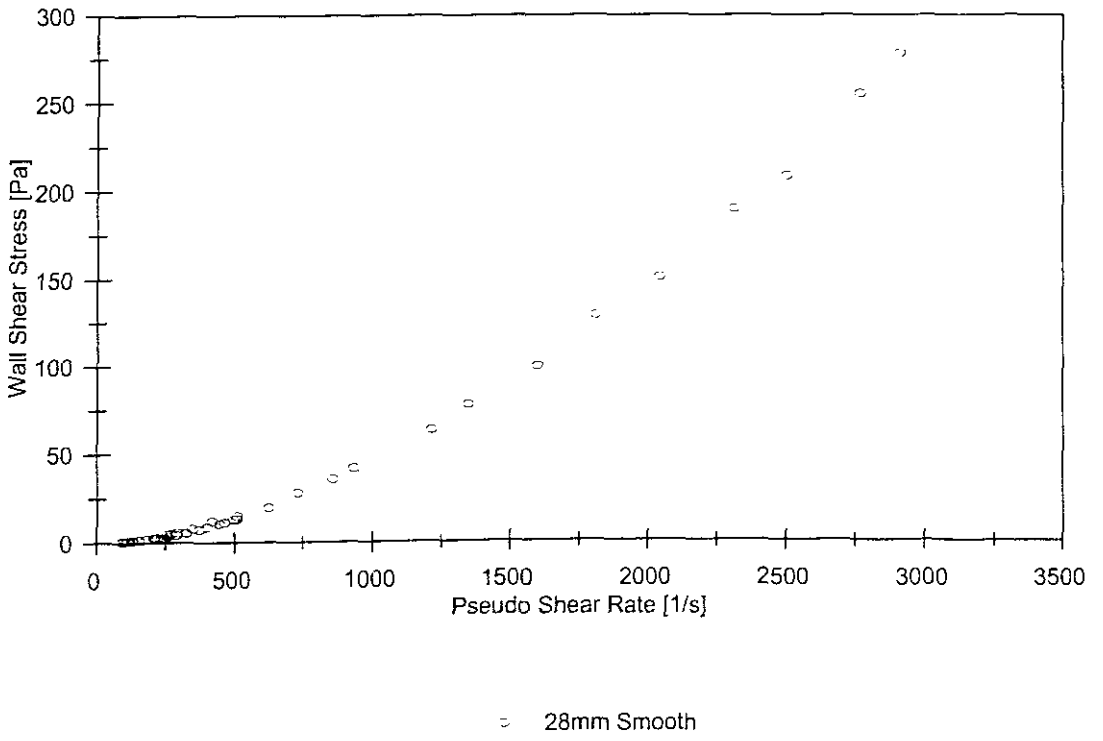

APPARATUS

Facility	BBTV
Pipe name	45 Smooth
Diameter (mm)	45.04
Pipe roughness (μm)	1.3
Material	CMC
Operator	FvS
Supervisor	PTS

SLURRY PROPERTIES

Solids Relative Density	N/A
Fluid Relative Density (S_m)	1.0129
Volumetric Concentration	N/A
Yield Stress, τ_y (Pa)	0
Fluid Consistency Index, K (Pa.s^n)	0.02592
Flow Behaviour Index, n	0.84959
Representative Particle Size	N/A

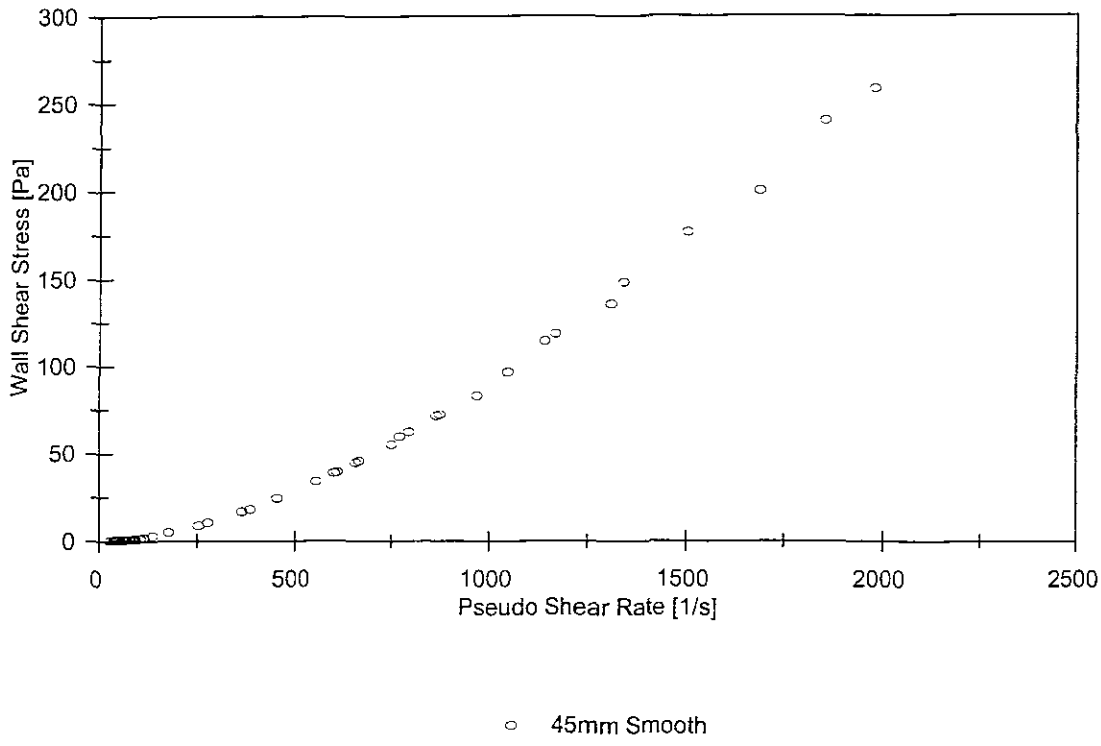

APPARATUS

Facility	BBTV
Pipe name	R28-1525
Diameter (mm)	27.03
Pipe roughness (μm)	136
Material	CMC
Operator	FvS
Supervisor	PTS

SLURRY PROPERTIES

Solids Relative Density	N/A
Fluid Relative Density (S_m)	1.0129
Volumetric Concentration	N/A
Yield Stress, τ_y (Pa)	0
Fluid Consistency Index, K (Pa.s^n)	0.02592
Flow Behaviour Index, n	0.84959
Representative Particle Size	N/A

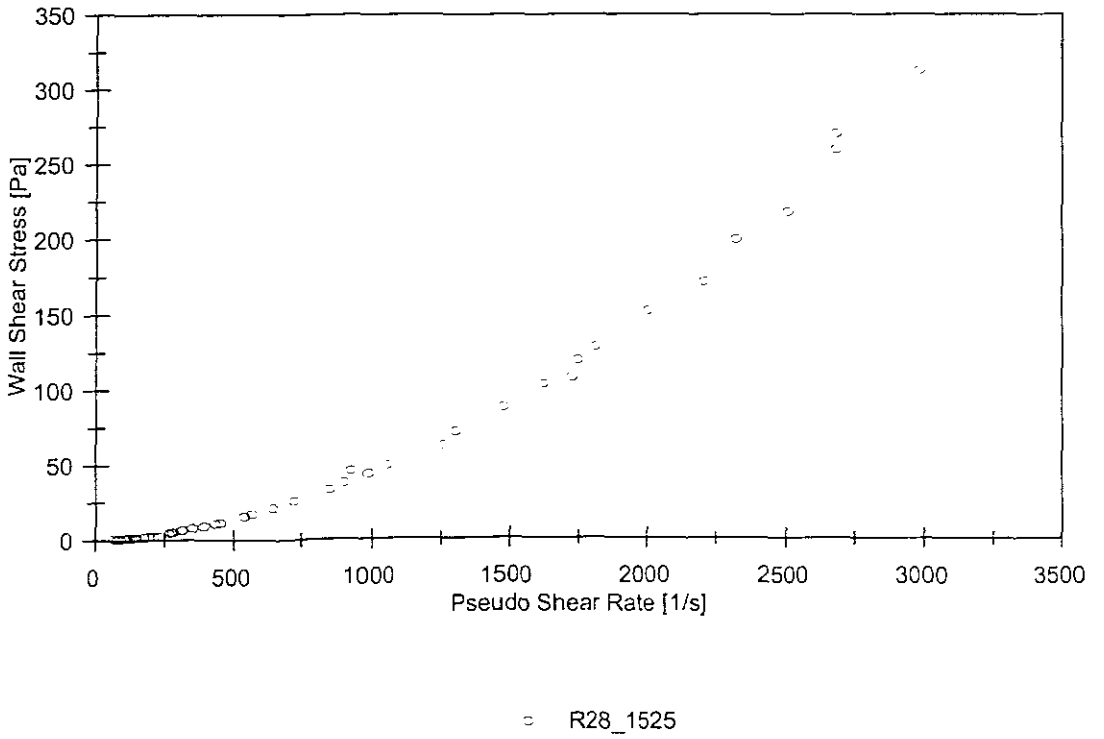

APPARATUS

Facility	BBTV
Pipe name	R28-3060
Diameter (mm)	27.17
Pipe roughness (μm)	291
Material	CMC
Operator	FvS
Supervisor	PTS

SLURRY PROPERTIES

Solids Relative Density	N/A
Fluid Relative Density (S_m)	1.0129
Volumetric Concentration	N/A
Yield Stress, τ_y (Pa)	0
Fluid Consistency Index, K (Pa.s^n)	0.02592
Flow Behaviour Index, n	0.84959
Representative Particle Size	N/A

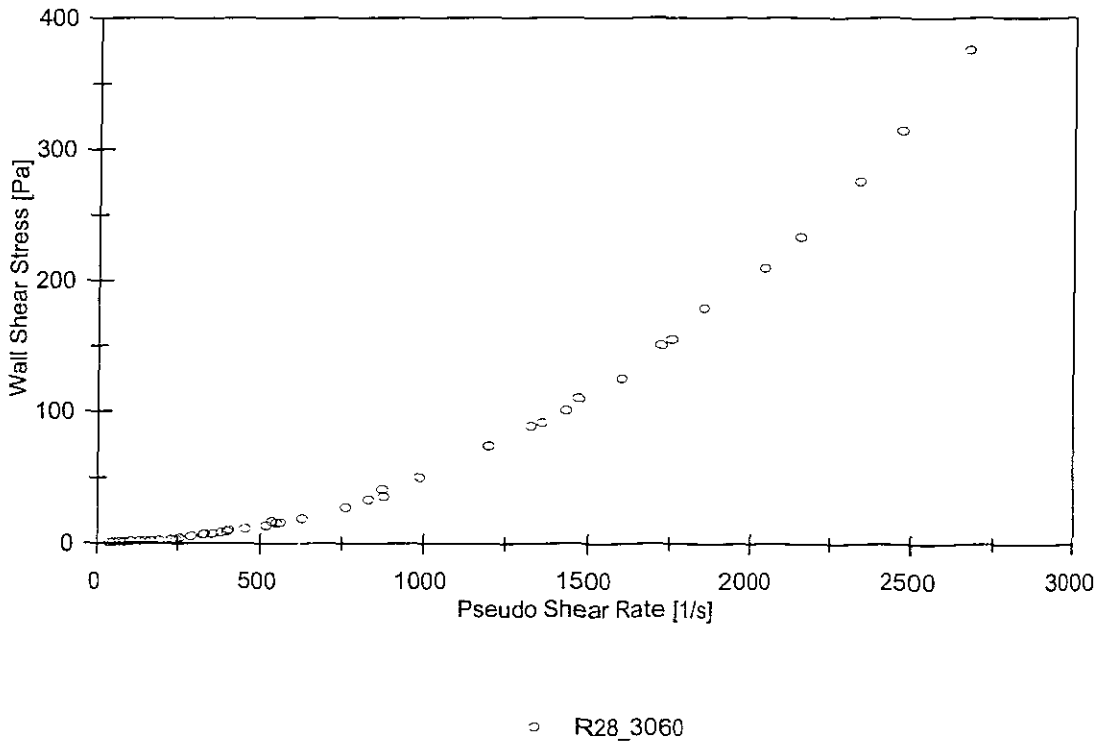

APPARATUS

Facility	BBTV
Pipe name	R45-1525
Diameter (mm)	44.73
Pipe roughness (μm)	42
Material	CMC
Operator	FvS
Supervisor	PTS

SLURRY PROPERTIES

Solids Relative Density	N/A
Fluid Relative Density (S_m)	1.0129
Volumetric Concentration	N/A
Yield Stress, τ_y (Pa)	0
Fluid Consistency Index, K (Pa.s^n)	0.02592
Flow Behaviour Index, n	0.84959
Representative Particle Size	N/A

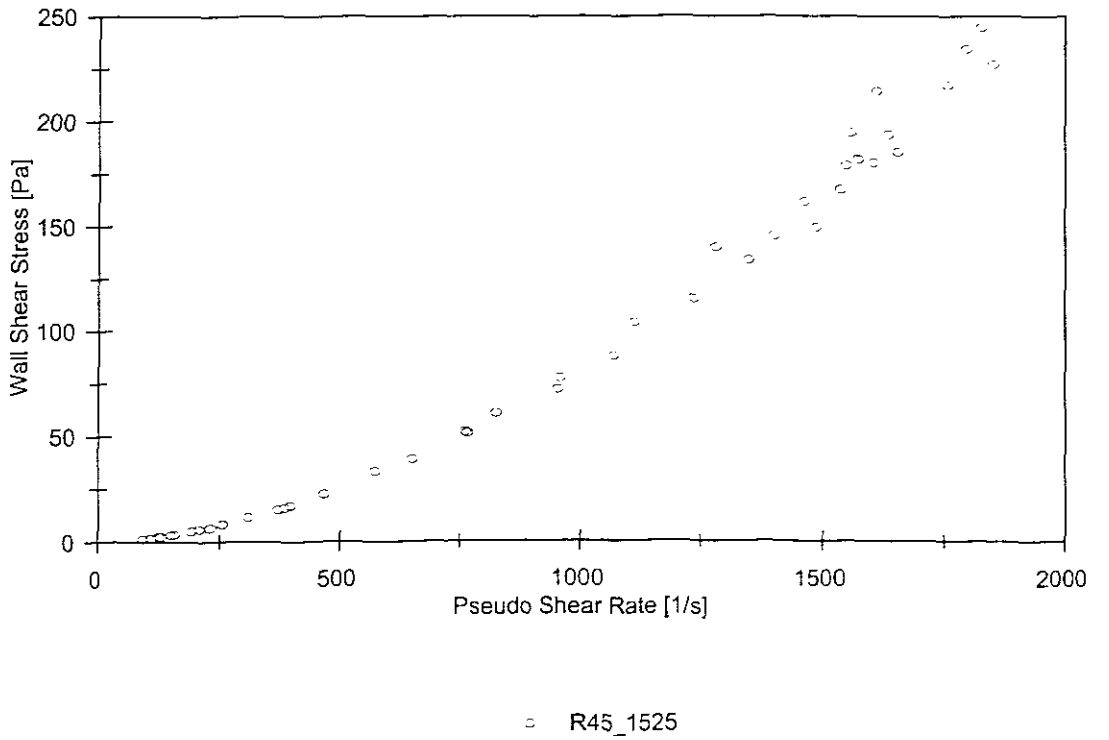

APPARATUS

Facility	BBTV
Pipe name	R45-3060
Diameter (mm)	45.44
Pipe roughness (μm)	672
Material	CMC
Operator	FvS
Supervisor	PTS

SLURRY PROPERTIES

Solids Relative Density	N/A
Fluid Relative Density (S_m)	1.0129
Volumetric Concentration	N/A
Yield Stress, τ_y (Pa)	0
Fluid Consistency Index, K ($Pa.s^n$)	0.02592
Flow Behaviour Index, n	0.84959
Representative Particle Size	N/A

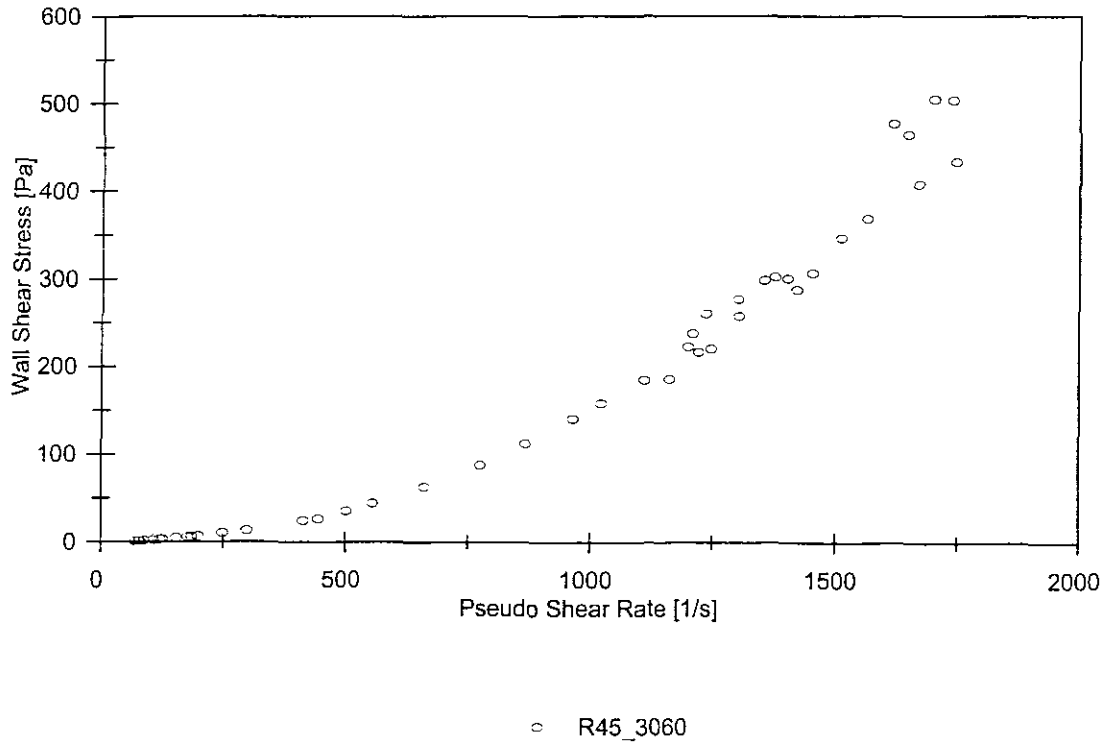

CMC TEST RESULTS $S_m = 1.0269$

APPARATUS

Facility	BBTV
Pipe name	5 Smooth
Diameter (mm)	5.78
Pipe roughness (μm)	1.1
Material	CMC
Operator	FvS
Supervisor	PTS

SLURRY PROPERTIES

Solids Relative Density	N/A
Fluid Relative Density (S_m)	1.0269
Volumetric Concentration	N/A
Yield Stress, τ_y (Pa)	0
Fluid Consistency Index, K (Pa.s^n)	0.12106
Flow Behaviour Index, n	0.82743
Representative Particle Size	N/A

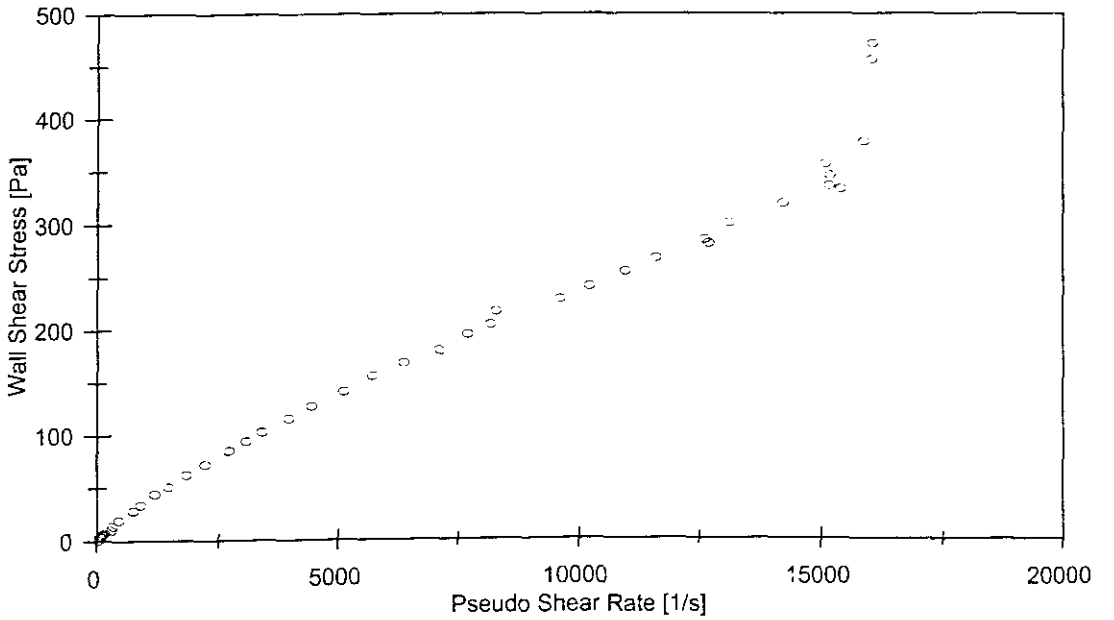

APPARATUS

Facility	BBTV
Pipe name	13 Smooth
Diameter (mm)	13.12
Pipe roughness (μm)	0.9
Material	CMC
Operator	FvS
Supervisor	PTS

SLURRY PROPERTIES

Solids Relative Density	N/A
Fluid Relative Density (S_m)	1.0269
Volumetric Concentration	N/A
Yield Stress, τ_y (Pa)	0
Fluid Consistency Index, K (Pa.s^n)	0.12106
Flow Behaviour Index, n	0.82743
Representative Particle Size	N/A

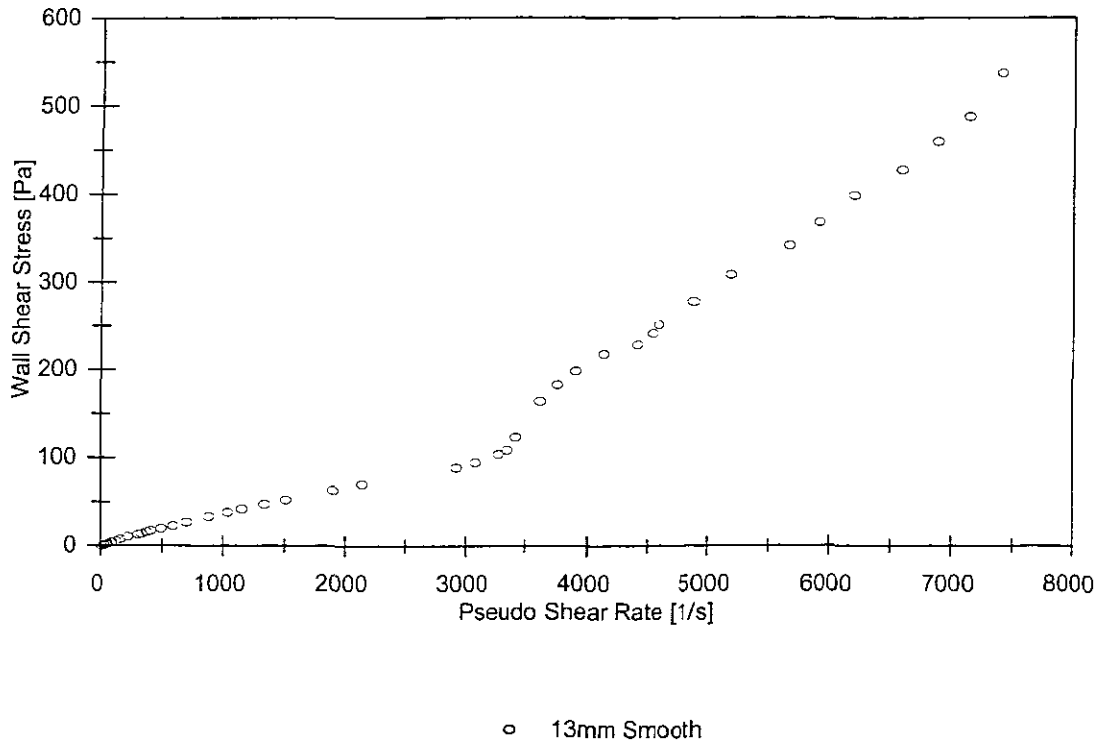

APPARATUS

Facility	BBTV
Pipe name	28 Smooth
Diameter (mm)	28.34
Pipe roughness (μm)	5.9
Material	CMC
Operator	FvS
Supervisor	PTS

SLURRY PROPERTIES

Solids Relative Density	N/A
Fluid Relative Density (S_m)	1.0269
Volumetric Concentration	N/A
Yield Stress, τ_y (Pa)	0
Fluid Consistency Index, K ($Pa.s^n$)	0.12106
Flow Behaviour Index, n	0.82743
Representative Particle Size	N/A

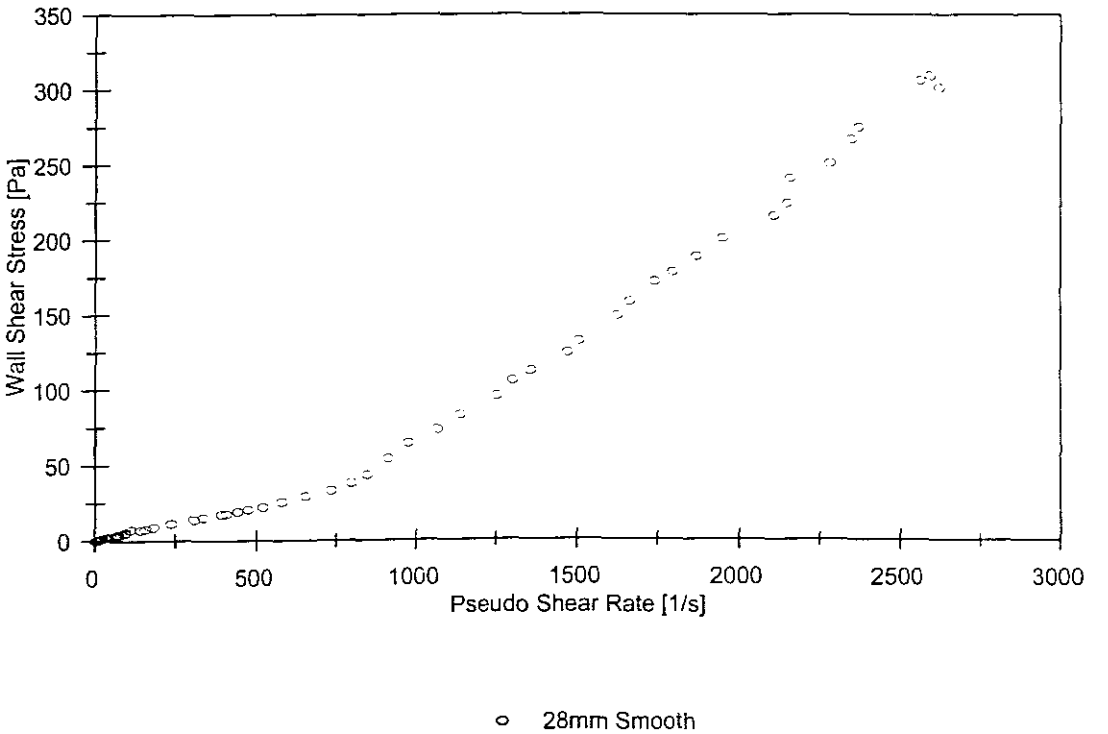

APPARATUS

Facility	BBTV
Pipe name	45 Smooth
Diameter (mm)	45.04
Pipe roughness (μm)	1.3
Material	CMC
Operator	FvS
Supervisor	PTS

SLURRY PROPERTIES

Solids Relative Density	N/A
Fluid Relative Density (S_m)	1.0269
Volumetric Concentration	N/A
Yield Stress, τ_y (Pa)	0
Fluid Consistency Index, K (Pa.s^n)	0.12106
Flow Behaviour Index, n	0.82743
Representative Particle Size	N/A

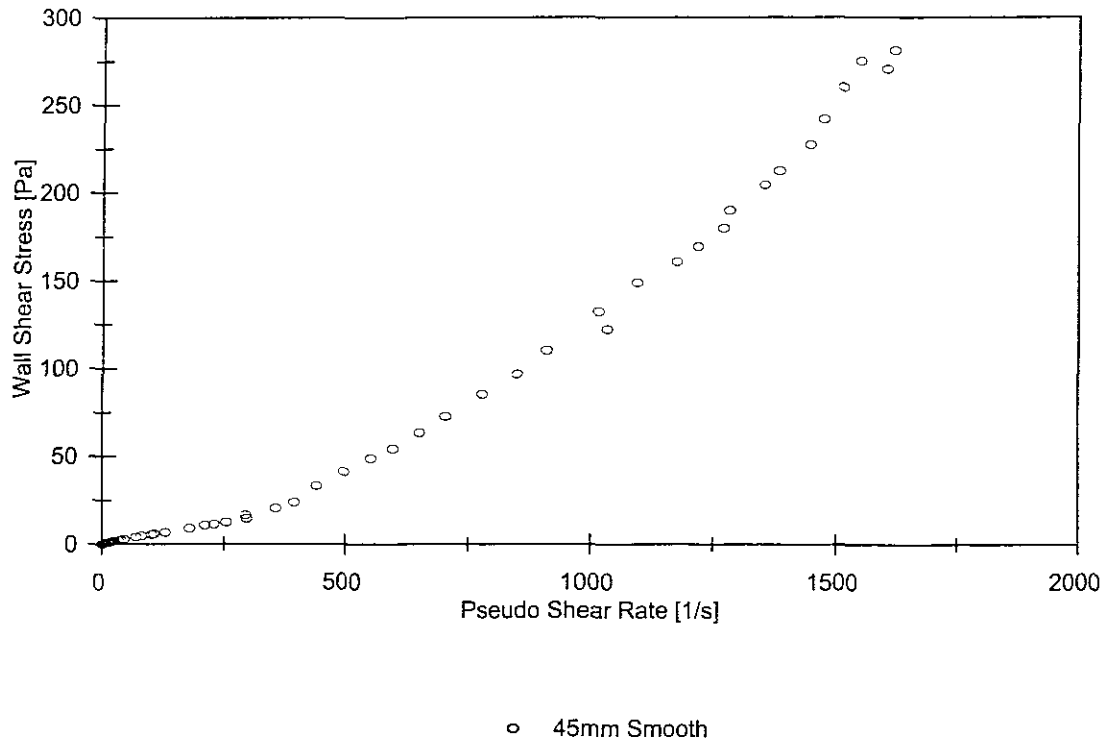

APPARATUS

Facility	BBTV
Pipe name	R28-1525
Diameter (mm)	27.03
Pipe roughness (μm)	136
Material	CMC
Operator	FvS
Supervisor	PTS

SLURRY PROPERTIES

Solids Relative Density	N/A
Fluid Relative Density (S_m)	1.0269
Volumetric Concentration	N/A
Yield Stress, τ_y (Pa)	0
Fluid Consistency Index, K ($Pa.s^n$)	0.12106
Flow Behaviour Index, n	0.82743
Representative Particle Size	N/A

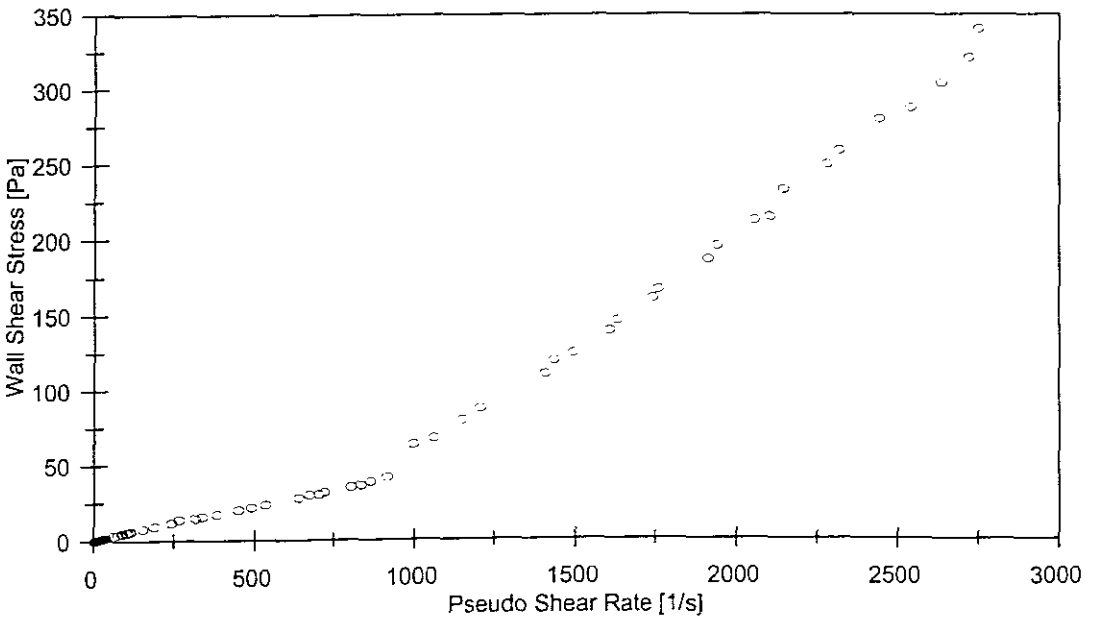

APPARATUS

Facility	BBTV
Pipe name	R28-3060
Diameter (mm)	27.17
Pipe roughness (μm)	291
Material	CMC
Operator	FvS
Supervisor	PTS

SLURRY PROPERTIES

Solids Relative Density	N/A
Fluid Relative Density (S_m)	1.0269
Volumetric Concentration	N/A
Yield Stress, τ_y (Pa)	0
Fluid Consistency Index, K (Pa.s^n)	0.12106
Flow Behaviour Index, n	0.82743
Representative Particle Size	N/A

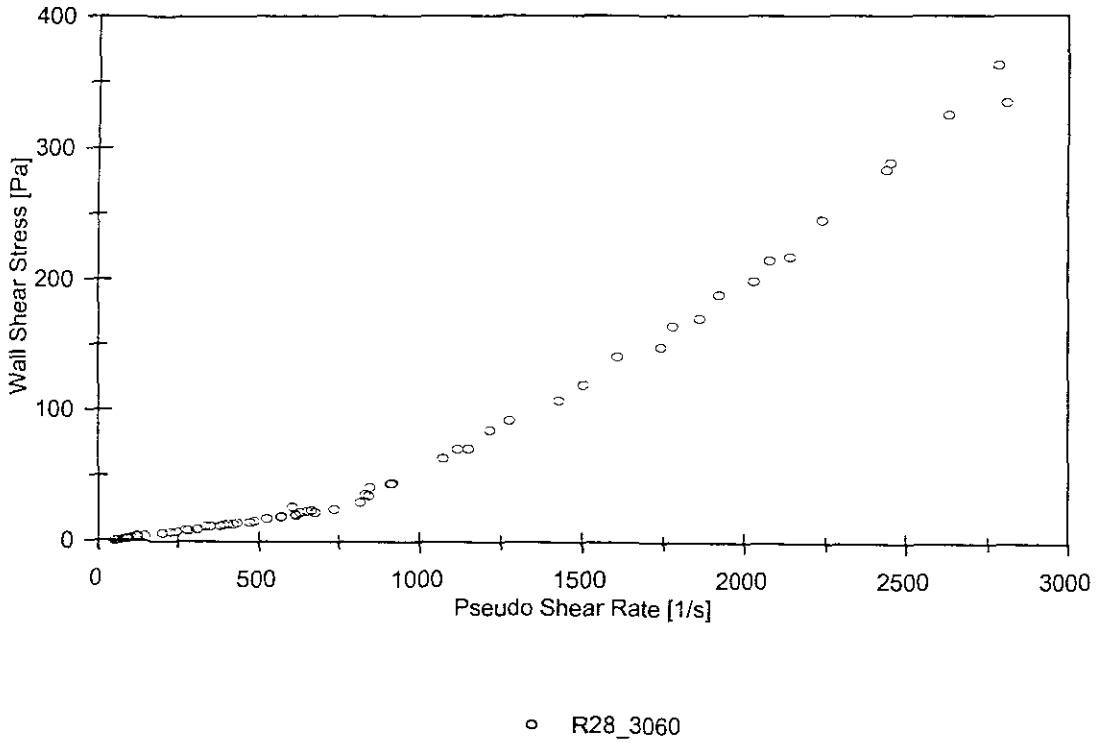

APPARATUS

Facility	BBTV
Pipe name	R45-1525
Diameter (mm)	44.73
Pipe roughness (μm)	42
Material	CMC
Operator	FvS
Supervisor	PTS

SLURRY PROPERTIES

Solids Relative Density	N/A
Fluid Relative Density (S_m)	1.0269
Volumetric Concentration	N/A
Yield Stress, τ_y (Pa)	0
Fluid Consistency Index, K (Pa.s^n)	0.12106
Flow Behaviour Index, n	0.82743
Representative Particle Size	N/A

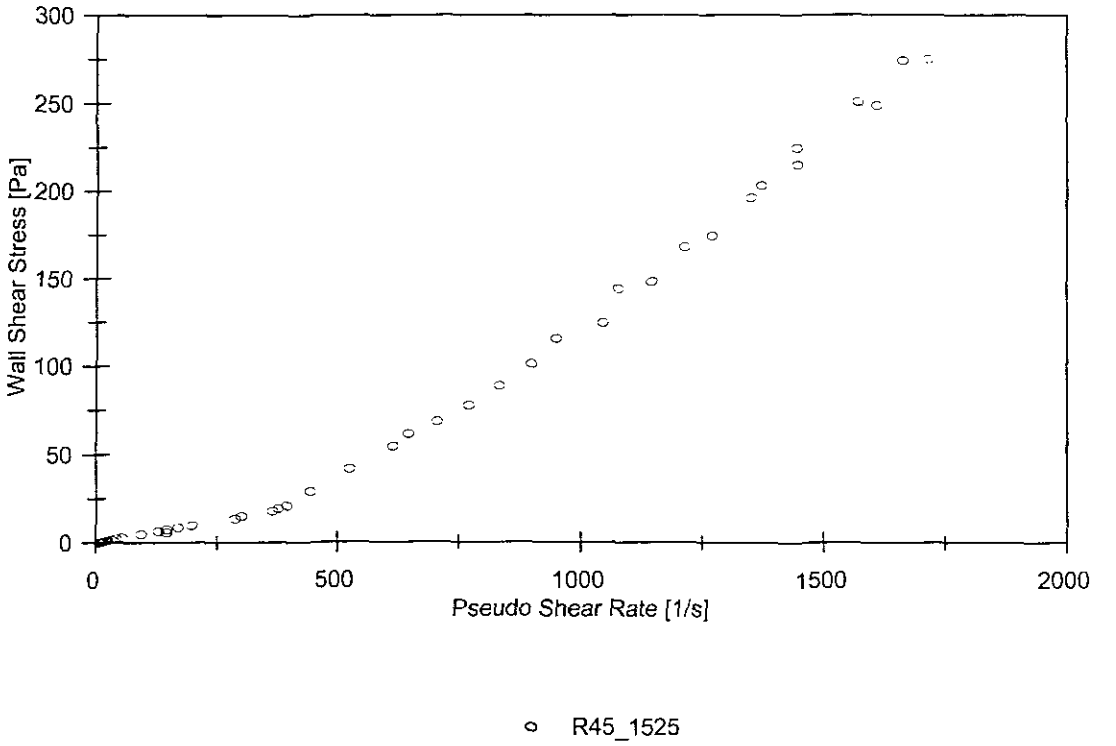

APPARATUS

Facility	BBTV
Pipe name	R45-3060
Diameter (mm)	45.44
Pipe roughness (μm)	672
Material	CMC
Operator	FvS
Supervisor	PTS

SLURRY PROPERTIES

Solids Relative Density	N/A
Fluid Relative Density (S_{rl})	1.0269
Volumetric Concentration	N/A
Yield Stress, τ_y (Pa)	0
Fluid Consistency Index, K (Pa.s^n)	0.12106
Flow Behaviour Index, n	0.82743
Representative Particle Size	N/A

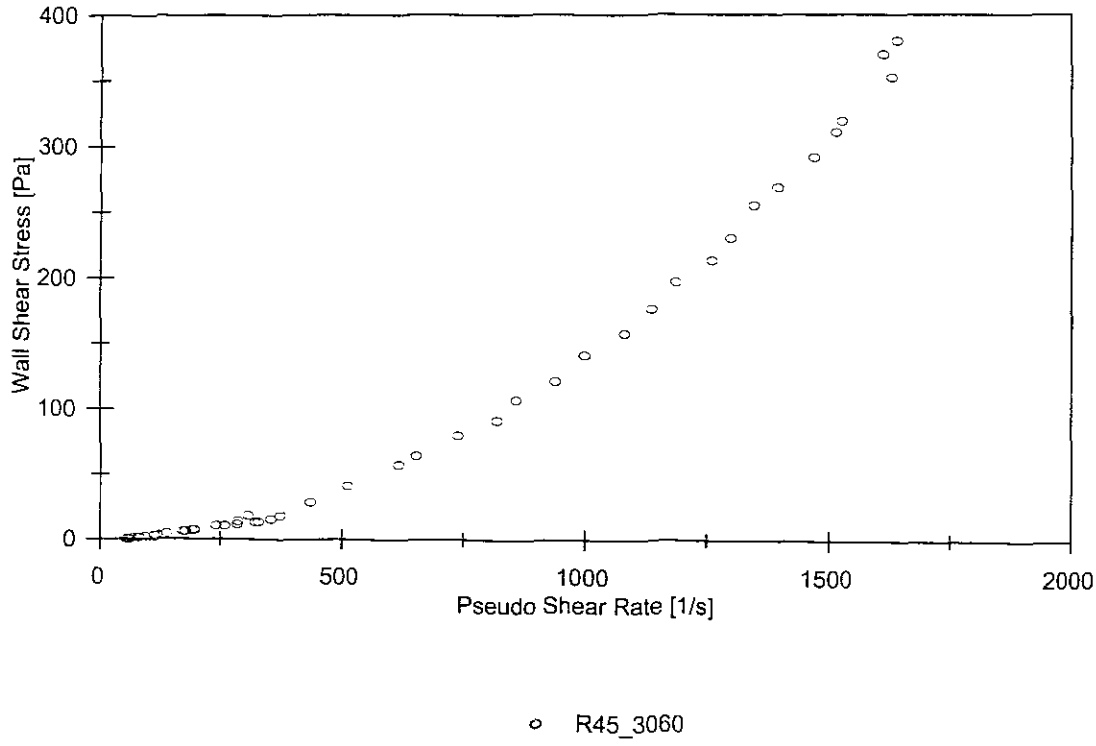

CMC TEST RESULTS $S_m = 1.0372$

APPARATUS	
Facility	BBTV
Pipe name	5 Smooth
Diameter (mm)	5.78
Pipe roughness (μm)	1.1
Material	CMC
Operator	FvS
Supervisor	PTS

SLURRY PROPERTIES	
Solids Relative Density	N/A
Fluid Relative Density (S_m)	1.0372
Volumetric Concentration	N/A
Yield Stress, τ_y (Pa)	0
Fluid Consistency Index, K (Pa.s^n)	0.37011
Flow Behaviour Index, n	0.78749
Representative Particle Size	N/A

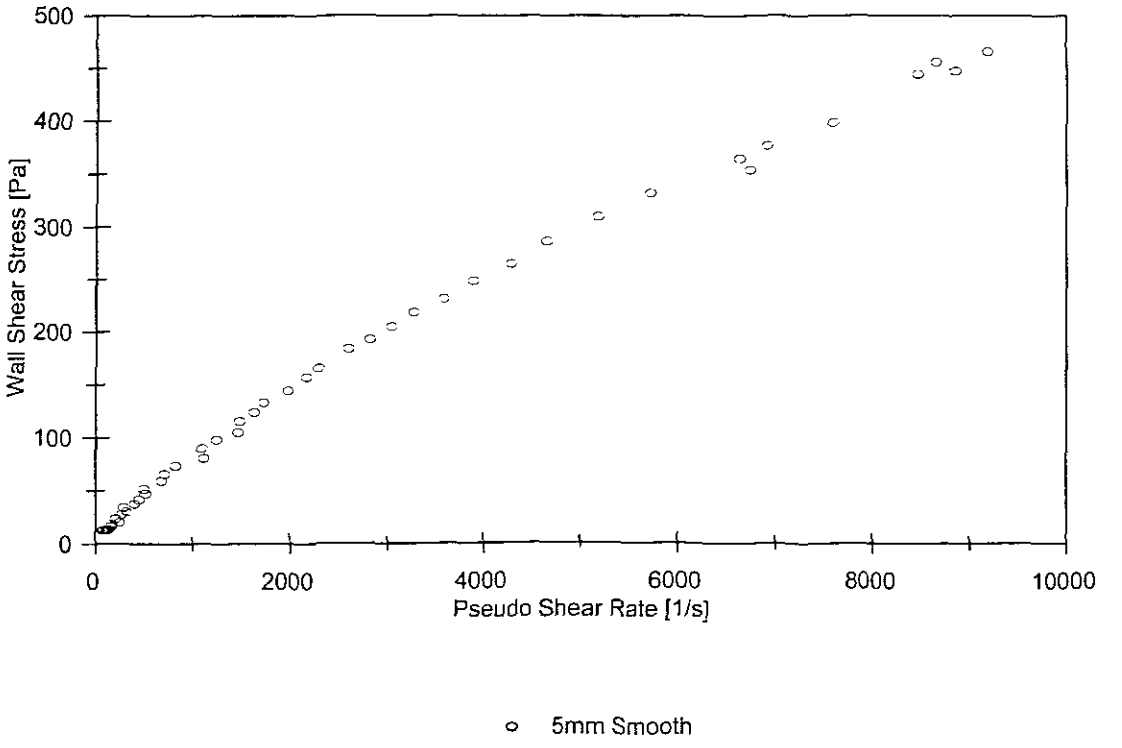

APPARATUS

Facility	BBTV
Pipe name	13 Smooth
Diameter (mm)	13.12
Pipe roughness (μm)	0.9
Material	CMC
Operator	FvS
Supervisor	PTS

SLURRY PROPERTIES

Solids Relative Density	N/A
Fluid Relative Density (S_m)	1.0372
Volumetric Concentration	N/A
Yield Stress, τ_y (Pa)	0
Fluid Consistency Index, K ($Pa.s^n$)	0.37011
Flow Behaviour Index, n	0.78749
Representative Particle Size	N/A

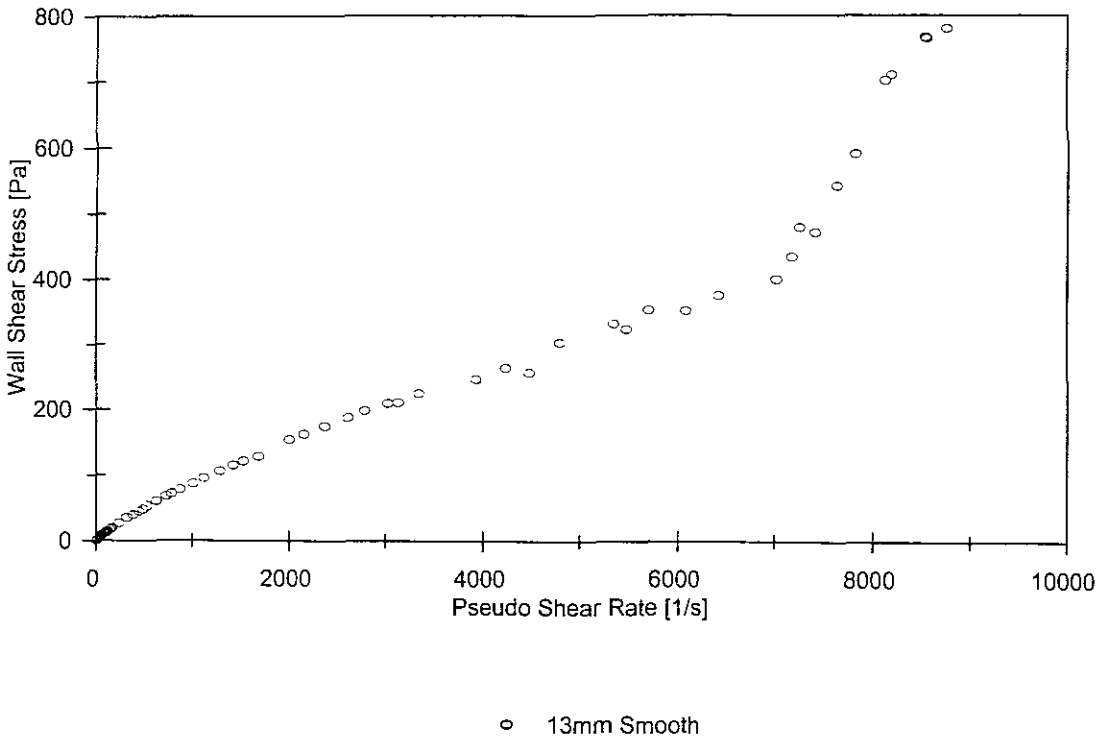

APPARATUS

Facility	BBTV
Pipe name	28 Smooth
Diameter (mm)	28.34
Pipe roughness (μm)	5.9
Material	CMC
Operator	FvS
Supervisor	PTS

SLURRY PROPERTIES

Solids Relative Density	N/A
Fluid Relative Density (S_m)	1.0372
Volumetric Concentration	N/A
Yield Stress, τ_y (Pa)	0
Fluid Consistency Index, K (Pa.s^n)	0.37011
Flow Behaviour Index, n	0.78749
Representative Particle Size	N/A

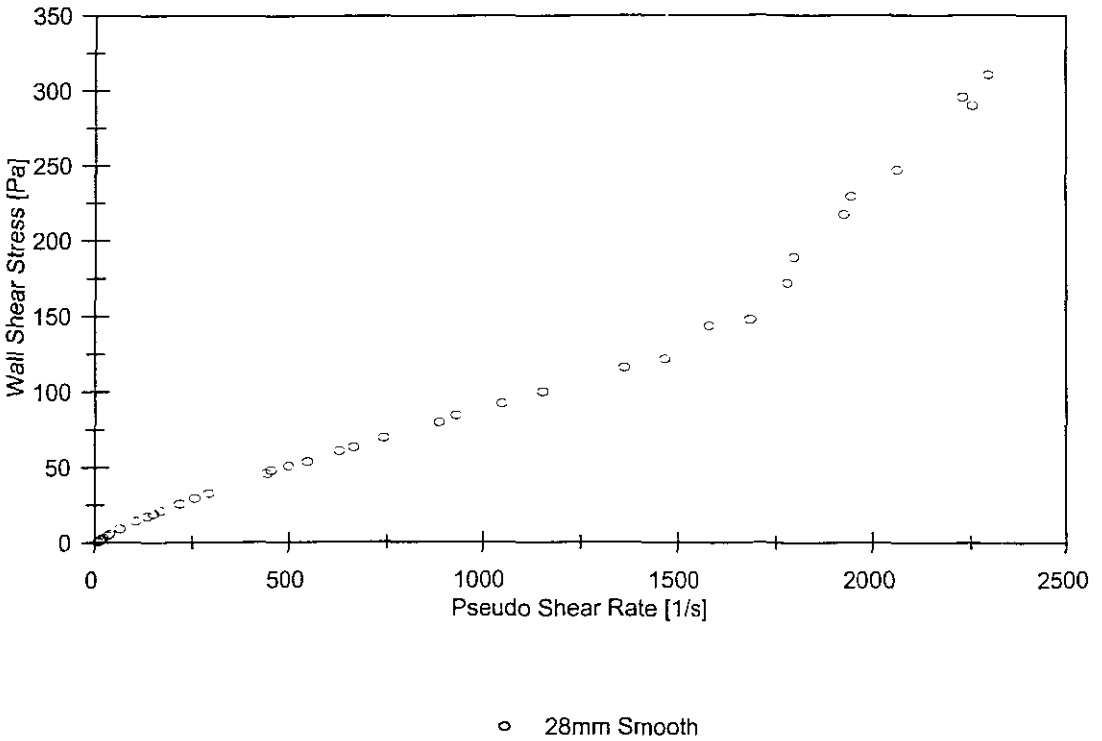

APPARATUS

Facility	BBTV
Pipe name	45 Smooth
Diameter (mm)	45.04
Pipe roughness (μm)	1.3
Material	CMC
Operator	FvS
Supervisor	PTS

SLURRY PROPERTIES

Solids Relative Density	N/A
Fluid Relative Density (S_m)	1.0372
Volumetric Concentration	N/A
Yield Stress, τ_y (Pa)	0
Fluid Consistency Index, K ($Pa.s^n$)	0.37011
Flow Behaviour Index, n	0.78749
Representative Particle Size	N/A

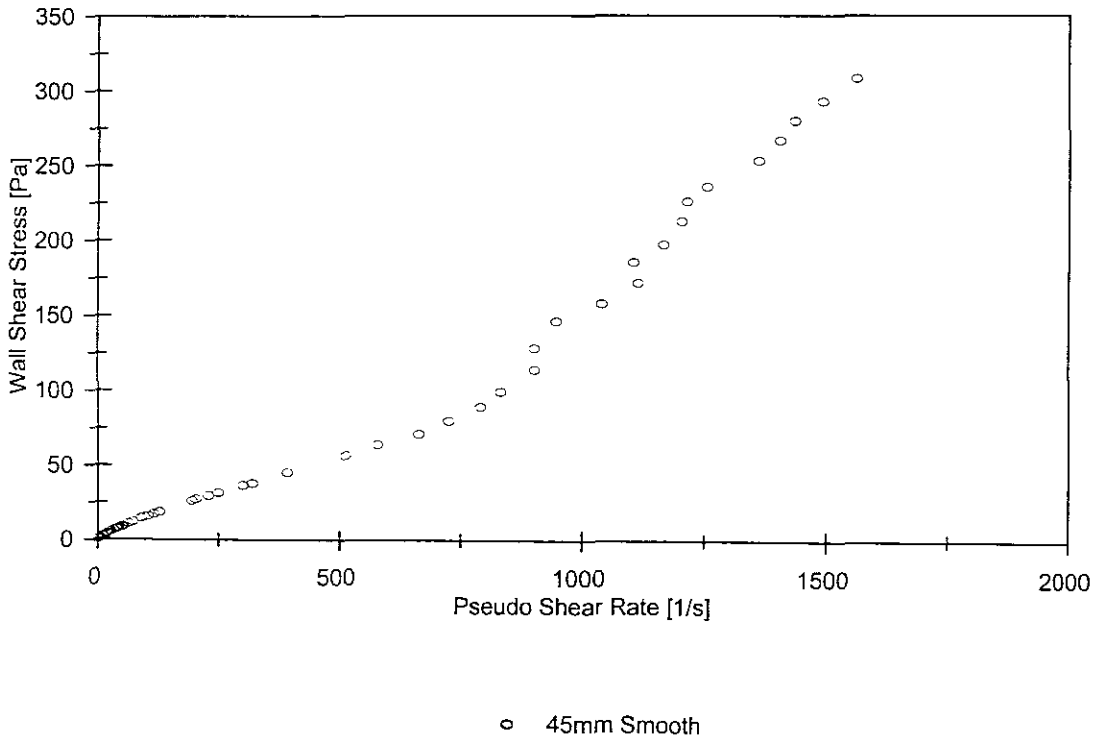

APPARATUS

Facility	BBTV
Pipe name	R28-1525
Diameter (mm)	27.03
Pipe roughness (μm)	136
Material	CMC
Operator	FvS
Supervisor	PTS

SLURRY PROPERTIES

Solids Relative Density	N/A
Fluid Relative Density (S_m)	1.0372
Volumetric Concentration	N/A
Yield Stress, τ_y (Pa)	0
Fluid Consistency Index, K (Pa.s^n)	0.37011
Flow Behaviour Index, n	0.78749
Representative Particle Size	N/A

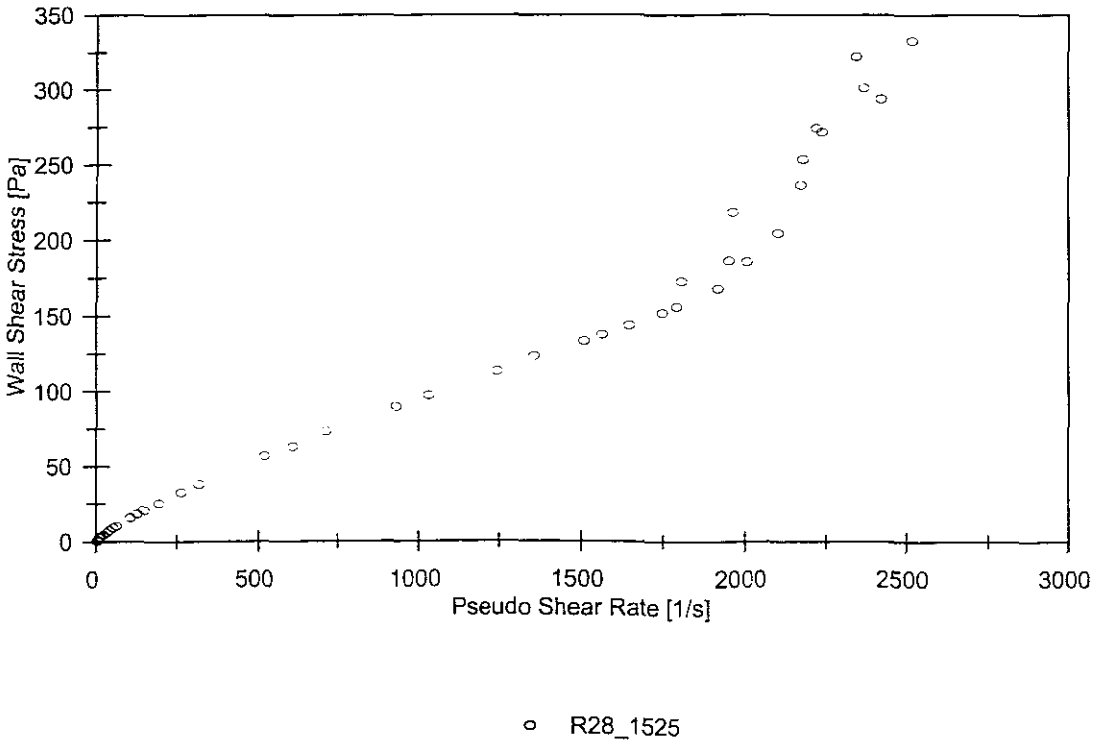

APPARATUS

Facility	BBTV
Pipe name	R28-3060
Diameter (mm)	27.17
Pipe roughness (μm)	291
Material	CMC
Operator	FvS
Supervisor	PTS

SLURRY PROPERTIES

Solids Relative Density	N/A
Fluid Relative Density (S_m)	1.0372
Volumetric Concentration	N/A
Yield Stress, τ_y (Pa)	0
Fluid Consistency Index, K (Pa.s^n)	0.37011
Flow Behaviour Index, n	0.78749
Representative Particle Size	N/A

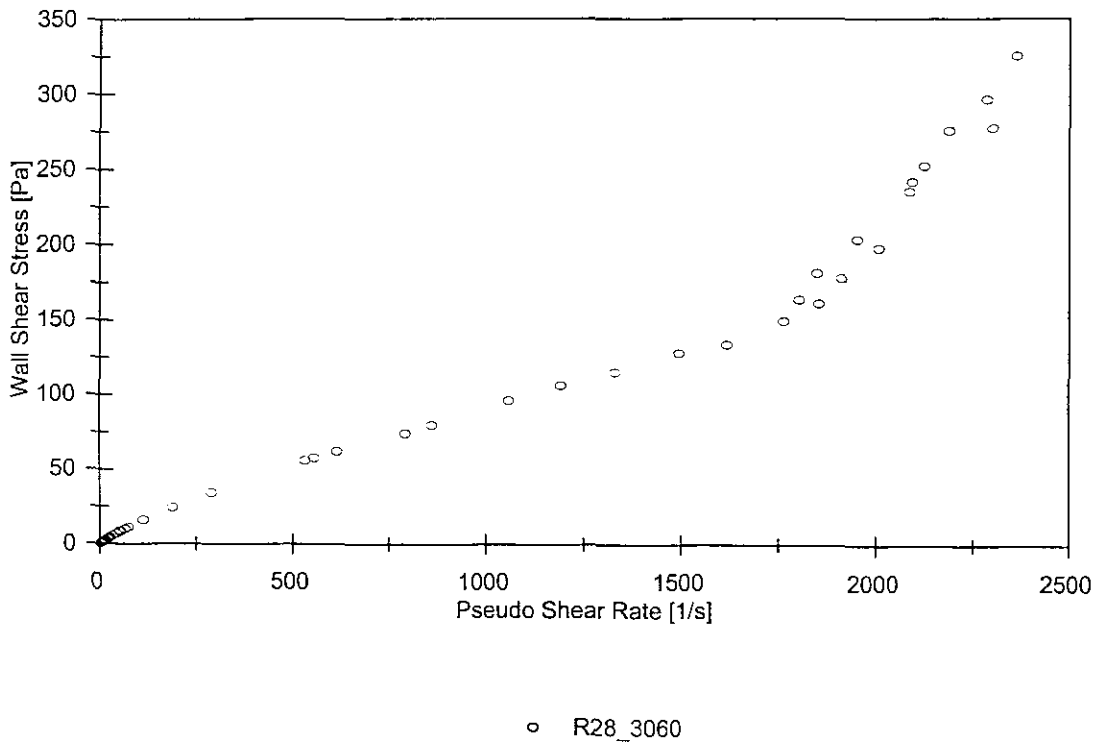

APPARATUS

Facility	BBTV
Pipe name	R45-1525
Diameter (mm)	44.73
Pipe roughness (μm)	42
Material	CMC
Operator	FvS
Supervisor	PTS

SLURRY PROPERTIES

Solids Relative Density	N/A
Fluid Relative Density (S_m)	1.0372
Volumetric Concentration	N/A
Yield Stress, τ_y (Pa)	0
Fluid Consistency Index, K (Pa.s^n)	0.37011
Flow Behaviour Index, n	0.78749
Representative Particle Size	N/A

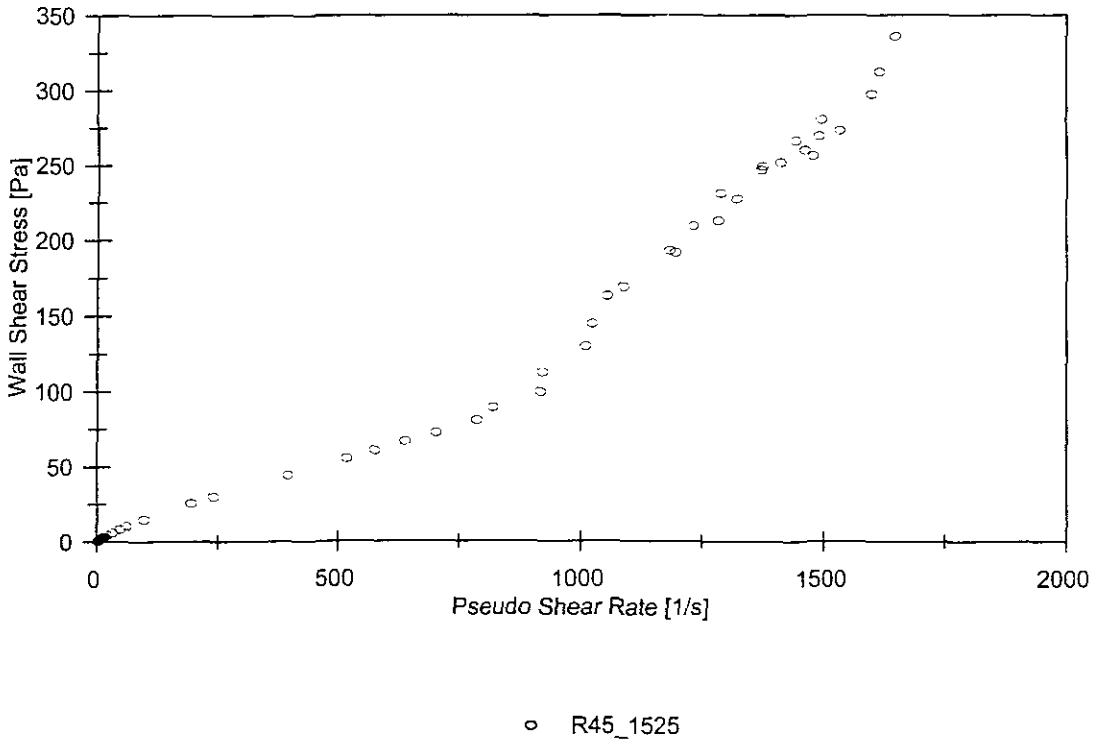

APPARATUS

Facility	BBTV
Pipe name	R45-3060
Diameter (mm)	45.44
Pipe roughness (μm)	672
Material	CMC
Operator	FvS
Supervisor	PTS

SLURRY PROPERTIES

Solids Relative Density	N/A
Fluid Relative Density (S_m)	1.0372
Volumetric Concentration	N/A
Yield Stress, τ_y (Pa)	0
Fluid Consistency Index, K (Pa.s^n)	0.37011
Flow Behaviour Index, n	0.78749
Representative Particle Size	N/A

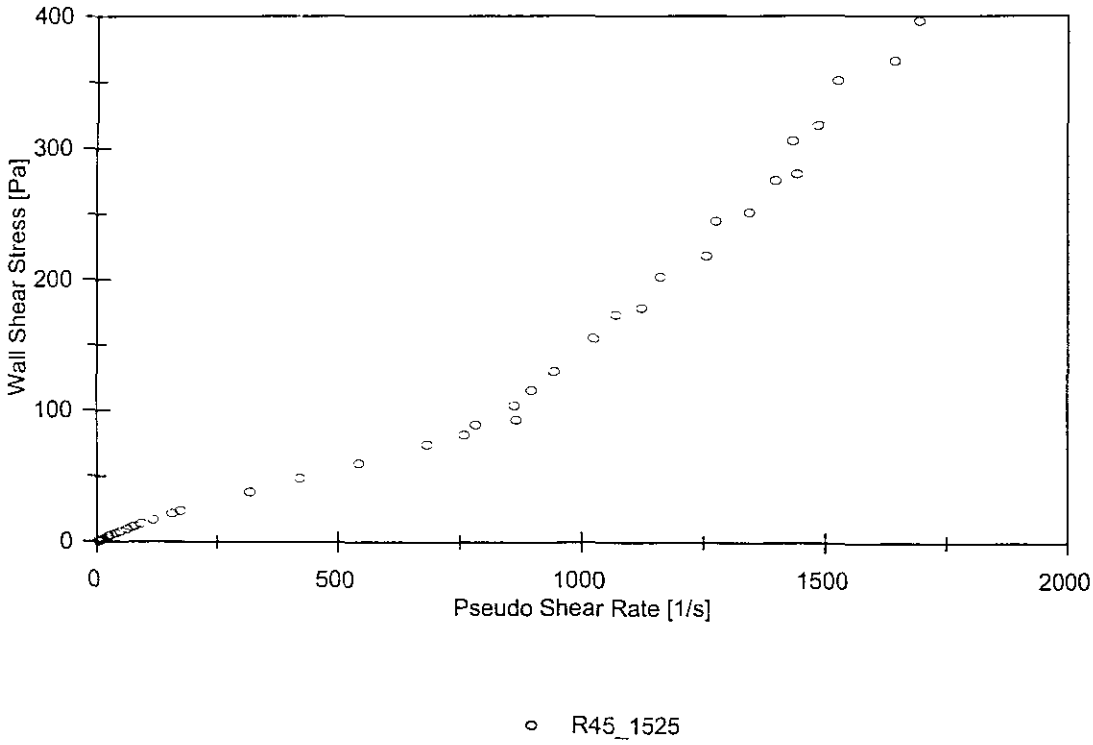

KAOLIN TEST RESULTS S_m = 1.0803

APPARATUS	
Facility	BBTV
Pipe name	5 Smooth
Diameter (mm)	5.78
Pipe roughness (μm)	1.1
Material	Kaolin
Operator	FvS
Supervisor	PTS

SLURRY PROPERTIES	
Solids Relative Density	2.65
Fluid Relative Density (S_m)	1.0803
Volumetric Concentration	4.85 %
Yield Stress, τ_y (Pa)	5.50494
Fluid Consistency Index, K (Pa.s^n)	0.28786
Flow Behaviour Index, n	0.46263
Representative Particle Size, d_{85}	15 μm

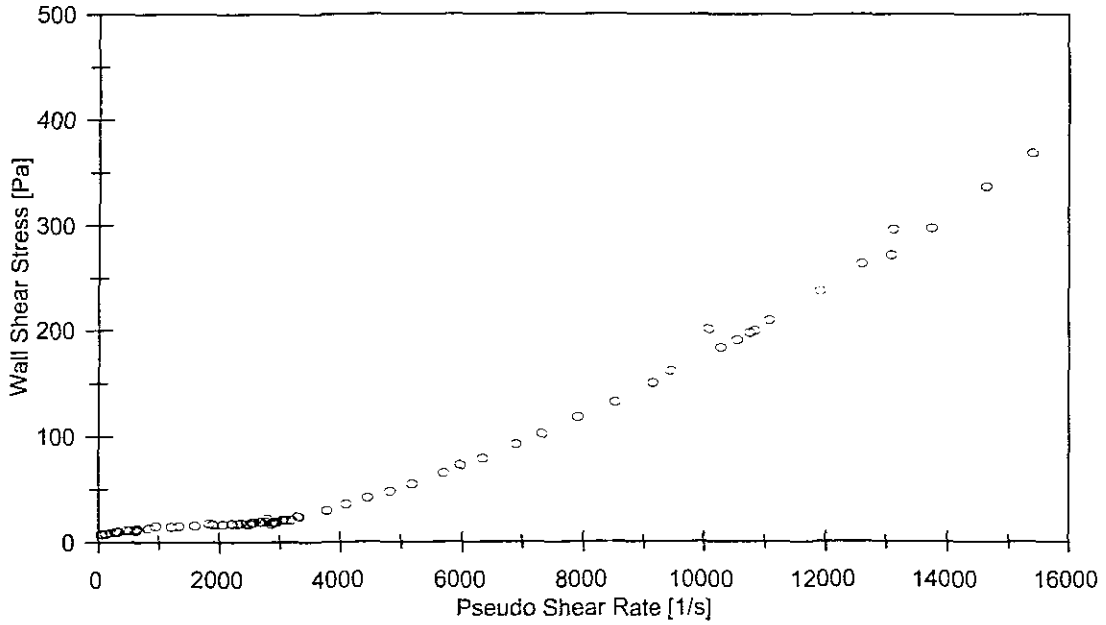

APPARATUS

Facility	BBTV
Pipe name	13 Smooth
Diameter (mm)	13.12
Pipe roughness (μm)	0.9
Material	Kaolin
Operator	FvS
Supervisor	PTS

SLURRY PROPERTIES

Solids Relative Density	2.65
Fluid Relative Density (S_m)	1.0803
Volumetric Concentration	4.85 %
Yield Stress, τ_y (Pa)	5.50494
Fluid Consistency Index, K ($Pa.s^n$)	0.28786
Flow Behaviour Index, n	0.46263
Representative Particle Size, d_{85}	15 μm

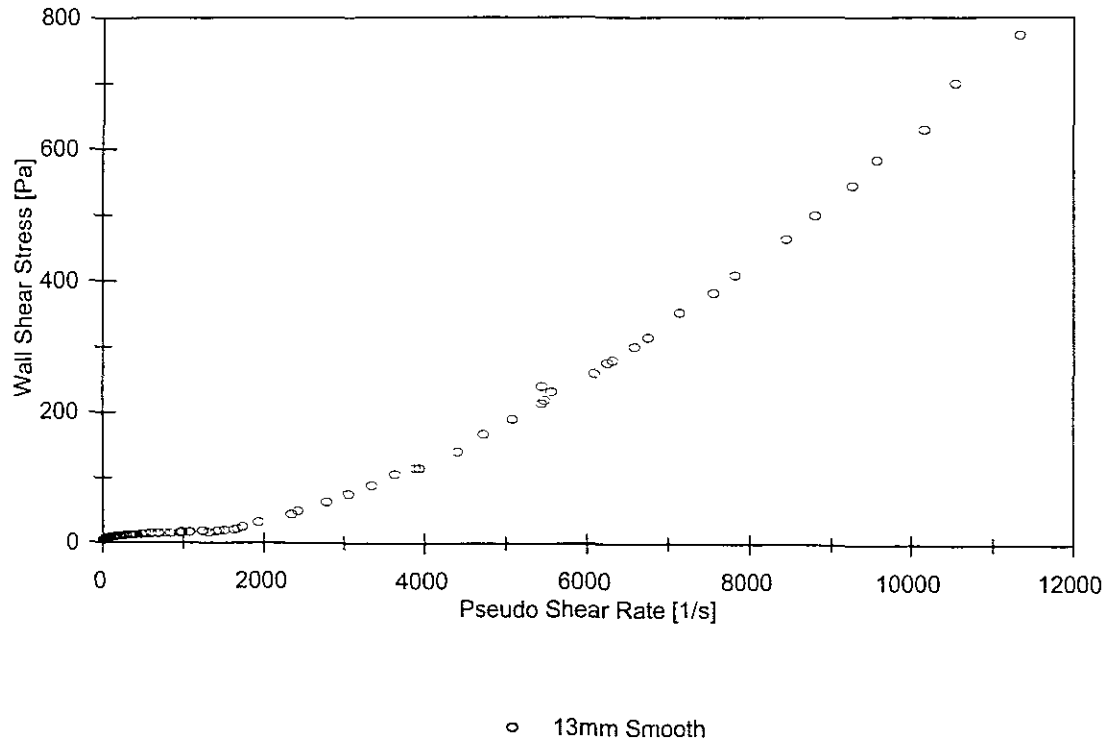

APPARATUS

Facility	BBTV
Pipe name	28 Smooth
Diameter (mm)	28.34
Pipe roughness (μm)	5.9
Material	Kaolin
Operator	FvS
Supervisor	PTS

SLURRY PROPERTIES

Solids Relative Density	2.65
Fluid Relative Density (S_m)	1.0803
Volumetric Concentration	4.85 %
Yield Stress, τ_y (Pa)	5.50494
Fluid Consistency Index, K (Pa.s^n)	0.28786
Flow Behaviour Index, n	0.46263
Representative Particle Size, d_{85}	15 μm

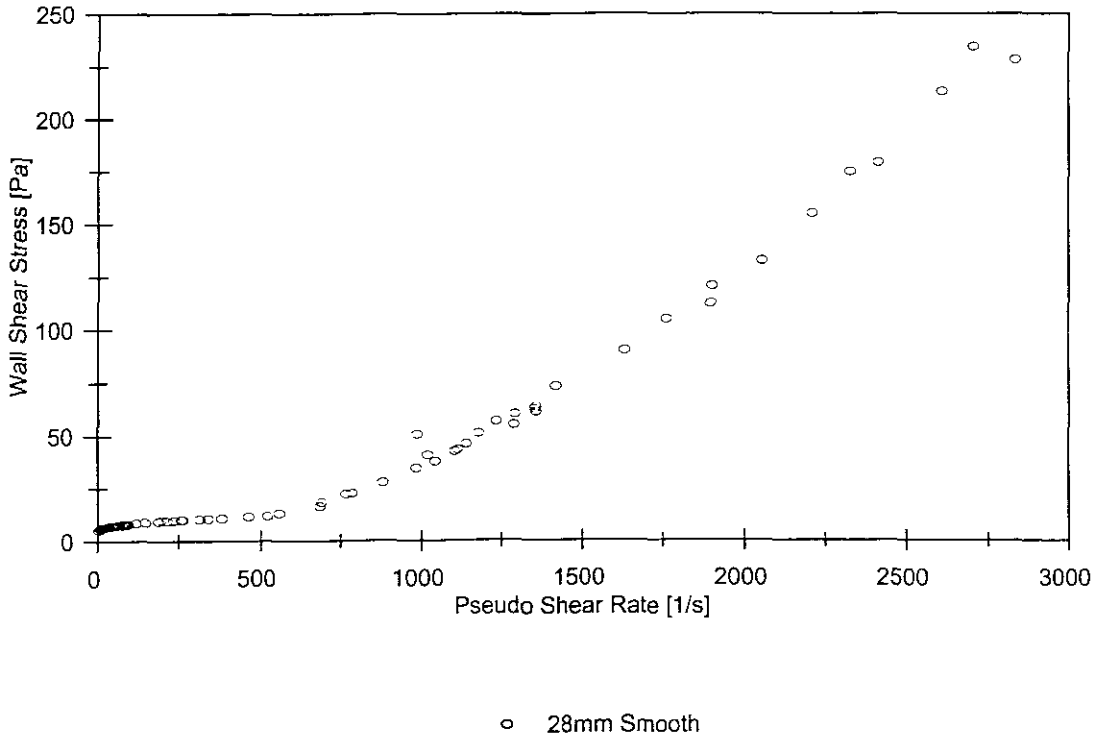

APPARATUS

Facility	BBTV
Pipe name	45 Smooth
Diameter (mm)	45.04
Pipe roughness (μm)	1.3
Material	Kaolin
Operator	FvS
Supervisor	PTS

SLURRY PROPERTIES

Solids Relative Density	2.65
Fluid Relative Density (S_m)	1.0803
Volumetric Concentration	4.85 %
Yield Stress, τ_y (Pa)	5.50494
Fluid Consistency Index, K ($Pa.s^n$)	0.28786
Flow Behaviour Index, n	0.46263
Representative Particle Size, d_{85}	15 µm

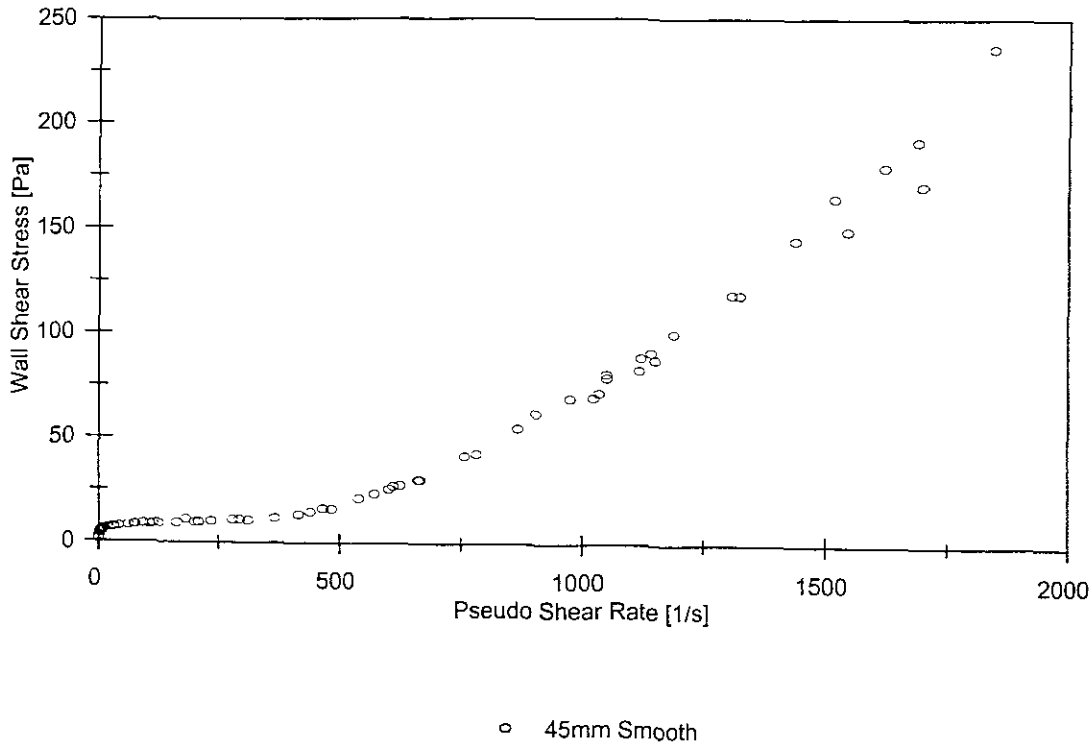

APPARATUS

Facility	BBTV
Pipe name	R28-1525
Diameter (mm)	27.03
Pipe roughness (μm)	136
Material	Kaolin
Operator	FvS
Supervisor	PTS

SLURRY PROPERTIES

Solids Relative Density	2.65
Fluid Relative Density (S_m)	1.0803
Volumetric Concentration	4.85 %
Yield Stress, τ_y (Pa)	5.50494
Fluid Consistency Index, K (Pa.s^n)	0.28786
Flow Behaviour Index, n	0.46263
Representative Particle Size, d_{85}	15 μm

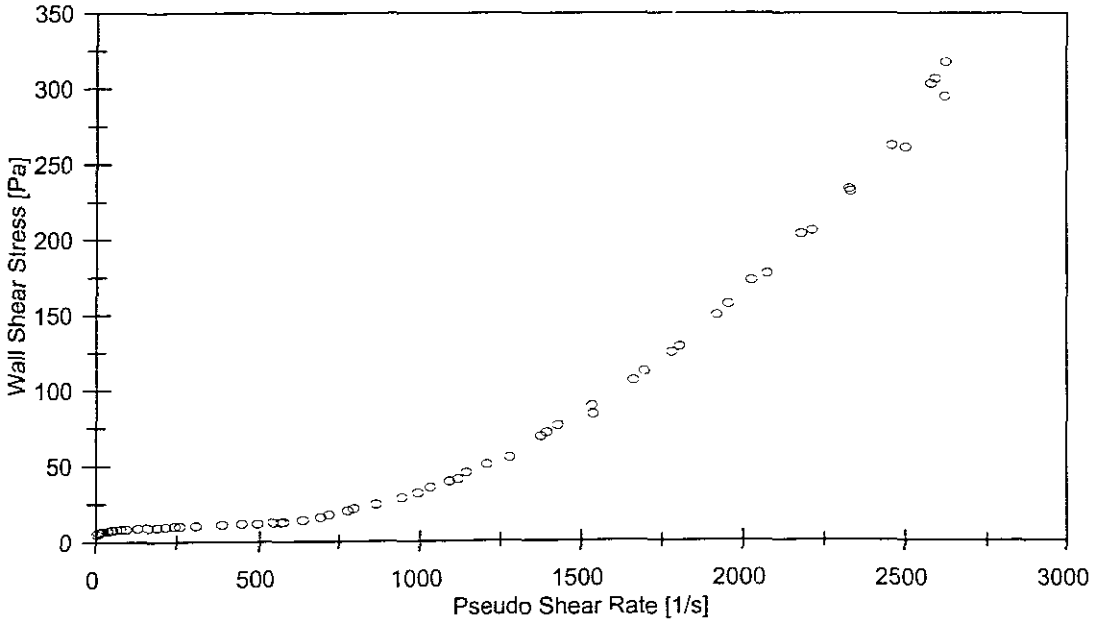

APPARATUS

Facility	BBTV
Pipe name	R28-3060
Diameter (mm)	27.17
Pipe roughness (μm)	291
Material	Kaolin
Operator	FvS
Supervisor	PTS

SLURRY PROPERTIES

Solids Relative Density	2.65
Fluid Relative Density (S_m)	1.0803
Volumetric Concentration	4.85 %
Yield Stress, τ_y (Pa)	5.50494
Fluid Consistency Index, K ($Pa.s^n$)	0.28786
Flow Behaviour Index, n	0.46263
Representative Particle Size, d_{85}	15 μm

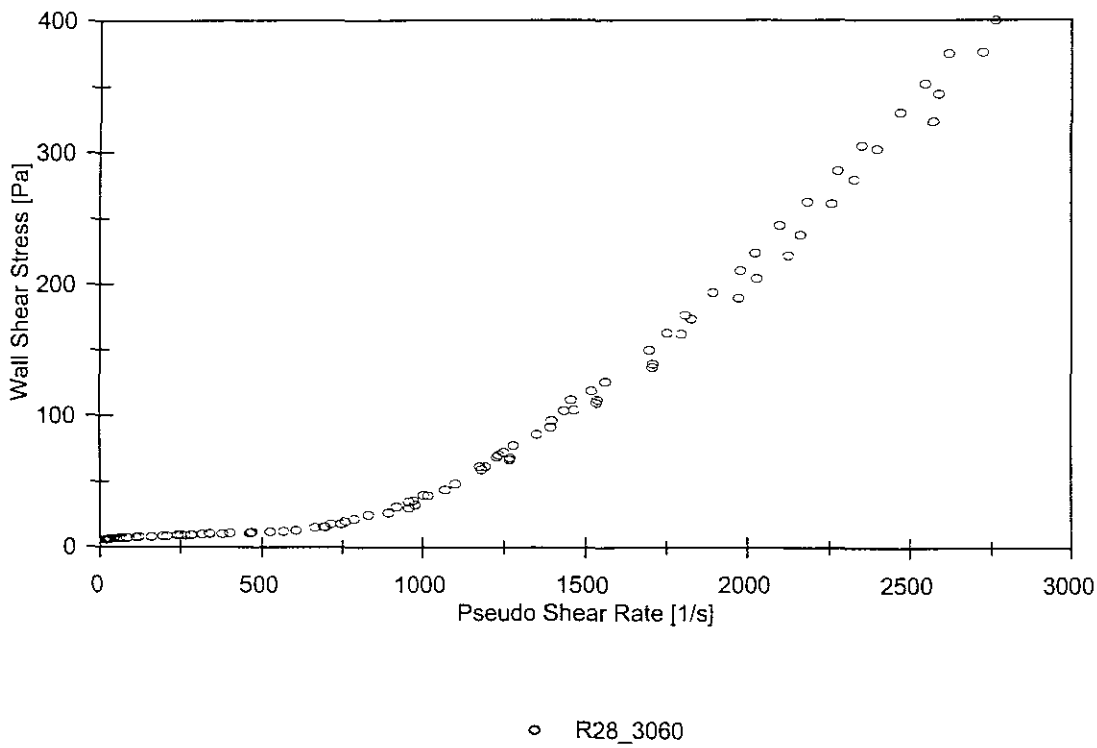

APPARATUS

Facility	BBTV
Pipe name	R45-1525
Diameter (mm)	44.73
Pipe roughness (μm)	42
Material	Kaolin
Operator	FvS
Supervisor	PTS

SLURRY PROPERTIES

Solids Relative Density	2.65
Fluid Relative Density (S_m)	1.0803
Volumetric Concentration	4.85 %
Yield Stress, τ_y (Pa)	5.50494
Fluid Consistency Index, K (Pa.s^n)	0.28786
Flow Behaviour Index, n	0.46263
Representative Particle Size, d_{85}	15 μm

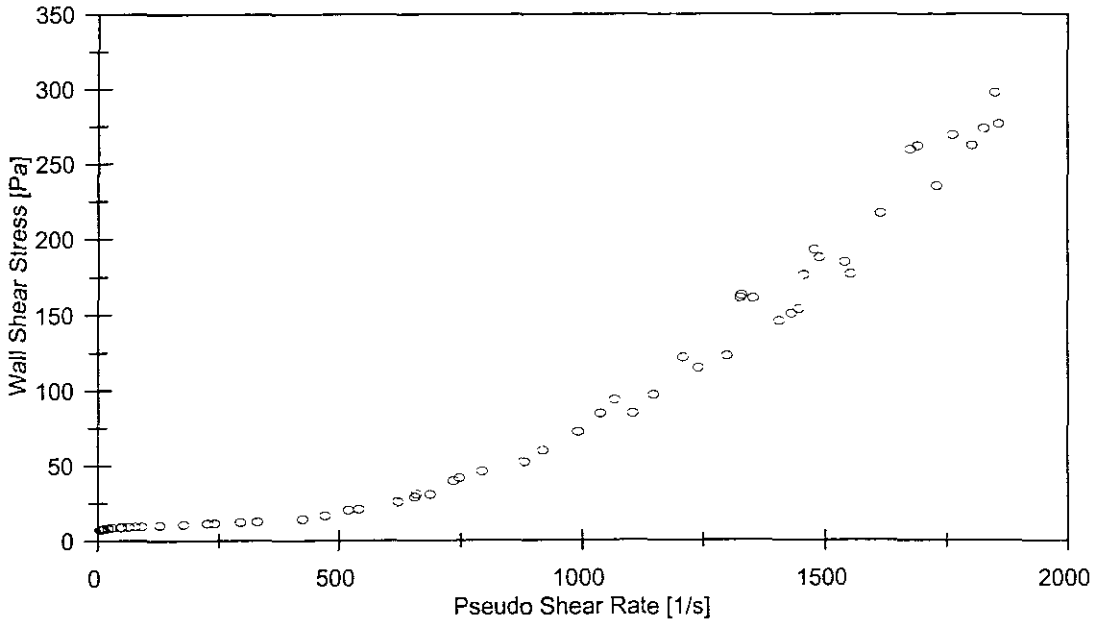

APPARATUS

Facility	BBTV
Pipe name	R45-3060
Diameter (mm)	45.44
Pipe roughness (μm)	672
Material	Kaolin
Operator	FvS
Supervisor	PTS

SLURRY PROPERTIES

Solids Relative Density	2.65
Fluid Relative Density (S_m)	1.0803
Volumetric Concentration	4.85 %
Yield Stress, τ_y (Pa)	5.50494
Fluid Consistency Index, K ($Pa.s^n$)	0.28786
Flow Behaviour Index, n	0.46263
Representative Particle Size, d_{85}	15 μm

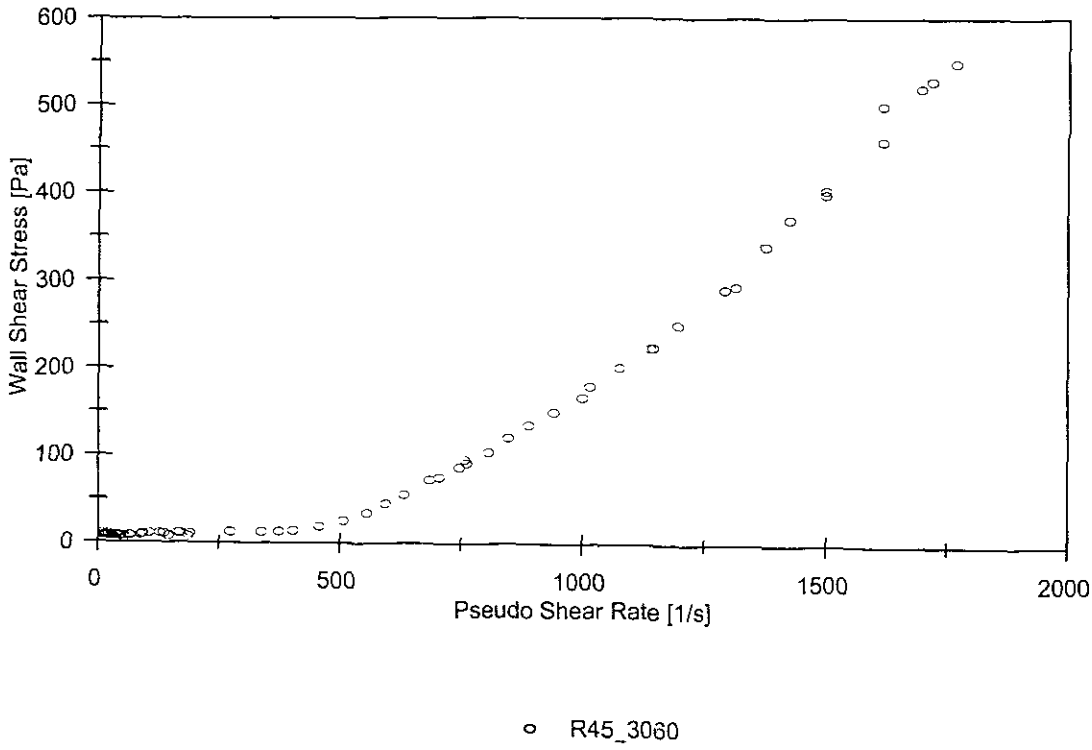

KAOLIN TEST RESULTS S_m = 1.146

APPARATUS	
Facility	BBTV
Pipe name	5 Smooth
Diameter (mm)	5.78
Pipe roughness (μm)	1.1
Material	Kaolin
Operator	FvS
Supervisor	PTS

SLURRY PROPERTIES	
Solids Relative Density	2.65
Fluid Relative Density (S_m)	1.146
Volumetric Concentration	8.85 %
Yield Stress, τ_y (Pa)	14.28570
Fluid Consistency Index, K (Pa.s^n)	0.87945
Flow Behaviour Index, n	0.44337
Representative Particle Size, d_{85}	15 μm

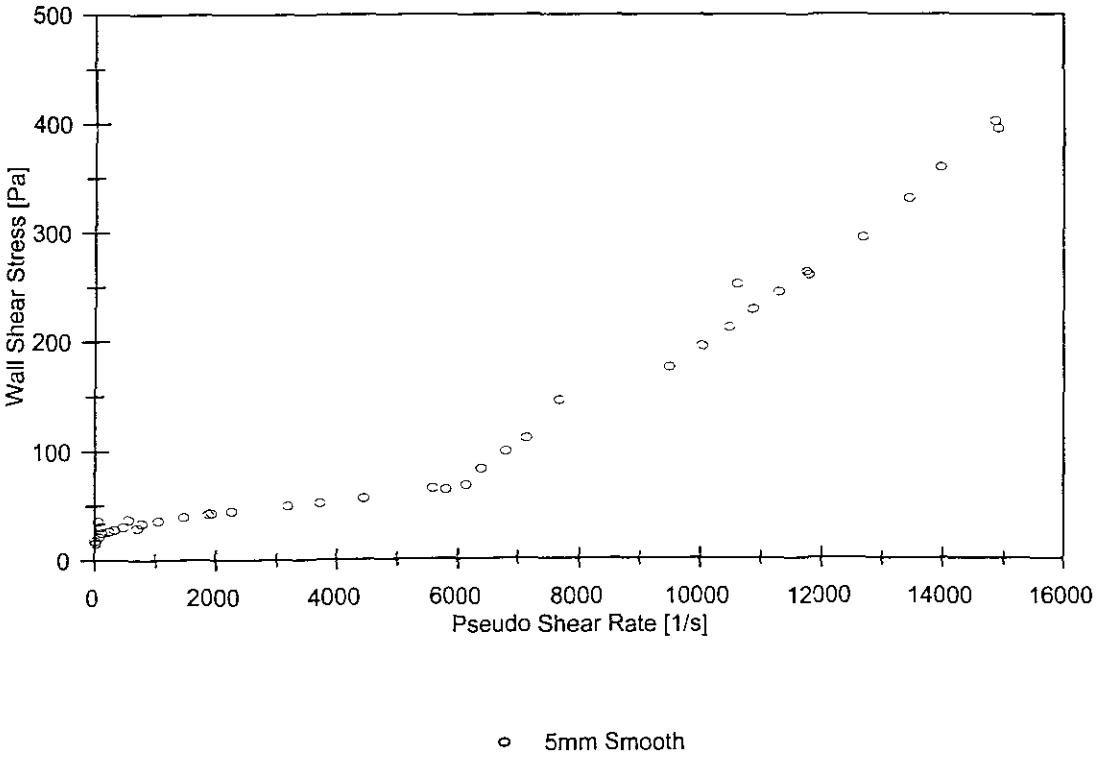

APPARATUS

Facility	BBTV
Pipe name	13 Smooth
Diameter (mm)	13.12
Pipe roughness (μm)	0.9
Material	Kaolin
Operator	FvS
Supervisor	PTS

SLURRY PROPERTIES

Solids Relative Density	2.65
Fluid Relative Density (S_m)	1.146
Volumetric Concentration	8.85 %
Yield Stress, τ_y (Pa)	14.28570
Fluid Consistency Index, K (Pa.s^n)	0.87945
Flow Behaviour Index, n	0.44337
Representative Particle Size, d_{85}	15 μm

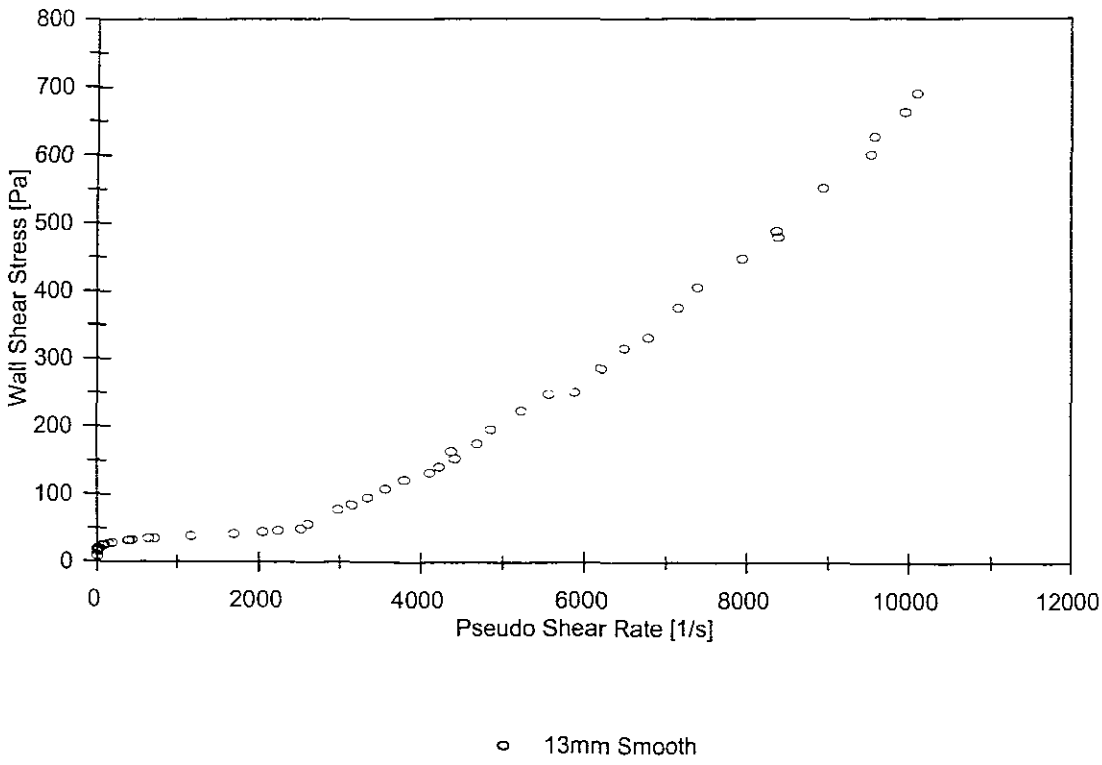

APPARATUS

Facility	BBTV
Pipe name	28 Smooth
Diameter (mm)	28.34
Pipe roughness (μm)	5.9
Material	Kaolin
Operator	FvS
Supervisor	PTS

SLURRY PROPERTIES

Solids Relative Density	2.65
Fluid Relative Density (S_m)	1.146
Volumetric Concentration	8.85 %
Yield Stress, τ_y (Pa)	14.28570
Fluid Consistency Index, K ($Pa.s^n$)	0.87945
Flow Behaviour Index, n	0.44337
Representative Particle Size, d_{85}	15 μm

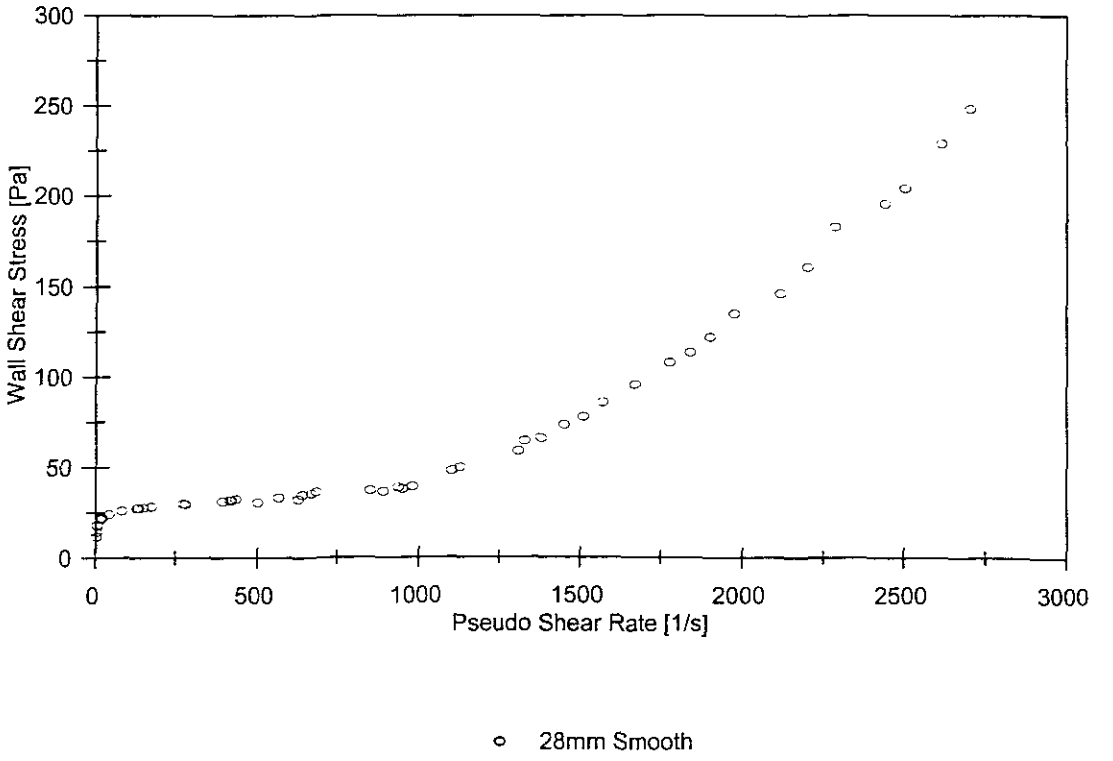

APPARATUS

Facility	BBTV
Pipe name	45 Smooth
Diameter (mm)	45.04
Pipe roughness (μm)	1.3
Material	Kaolin
Operator	FvS
Supervisor	PTS

SLURRY PROPERTIES

Solids Relative Density	2.65
Fluid Relative Density (S_m)	1.146
Volumetric Concentration	8.85 %
Yield Stress, τ_y (Pa)	14.28570
Fluid Consistency Index, K ($Pa.s^n$)	0.87945
Flow Behaviour Index, n	0.44337
Representative Particle Size, d_{85}	15 μm

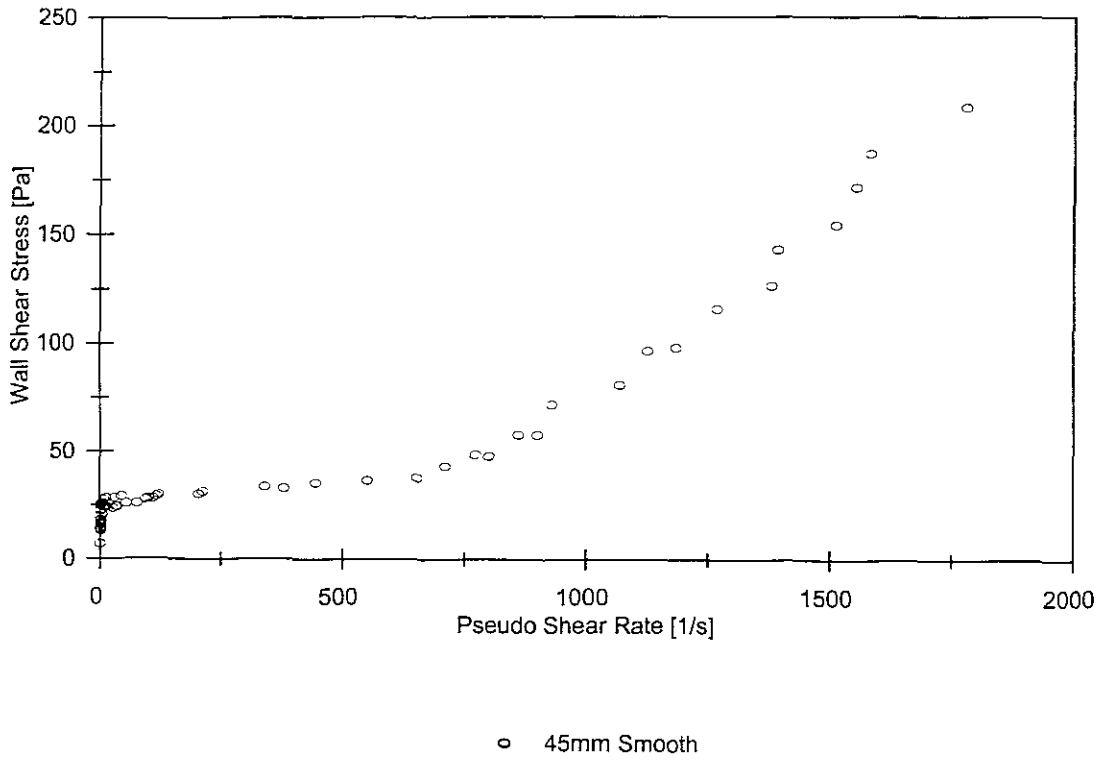

APPARATUS

Facility	BBTV
Pipe name	R28-1525
Diameter (mm)	27.03
Pipe roughness (μm)	136
Material	Kaolin
Operator	FvS
Supervisor	PTS

SLURRY PROPERTIES

Solids Relative Density	2.65
Fluid Relative Density (S_m)	1.146
Volumetric Concentration	8.85 %
Yield Stress, τ_y (Pa)	14.28570
Fluid Consistency Index, K ($Pa.s^n$)	0.87945
Flow Behaviour Index, n	0.44337
Representative Particle Size, d_{85}	15 μm

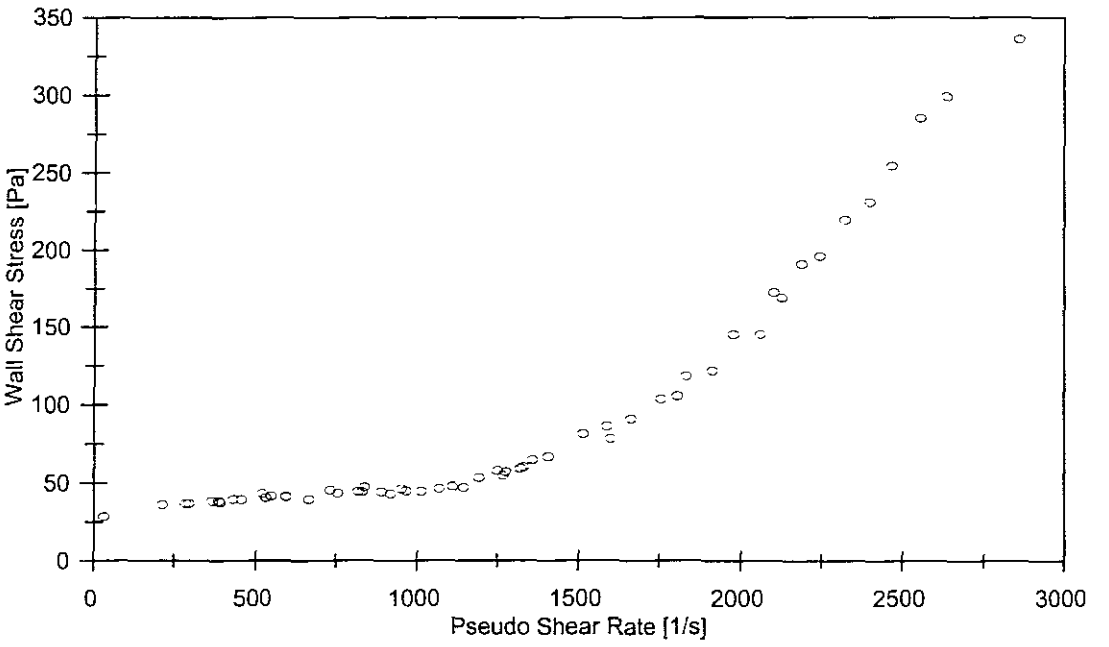

APPARATUS

Facility	BBTV
Pipe name	R28-3060
Diameter (mm)	27.17
Pipe roughness (μm)	291
Material	Kaolin
Operator	FvS
Supervisor	PTS

SLURRY PROPERTIES

Solids Relative Density	2.65
Fluid Relative Density (S_m)	1.146
Volumetric Concentration	8.85 %
Yield Stress, τ_y (Pa)	14.28570
Fluid Consistency Index, K ($Pa.s^n$)	0.87945
Flow Behaviour Index, n	0.44337
Representative Particle Size, d_{85}	15 μm

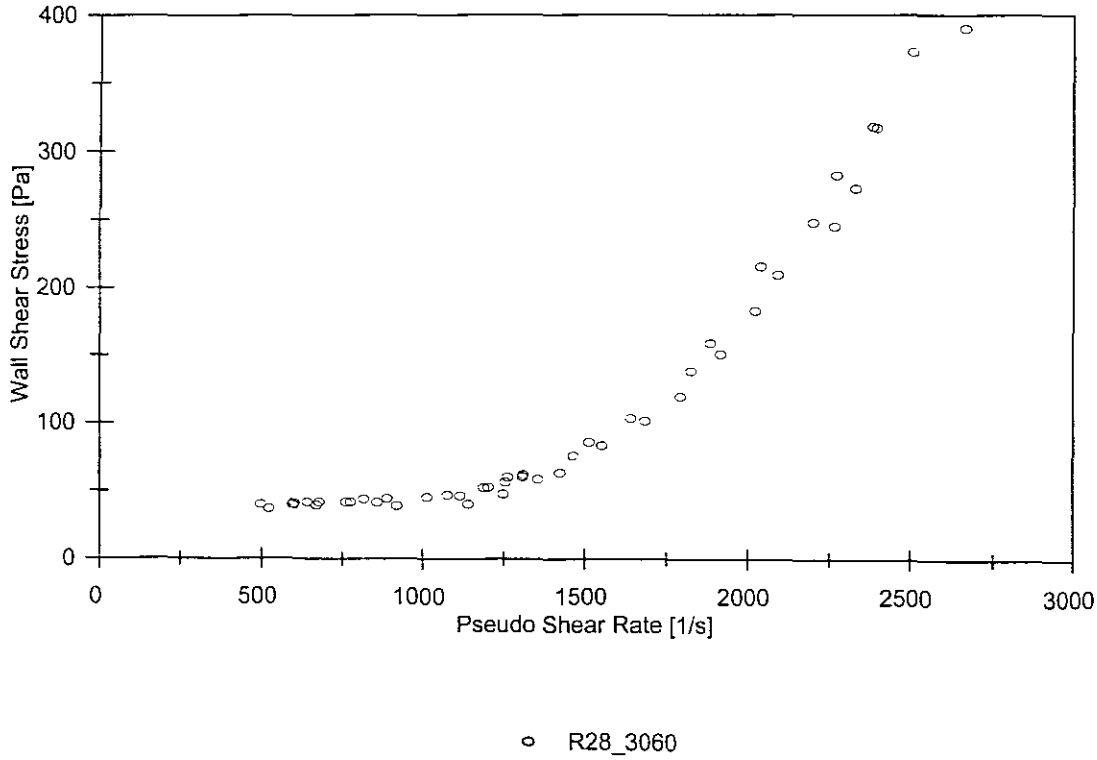

APPARATUS

Facility	BBTV
Pipe name	R45-1525
Diameter (mm)	44.73
Pipe roughness (μm)	42
Material	Kaolin
Operator	FvS
Supervisor	PTS

SLURRY PROPERTIES

Solids Relative Density	2.65
Fluid Relative Density (S_m)	1.146
Volumetric Concentration	8.85 %
Yield Stress, τ_y (Pa)	14.28570
Fluid Consistency Index, K ($Pa.s^n$)	0.87945
Flow Behaviour Index, n	0.44337
Representative Particle Size, d_{85}	15 μm

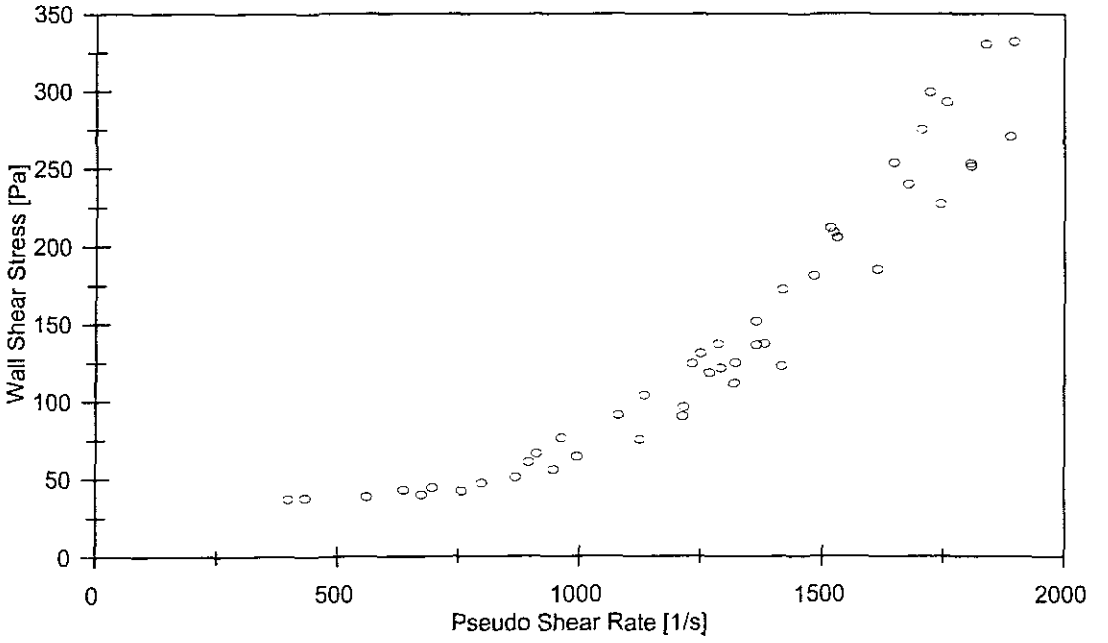

APPARATUS

Facility	BBTV
Pipe name	R45-3060
Diameter (mm)	45.44
Pipe roughness (μm)	672
Material	Kaolin
Operator	FvS
Supervisor	PTS

SLURRY PROPERTIES

Solids Relative Density	2.65
Fluid Relative Density (S_m)	1.146
Volumetric Concentration	8.85 %
Yield Stress, τ_y (Pa)	14.28570
Fluid Consistency Index, K (Pa.s^n)	0.87945
Flow Behaviour Index, n	0.44337
Representative Particle Size, d_{85}	15 μm

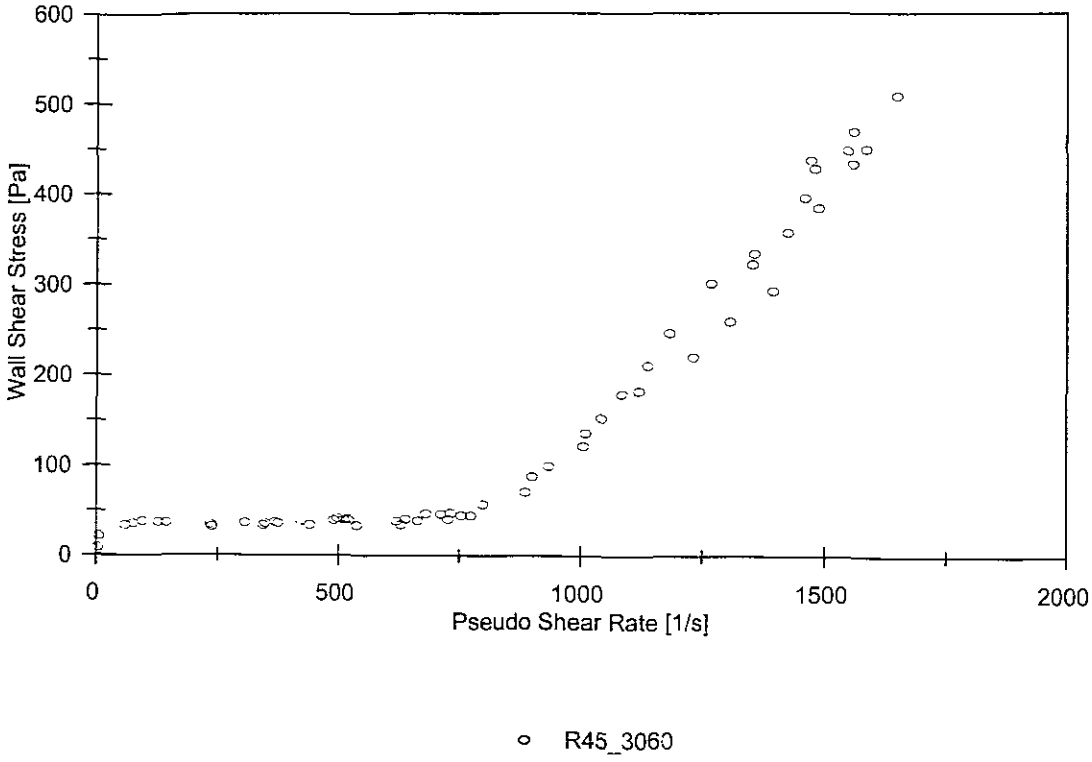

KAOLIN TEST RESULTS $S_m = 1.1779$

APPARATUS

Facility	BBTV
Pipe name	5 Smooth
Diameter (mm)	5.78
Pipe roughness (μm)	1.1
Material	Kaolin
Operator	FvS
Supervisor	PTS

SLURRY PROPERTIES

Solids Relative Density	2.65
Fluid Relative Density (S_m)	1.146
Volumetric Concentration	10.73 %
Yield Stress, τ_y (Pa)	35.7885
Fluid Consistency Index, K (Pa.s^n)	0.27887
Flow Behaviour Index, n	0.61650
Representative Particle Size, d_{85}	15 μm

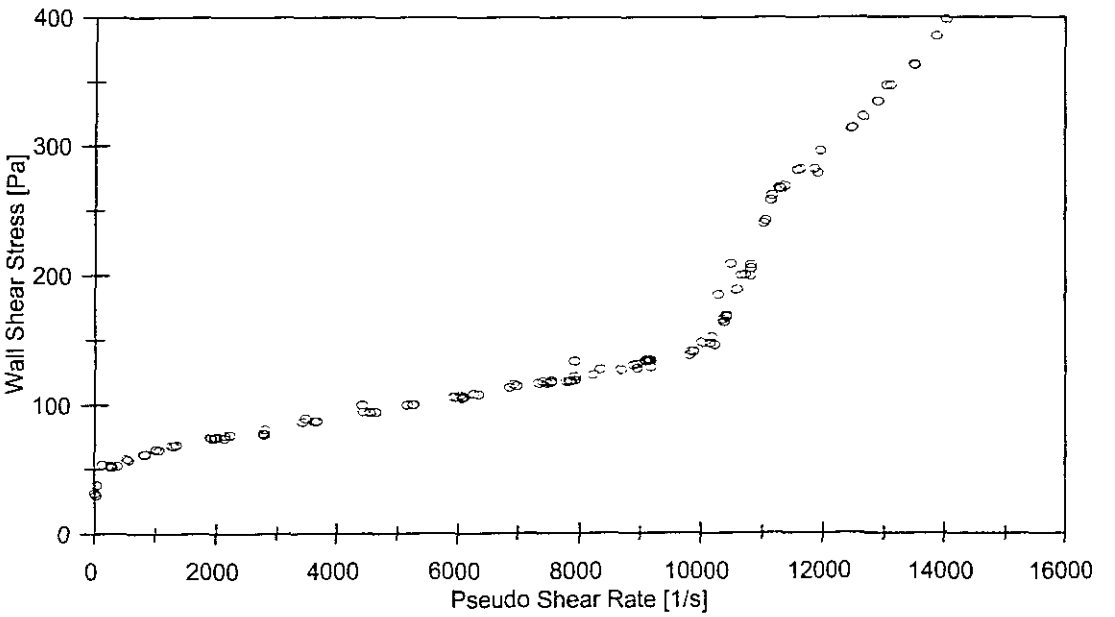

APPARATUS

Facility	BBTV
Pipe name	13 Smooth
Diameter (mm)	13.12
Pipe roughness (μm)	0.9
Material	Kaolin
Operator	FvS
Supervisor	PTS

SLURRY PROPERTIES

Solids Relative Density	2.65
Fluid Relative Density (S_m)	1.146
Volumetric Concentration	10.73 %
Yield Stress, τ_y (Pa)	35.7885
Fluid Consistency Index, K ($Pa.s^n$)	0.27887
Flow Behaviour Index, n	0.61650
Representative Particle Size, d_{85}	15 µm

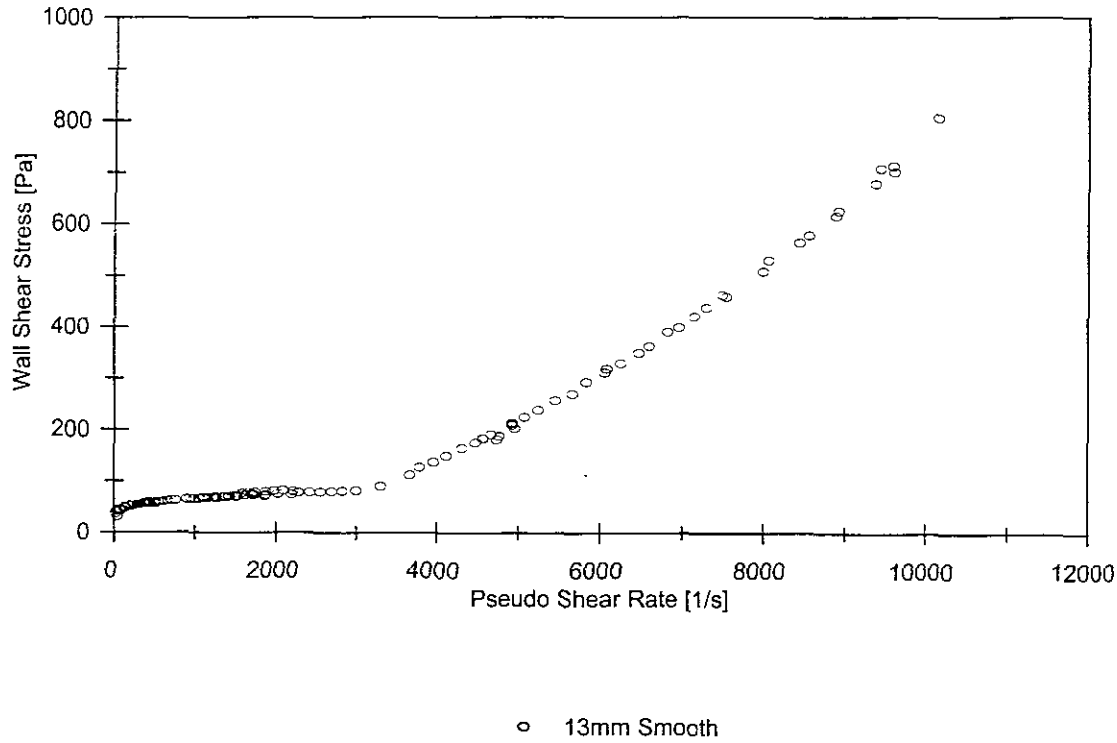

APPARATUS

Facility	BBTV
Pipe name	28 Smooth
Diameter (mm)	28.34
Pipe roughness (μm)	5.9
Material	Kaolin
Operator	FvS
Supervisor	PTS

SLURRY PROPERTIES

Solids Relative Density	2.65
Fluid Relative Density (S_m)	1.146
Volumetric Concentration	10.73 %
Yield Stress, τ_y (Pa)	35.7885
Fluid Consistency Index, K ($Pa.s^n$)	0.27887
Flow Behaviour Index, n	0.61650
Representative Particle Size, d_{85}	15 μm

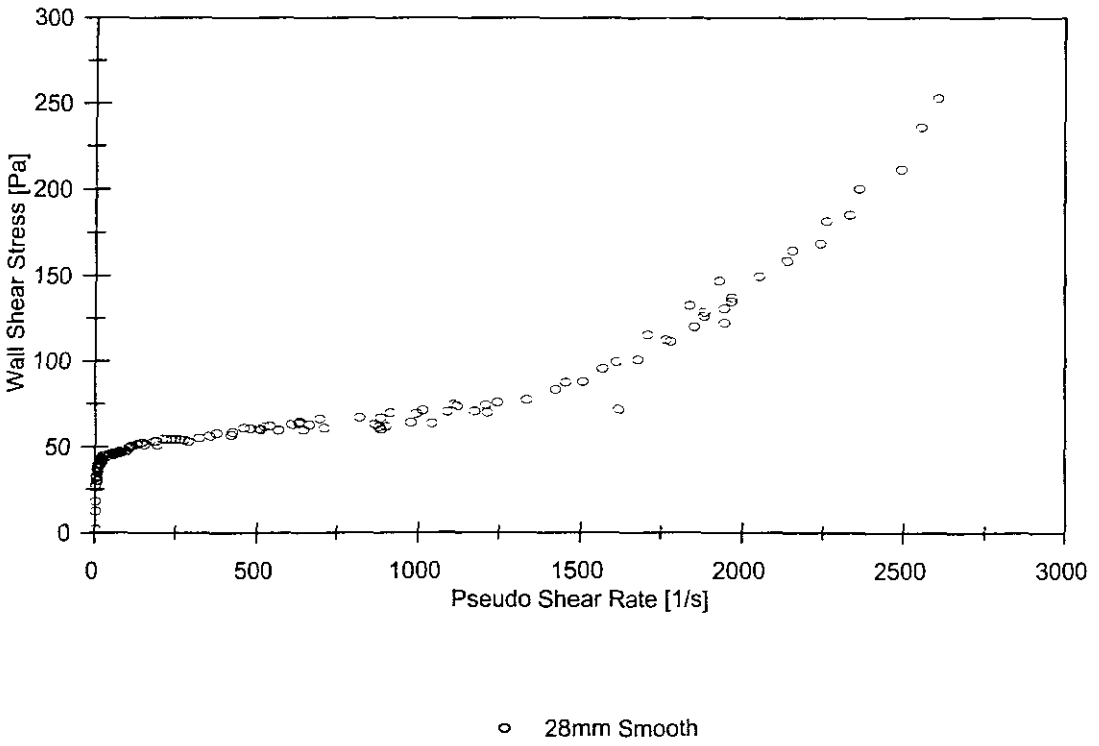

APPARATUS

Facility	BBTV
Pipe name	45 Smooth
Diameter (mm)	45.04
Pipe roughness (μm)	1.3
Material	Kaolin
Operator	FvS
Supervisor	PTS

SLURRY PROPERTIES

Solids Relative Density	2.65
Fluid Relative Density (S_m)	1.146
Volumetric Concentration	10.73 %
Yield Stress, τ_y (Pa)	35.7885
Fluid Consistency Index, K ($Pa.s^n$)	0.27887
Flow Behaviour Index, n	0.61650
Representative Particle Size, d_{85}	15 μm

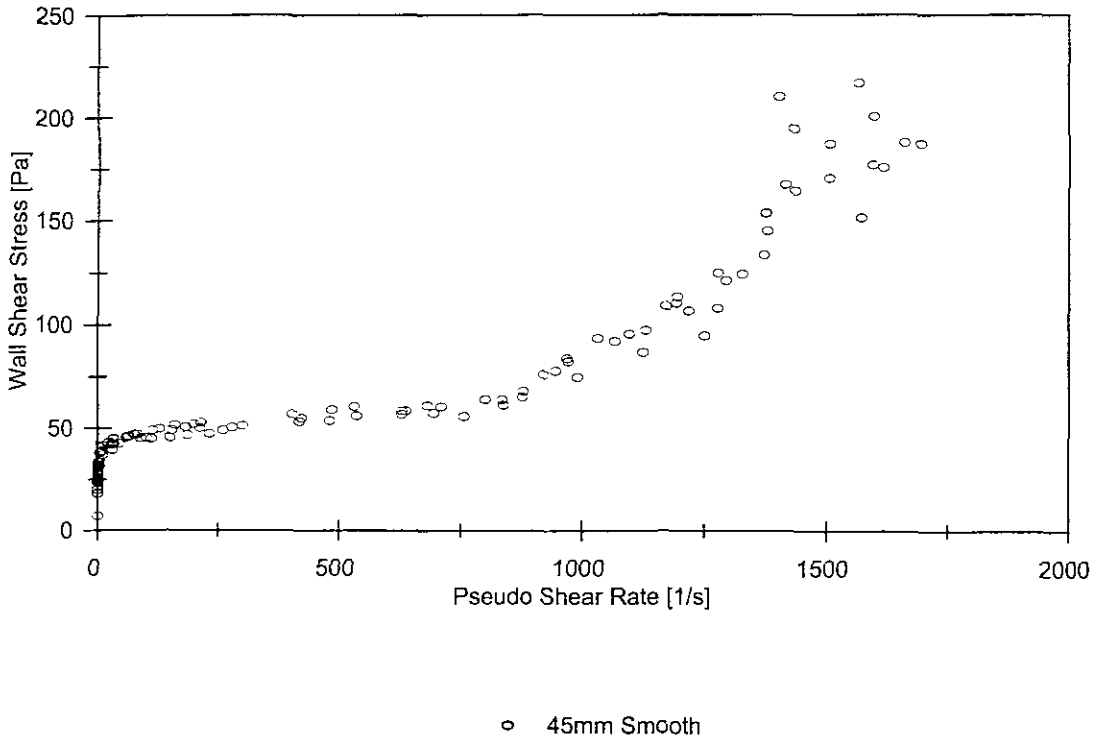

APPARATUS

Facility	BBTV
Pipe name	R28-1525
Diameter (mm)	27.03
Pipe roughness (μm)	136
Material	Kaolin
Operator	FvS
Supervisor	PTS

SLURRY PROPERTIES

Solids Relative Density	2.65
Fluid Relative Density (S_m)	1.146
Volumetric Concentration	10.73 %
Yield Stress, τ_y (Pa)	35.7885
Fluid Consistency Index, K (Pa.s^n)	0.27887
Flow Behaviour Index, n	0.61650
Representative Particle Size, d_{85}	15 μm

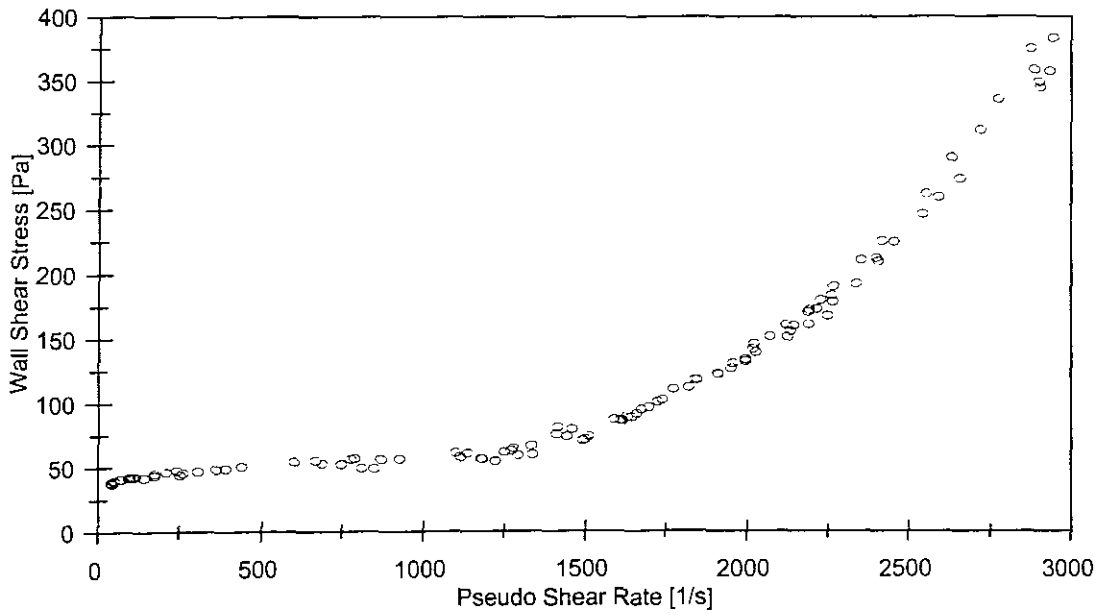

APPARATUS

Facility	BBTV
Pipe name	R28-3060
Diameter (mm)	27.17
Pipe roughness (μm)	291
Material	Kaolin
Operator	FvS
Supervisor	PTS

SLURRY PROPERTIES

Solids Relative Density	2.65
Fluid Relative Density (S_m)	1.146
Volumetric Concentration	10.73 %
Yield Stress, τ_y (Pa)	35.7885
Fluid Consistency Index, K ($Pa.s^n$)	0.27887
Flow Behaviour Index, n	0.61650
Representative Particle Size, d_{85}	15 µm

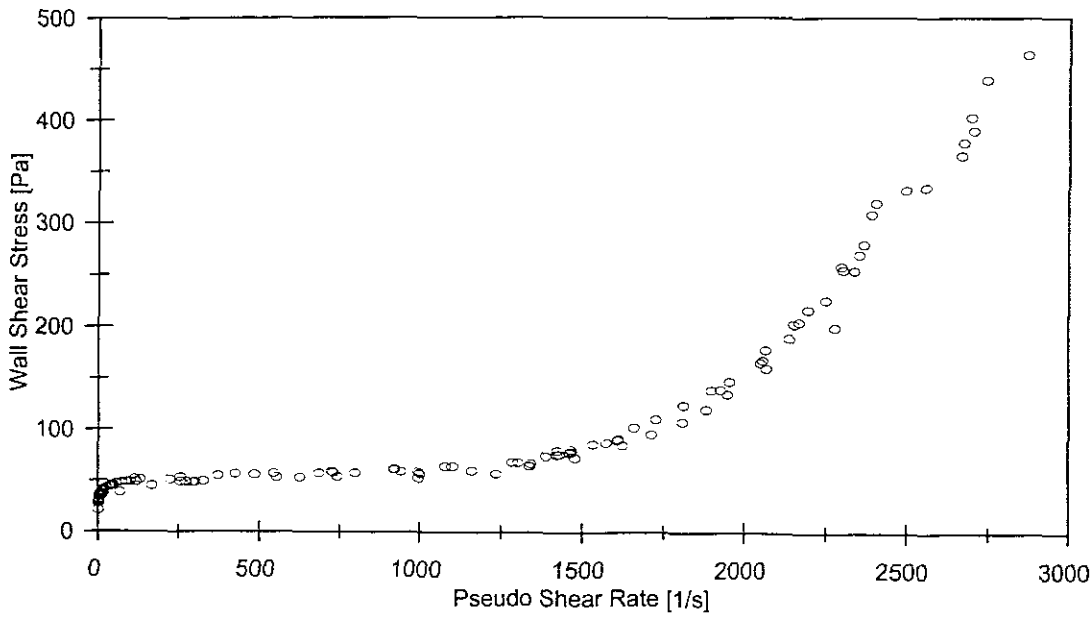

APPARATUS

Facility	BBTV
Pipe name	R45-1525
Diameter (mm)	44.73
Pipe roughness (μm)	42
Material	Kaolin
Operator	FvS
Supervisor	PTS

SLURRY PROPERTIES

Solids Relative Density	2.65
Fluid Relative Density (S_m)	1.146
Volumetric Concentration	10.73 %
Yield Stress, τ_y (Pa)	35.7885
Fluid Consistency Index, K (Pa.s^n)	0.27887
Flow Behaviour Index, n	0.61650
Representative Particle Size, d_{85}	15 μm

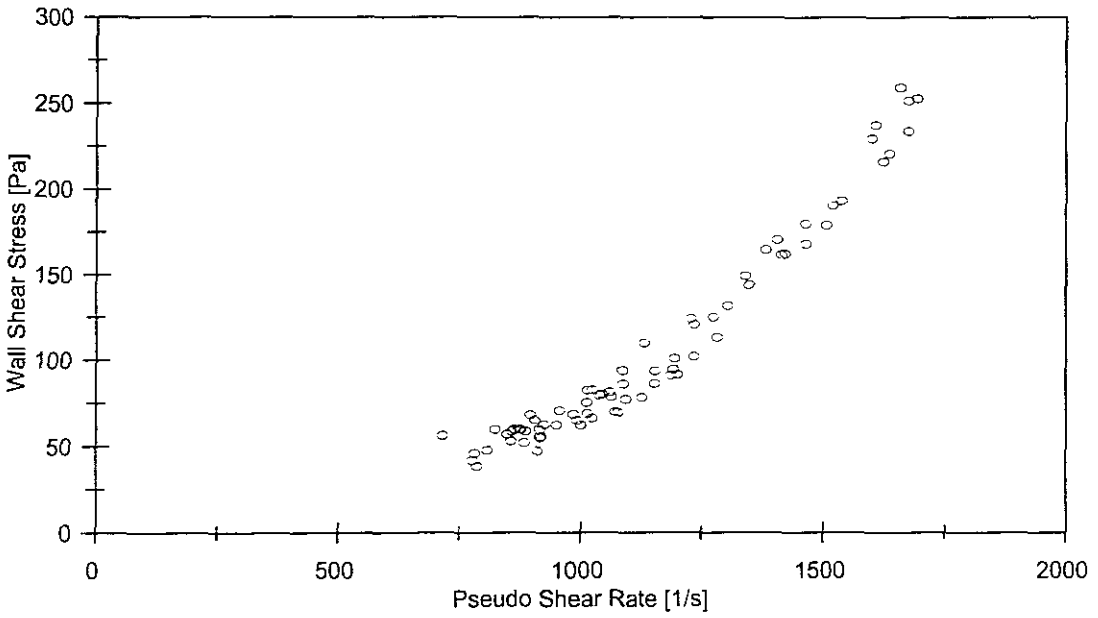

APPARATUS

Facility	BBTV
Pipe name	R45-3060
Diameter (mm)	45.44
Pipe roughness (μm)	672
Material	Kaolin
Operator	FvS
Supervisor	PTS

SLURRY PROPERTIES

Solids Relative Density	2.65
Fluid Relative Density (S_m)	1.146
Volumetric Concentration	10.73 %
Yield Stress, τ_y (Pa)	35.7885
Fluid Consistency Index, K (Pa.s^n)	0.27887
Flow Behaviour Index, n	0.61650
Representative Particle Size, d_{85}	15 μm

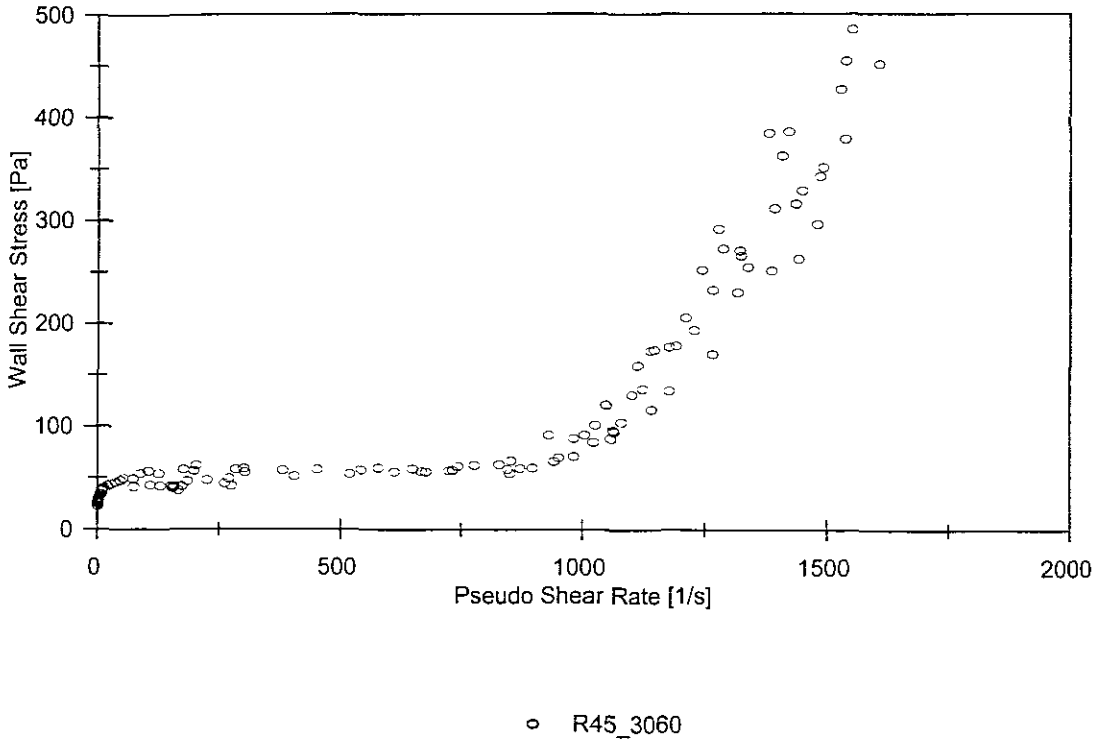

TAILINGS TEST RESULTS $S_m = 1.7309$

APPARATUS	
Facility	BBTV
Pipe name	5 Smooth
Diameter (mm)	5.78
Pipe roughness (μm)	1.1
Material	Tailings
Operator	FvS
Supervisor	PTS

SLURRY PROPERTIES	
Solids Relative Density	3.70
Fluid Relative Density (S_m)	1.146
Volumetric Concentration	27.07 %
Yield Stress, τ_y (Pa)	2.5839
Fluid Consistency Index, K (Pa.s^n)	0.00287
Flow Behaviour Index, n	1.20220
Representative Particle Size, d_{85}	85 μm

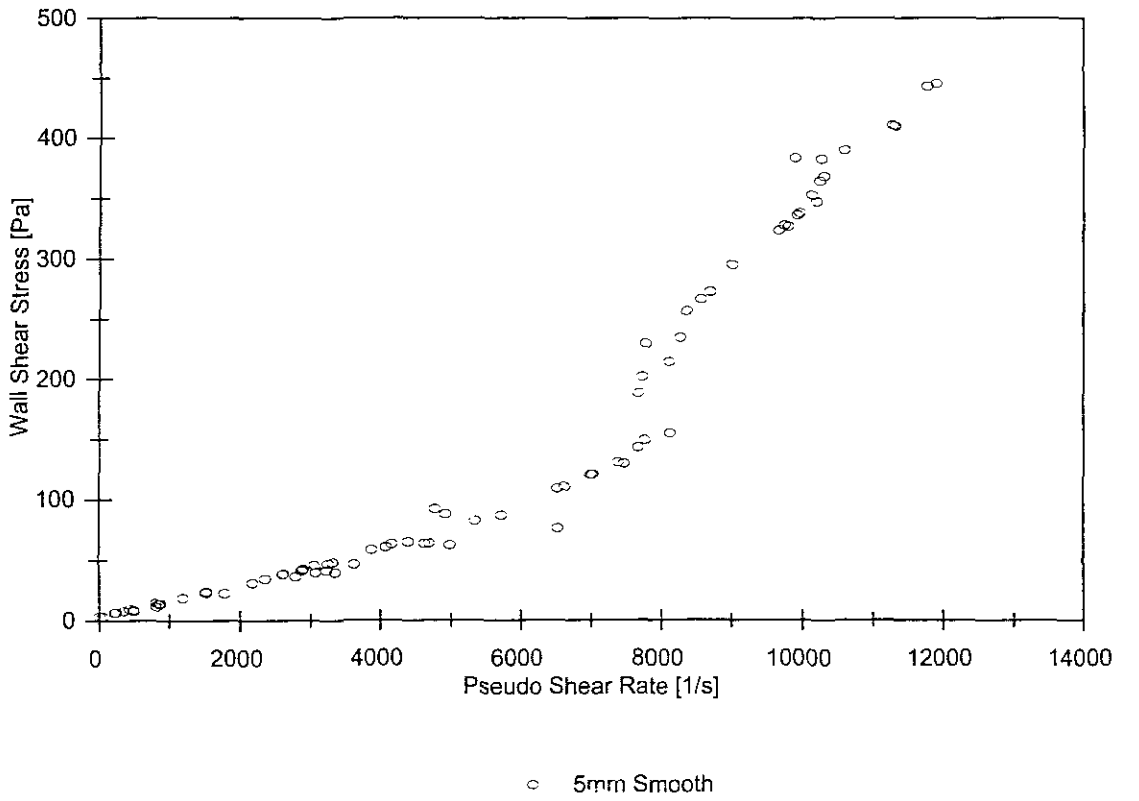

APPARATUS

Facility	BBTV
Pipe name	13 Smooth
Diameter (mm)	13.12
Pipe roughness (μm)	0.9
Material	Tailings
Operator	FvS
Supervisor	PTS

SLURRY PROPERTIES

Solids Relative Density	3.70
Fluid Relative Density (S_m)	1.146
Volumetric Concentration	27.07 %
Yield Stress, τ_y (Pa)	2.5839
Fluid Consistency Index, K ($Pa.s^n$)	0.00287
Flow Behaviour Index, n	1.20220
Representative Particle Size, d_{85}	85 μm

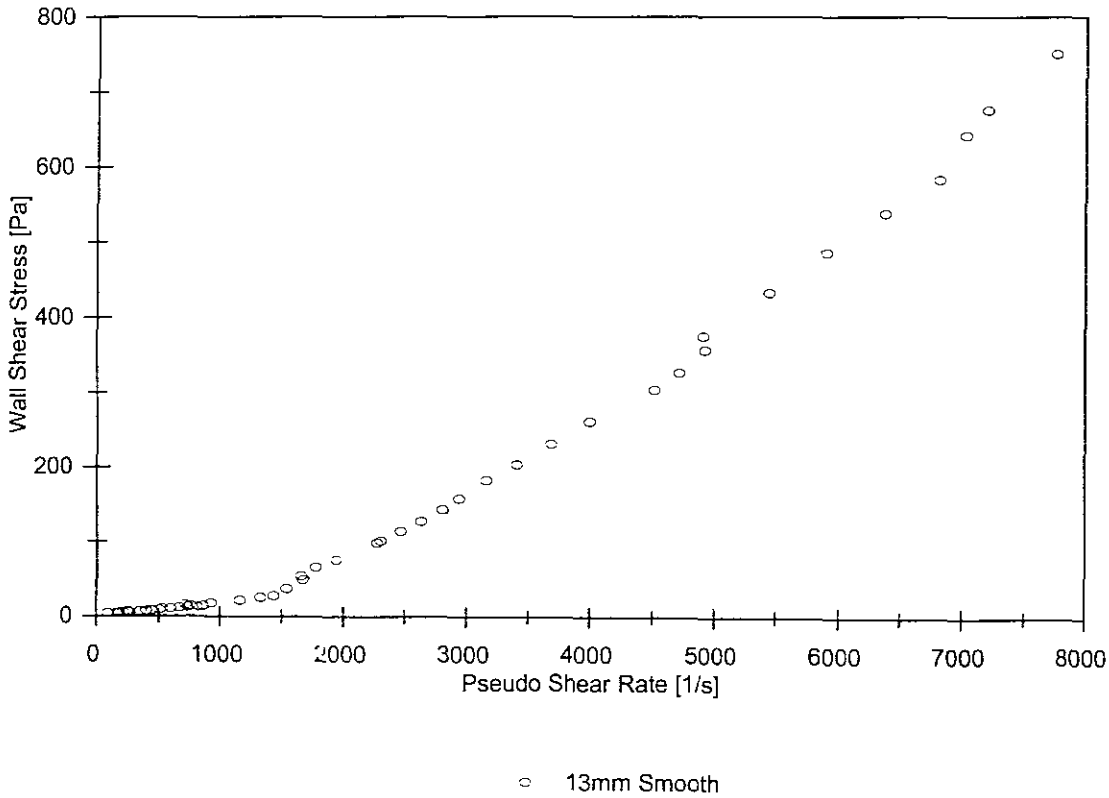

APPARATUS

Facility	BBTV
Pipe name	28 Smooth
Diameter (mm)	28.34
Pipe roughness (μm)	5.9
Material	Tailings
Operator	FvS
Supervisor	PTS

SLURRY PROPERTIES

Solids Relative Density	3.70
Fluid Relative Density (S_m)	1.146
Volumetric Concentration	27.07 %
Yield Stress, τ_y (Pa)	2.5839
Fluid Consistency Index, K (Pa.s^n)	0.00287
Flow Behaviour Index, n	1.20220
Representative Particle Size, d_{85}	85 μm

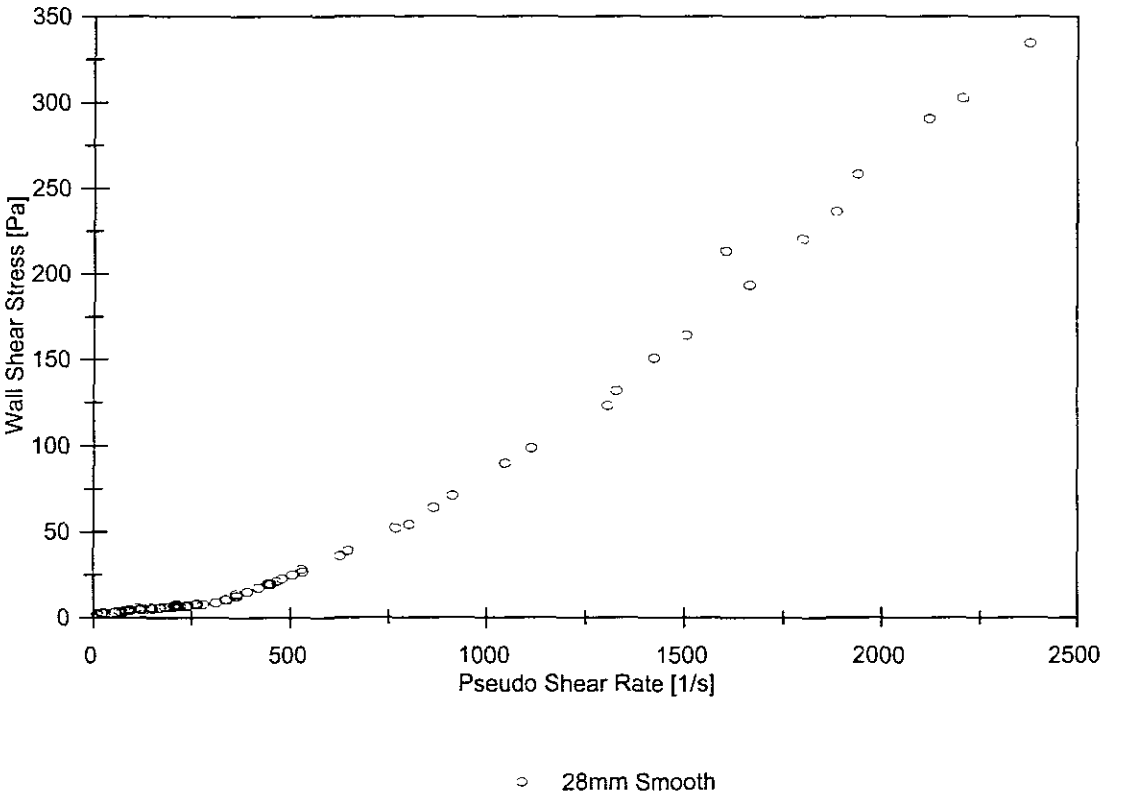

APPARATUS

Facility	BBTV
Pipe name	45 Smooth
Diameter (mm)	45.04
Pipe roughness (μm)	1.3
Material	Tailings
Operator	FvS
Supervisor	PTS

SLURRY PROPERTIES

Solids Relative Density	3.70
Fluid Relative Density (S_m)	1.146
Volumetric Concentration	27.07 %
Yield Stress, τ_y (Pa)	2.5839
Fluid Consistency Index, K ($Pa.s^n$)	0.00287
Flow Behaviour Index, n	1.20220
Representative Particle Size, d_{85}	85 μm

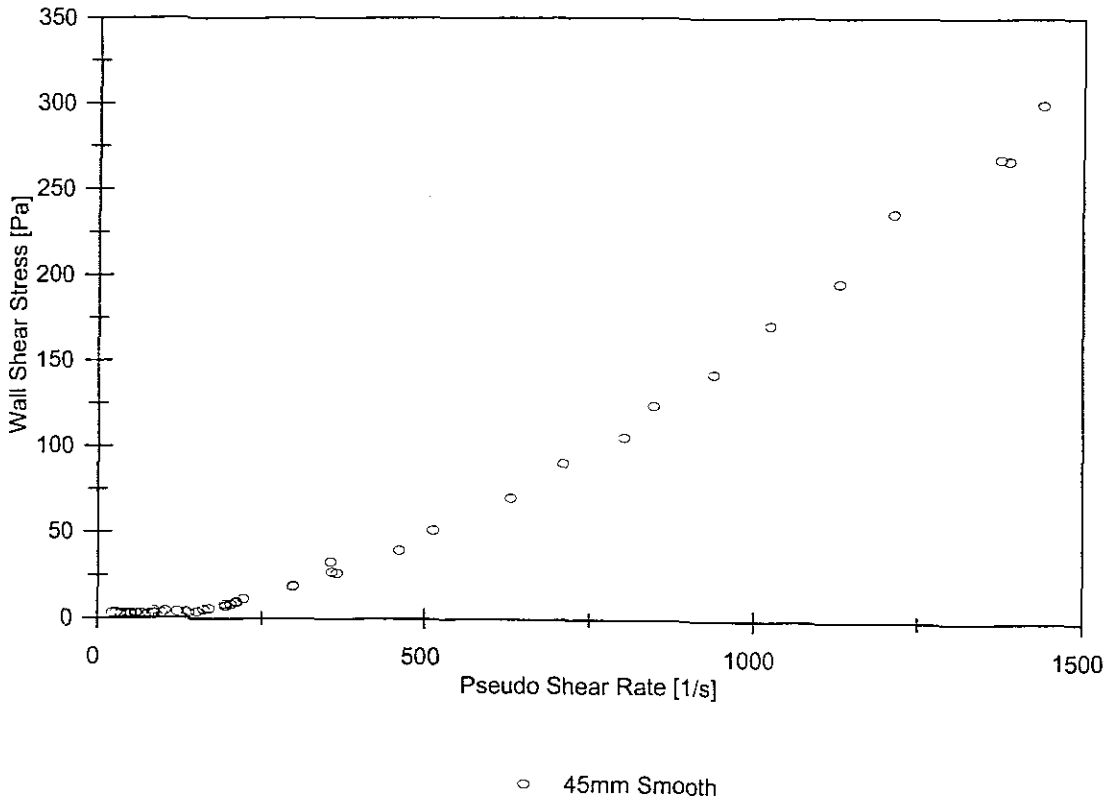

APPARATUS

Facility	BBTV
Pipe name	R28-1525
Diameter (mm)	27.03
Pipe roughness (μm)	136
Material	Tailings
Operator	FvS
Supervisor	PTS

SLURRY PROPERTIES

Solids Relative Density	3.70
Fluid Relative Density (S_m)	1.146
Volumetric Concentration	27.07 %
Yield Stress, τ_y (Pa)	2.5839
Fluid Consistency Index, K ($Pa.s^n$)	0.00287
Flow Behaviour Index, n	1.20220
Representative Particle Size, d_{85}	85 μm

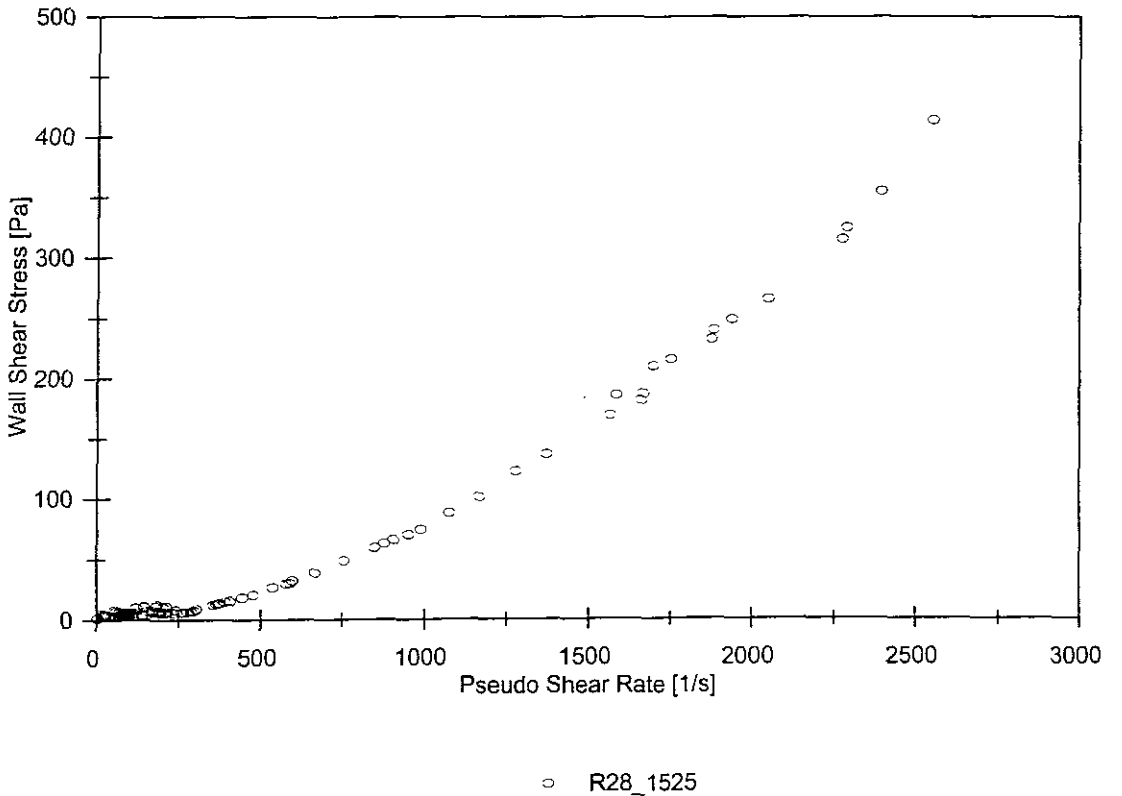

APPARATUS

Facility	BBTV
Pipe name	R28-3060
Diameter (mm)	27.17
Pipe roughness (μm)	291
Material	Tailings
Operator	FvS
Supervisor	PTS

SLURRY PROPERTIES

Solids Relative Density	3.70
Fluid Relative Density (S_{rf})	1.146
Volumetric Concentration	27.07 %
Yield Stress, τ_y (Pa)	2.5839
Fluid Consistency Index, K (Pa.s^n)	0.00287
Flow Behaviour Index, n	1.20220
Representative Particle Size, d_{85}	85 μm

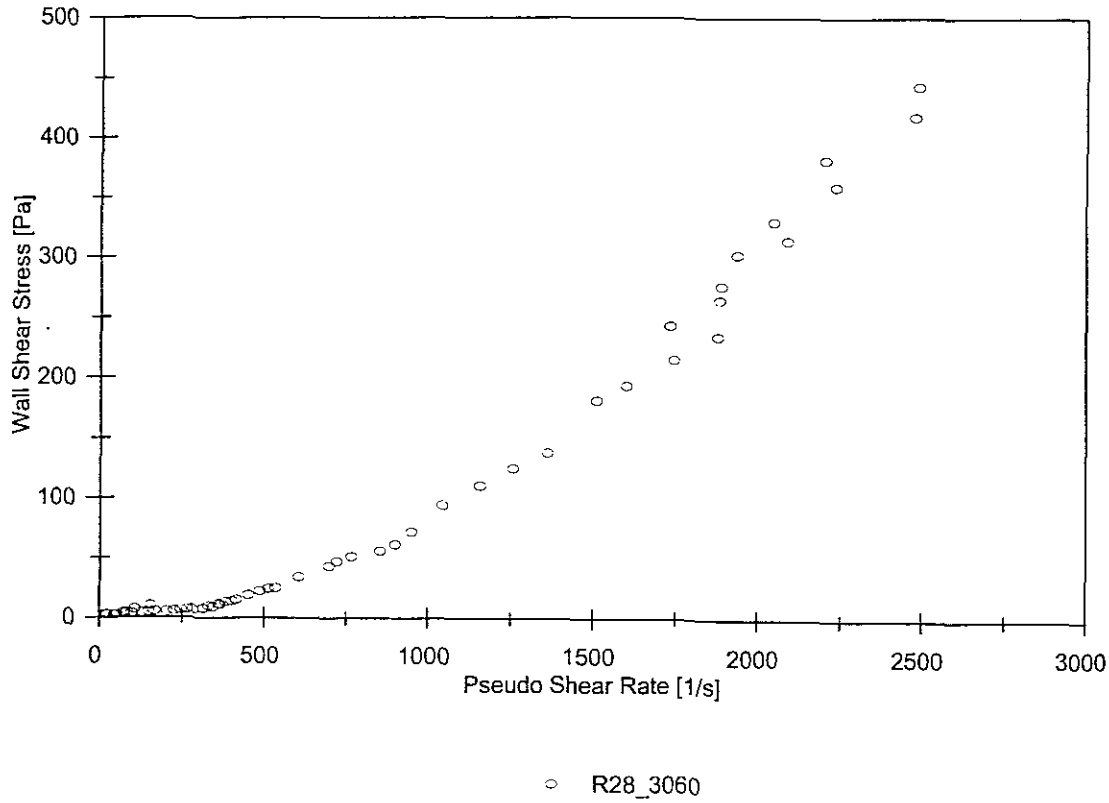

APPARATUS

Facility	BBTV
Pipe name	R45-1525
Diameter (mm)	44.73
Pipe roughness (μm)	42
Material	Tailings
Operator	FvS
Supervisor	PTS

SLURRY PROPERTIES

Solids Relative Density	3.70
Fluid Relative Density (S_m)	1.146
Volumetric Concentration	27.07 %
Yield Stress, τ_y (Pa)	2.5839
Fluid Consistency Index, K (Pa.s^n)	0.00287
Flow Behaviour Index, n	1.20220
Representative Particle Size, d_{85}	85 μm

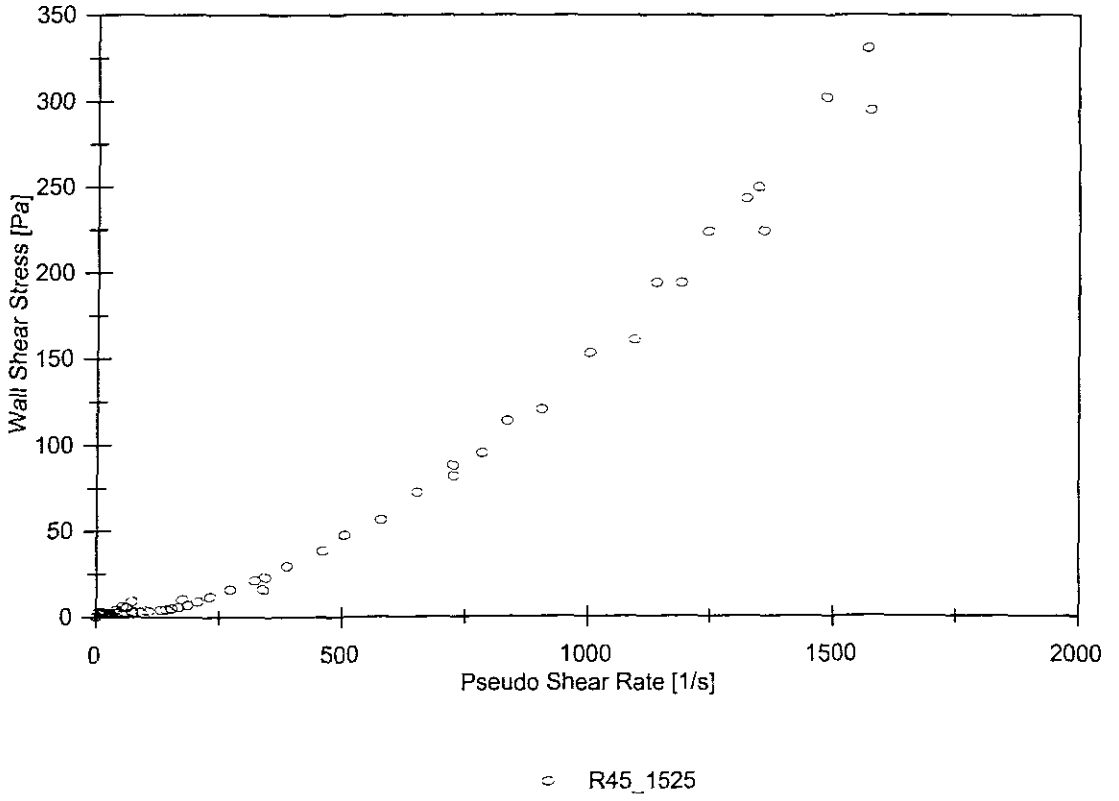

APPARATUS

Facility	BBTV
Pipe name	R45-3060
Diameter (mm)	45.44
Pipe roughness (μm)	672
Material	Tailings
Operator	FvS
Supervisor	PTS

SLURRY PROPERTIES

Solids Relative Density	3.70
Fluid Relative Density (S_m)	1.146
Volumetric Concentration	27.07 %
Yield Stress, τ_y (Pa)	2.5839
Fluid Consistency Index, K (Pa.s^n)	0.00287
Flow Behaviour Index, n	1.20220
Representative Particle Size, d_{85}	85 μm

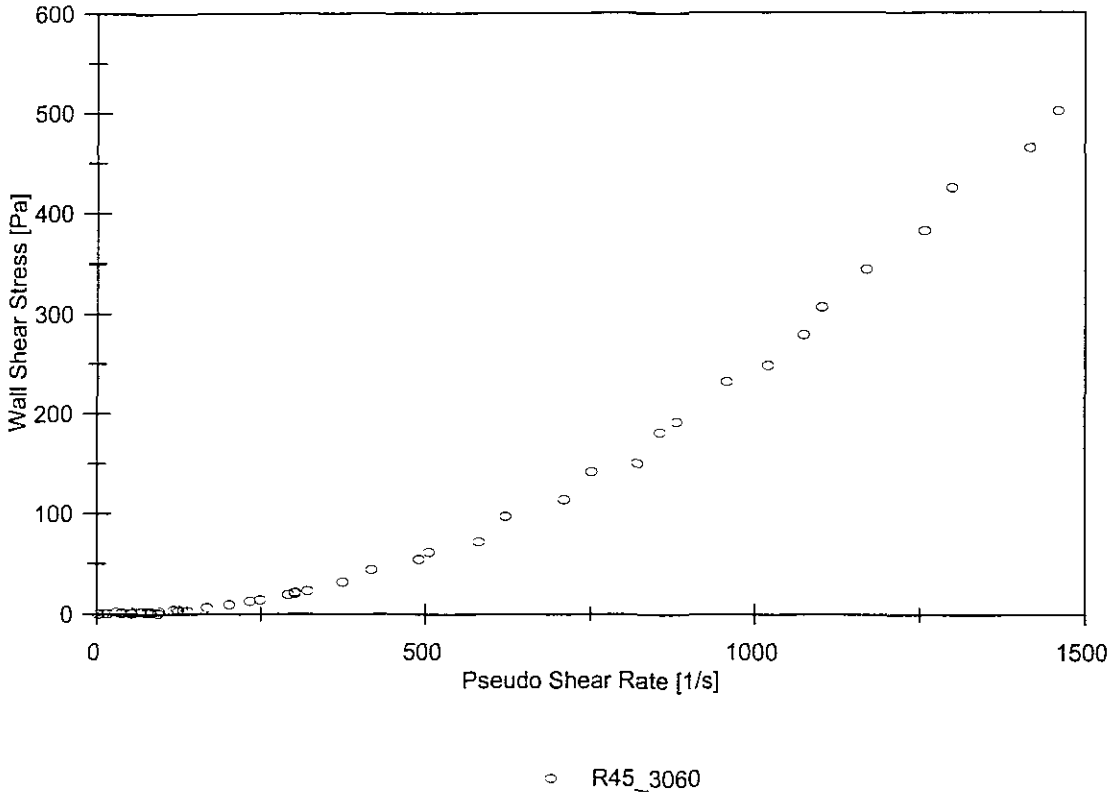

TAILINGS TEST RESULTS $S_m = 1.8012$

APPARATUS

Facility	BBTV
Pipe name	5 Smooth
Diameter (mm)	5.78
Pipe roughness (μm)	1.1
Material	Tailings
Operator	FvS
Supervisor	PTS

SLURRY PROPERTIES

Solids Relative Density	3.70
Fluid Relative Density (S_m)	1.146
Volumetric Concentration	29.67 %
Yield Stress, τ_y (Pa)	4.9599
Fluid Consistency Index, K (Pa.s^n)	0.01689
Flow Behaviour Index, n	1.00129
Representative Particle Size, d_{85}	85 μm

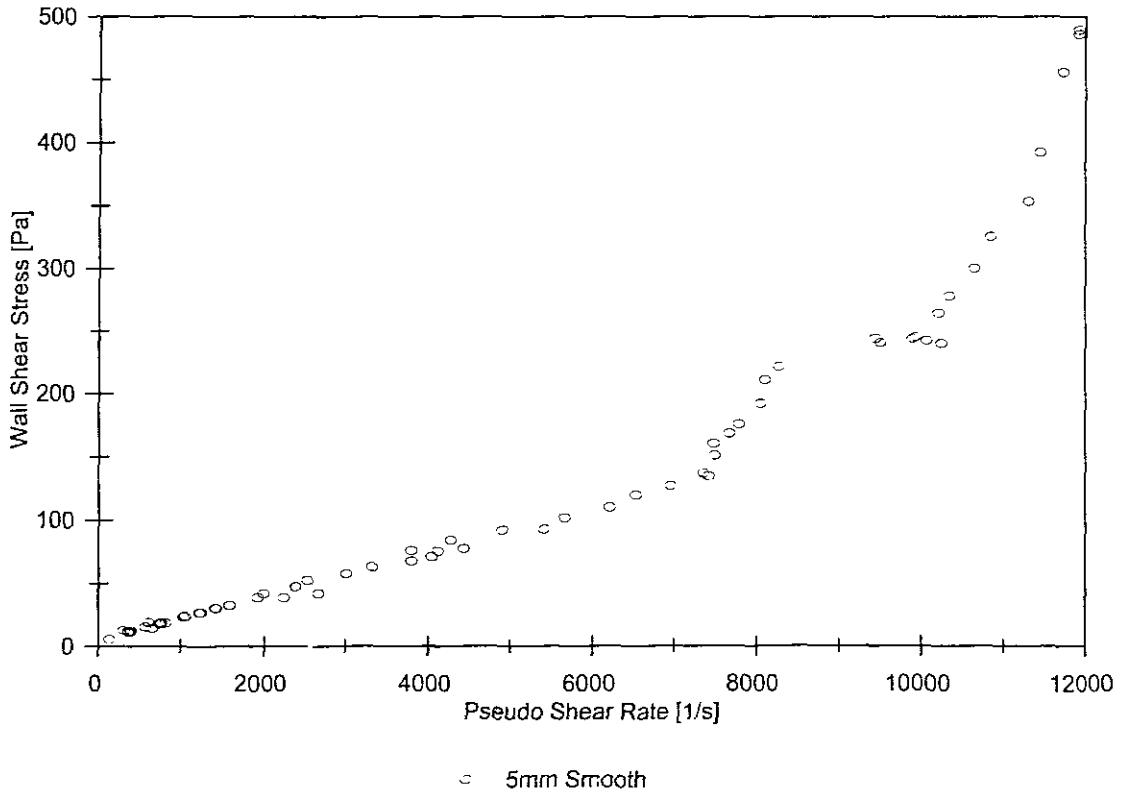

APPARATUS

Facility	BBTV
Pipe name	13 Smooth
Diameter (mm)	13.12
Pipe roughness (μm)	0.9
Material	Tailings
Operator	FvS
Supervisor	PTS

SLURRY PROPERTIES

Solids Relative Density	3.70
Fluid Relative Density (S_m)	1.146
Volumetric Concentration	29.67 %
Yield Stress, τ_y (Pa)	4.9599
Fluid Consistency Index, K ($Pa.s^n$)	0.01689
Flow Behaviour Index, n	1.00129
Representative Particle Size, d_{85}	85 µm

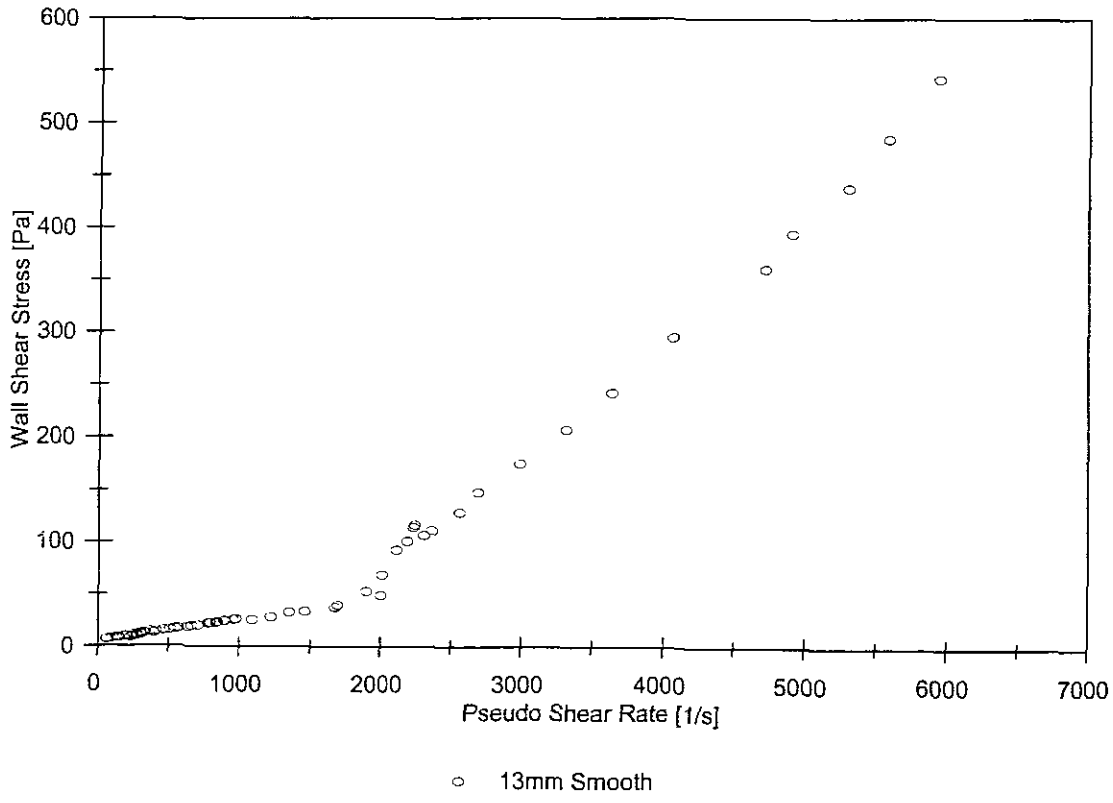

APPARATUS

Facility	BBTV
Pipe name	28 Smooth
Diameter (mm)	28.34
Pipe roughness (μm)	5.9
Material	Tailings
Operator	FvS
Supervisor	PTS

SLURRY PROPERTIES

Solids Relative Density	3.70
Fluid Relative Density (S_m)	1.146
Volumetric Concentration	29.67 %
Yield Stress, τ_y (Pa)	4.9599
Fluid Consistency Index, K ($Pa.s^n$)	0.01689
Flow Behaviour Index, n	1.00129
Representative Particle Size, d_{85}	85 μm

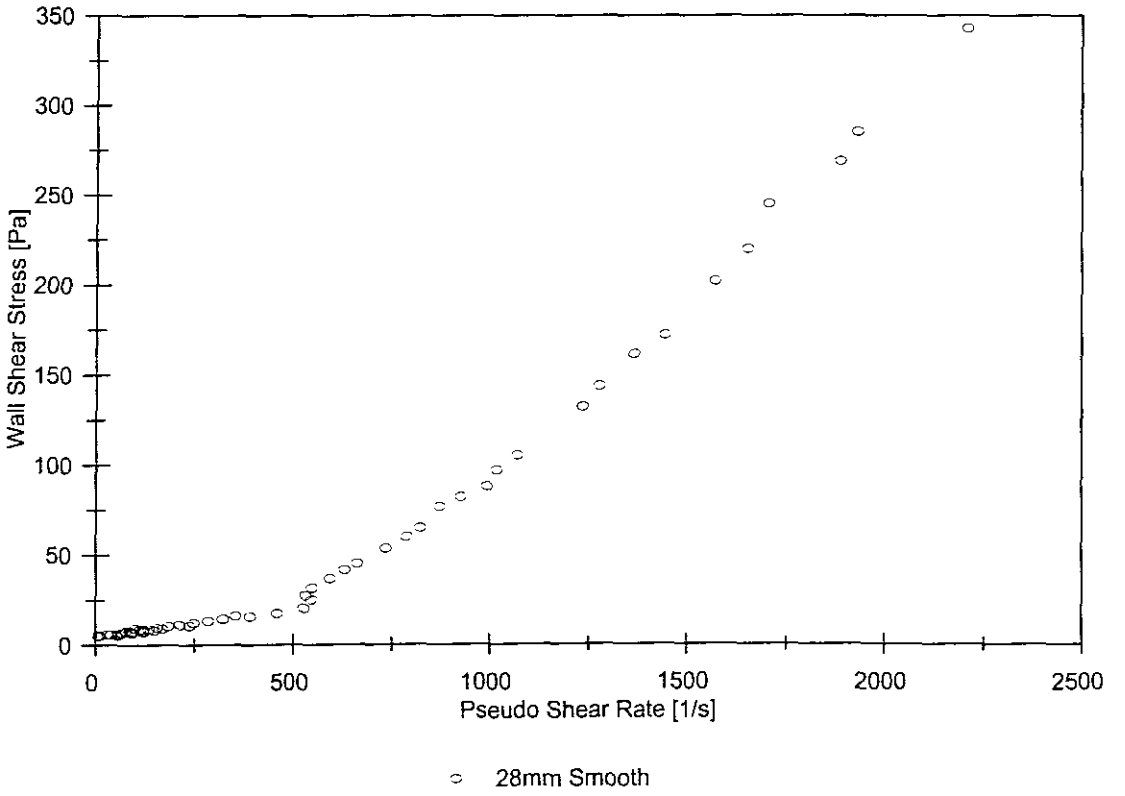

APPARATUS

Facility	BBTV
Pipe name	45 Smooth
Diameter (mm)	45.04
Pipe roughness (μm)	1.3
Material	Tailings
Operator	FvS
Supervisor	PTS

SLURRY PROPERTIES

Solids Relative Density	3.70
Fluid Relative Density (S_m)	1.146
Volumetric Concentration	29.67 %
Yield Stress, τ_y (Pa)	4.9599
Fluid Consistency Index, K ($Pa.s^n$)	0.01689
Flow Behaviour Index, n	1.00129
Representative Particle Size, d_{85}	85 µm

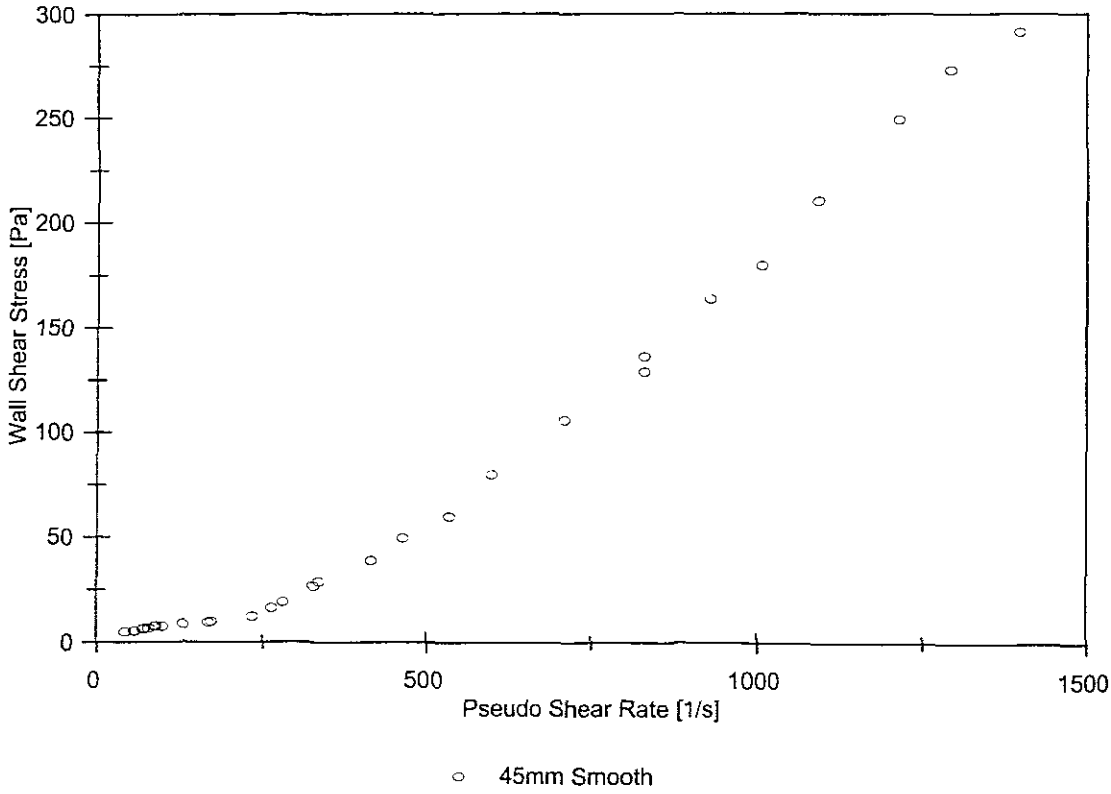

APPARATUS

Facility	BBTV
Pipe name	R28-1525
Diameter (mm)	27.03
Pipe roughness (μm)	136
Material	Tailings
Operator	FvS
Supervisor	PTS

SLURRY PROPERTIES

Solids Relative Density	3.70
Fluid Relative Density (S_m)	1.146
Volumetric Concentration	29.67 %
Yield Stress, τ_y (Pa)	4.9599
Fluid Consistency Index, K (Pa.s^n)	0.01689
Flow Behaviour Index, n	1.00129
Representative Particle Size, d_{85}	85 μm

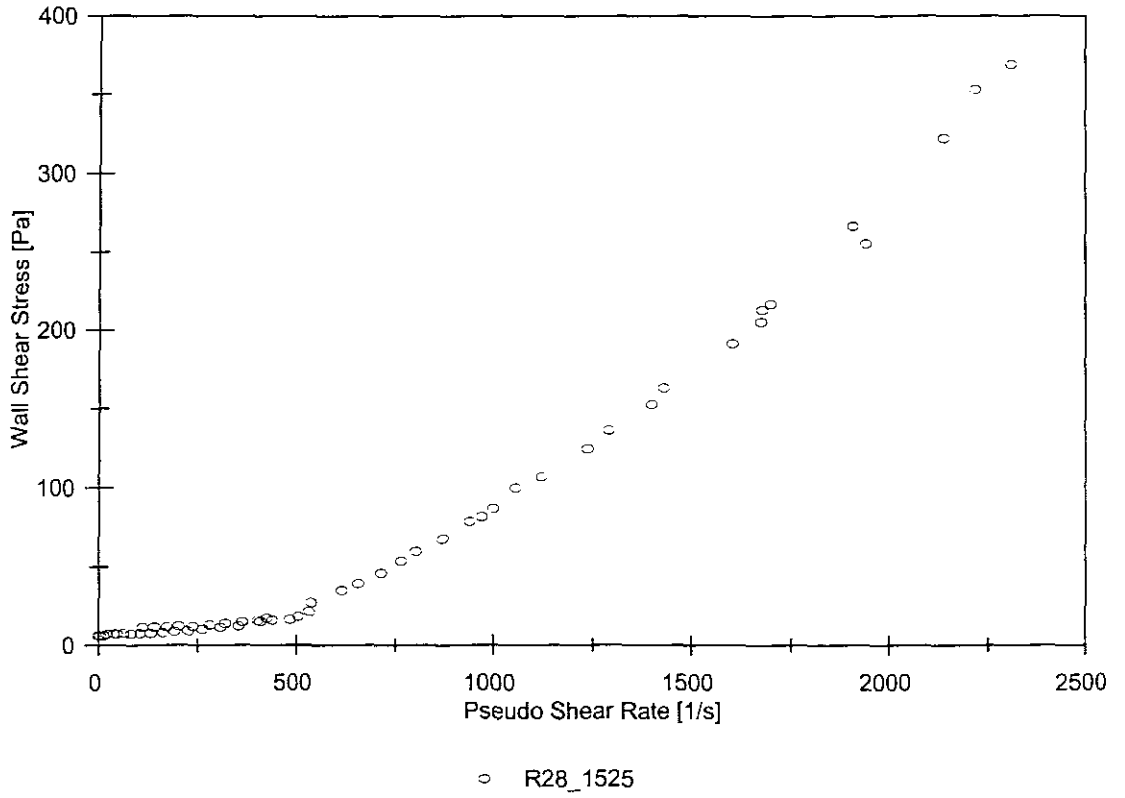

APPARATUS

Facility	BBTV
Pipe name	R28-3060
Diameter (mm)	27.17
Pipe roughness (μm)	291
Material	Tailings
Operator	FvS
Supervisor	PTS

SLURRY PROPERTIES

Solids Relative Density	3.70
Fluid Relative Density (S_m)	1.146
Volumetric Concentration	29.67 %
Yield Stress, τ_y (Pa)	4.9599
Fluid Consistency Index, K ($Pa.s^n$)	0.01689
Flow Behaviour Index, n	1.00129
Representative Particle Size, d_{85}	85 μm

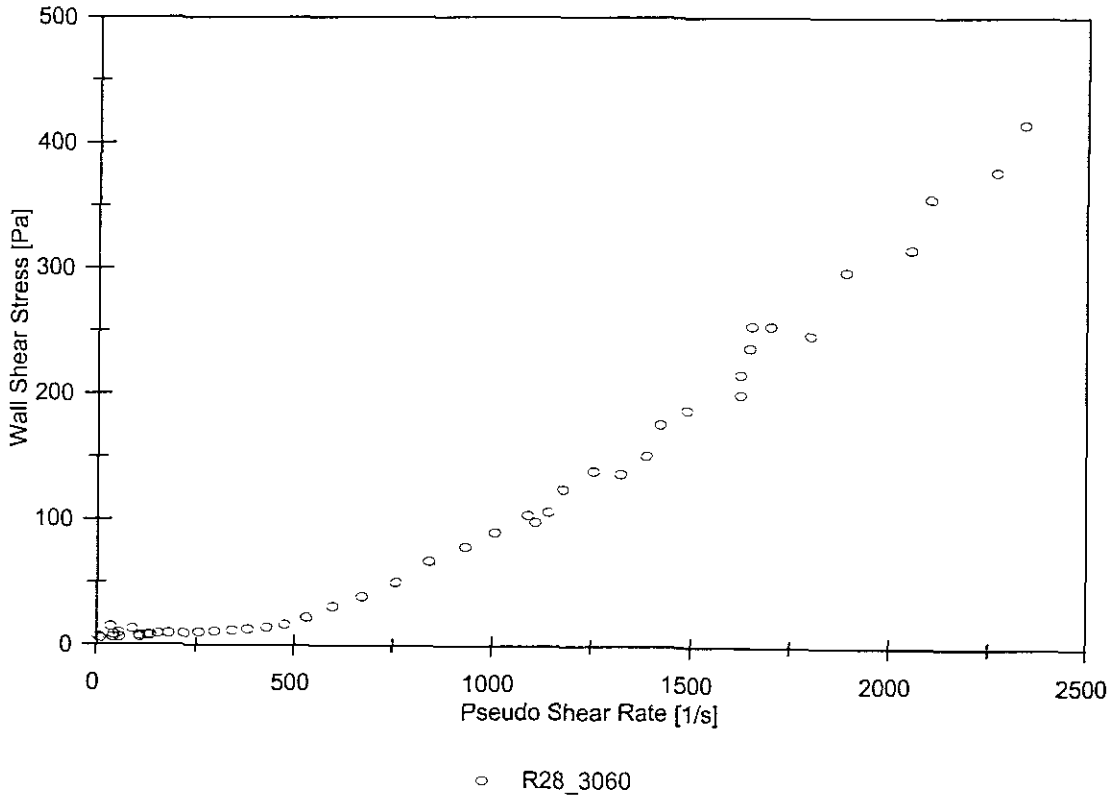

APPARATUS

Facility	BBTV
Pipe name	R45-1525
Diameter (mm)	44.73
Pipe roughness (μm)	42
Material	Tailings
Operator	FvS
Supervisor	PTS

SLURRY PROPERTIES

Solids Relative Density	3.70
Fluid Relative Density (S_m)	1.146
Volumetric Concentration	29.67 %
Yield Stress, τ_y (Pa)	4.9599
Fluid Consistency Index, K (Pa.s^n)	0.01689
Flow Behaviour Index, n	1.00129
Representative Particle Size, d_{85}	85 μm

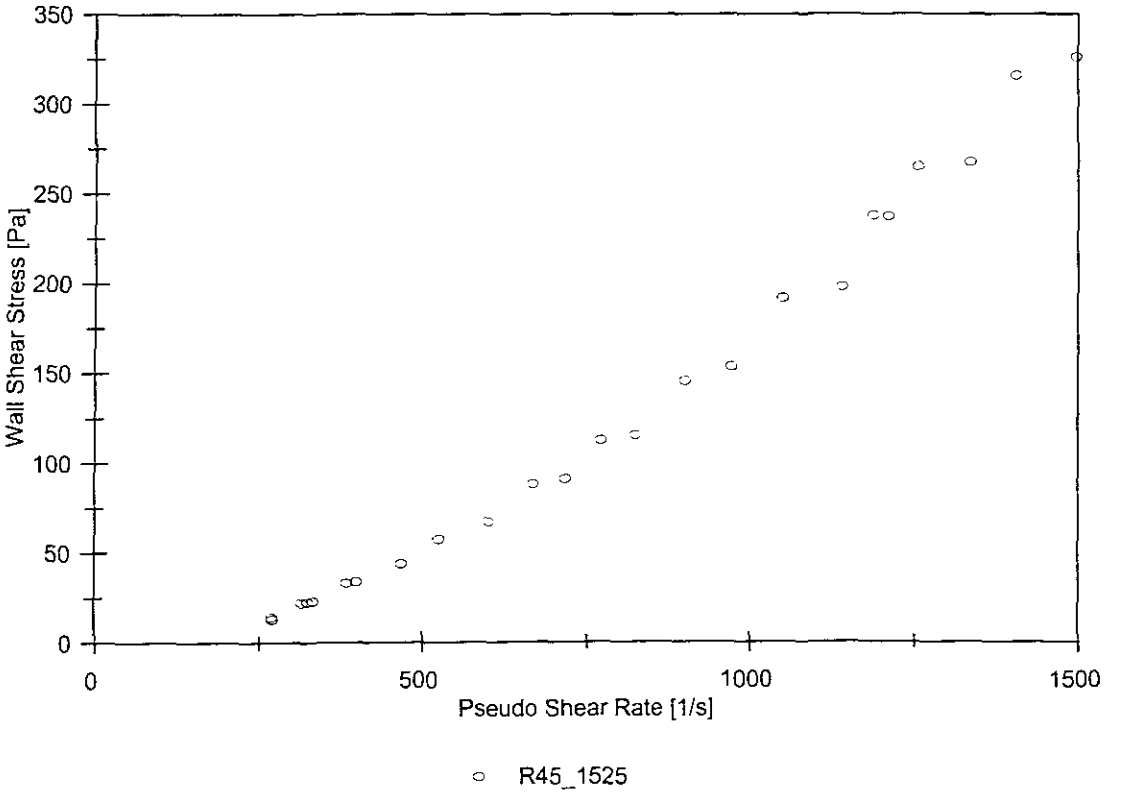

APPARATUS

Facility	BBTV
Pipe name	R45-3060
Diameter (mm)	45.44
Pipe roughness (μm)	672
Material	Tailings
Operator	FvS
Supervisor	PTS

SLURRY PROPERTIES

Solids Relative Density	3.70
Fluid Relative Density (S_m)	1.146
Volumetric Concentration	29.67 %
Yield Stress, τ_y (Pa)	4.9599
Fluid Consistency Index, K ($Pa.s^n$)	0.01689
Flow Behaviour Index, n	1.00129
Representative Particle Size, d_{85}	85 μm

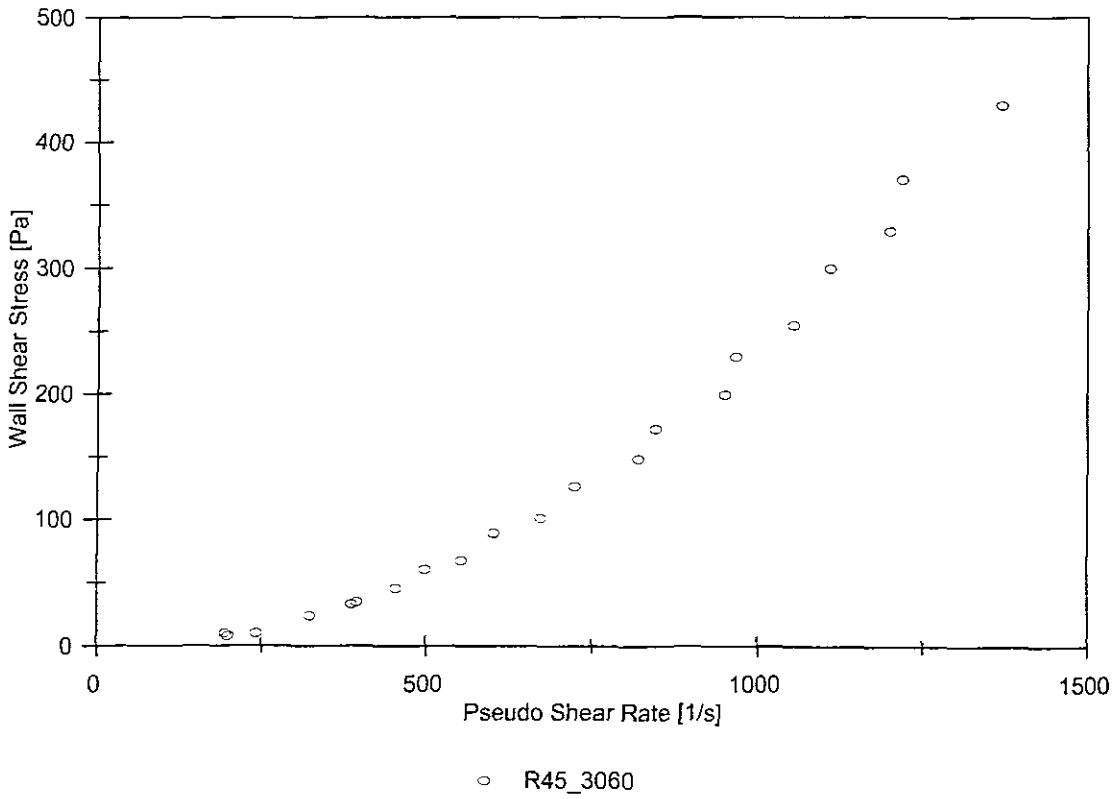

APPENDIX B

RHEOLOGICAL CHARACTERIZATION

B1 Introduction

The rheological characterization is the first step of analysis before the turbulent flow of the smooth and rough pipes can be examined. It is therefore of utmost importance that the rheological characterization is done properly, as the result will influence the turbulent flow analysis.

In all the tests the laminar flow was analyzed using the generalized pseudo plastic model (Govier & Aziz, 1972). In all the rheological analysis presented a table is provided showing the best fit model, the rheological parameters and the error in the model fitted to the data.

Only the smooth pipe laminar flow data was used for the rheological characterization for reasons discussed in Chapter 4 and Section B3 of this Appendix.

B2 Rheological Characterization

B2.1 Correlation Errors

A graphical and a analytical technique are used to compare the errors between experimentally determined and analytically derived values.

The most meaningful analytical comparison was considered by Lazarus and Nielson (1978) to be a log standard error rather than a correlation coefficient. The equation used is given by;

$$S = \frac{\sqrt{\sum_{i=1}^{n}\left[\log(\text{observed}) - \log(\text{calculated})\right]^2}}{(n-1)}; \qquad \text{(B.1)}$$

where S is the root mean square deviation of the log of observed points from the log of calculated points.

Figure B.1 shows the value of S in the logarithmic domain and its transformation into the linear domain. The value ε is the expected average error above (positive) and below (negative) the actual value.

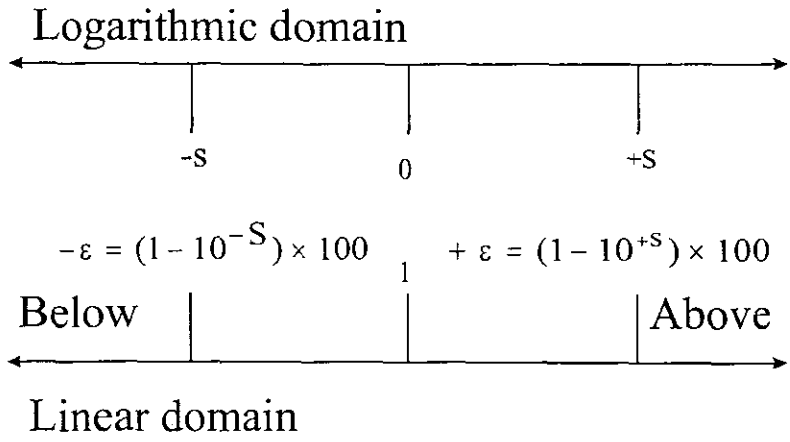

Figure 1: Definition diagram for log standard error

The log standard error should be used with some care since the error values are average values and not maximum expected values. Average error values of below 2% (Log Err below 0.0095) should be considered the upper limit for a good correlation of the data.

B2.2 Glycerol Test Results

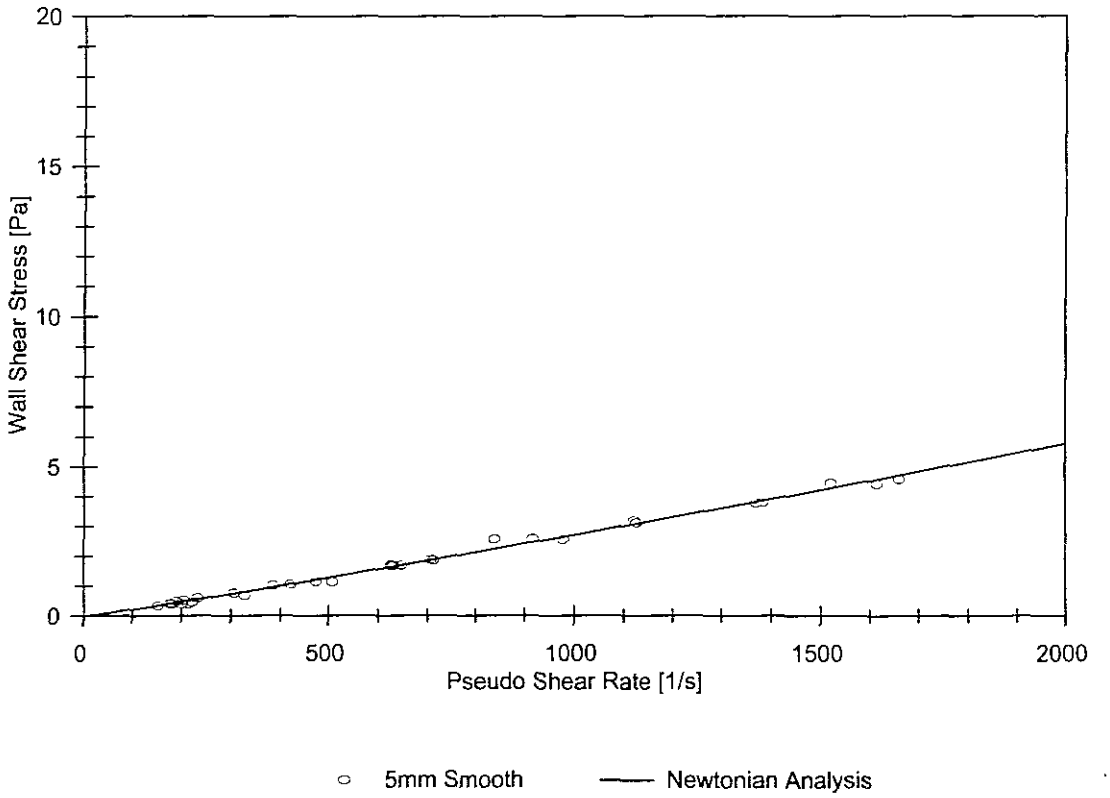

Glycerol at Solution Relative Density of 1.0906

Glycerol at relative density of 1.0906 was analyzed as a Newtonian fluid. Because of the low slurry relative density, laminar flow was only obtained in the 5.78 mm smooth pipe. Laminar data was measured at pseudo shear rates between 150 to 1700 1/s, and the wall shear stress ranged from 0.3 to 5 Pa.

Rheological Model	Yield Stress τy [Pa]	Fluid Consistency Index K	Flow Behavior Index n	Log Std Error
Newtonian Analysis	0	0.002736	1.000	0.0106

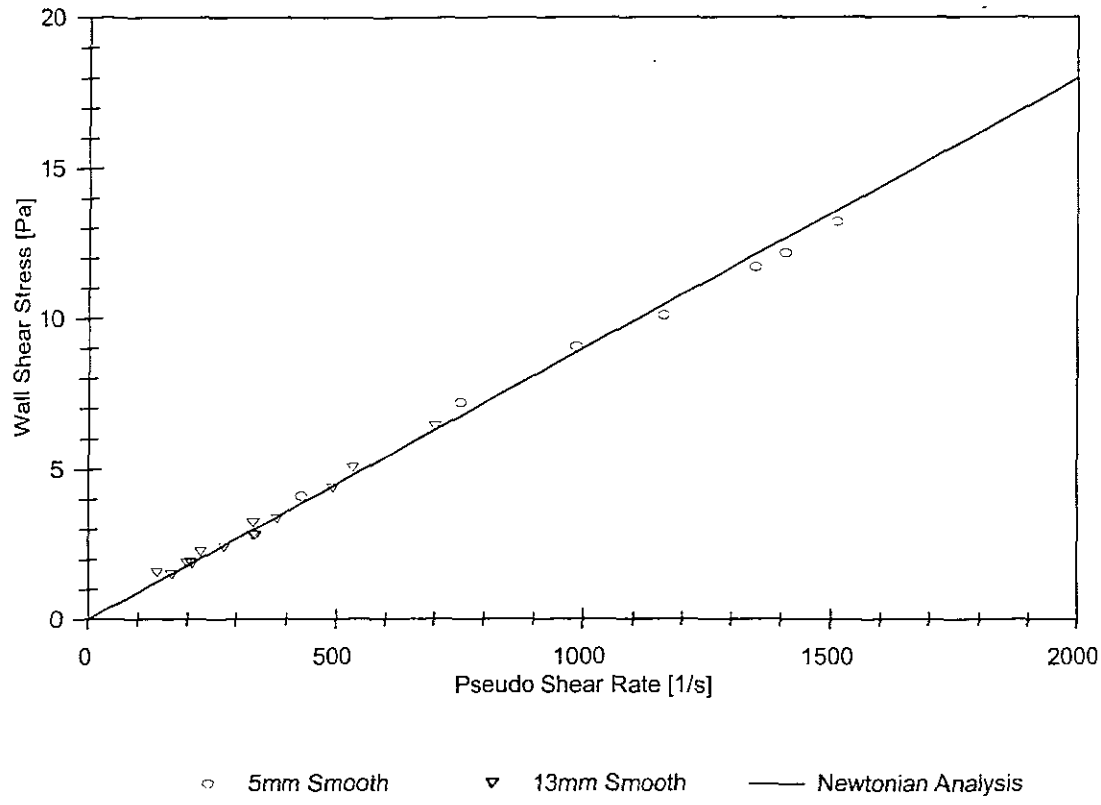

Glycerol at a Solution Relative Density of Sm 1.1433

Glycerol at relative density of 1.1433 was analyzed as a Newtonian fluid. The Newtonian model was used and applied to turbulent flow analysis. Laminar data was obtained in both the 5.78 mm and 13.13 mm smooth pipes. Pseudo shear rates ranged from 100 to 4150 1/s and the wall shear stress ranged from 1 and 34 Pa in the laminar region.

Rheological Model	Yield Stress τy [Pa]	Fluid Consistency Index K	Flow Behavior Index n	Log Std Error
Newtonian Analysis	0	0.00900	1.000	0.0072

B2.3 CMC Test Results

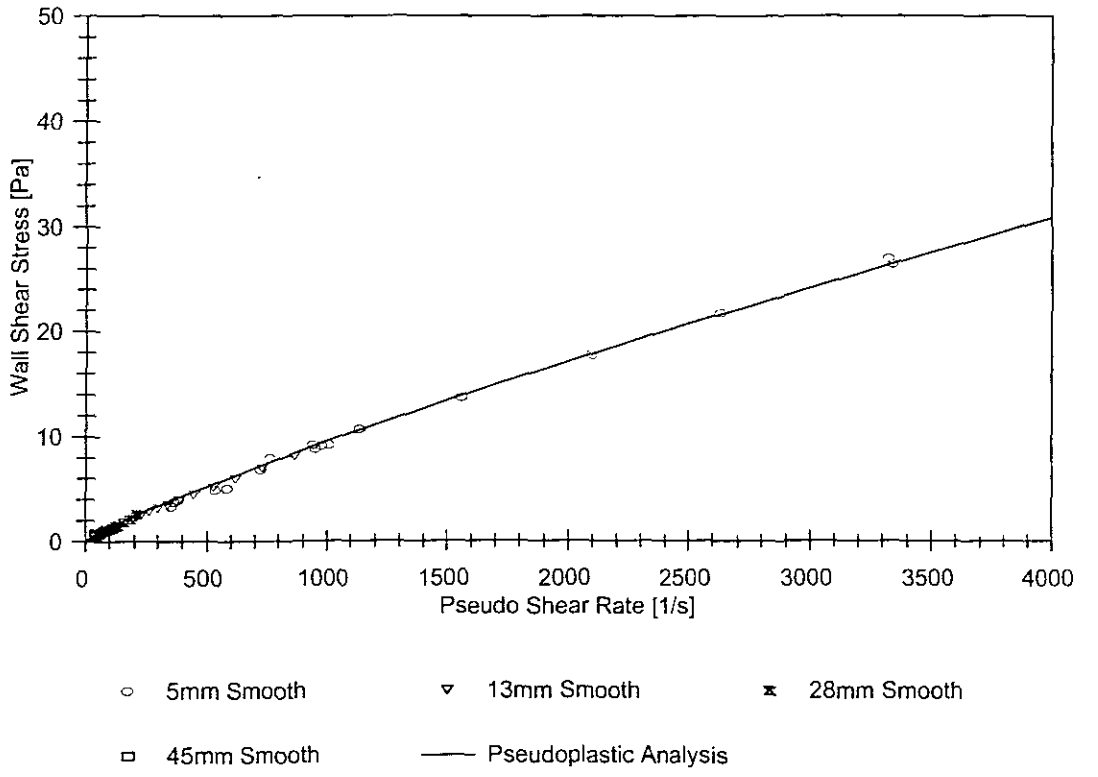

CMC at a Solution Relative Density of 1.0129

CMC at relative density of 1.0129 was analyzed as a Pseudoplastic fluid. Pseudo shear rates ranged from 30 and 3500 1/s and wall shear stress ranged between 0.2 and 28 Pa. Laminar flow was achieved in all four smooth pies. Laminar flow was also achieved in the rough pipes but was not used in the rheological characterization.

Rheological Model	Yield Stress τy [Pa]	Fluid Consistency Index K	Flow Behavior Index n	Log Std Error
Pseudoplastic Analysis	0	0.84959	0.026	0.0046

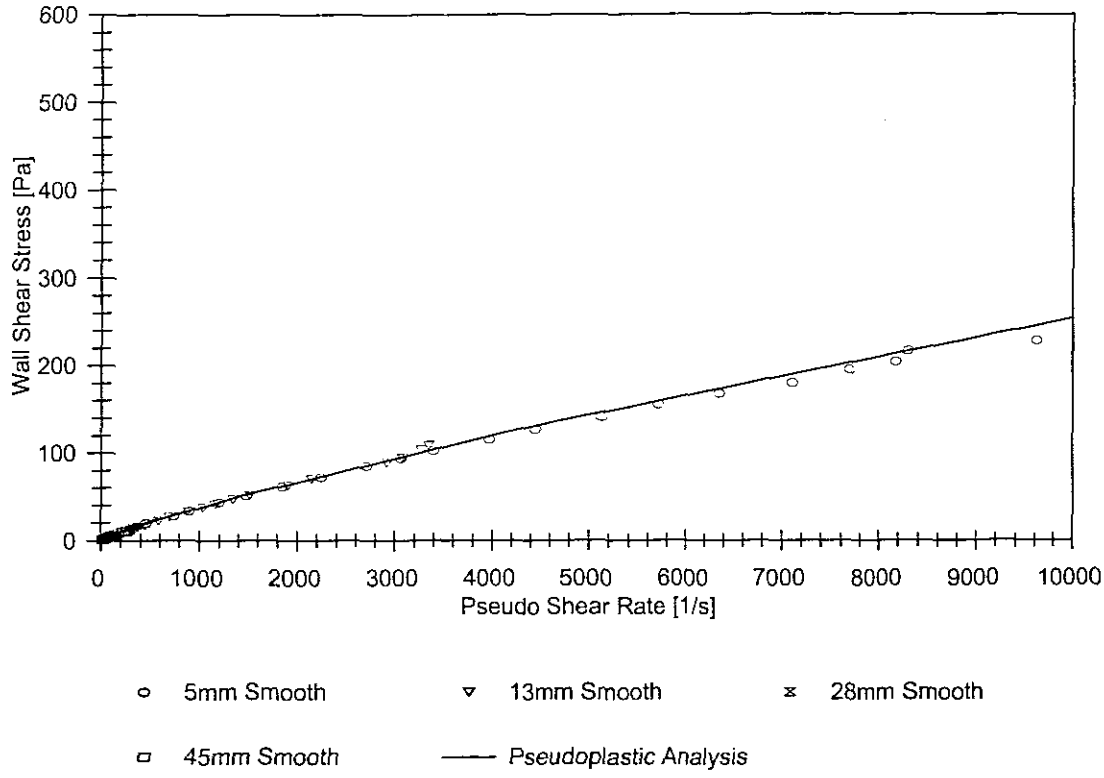

CMC at Slurry Relative Density of 1.0269

CMC at a slurry relative density of 1.0269 was analyzed as a Pseudoplastic fluid. Pseudo shear rates ranged from 10 to 16000 1/s and the wall shear stress ranged from 0.6 to 320Pa. Laminar flow was achieved in all the smooth pipes as well as in the rough pipes. Only the smooth pipes were used for the rheological characterization.

Rheological Model	Yield Stress τy [Pa]	Fluid Consistency Index K	Flow Behavior Index n	Log Std Error
Pseudoplastic Analysis	0	0.12106	0.827	0.0061

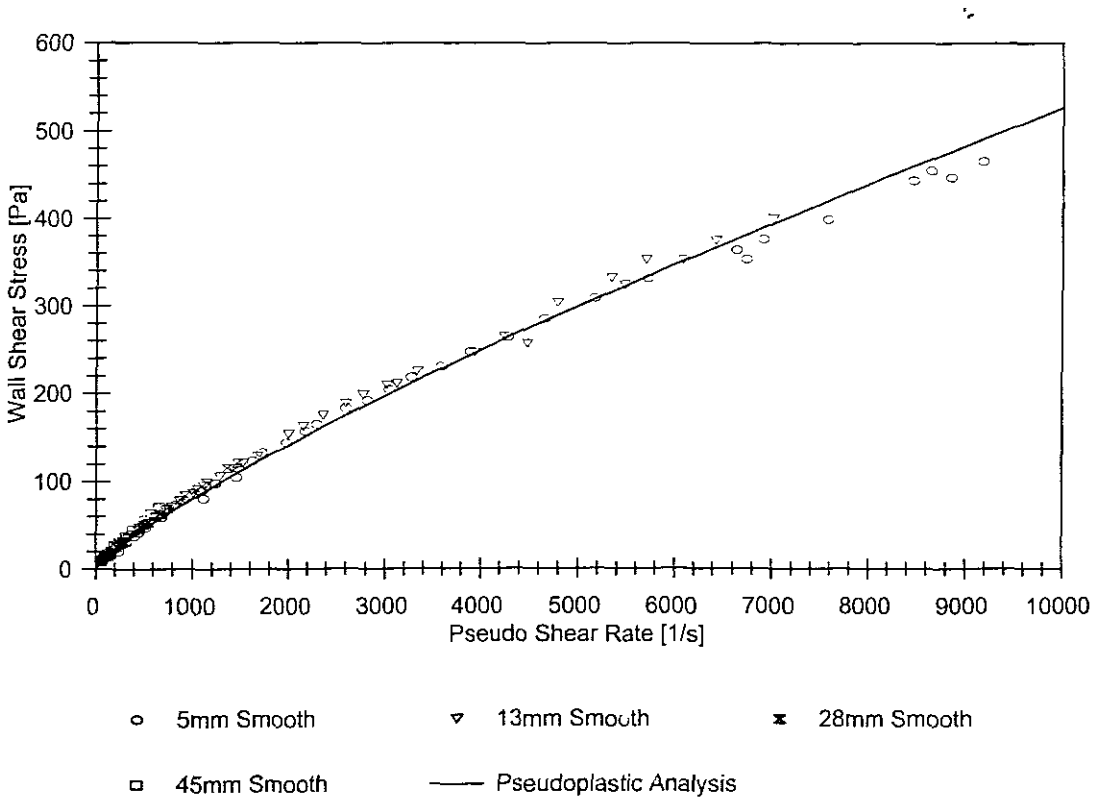

Cmc at a Slurry Relative Density of 1.0372

CMC at a slurry relative density of 1.0372 was analyzed as a Pseudoplastic fluid. Pseudo shear rates ranged from 40 to 9200 1/s and the wall shear stress ranged between 5 and 500Pa. Laminar flow was achieved in both smooth and rough pipes. Only the smooth pipes were used for rheological characterization.

Rheological Model	Yield Stress τy [Pa]	Fluid Consistency Index K	Flow Behavior Index n	Log Std Error
Pseudoplastic Analysis	0	0.27485	0.816	0.0018

B2.4 Kaolin Test Results

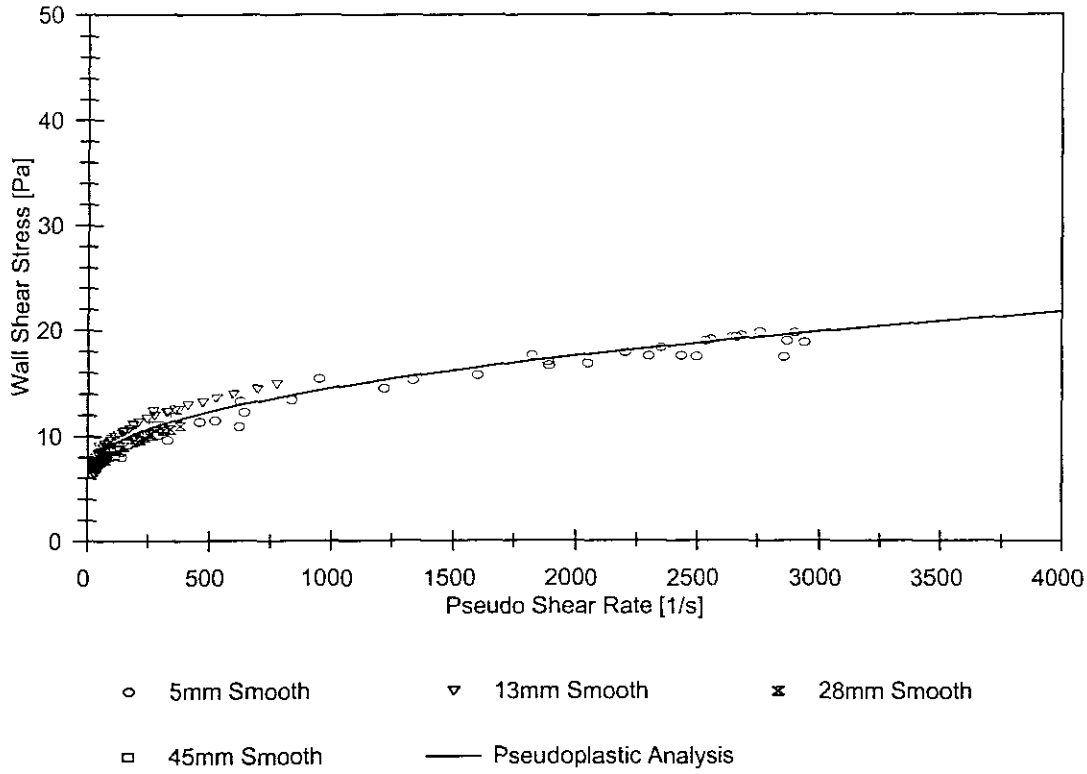

Kaolin at Sm 1.0803

Kaolin at a slurry relative density of 1.0803 was analyzed as a Yield Pseudoplastic fluid. Pseudo shear rates ranged between 10 and 3100 1/s and the wall shear stress between 5 and 20 Pa. Laminar flow was achieved in all the smooth and rough pipes. Only the laminar flow obtained from the smooth pipes were used for rheological characterization.

Rheological Model	Yield Stress τy [Pa]	Fluid Consistency Index K	Flow Behavior Index n	Log Std Error
Yield Pseudoplastic Analysis	5.50494	0.28786	0.463	0.0028

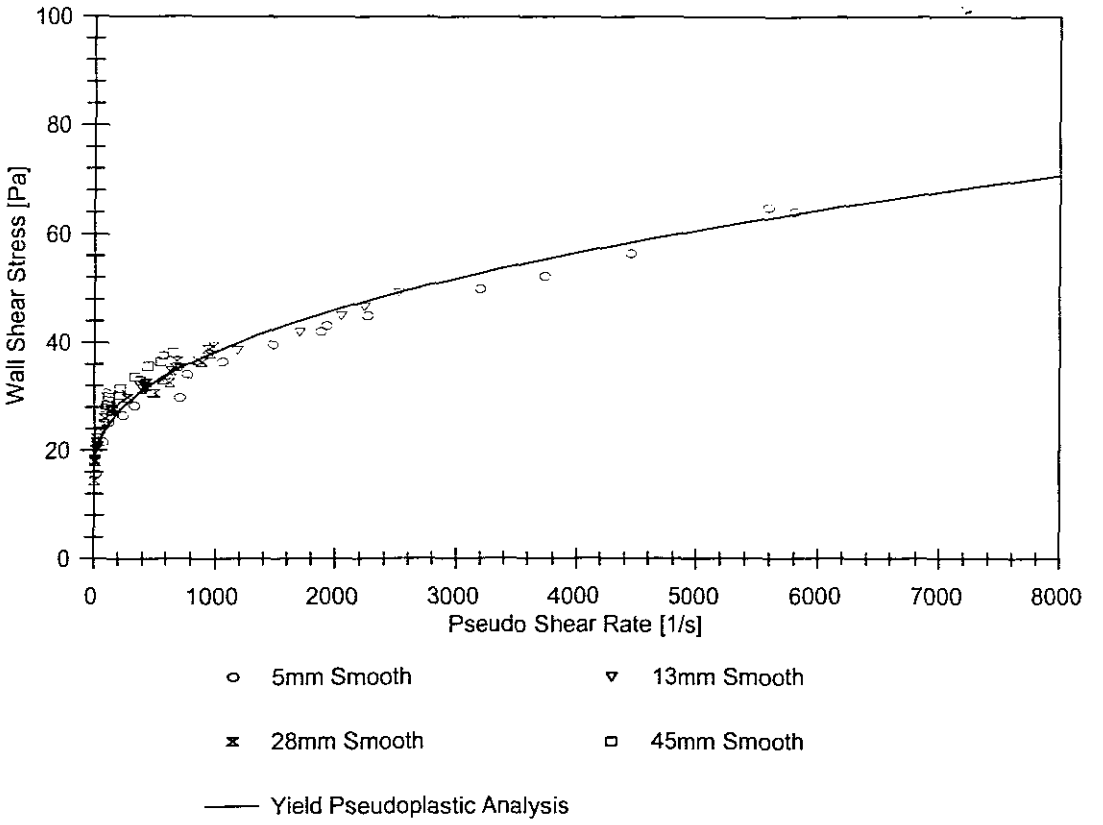

Kaolin at a Slurry Relative Density of 1.146

Kaolin at a slurry relative density of 1.146 was analyzed as a Yield Pseudoplastic fluid. Pseudo shear rates ranged from 1 to 6000 1/s and the wall shear stress from 12 to 60 Pa. Laminar flow was achieved in all smooth and rough pipes. Only the laminar flow from the smooth pipes was used for the rheological characterization.

Rheological Model	Yield Stress τ_y [Pa]	Fluid Consistency Index K	Flow Behavior Index n	Log Std Error
Yield Pseudoplastic Analysis	14.28570	0.87945	0.443	0.0041

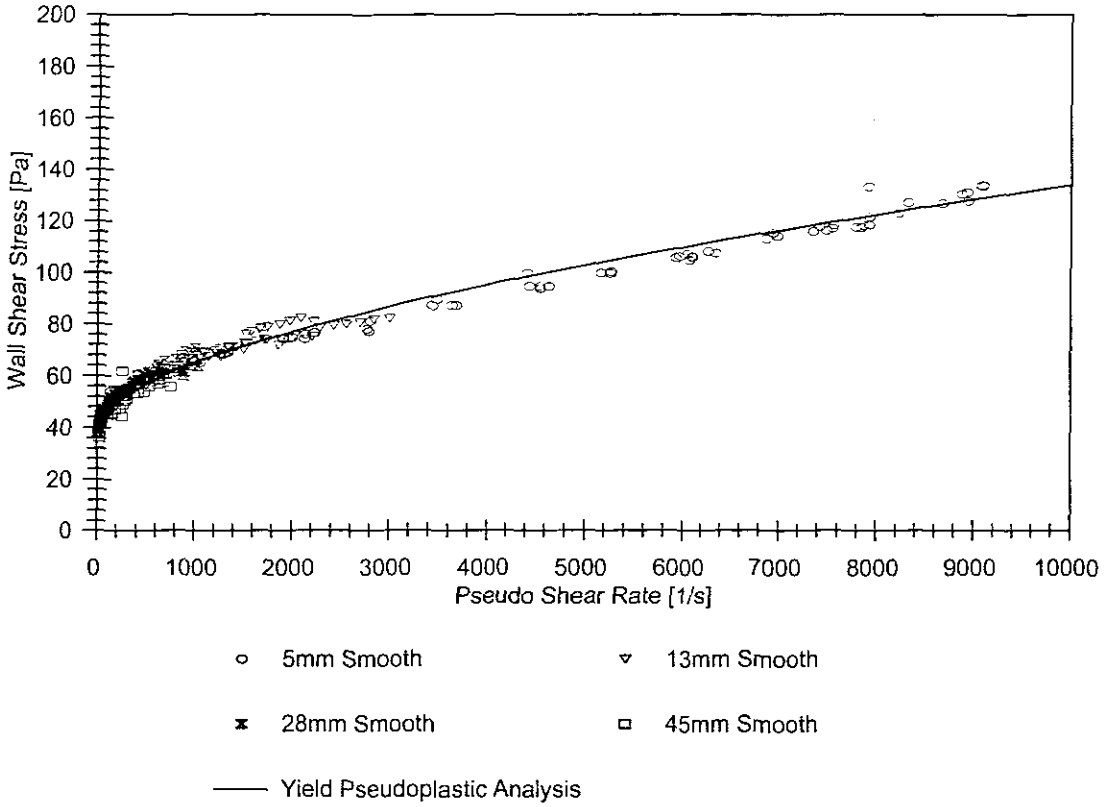

Kaolin at a Slurry Relative Density of 1.1779

Kaolin at a slurry relative density of 1.1779 was analyzed as a Yield Pseudoplastic fluid. Pseudo shear rates ranged between 10 and 9400 1/s. The wall shear stress ranged between 30 and 130 Pa. Laminar flow was achieved in all the smooth and rough pipes. Only the smooth pipe laminar flow data was used for rheological characterization.

Rheological Model	Yield Stress τ_y [Pa]	Fluid Consistency Index K	Flow Behavior Index n	Log Std Error
Yield Pseudoplastic Analysis	35.7885	0.27887	0.617	0.0013

B2.5 Tailings Test Results

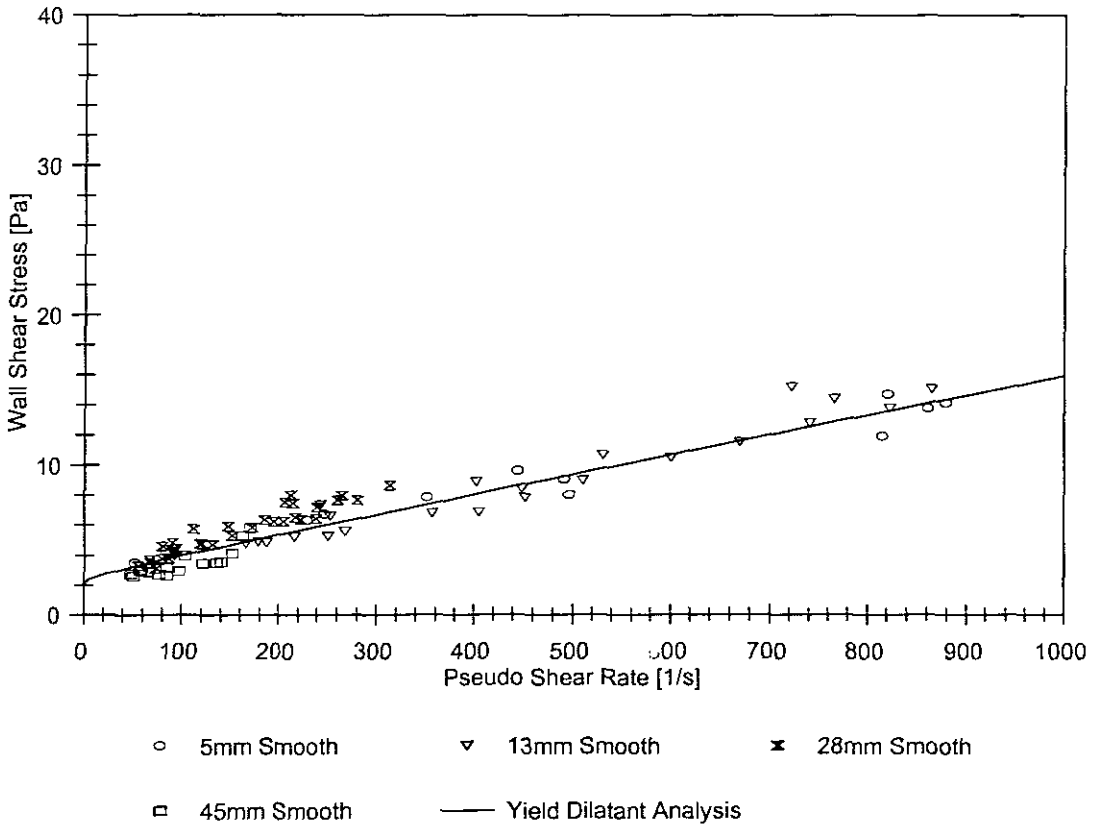

Tailings at a Slurry Relative Density of 1.7309

Tailings at a slurry relative density of 1.7309 were analyzed as a Yield Dilatant fluid Pseudo shear rates varied between 30 and 900 1/s and the wall shear stress varied between 2 and 16 Pa. Laminar flow was observed in all the smooth and rough pipes. Only the data from the smooth pipes were used for rheological characterization.

Rheological Model	Yield Stress τy [Pa]	Fluid Consistency Index K	Flow Behavior Index n	Log Std Error
Yield Dilatant Analysis	2.503	0.00653	1.100	0.0026

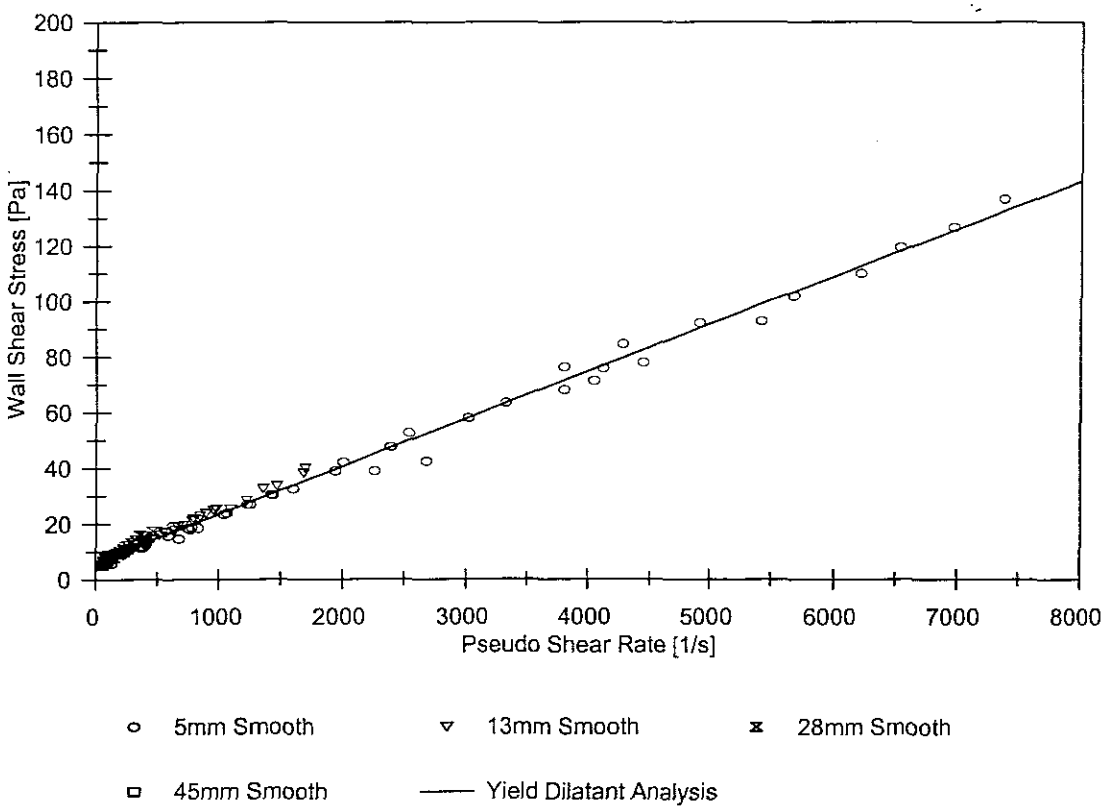

Tailings at a Slurry Relative Density of 1.8012

Tailings at a slurry relative density of 1.8012 were analyzed as a Yield Dilatant fluid Pseudo shear rates varied between 40 and 7200 1/s and the wall shear stress varied between 4 and 140 Pa. Laminar data were achieved in all the smooth and rough pipes. Only the data obtained in the smooth pipes were used for rheological characterization.

Rheological Model	Yield Stress τy [Pa]	Fluid Consistency Index K	Flow Behavior Index n	Log Std Error
Yield Dilatant Analysis	4.960	0.01689	1.001	0.0041

B3 Laminar Flow in Rough Pipes.

In most cases the laminar flow of the smooth and rough pipes were coincident. However, there were cases where some variation was noted. Only the laminar flow in the smooth pipes was used for rheological characterization. This variation in laminar flow will be discussed further in this Section.

B3.1 Glycerol at Relative Density of 1.1433

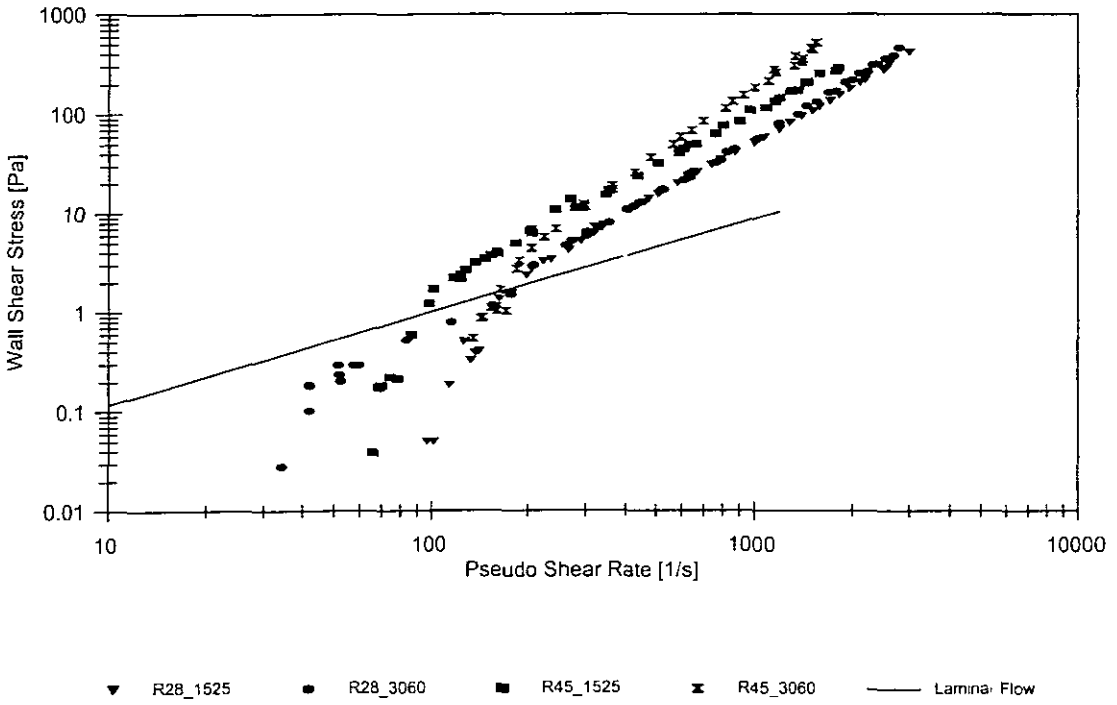

Glycerol at a Slurry Relative Density 1.1433

The laminar flow of glycerol in the rough pipes at a slurry relative density of 1.1433 behaved differently from the smooth pipe laminar flow. At the low pseudo shear rates the rough pipe data were below the Newtonian prediction for laminar flow of the smooth pipes. The laminar flow data of the rough pipes also indicates that the data is separated by a roughness effect. The rough pipe with the lowest hydraulic roughness is shifted to the left of the curve and the rough pipe with the highest hydraulic roughness is shifted to the right of the curve. In sufficient data was achieved in the R45_3060 rough pipe to determine its pattern. The rough pipe data in the early turbulent flow region also behaves differently from the smooth pipe data.

B3.2 CMC at a Slurry Relative Density of 1.1269

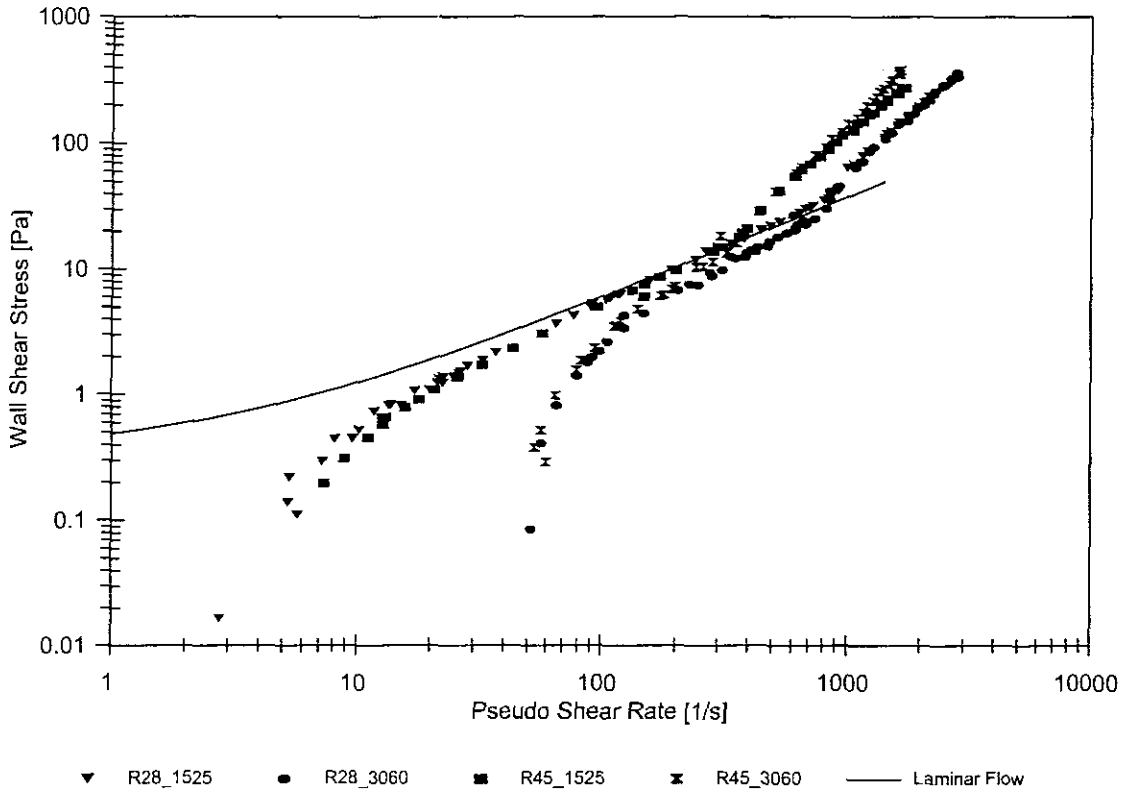

The laminar flow of CMC in the smooth and rough pipes behaved distinctly differently from each other. The laminar flow line on the graph shows the prediction of the smooth pipe data. The laminar flow of the rough pipe data indicates that there is a roughness effect and the data behaves distinctly differently from the smooth pipe data. In this case the laminar flow seems only to be affected by the hydraulic roughness as the pipes with similar hydraulic roughness are grouped together. No diameter effect was detected.

The transition from laminar to turbulent flow is the same for both the smooth and the rough pipes.

B3.3 CMC at a Slurry Relative Density of 1.0372

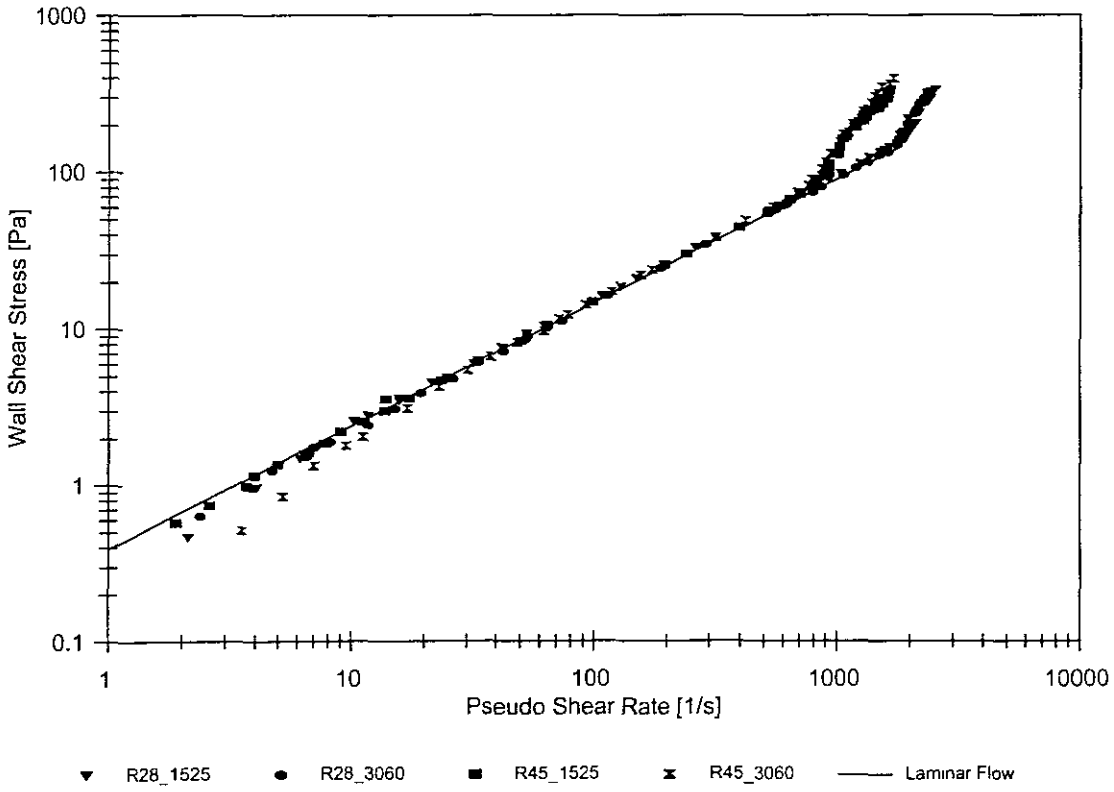

The laminar data of the rough pipes for CMC at a slurry relative density of 1.0362 deviates from the smooth pipe data at very low pseudo shear rates. The data are separated by pipe roughness where the pipe of the greatest roughness starts to deviate first. This phenomenon seems to be independent of the pipe diameter.

B4 Conclusions

- Laminar flow for the smooth and the rough pipes was presented for all the test fluids. All the smooth pipe laminar data is coincident in all the cases for the different tests.

- The rough pipe laminar flow data was not consistent. In some cases the laminar flow of the rough pipes behaved differently from the smooth pipe data. The laminar flow in these isolated cases seems to be influenced by a roughness effect.

- Not enough data were achieved to quantify this phenomenon but there is certainly scope for more intensive research in this field.

APPENDIX C

SMOOTH PIPE ANALYSIS

Test Fluid	Solids density (S_s)	Slurry Relative Density (S_m)	Solids Concentration (C_v) %	Page
Glycerol	N/A	1.090	N/A	C2
		1.143	N/A	C2
CMC	N/A	1.013	N/A	C3
		1.027	N/A	C3
		1.037	N/A	C4
Kaolin	2.65	1.080	4.85	C5
		1.146	8.85	C5
		1.177	10.73	C6
Tailings	3.70	1.731	27.07	C7
		1.801	29.67	C7

SMOOTH PIPE TEST RESULTS

GLYCEROL SMOOTH PIPE TEST RESULTS

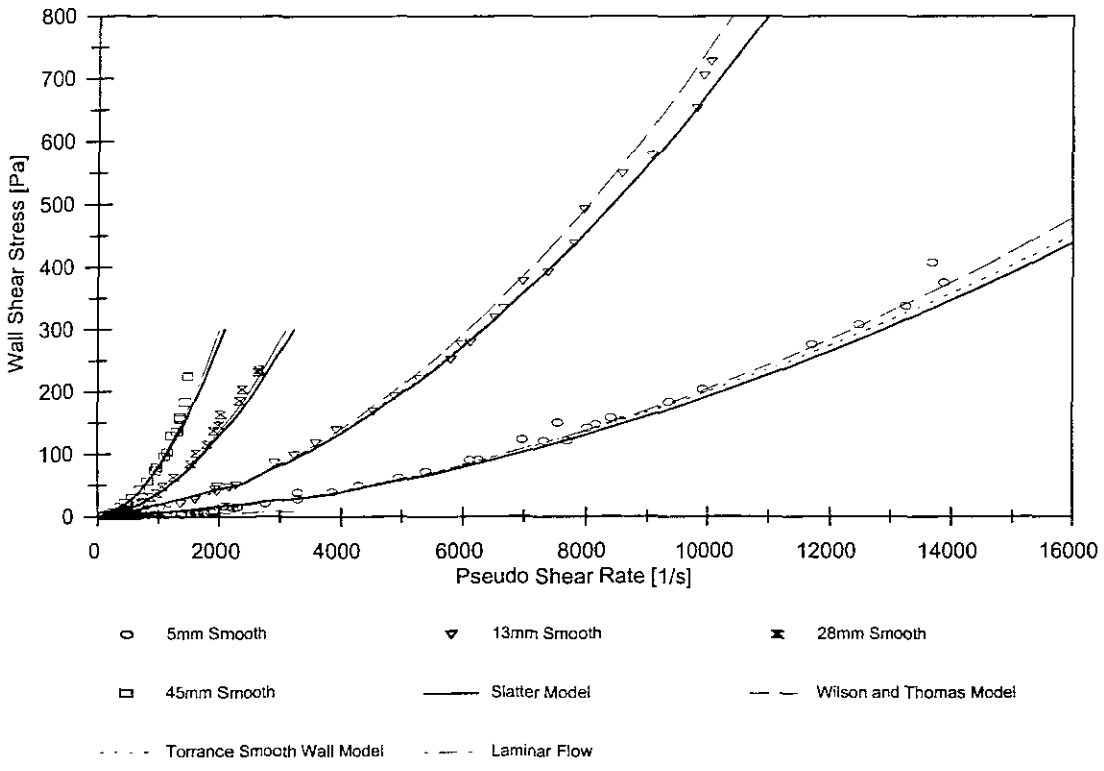

Glycerol Smooth Models at a Slurry Relative Density of 1.090

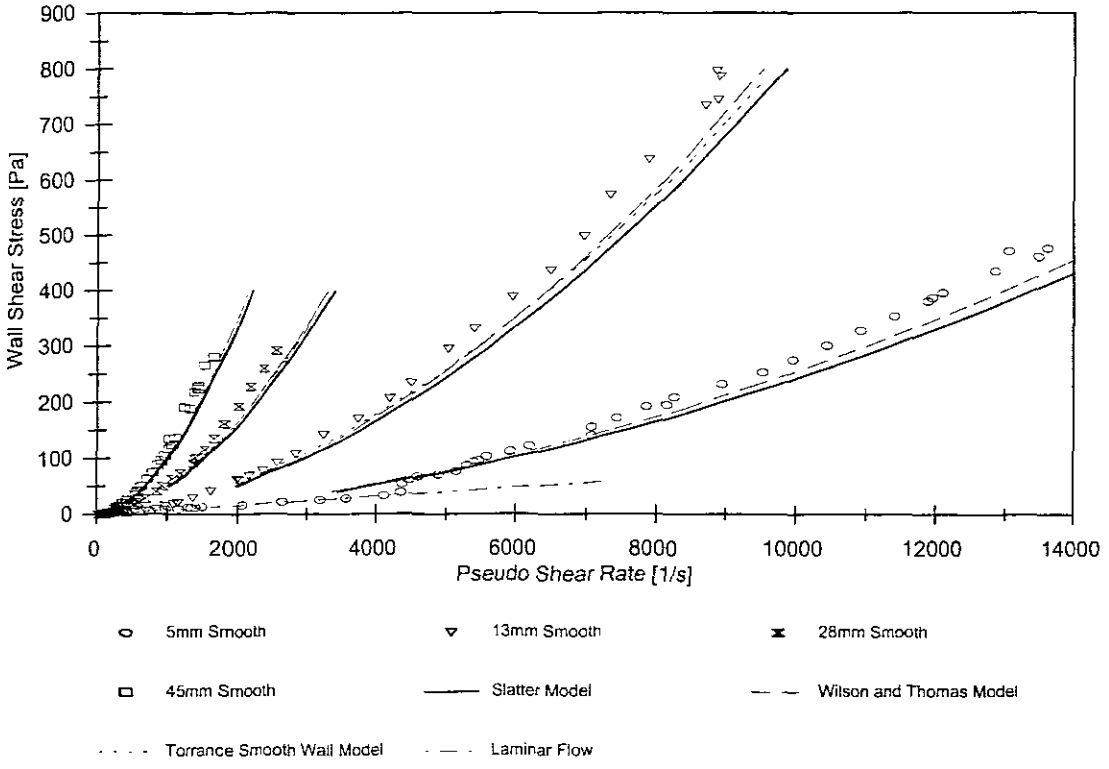

Glycerol Smooth Models at a Slurry Relative Density of 1.143

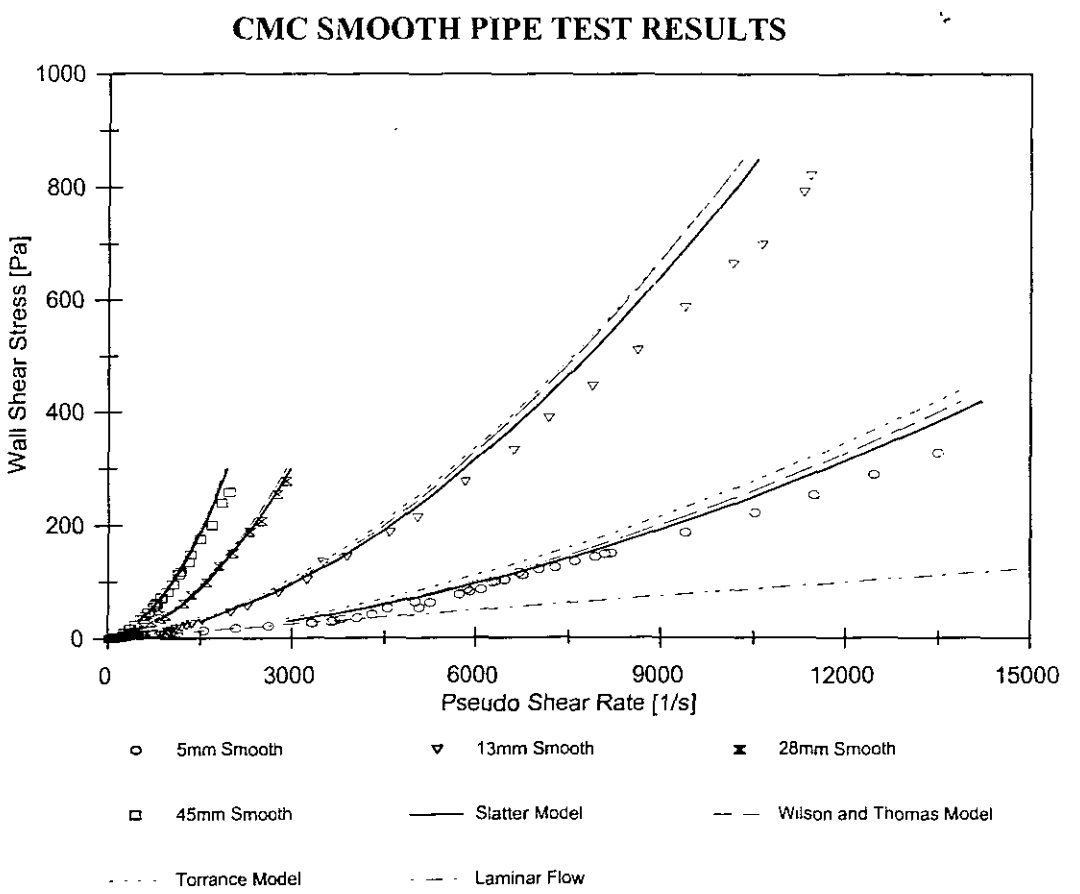

CMC Smooth Pipe Models at a Slurry Relative Density of 1.013

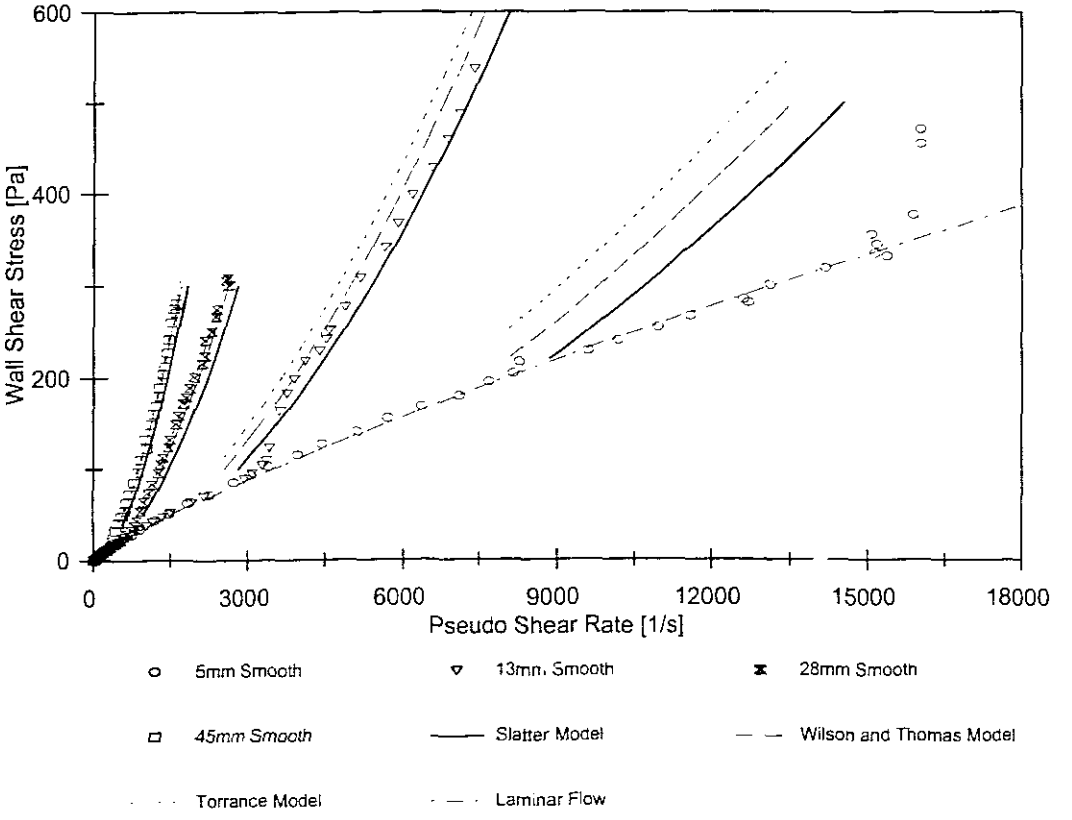

CMC Smooth Pipe Models at a Slurry Relative Density of 1.027

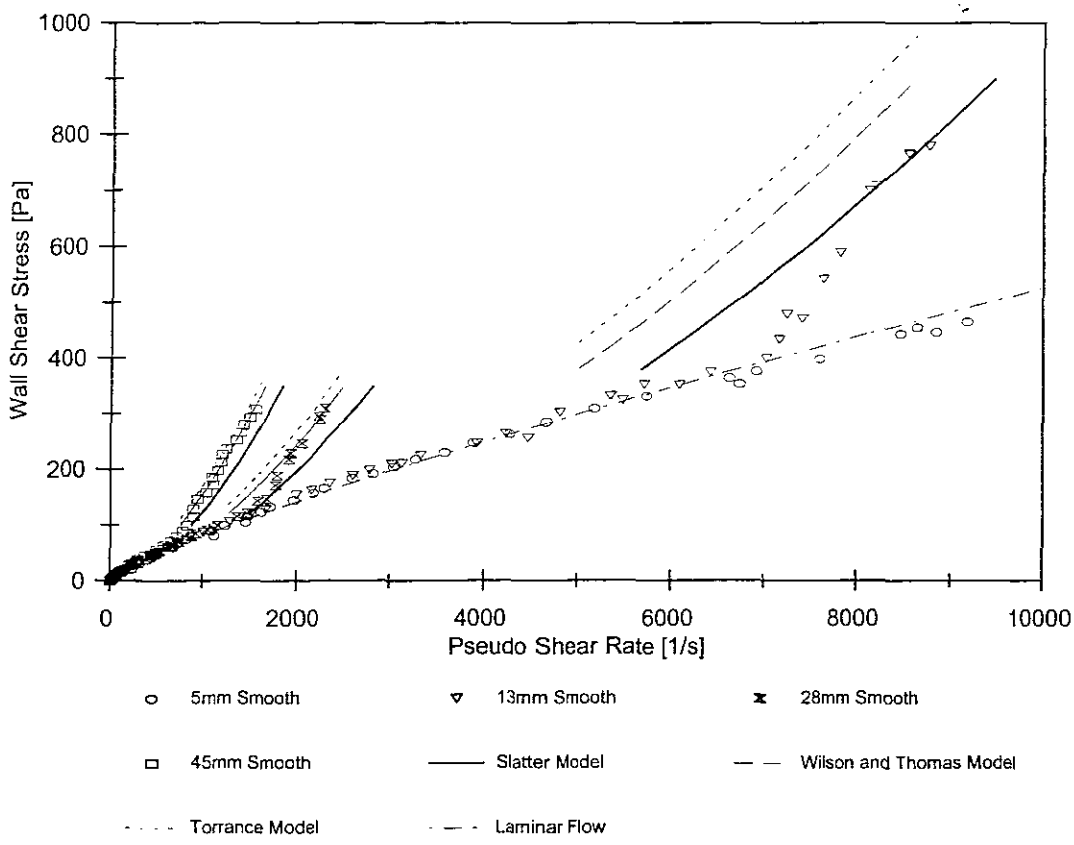

CMC Smooth Pipe Models at a Slurry Relative Density of 1.037

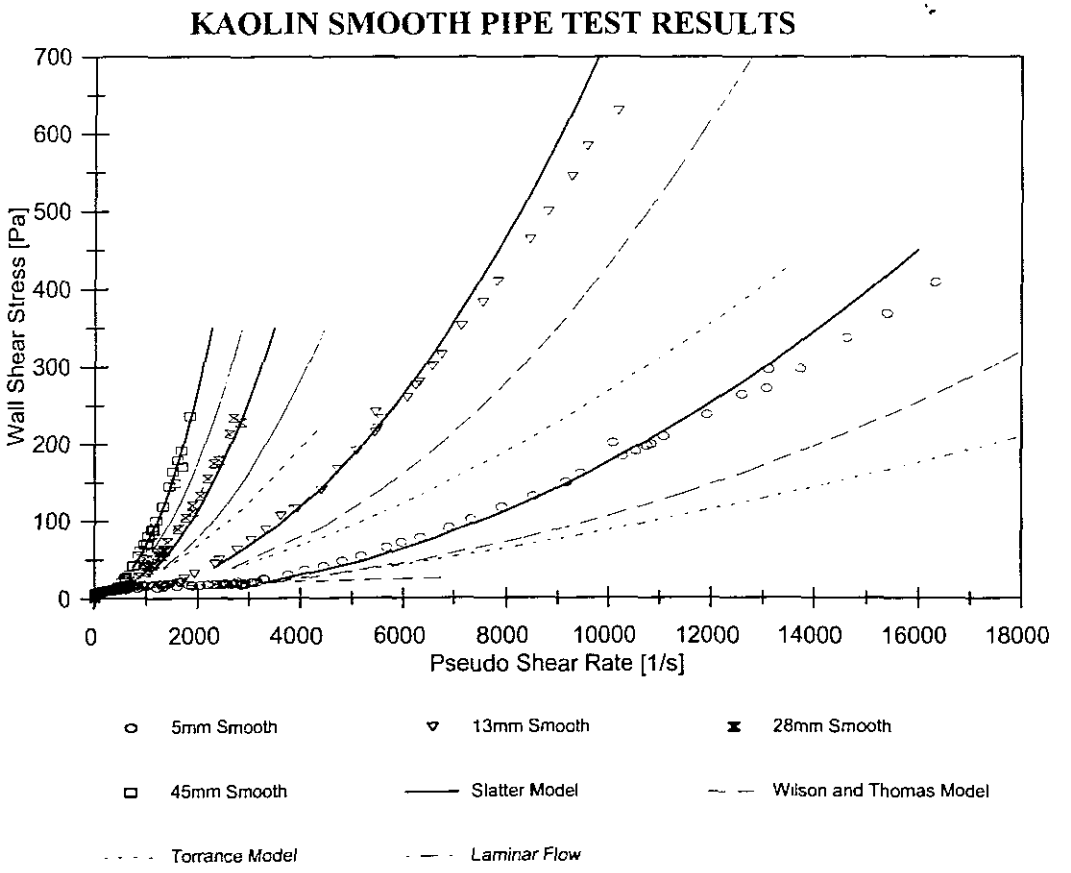

Kaolin Smooth Pipe Models at a Slurry Relative Density of 1.080

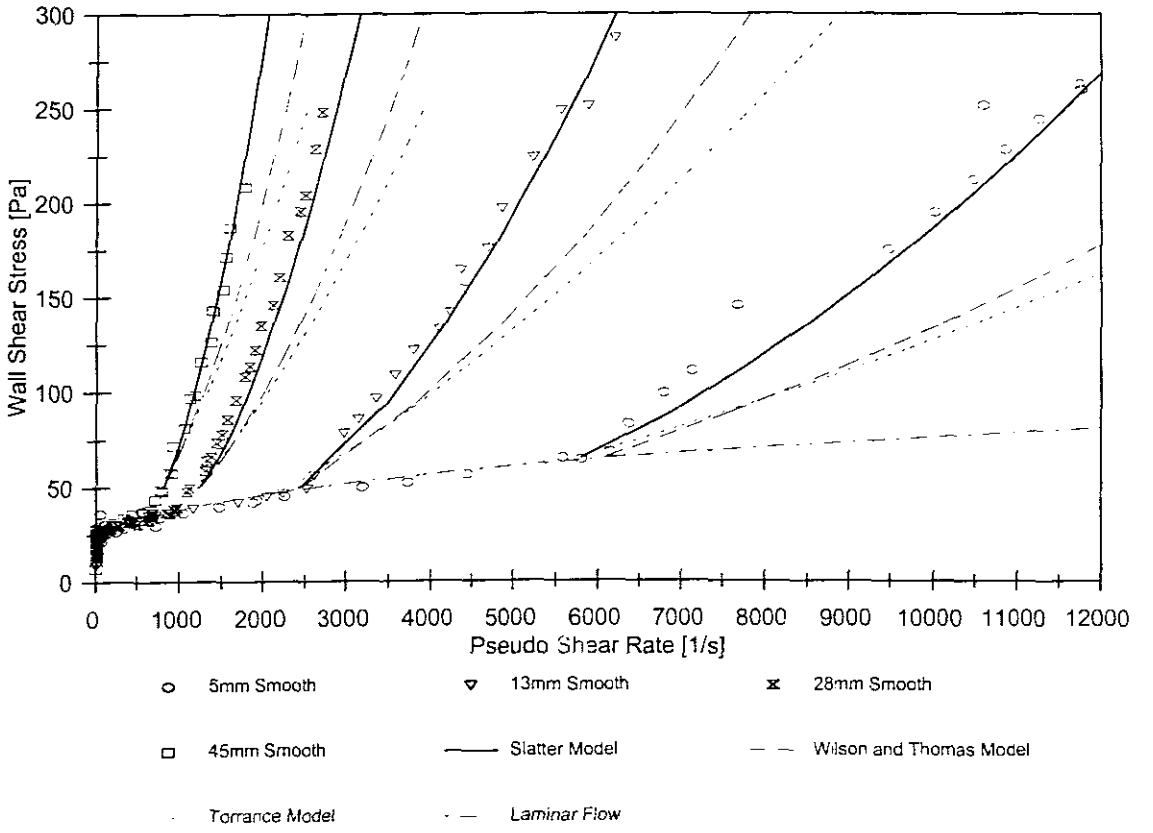

Kaolin Smooth Pipe Models at a Slurry Relative Density 1.146

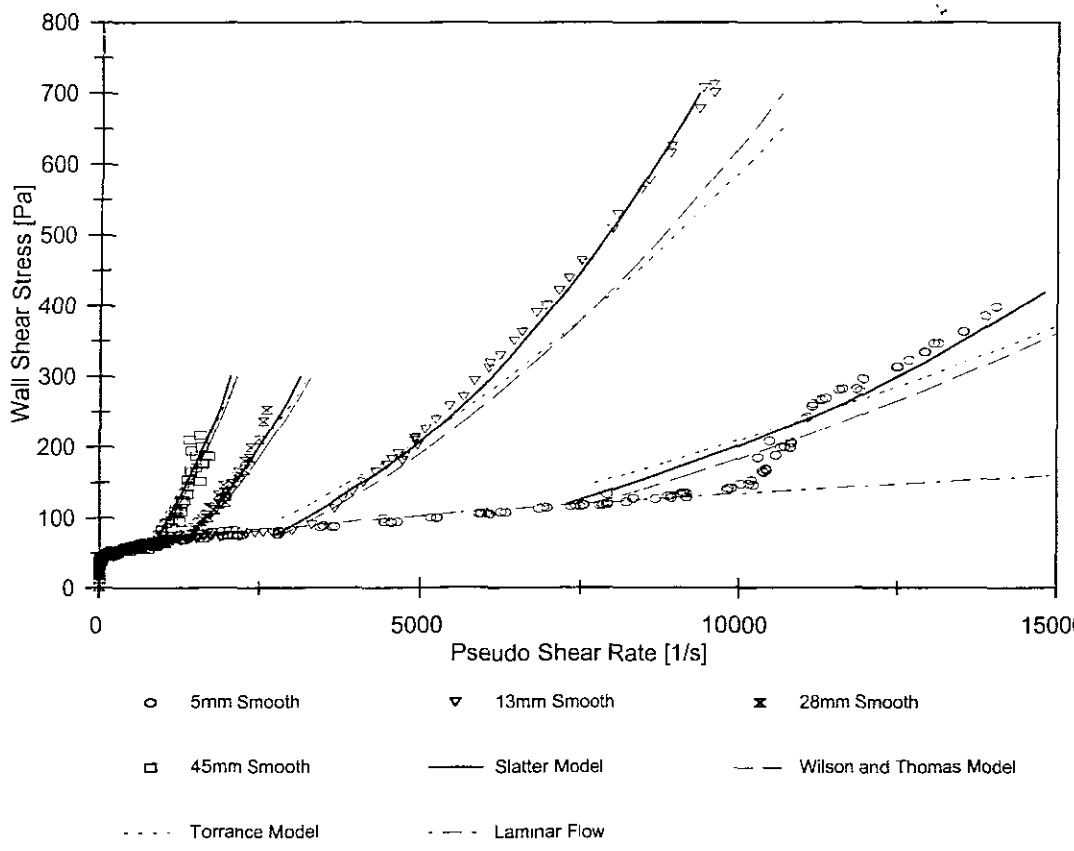

Kaolin Smooth Pipe Models at a Slurry Relative Density of 1.177

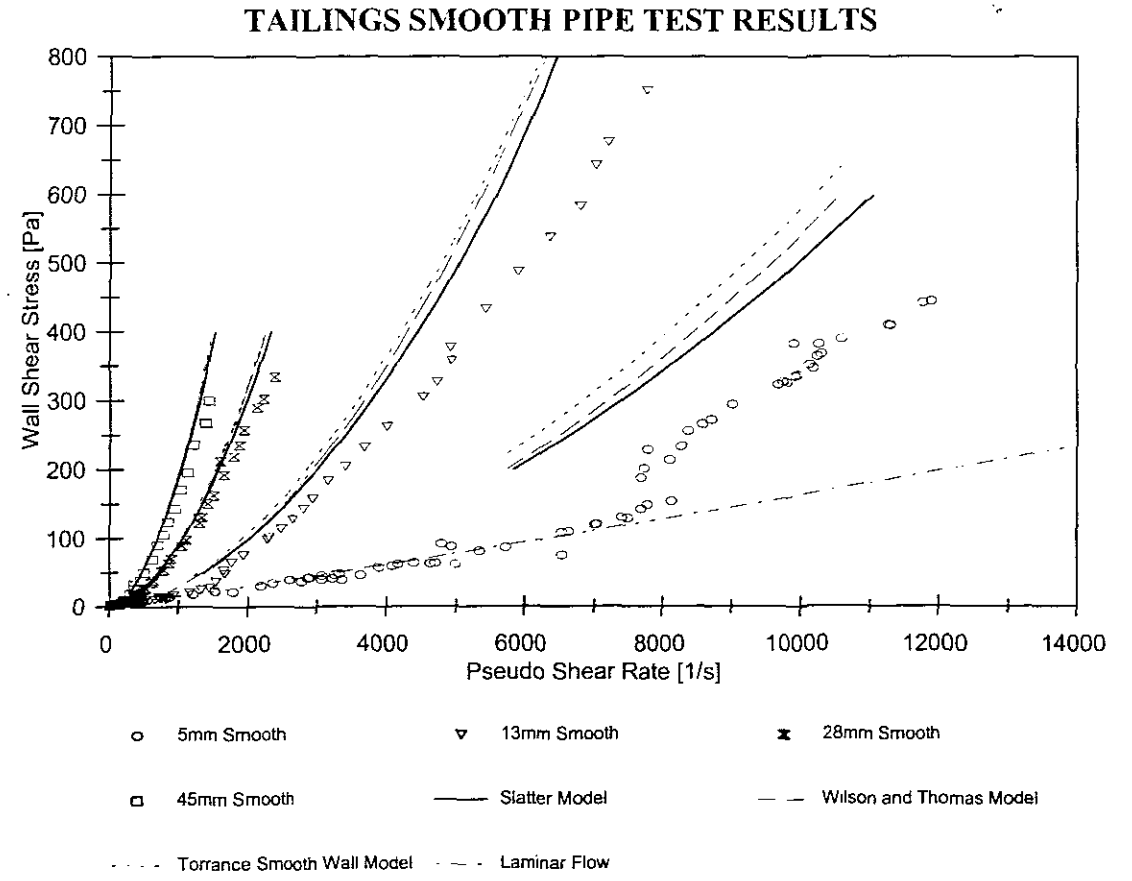

Tailings Smooth Pipe Models at a Slurry Relative Density of 1.731

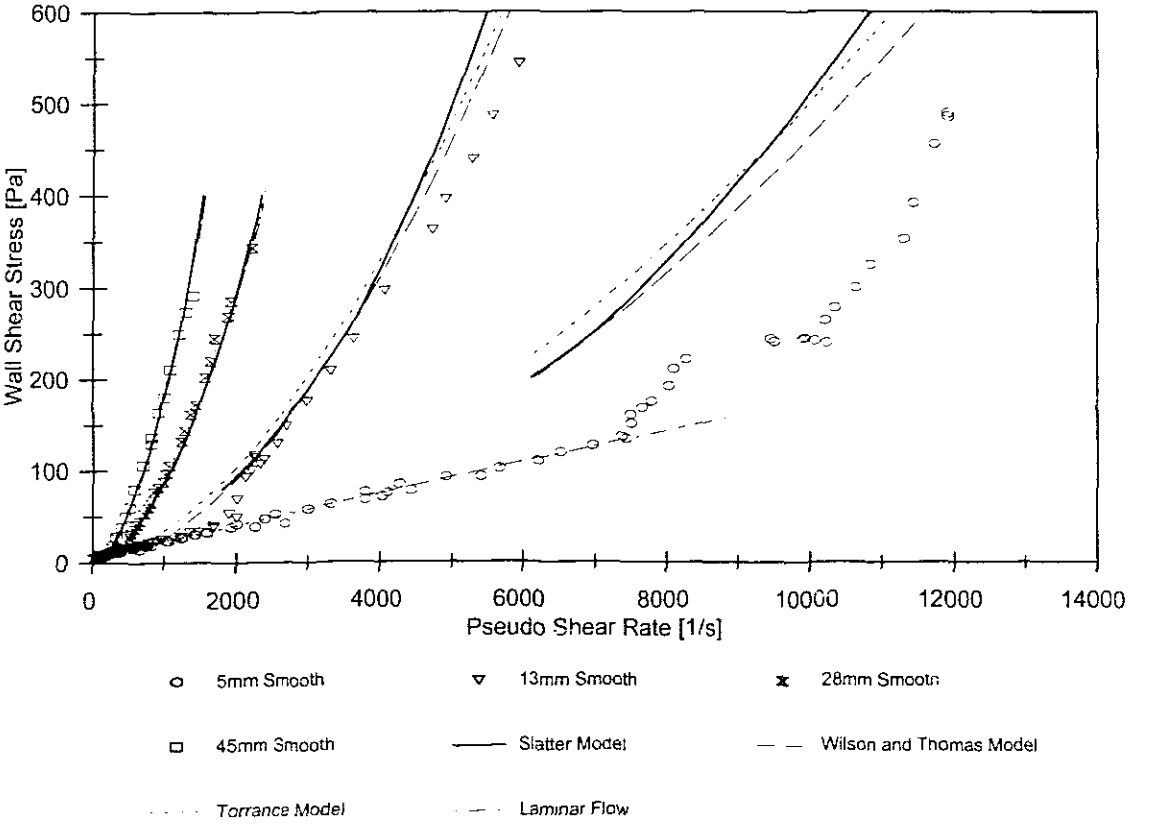

Tailings Smooth Pipe Models at a Slurry Relative Density of 1.801

APPENDIX D

APPARATUS

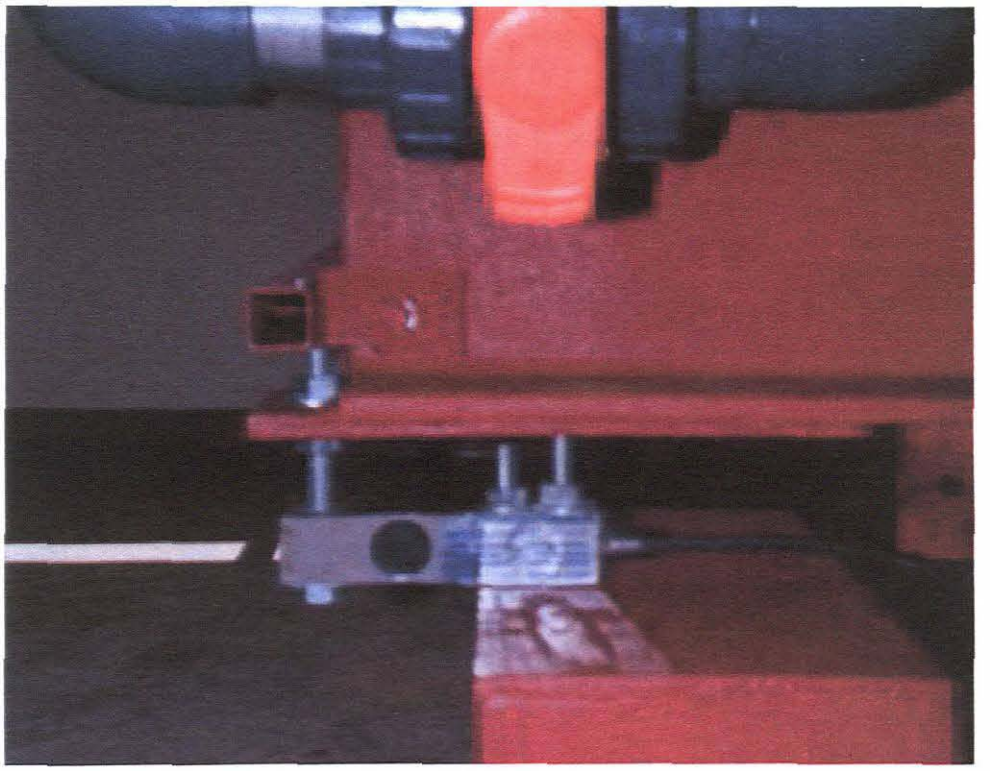

The load cell fixed to the I-beam of the BBTV.

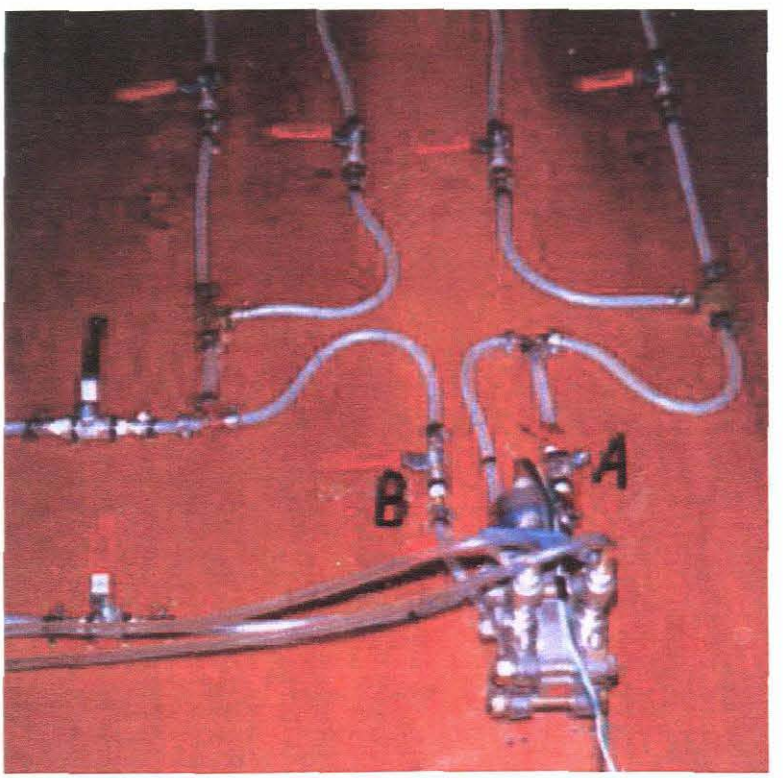

Differential pressure transducer (DPT) and manometer board.

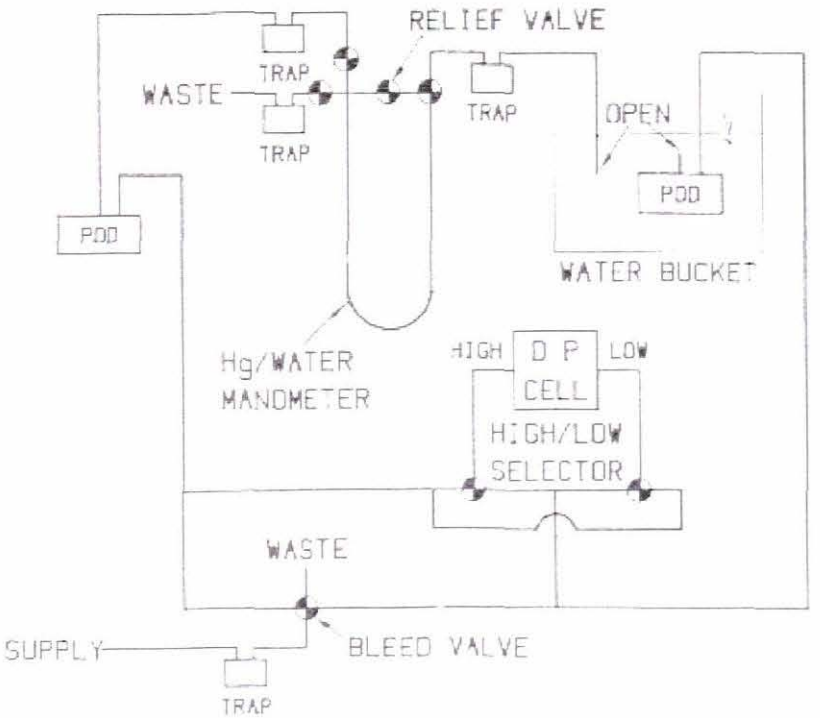

DPT calibration connection.

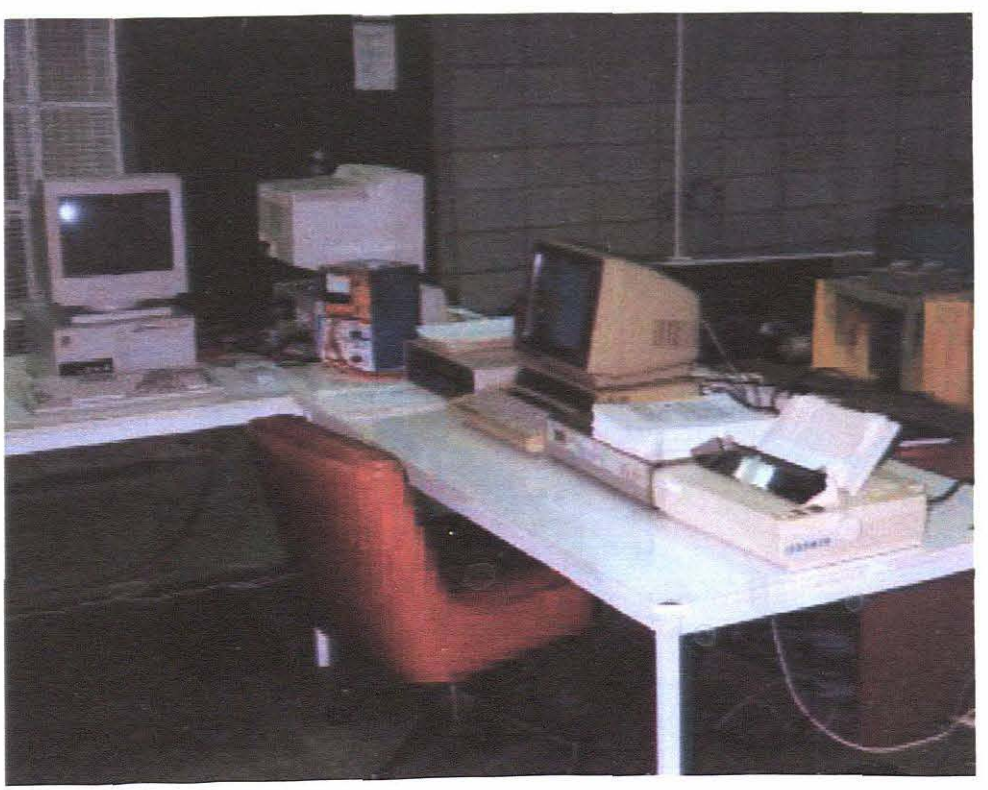

Data acquisition unit and computer.

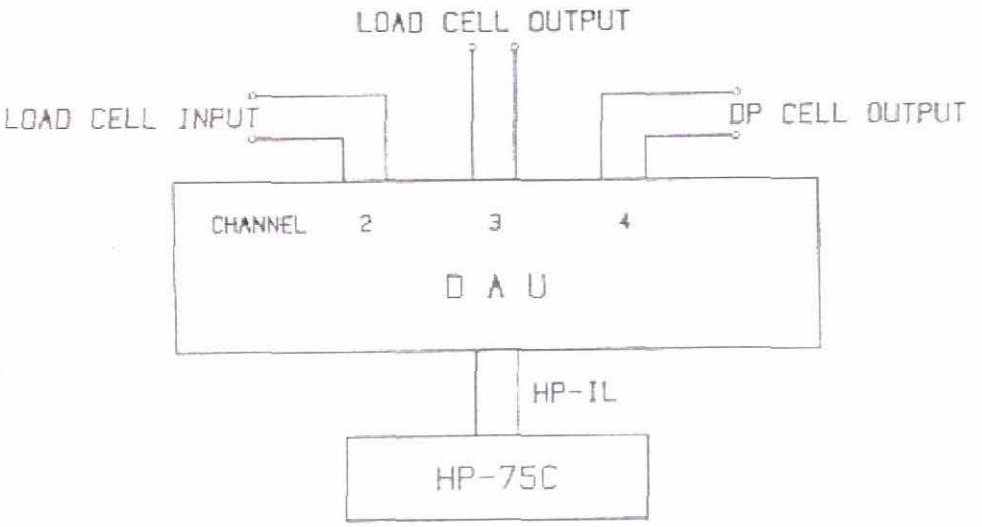

Data acquisition unit and computer connection diagram.

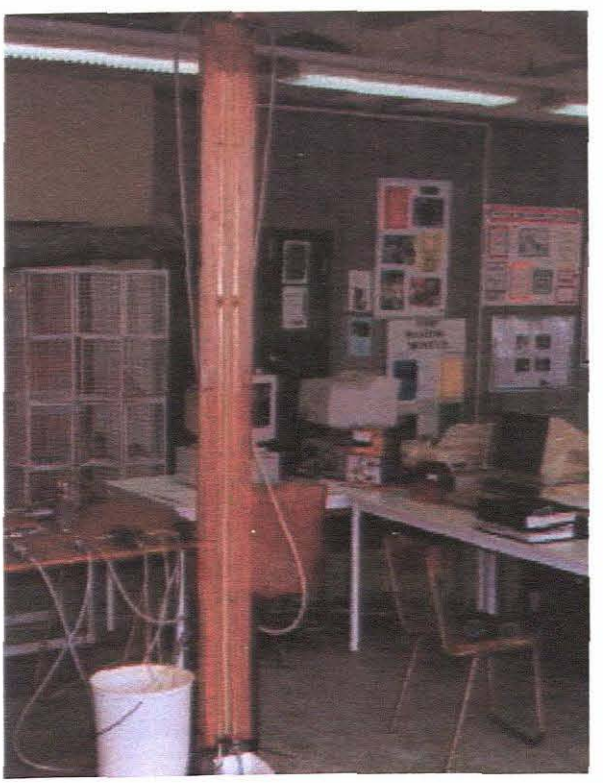

Water over mercury manometer board.

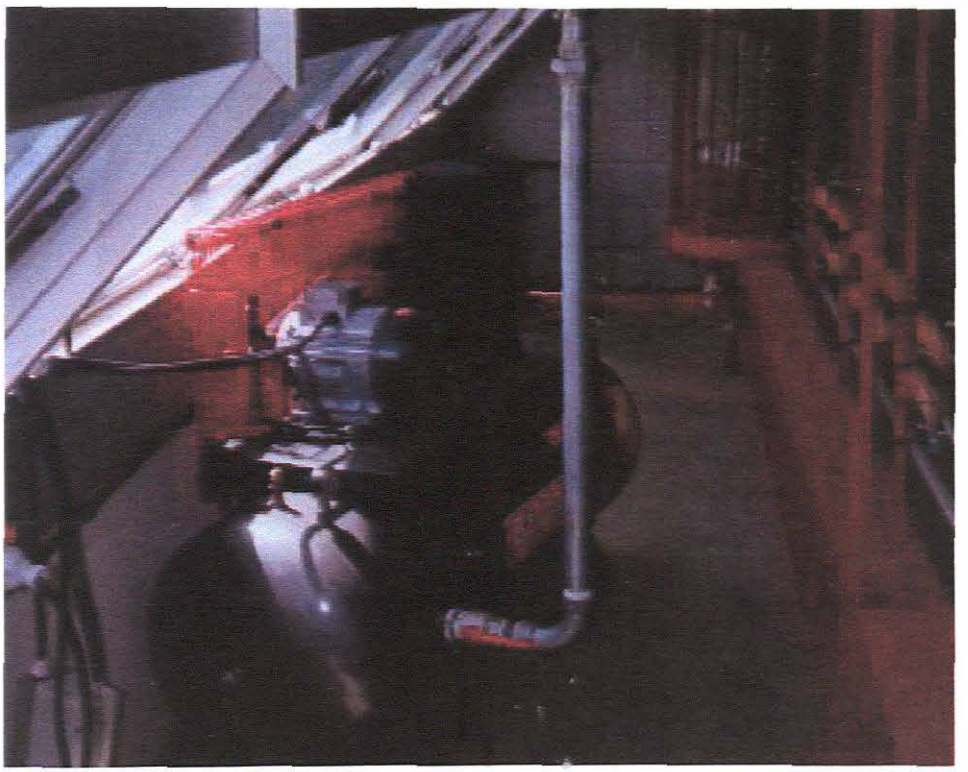

The compressor supplying the compressed air to the BBTV.

The BBTV is balanced on a knife edge.

APPENDIX E

Acaroglu, E. R., "Friction Factors in Solid Material Laden Systems". Proceedings ASCE, Vol. 89, No. HY4, April 1972, p.681.

Bewersdorff, H, and Berman, N. S., "Effect of Roughness on Drag Reduction for Commercially Smooth Pipes," J. Non - Newtonian Fluid Mec. (1987) 24, 365.

Bowen, R.L. Jr.: "Designing Turbulent Flow Systems," Chem. Eng. (July 24, 1961) p143-150.

BS 1377, "Methods of test for soils for civil engineering purposes", British Standards Institution, London (1975).

Casson, N., "Rheology of Disperse Systems," Ed. By C. C. Mill, Pergamon Press, London (1959), p.59. "A Flow Equation for Pigment-Oil Suspensions of the Printing Ink Type."

Chen, N.H., "An Explicit Equation for Friction Factor in Pipe," Ind. Eng. Chem. *Fund.* (1979) 18, No.3, 296-97.

Churchill, S. W., "Empirical Expressions for the Shear Stress in Turbulent Flow in Commercial Pipe," AIChEJ. (1973) 19, No.2, p375-376.

Clapp, R. M., "Turbulent heat transfer in pseudoplastic non-Newtonian fluids." International developments in heat transfer, ASME Part III (1961), Section A, 652.

Colebrook, C.F., "Turbulent flow in Pipes With Particular Reference to the Transition Between the Smooth and Rough Pipe Laws," J. Inst. Civil Eng.(1938-39) 11, p133-156.

Colebrook, C F and White, C M., "Experiments with fluid friction in roughened pipes." Proc, Royal Society of London, (1937), Vol 161: p367-381.

Darby, R. and Chang, H. D., "Generalized Correlation for Friction Loss in Drag Reducing Polymer Solutions," AICHEJ. (1984) 30, No. 2, p274-80.

Dodge, D. W. and Metzner, A.B., "Turbulent Flow of non-Newtonian systems." AIChe Journal. (1959), Vol. 5, No. 2, p189-204.

Dodge, D.W., "Turbulent Flow of non - Newtonian Fluids in Smooth, Round Tubes," PhD discretion, U. of Delaware, Newark (1957).

Drew, T.B., Koo, E.C., and McAdams, W.H., "The Factors for Clear Round Pipes.", Trans., AIChE (1932) 28, p56-72.

Durst, F. and Rastogi, A.K., "Calculations of Turbulent Boundary Layer Flows With Drag Reducing Polymer Additives," Phys. Fluids (1977) 20, No. 12 1975 (1977).

Einstein, H. A. and N. L. Barbarossa, River Channel Roughness, Transactions, ASCE, Vol. 117, (1952) p1121-1146.

Fritsch, W., "Einfluβ der Wandrauhigkeit auf die turbulente Geschwindigkeitsverteilung

in Rinnen." ZAMM 8, (1928) p199.

Fromm, K., "Strömungswiderstand in raun Rohren". Zamm 3, 339 (1923) and W. Fritsch (W. Fritsch, "EinfluB der Wandrauhigkeit auf die turbulente Geschwindigkeitsverteilung in Rinnen". ZAMM 8, 1928).

Govier, G. W. and Aziz, K., "The Flow of Complex Mixtures in Pipes" van Nostrand Reinhold Co. (1972)

Hanks R W, Course notes. "Hydraulic design for flow of complex fluids.", 1981 Richard W Hanks Associates, Inc. Orem, Utah. USA (1981).

Hanks R. W., "The axial laminar flow of yield-pseudoplastic fluids in a concentric annulus", Ind Eng Chem Process Des Dev, 18, 3 (1979).

Hanks, R.W. and Pratt., D.R., "On the Flow of Bingham Plastic Slurries in Pipes and Between Parallel Plates," SPEJ (Dec.1967) 342-46; Trans.,AIME, p240.

Hedström, B. O. A., "Flow of Plastics Materials in Pipes" Industrial and Engineering Chemistry, (1952), v.44 No.3.

Heerman, D F., "Characterization of hydraulic roughness." PhD thesis, Colorado State University, Colorado (1968).

Henderson, F. M.., "Open Channel Flow, MacMillan", 1971, p. 94.

Herschel, W. H. and R. Bulkley.,"Measurement of consistency as applied to rubber-benzene solutions", Proc ASTM, V. 26 Part 2, pp.621 - 633 (1926).

Heywood, N.I., Mehta, K. B. and Poplar, D., "Evaluation of seven commercially available electromagnetic flowmeters with Newtonian and non-Newtonian china clay slurry in pipeflow." 12th Int. Conf. on slurry handling and pipeline transport, Hydrotransport 12 (1993), BHR Group, p353.

Hopf, L., "Die Messung der Hydraulischen Rauhigkeit." ZAMM 3, (1923) 329

Johnson, M., "Non-Newtonian fluid system design - some problems and their solutions." 8th Int. Conf. on the hydraulic transport of solids in pipes, Hydrotransport 8 Paper F3 (1982).

Kamphuis, J. W., "Determination of Sand Roughness For Fixed Beds," Journal of Hydraulic *Research*. 12 (1974) no. 2.

Laufer, J., "The Structure of Turbulence in Fully Developed Pipe Flow", NACA Technical Note 2954, June 1953, see also NACA Report 1175, 1954.

Lazarus, J.H. and Slatter, P.T., "A method for the rheological characterization of tube viscometer data." Journal of pipelines, v. 7. (1988)

Lazarus, J.H. and Sive, A.W., "A novel balanced beam tube viscometer and the rheological characterization of high concentration fly ash slurries." 9th Int. Conf. on the hydraulic

transport of solids in pipes (1984), Hydrotransport 9, Paper E1.

Lazarus J. H. and Slatter P. T., "Comparitive Rheological Characterisation Using a Balanced Beam Tube Viscometer and Rotary Viscometer" 10th Int. Conf. On the Hydraulic Transport of Solids in Pipes, (1986), Hydrotransport 10, Paper J2.

Lord, D.L., Hulsey, B.W., and Melton, L.L., "General Turbulent Pipe Flow Scale-Up Correlation Complex Fluid," SPEJ (Sept. 1967) 252-58; Trans., AIME, 240.

McComb, 1990

Melton, L.L. and Malone, W.T., "Fluid Mechanics Research and Engineering Applications in non-Newtonian Fluid Systems," SPEJ (March 1964) p56-66: Trans., AIME, p231.

Metzner, A.B. and Reed, J.C., "Flow of non-Newtonian Fluids-Correlation of the Laminar, Transition and Turbulent Flow Regions," AIChE J. (1955) 1, No. 4, p434-440.

Moody, L. F., "Friction factors for pipe flow." Trans. Amer. Soc. Mech. Eng. **66** p671 (1944).

Moody, L.F., "Friction factors for pipe flow." Trans . ASME November (1944).

Morris, H. M., "Flow in Rough conduits. Transaction, American Society of Civil Engineers, Vol 120: 373-410 (1955).

Mun, R., "Turbulent pipe flow of yield stress fluids." M Eng Sci Thesis (1988), University of Melbourne.

Neill, R. I. G., "The rheology and flow behavior of high concentration mineral slurries." Msc Dissertation (1988), University of Cape Town.

Nikuradse, J., "Stömungsgesetze in rauhen Rohren", VDI-Forschungsheft p361. Beilage zu Forschung auf dem Gebiete des Ingenieurswesens, Ausgabe B, Band July/August 1933.

Nikuradse, J., Forschungsh. Ver. Dtsch. Ing. (1932) p356.

O'Loughlin, E. M. and E. G. MacDonald., "Some Roughness-Concentration Effects on Boundry Resistance", La Houille Blanche, No. 7, 1964, p773-783.

Park, J. T., Mannheimer, R.J. Grimley, T.A., Morrow, T.B.: "Pipe flow measurements of a transparent non-Newtonian slurry." Journal of fluids engineering (1989), Vol. 111, p331-336.

Paterson A and Cooke R, Course notes. "The Design of Slurry Pipeline Systems", 1997 Paterson & Cooke Consulting Engineers, Claremont, South Africa.

Paterson A. J. C.: "The hydraulic transportation of High Concentration Stabilized Flow Full Plant Mineral Tailings." Ph.D. thesis, (1991), University of Cape Town.

Prandtl, L.. "Über den Reibungswiderstand strömender Luft. Erbebnisse Aerodyn. Versuchsanst. Göttingen", III series, München (1927)

Raudkivi, A. J., "Loose boundary Hydraulics", 1st ed. Pergamon Press, London, England, 1967.

Reynolds, O., Roy. Soc. Phil. Trans., Ser. A, p174, 935 (1883)

Riedel, H. P., "Direct Measurement of Bed Shear Stress Under Waves", Queen's University Ph.D. Thesis, 1972.

Rothfus, R. R., Doctoral Dissertation, Carnegie Institute of Technology, Pittsburgh, Pa., 1948.

RP 39, "Recommended Practices for Standard Procedures for Evaluation of Hydraulic Fracturing Fluids", second edition, API, Dallas (Jan. 1983).

Saph V. and Schoder, E.H., "An Experimental Study of the Resistance to the Flow of Water in pipes". Trans. Amer. Soc. Civ. Engr. 51, 944 (1903).

Schlichting, H., "Boundary Layer Theory." 4th edition, (1960) McGraw-Hill, New York, Chapter XX.

Senecal, V. E, and R.R. Rothfus, Chem. Eng. Progress, 49, 533 (1953).

Serghides, T. K., "Estimate Friction Factor Accurately," Chem. Eng. (March 5, 1984) p63-64.

Shah, S.N., "Correlations Predict Friction Pressures of Fracturing Gels," Oil & Gas J. (Jan. 16, 1984) p92-98.

Shook, C. A. and Roco M. C., "Slurry Flow: Principles and Practice." Butterworth-Heineman, (1991).

Sive A. W., "An Analytical and Experimental Investigation of the Hydraulic Transport of High Concentration Mixed Regime Slurries." Ph.D Thesis, (1988), University of Cape Town.

Slatter P T and Lazarus J. H., "The application of viscometry to the hydraulic transport of backfill material", Conf. Backfill in South African mines. (SAIMM) (1988).

Slatter, P. T., "The Rheological Characterasition of non-Newtonian Slurries Using a Novel Balanced Beam Tube Viscometer." M.Sc Dissertation, (1986), University of Cape Town.

Slatter, P.T. and Van Sittert, F. P., "The effect of pipe roughness on non-Newtonian turbulent flow." 9th International conference on Transport and Sedimentation of Solid Particles (1997) Cracow.

Slatter, P.T. and Lazarus, J. H.: "Critical flow in slurry pipelines." 12th Int. Conf. on slurry handling and pipeline transport, Hydrotransport12 (1993), BHR Group, p639.

Slatter, P.T., "Transitional and Turbulent Flow of non-Newtonian Slurries in Pipes." Ph.D Thesis, (1994), University of Cape Town.

Slatter, P.T., "Turbulent flow of non-Newtonian slurries in pipes." 8th International Conference on Transport and Sedimentation of Solid Particles (1995) - Prage.

Stanton, T. E., Proc. Royal Soc., Ser. A, 85, p366 (1911).

Stanton, T. E., and J. R. Pannell, Roy. Soc. Phil. Trans., Ser. A, 214, p199 (1914)

Streeter, V. L., "Frictional Resistance in Artificially Roughened Pipes. Proc. Amer. Soc. Civil Engr. 61, p163 (1935).

Thomas A. D. and Wilson K. C., "New Analysis of non-Newtonian Flow Yield Power-Law Fluids." Can T Chem Eng, (1987), 65 p335-338.

Torrance, B. McK., "Friction Factors for Turbulent non-Newtonian Flow in Circular Pipes." S. A. Mechanical Engineer, (1963), v.13.

Vanoni, V. a., "Hydraulic Relations for Alluvial Streams", Proceedings ASCE, Vol. 97, Hy1, January 1971, p101.

Virk, P.S.: "Drag Reduction in Rough Pipes," J. Fluid Mech. (1971) 45, Part 2, p225.

von Karman, T., Natl. Advisory Committee for Aeronautics Technical Memo No. 611, Washington(1931).

Williamson, J., "The Laws of Flow in Rough Pipes", La Houilie Blanche, Vol. 6, No. 5, September 1951, p738.

Wilson, K.C., Addie G. R. and Clift R., "Slurry transport using centrifugal pumps." Elsevier Science Publishers Ltd, Essex, (1992) England.

Wilson, K. C. and Thomas, A. D., "A new analysis of the turbulent flow of non-Newtonian fluids. Can. J. Chem. Eng. (1985) 63, p539-546.

Yalin, M. S., Mechanics of Sediment Transport, Pergamon, 1972.

Zigrang, D.J. and Sylvester, N.D., "Explicit Approximations to the Solution of Colebrook's Friction Factor Equation," AIChEJ. (1982) 28, No. 3. 514-15.

APPENDIX F

INTERNATIONAL PAPERS PRESENTED BY THE AUTHOR

1. THE EFFECT OF PIPE ROUGHNESS ON NON-NEWTONIAN TURBULENT FLOW by Paul T. Slatter and Fritz P. van Sittert

   9th International Conference on TRANSPORT AND SEDIMENT OF SOLID PARTICLES
   2-5 September 1997, Cracow, Poland

2. ANALYSIS OF ROUGH WALL NON-NEWTONIAN TURBULENT FLOW by P T Slatter, School of Civil Engineering, Cape Town, South Africa and F P van Sittert, Paterson & Cooke Consulting Engineers (Pty) Limited, South Africa

   HYDROTRANSPORT 14 on SLURRY HANDLING AND PIPELINE TRANSPORT
   8-10 September 1999, The Netherlands, Maastricht